

# Design-to-Fabrication Workflow for Raw-Sawn-Timber using Joinery Solver

THIS IS A TEMPORARY TITLE PAGE  
It will be replaced for the final print by a version  
provided by the registrar's office.

Thèse n. 8928  
présentée le 5 juillet 2021 à la Faculté des sciences de base  
laboratoire IBOIS  
programme doctoral en EDAR  
École polytechnique fédérale de Lausanne  
pour l'obtention du grade de Docteur ès Sciences  
par

Petras Vestartas

acceptée sur proposition du jury :

Prof Jeffrey Huang, président du jury  
Prof Yves Weinand, directeur de thèse  
Prof Niels Martin Larsen, rapporteur  
Prof Phil Ayres, rapporteur  
Prof Marco Bakker, rapporteur

Lausanne, EPFL, 2021





# Acknowledgements

Firstly, I am grateful to my supervisor, civil engineer and architect Prof. Dr. Yves Weinand, who has given me an opportunity to work with timber in its natural form in an interdisciplinary research environment and supported me during the thesis.

It was a pleasure to meet, work and collaborate with my colleagues and friends at IBOIS, notably Julien Gamerro, Anh Chi Nguyen, Aryan Rezaei Rad, Martin Thomas Nakad, Omar Geneidy, Leo Pommereul, Maxence Grangeot, Andrea Settimi, Nicolas Rogeau, Francine Sallin, Francois Perrin, Violaine Prevost, Christopher Robeller, Andrea Stitic, Stéphane Roche, Aymeric Broyet.

A special thanks to Swiss industrial collaborators: Rossiniere forestry (Frederic Blum and Jean Pierre Neff) who introduced to the mountain forest harvesting, Lausanne forestry and Chavornay saw-mill for the material support. In addition to this, Belgium company Mobic (ImaxPro) helped to apply robotic fabrication for whole timber processing.

Without the technical support of Groupe Ingenierie des Structures (GIS) at ENAC , demonstrators and setups would be hardly possible.

I would also like to thank the members of the thesis jury Prof. Jeffrey Huang, who has accepted the role of the president, and the experts, Prof. Niels Martin Larsen, Prof. Phil Ayres, Prof. Marco Bakker, for their examination of the work and for their valuable advice and support.

Finally, I would like to thank my wife Lina, for your unconditional support and encouragement. The advice, assistance and understanding were necessary to go through all kinds of the different days of this journey. I am also grateful to my parents Ilona Girciene and Vytautas Gircys to reach this goal.

*Lausanne, August 31, 2021*

P. V.



# Abstract

Currently, the Swiss timber industry in mountain areas largely exports unprocessed lumber and imports finished timber products due to the lack of digital tools. By using new digital design-to-production workflows, it is possible to investigate new building systems for small-scale structures using local timber for local applications.

While automation in raw wood fabrication is a well-studied field, there is a lack of integration into the local timber industry. In addition, a few large robotic companies focus on raw-sawn-timber fabrication, leading to the high-level automation in fabrication but do not offer any architectural design methods. Architect and fabricator, in the raw wood context, are seen as two different parties. Research in architectural digital manufacturing demonstrate the potential in design with raw timber without the dependence on the large centralized timber companies. Often the focus is given to single case studies without questioning the automation in the local circular economies resulting in the small-scale semi-automated fab-lab workshops. Consequently, it is necessary to revisit individual design-to-fabrication workflows for whole timber structures and propose new open-source, extendable and reusable techniques.

First, a joinery algorithm is proposed to ease the drafting process of pair-wise wood-wood connections. The idea of the joinery algorithm is based on a design modelling separation into two independent algorithms: a) global architectural design, and b) local automation of wood-wood connections. These are the principal design requirements for the algorithm: a) re-usability of joinery methods for more than one case study, b) joinery library, c) automatic wood-wood connection generation, d) ensuring fabrication constraints e) propose a fast collision-based graph method, f) integrate joinery algorithm into a common CAD modelling environment, and g) employ minimal models for fast computation.

Second, the geometrical irregularities of raw wood require laser-scanning and robotic integration. The Scanning part proposes novel solutions for raw wood fabrication: a) point-cloud processing, b) market-less alignment within a robotic setup, and c) calibration guidelines for laser scanners. The robotic section proposes a tool-path planning algorithm to shorten the fabrication file preparation. The design recommendations for machining setups are given to

## **Abstract**

---

ensure secure, stable and accurate fabrication.

Third, timber joinery prototypes are assembled to validate the proposed workflow. Three types are developed: segmented timber shells, Nexorades and a truss from tree forks. Additionally, the modelling framework is interconnected with tool-path planning to manifest the validity of fabrication concerning a joint geometry. Finally, the developed algorithms are open-sourced.

In conclusion, the design-to-fabrication workflow proves that it is possible to detect wood joinery types based on minimal CAD models. From a user perspective, these models do not require hard-coded parametric skills and, as a result, applicable to CAD modelling interfaces. Finally, the integration of the low resolution referencing system of the laser scanner and the industrial robotic arm into the joinery generation method verifies the link between architectural design and manufacturing processes.

**Keywords:** Wood-wood Connections, Joinery, Robotic Fabrication, Raw-Timber, Assembly, Whole Timber, Scanning, Point-cloud Processing.

## Résumé

Aujourd’hui, l’industrie du bois des zones montagneuses exporte une grande partie de bois non transformé et importe des produits finis en bois pour les constructions locales. Grâce aux nouveaux processus de travail numériques de la conception à la production, il est possible d’étudier de nouveaux systèmes de construction pour des structures locales à petite échelle utilisant du bois brut scié.

Si l’automatisation dans la fabrication du bois brut est un domaine bien étudié, il y a un manque d’intégration dans l’industrie locale du bois. De plus, quelques grandes sociétés de robotique se concentrent sur la fabrication de bois brut scié, conduisant à une automatisation de la fabrication de haut niveau, mais elles ne proposent pas de méthodes de conception architecturale. Dans le contexte du bois brut, l’architecte et le fabricant sont considérés comme deux parties différentes. Des méthodes de recherche architecturales avancées, intégrées à la fabrication numérique, montrent un potentiel dans les économies circulaires numérisées sans dépendance à la grande industrie centralisée du bois. Toutefois, l’accent est mis uniquement sur des études de cas uniques sans remettre en question l’automatisation dans la construction et les méthodes fab-lab semi-automatisées à petite échelle. Par conséquent, il est nécessaire de revoir les processus de travail individuels de la conception à la production pour les structures en bois entier et de proposer de nouvelles techniques open-source, extensibles et recyclables.

Un algorithme de menuiserie est proposé pour faciliter le processus d’élaboration des raccords bois-bois par paire liés à la conception et la fabrication. L’idée de l’algorithme de menuiserie est basée sur une séparation de modélisation de la conception en deux algorithmes indépendants : a) les méthodes d’élaboration (échelle macro) et b) l’automatisation des raccords bois-bois (échelle micro). Voici les principales exigences de conception utilisées pour développer l’algorithme : a) la réutilisation des méthodes de menuiserie pour plus d’une étude de cas, b) la collection d’une bibliothèque de menuiserie à partir de multiples projets, c) la conception de structures en bois avec une génération de raccords bois-bois automatiques, d) garantir les contraintes de fabrication et la sécurité, e) interconnecter les éléments linéaires (poutres) et les éléments plans (plaques), f) proposer une méthode alternative de construction de graphique rapide au lieu d’utiliser une structure de données de graphique prédéfinie telle que le maillage, g) intégrer l’algorithme de menuiserie dans un environnement de modélisation CAO commun pour l’interconnecter avec d’autres techniques de modélisation CAO, et h) utiliser des modèles minimaux pour une rapidité des calculs.

## Résumé

---

Les irrégularités géométriques du bois brut nécessitent un balayage laser et une intégration robotique. La partie numérisation propose de nouvelles solutions pour la fabrication de bois brut : a) une bibliothèque de traitement de nuages de points traduite des langages de bas niveau vers un environnement CAO largement utilisé, b) un alignement sans marché dans une configuration robotique, et c) des directives d'étalonnage pour les scanners lasers. La section robotique propose un algorithme de planification de trajectoire d'outil pour raccourcir la préparation du fichier de fabrication. La méthode relie l'accessibilité du robot et la détection des collisions à la génération d'articulations en bois. De plus, la fabrication du bois entier est liée aux configurations d'usinage. Des recommandations de conception pour cette configuration sont données pour assurer une fabrication sûre, stable et précise.

La méthodologie montre qu'il est possible de détecter les types de menuiserie en bois sur la base d'un modèle architectural low-poly. Ces modèles ne nécessitent pas de modèles paramétriques codés en dur et, par conséquent, ils sont applicables aux interfaces de modélisation CAO. Le cadre proposé prend en compte divers types d'éléments en bois, en accordant une attention toute particulière au bois brut scié. Une série de prototypes de raccord bois-bois sont ainsi usinés en utilisant du bois brut scié pour valider le processus de travail. Deux démonstrateurs ont été construits pour prouver avec succès la faisabilité des méthodes proposées : a) des structures de coque utilisant des connexions latérales et b) des nexorades utilisant une menuiserie latérale et croisée. Le cadre proposé a également permis de réaliser un système d'armature à partir de fourches d'arbres et d'une menuiserie polyvalente.

Dans cette thèse, une topologie de la menuiserie recyclable est développée et mise en œuvre avec succès dans plusieurs prototypes. Le cadre est développé pour ne pas imposer un modèle de conception spécifique tout en résolvant la modélisation de la menuiserie locale. De plus, la bibliothèque de traitement de nuages de points développée montre un alignement nuage-nuage indépendant de la forme sans marché pour la fabrication de robotique. Ainsi, le cadre de modélisation est interconnecté avec la planification de trajectoire de l'outil pour manifester la validité de la fabrication concernant la géométrie d'assemblage. Enfin, la méthodologie est applicable en dehors de l'environnement d'un laboratoire fermé en utilisant le cadre du logiciel proposé qui est accessible au public.

**Mots-clés :** raccords bois-bois, menuiserie, fabrication de robotique, bois brut, assemblage, bois entier, numérisation, traitement de nuages de points.

# Contents

<b>Acknowledgements</b>	<b>i</b>
<b>Abstract (English/Français)</b>	<b>iii</b>
<b>I Introduction</b>	<b>1</b>
<b>State-of-the-Art Classification</b>	<b>3</b>
<b>1 Material Properties of Raw Wood</b>	<b>5</b>
1.1 Raw Wood Properties . . . . .	5
1.2 Swiss Context . . . . .	9
<b>2 Digital Fabrication Methods of Raw Wood</b>	<b>13</b>
2.1 Scanning . . . . .	13
2.2 Connections . . . . .	21
2.3 Digital Fabrication . . . . .	26
2.4 Differences between Research and Industrial Applications . . . . .	32
2.5 Stock Assignment . . . . .	33
<b>3 Architectural Design Methods using Raw Wood</b>	<b>35</b>
3.1 Historical Record . . . . .	35
3.2 Applications using Straight Wood . . . . .	37
3.3 Applications using Forks . . . . .	43
3.4 Applications using Crooked Curved Wood . . . . .	47
<b>4 Research Motivation</b>	<b>51</b>
4.1 Two Challenges: Architectural Design and Fabrication . . . . .	51
4.1.1 Challenge 1 - Building Better Models for the Digital Joint Design . . . . .	51
4.1.2 Challenge 2 - Scanning-to-Fabrication . . . . .	52
4.2 Small Radius Timber . . . . .	53
4.3 Motivation and Overview of the Proposed Workflow . . . . .	54
4.4 Thesis Structure . . . . .	56

## Contents

---

<b>II Methodology</b>	<b>59</b>
<b>Foreword of Methodology</b>	<b>61</b>
<b>5 Joinery Solver</b>	<b>63</b>
5.1 Foreword . . . . .	63
5.2 Introduction . . . . .	65
5.3 Data-structures . . . . .	67
5.4 Search Methods for Connection Zones . . . . .	74
5.5 Connection Types in a Model . . . . .	77
5.6 Boolean Methods for 2D Polyline and 3D Solid Meshes . . . . .	111
5.7 Conclusion . . . . .	112
<b>6 Scanning</b>	<b>115</b>
6.1 Foreword . . . . .	115
6.2 Introduction . . . . .	117
6.3 Laser Scanner and Industrial Robot Arm Synchronization . . . . .	123
6.4 Point-cloud Processing for Raw Wood Fabrication . . . . .	133
6.5 Conclusion . . . . .	150
<b>7 Robotic Fabrication</b>	<b>151</b>
7.1 Foreword . . . . .	151
7.2 Introduction . . . . .	153
7.3 Physical Setup . . . . .	156
7.4 Robot Control . . . . .	165
7.5 Robotic Tool-path Generation within Joinery Solver . . . . .	171
7.6 Conclusion . . . . .	175
<b>Conclusion of Methodology</b>	<b>179</b>
<b>III Demonstrators</b>	<b>181</b>
<b>Foreword of Demonstrators</b>	<b>183</b>
<b>8 Side-to-side Joints for Shell Structures</b>	<b>185</b>
8.1 Foreword . . . . .	185
8.2 Introduction . . . . .	186
8.3 Surface Discretization . . . . .	187
8.4 Prototypes . . . . .	188
8.5 Results . . . . .	192
8.6 Conclusion . . . . .	197
<b>9 Raw wood Cross and Top-to-side Joints for Nexorades</b>	<b>199</b>
9.1 Foreword . . . . .	199

9.2 Introduction . . . . .	200
9.3 Workflow for Nexorades in Raw Timber . . . . .	206
9.4 Prototypes . . . . .	211
9.5 Assignment Problem . . . . .	214
9.6 Conclusion . . . . .	216
<b>Conclusion of Demonstrators</b>	<b>217</b>
<b>IV Conclusion and Future Work</b>	<b>219</b>
<b>10 Conclusion</b>	<b>221</b>
<b>11 Future Work</b>	<b>225</b>
<b>V Appendices</b>	<b>227</b>
<b>A Timber Joinery and Teaching</b>	<b>229</b>
A.1 Introduction . . . . .	229
A.2 Side-to-top Joints Multi-valence Joint . . . . .	230
A.3 Truss from Tree Forks . . . . .	232
A.4 Conclusion . . . . .	237
<b>B Rossiniere Forestry</b>	<b>239</b>
B.1 Introduction . . . . .	239
B.2 Local Circular Economy . . . . .	240
B.3 Visit 1 - Absence of Digital Fabrication . . . . .	240
B.4 Visit 2 - Available Tree Topologies . . . . .	242
B.5 Visit 3 - Harvesting Trees . . . . .	243
B.6 Conclusion . . . . .	244
<b>C Software Frameworks</b>	<b>245</b>
C.1 NGon - Mesh Processing and Joinery Solver . . . . .	245
C.2 OpenNest - Packing 2D Objects for Fabrication . . . . .	246
C.3 Cockroach - PointCloud Processing . . . . .	247
C.4 FaroSharp - Laser Scanner Control for .NET Applications . . . . .	248
C.5 IBOIS-CNC - Tool-path Generation for 5-Axis CNC . . . . .	249
<b>List of figures</b>	<b>251</b>
<b>Bibliography</b>	<b>259</b>
<b>Curriculum Vitae</b>	<b>275</b>



# **Introduction Part I**



# **State-of-the-Art Classification**

The State-of-Art classification is divided into three parts: "Material Properties of Raw Wood", "Digital Fabrication Methods of Raw Wood" and "Architectural Design Methods using Raw Wood". The three parts are examined based on the existing commercial and research methods to design and fabricate the non-standard wood structures (see Figure 1).

Whole timber has distinctive linear material properties that are different to standardized timber. Raw timber is not often sold for everyday use, and such practice requires creating a dialogue between the research and the industry. Raw wood has several advantages compared to sawn timber: (a) there is a need to use more local timber due to the overstocking of forests, (b) low economic value, (c) lower embodied energy (d) structural performance, (e) minimal processing. This type of wood has a lower cost, including the digital fabrication process, due to the minimal physical transformation and transportation needs. Therefore, it has gained a commercial interest to join the robotic fabrication and the architectural design.

Industrial robots can transform trees into a building material with a minimal processing time. These tools usually have a) computer-vision, b) cutting methods to alter tree shapes' irregularity c) and cut wood-wood connections based on a pre-measured timber stock. The locally sawn timber also requires a skilled integration of the customized workflows such as lathes, band-saws, chain-saws, scanners and interpreting their communication with CAD applications. These tools have to be combined in a higher-level workflow while solving each of their low-level integration. As a result, there is a close relation between the material, fabrication and design processes.

Design methods must be analyzed to understand the relation between the micro-scale of timber connections and the macro architectural scale. The wood-wood connections differ from the joinery used in traditional timber, taking into account irregular timber shape: a) straight, b) bifurcated, or c) crooked. The raw timber has a linear fibre orientation that has a direct relation to possible structural models. Furthermore, models such as frames, trusses, grid-shells, Nexorades, solid walls, and slabs follow timber stock availability. Additionally, design models could be specific to their forest contexts. Thus, it is necessary to understand the common principles repeated throughout the case studies.

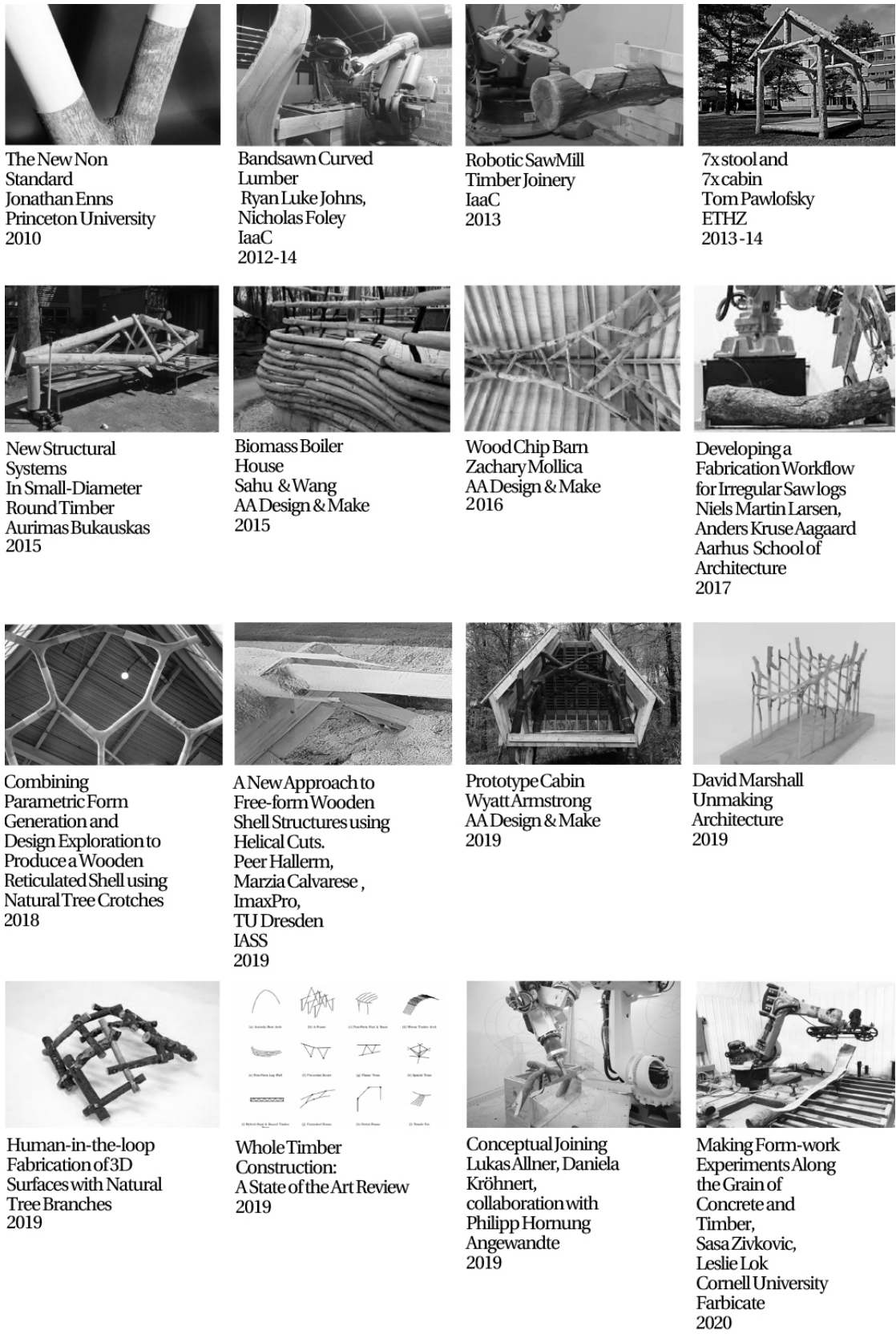


Figure 1 – Architectural research with locally sawn timber.

# 1 Material Properties of Raw Wood

## 1.1 Raw Wood Properties

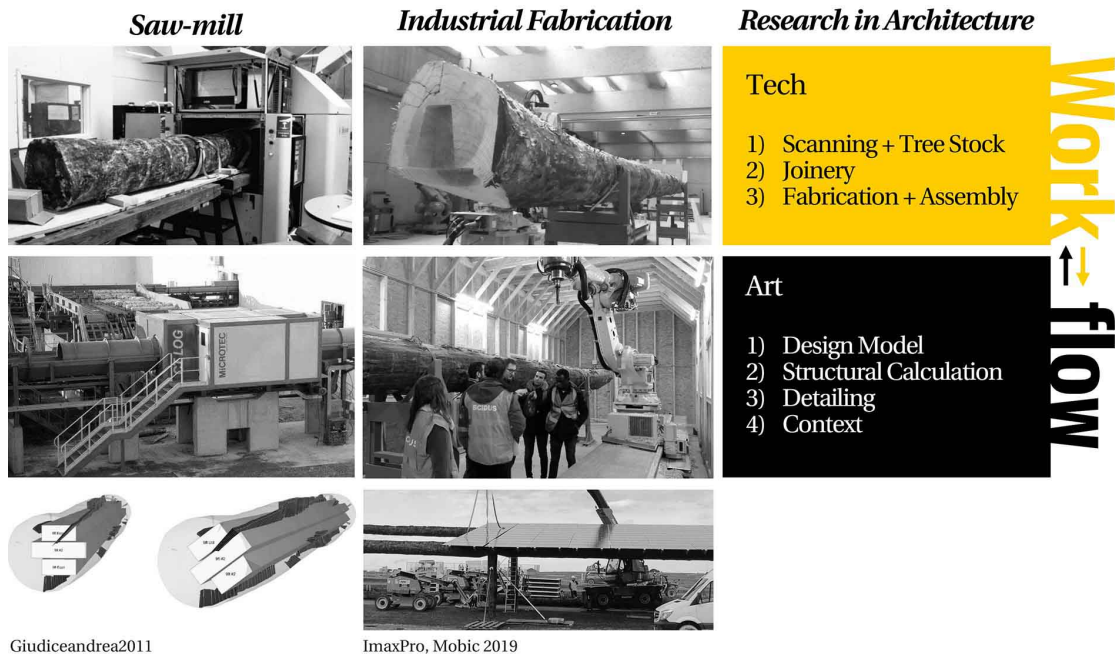
### Overstocking

Starting from the 1960s and continuing to the present, governments in forested regions around the world have increasingly faced a major forestry challenge: an overabundance of small-diameter trees (10-25 cm in diameter). This issue sets forests at increased risk of destructive high-intensity wildfires, diseases, and insect attacks, while suppressing the growth of trees [45, 51, 89, 145]. This overstocking is mainly caused by insufficient low-intensity burning in fire-prone forests and poor early harvests in planted forests. In plantation forestry, trees are typically planted in tight spacing to promote straightness and high growth ring density, generally requiring trees to be thinned one or two times before the final harvest. Thinning is expensive, and the value of small-diameter trees is low in most regions, meaning that forest managers often cannot cover the thinning costs necessary to ensure their forests' health and profitability till the final harvest.

### Increasing Interest in Business and Research

Several whole timber structural product suppliers and fabricators have been established such as WholeTrees, TTT Products, Loggo, Forest Engineering and Economics Laboratory, Mobic SA, Balmer Systems and Twig&Bot. This demonstrates the market potential for the increased use of whole timber in high-value structural applications. These businesses have developed and marketed standardised prefabricated whole timber construction elements, such as floor and wall elements, beams, roof truss elements, space trusses, and foundation systems at relatively high production volumes, and the potential for significant scaling in the future (see Figure 1.1).

## Chapter 1. Material Properties of Raw Wood



Giudiceandrea2011

ImaxPro, Mobic 2019

Figure 1.1 – Existing advanced industrial workflows focus on wood manufacturing without integration of a design process, whereas research in architecture tries to bridge the technology and the integrated architectural design techniques.

### Embodied Energy in Raw Wood and Local-circular Economies

Raw wood fabrication and application are highly relevant in local circular economies. Locally-sawn-timber is the cheapest material, even including robotic cutting, as indicated in Figure 1.2 (left). Also, the available stock of timber is higher than its demand for timber construction. It is only efficient to use raw wood locally when the long-distance transportation is not required. Otherwise it is advised to rely on large timber industries that could offer engineered timber products. Whole-timber has a lower embodied CO<sub>2</sub> emission than dimensioned lumber because it requires a minimal processing. The lower embodied energy includes harvesting, transport and production. Therefore the use of raw wood is closely linked to its use in local-circular economies. Additionally, whole-timbers require much less energy to be processed into structural elements, as they do not need to be sawn or kiln-dried. Thus, raw wood has an even lower embodied carbon than conventional timber in the form of dimensioned lumber and can achieve equivalent structural performance with even less material. Using wood in construction has a positive impact on the carbon dioxide emission level as well [87]. Consequently, raw wood research becomes a part of a sustainable discourse when crooked timber is applied in architectural applications rather than sold as fuel or wasted.

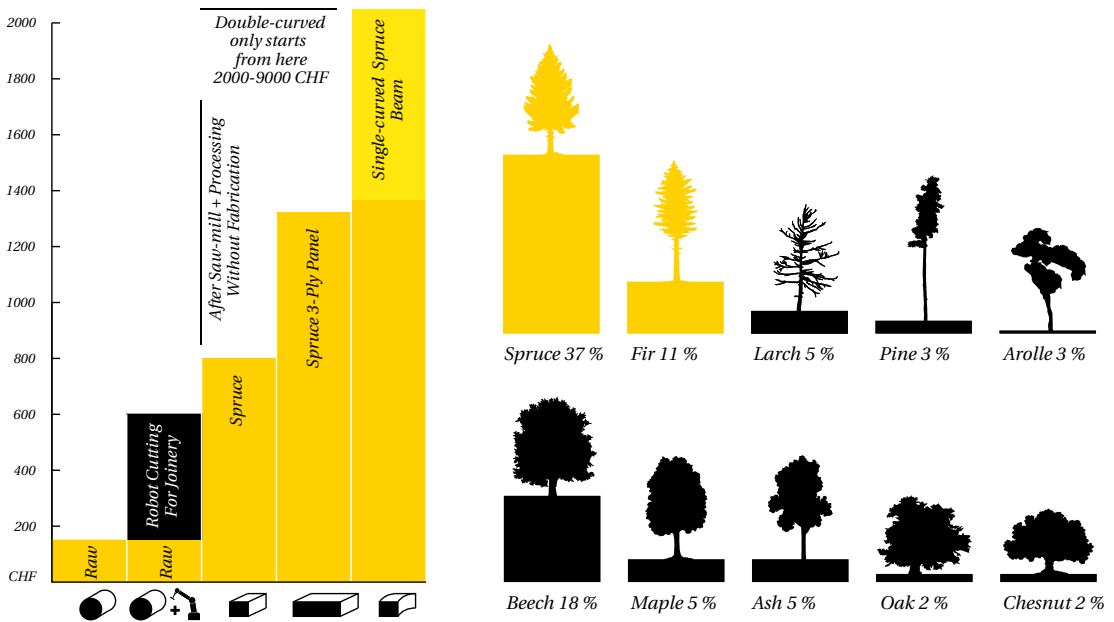


Figure 1.2 – Raw wood is the cheapest timber product, including robotic cutting, in comparison with 1 m<sup>3</sup> of regular lumber, engineered timber plates or glued laminated timber (left). The research employs two timber species: a) spruce, b) and fir. These two species are used due to the local collaboration with the publicly owned forest in Rossiniere (right). Spruce and fir are the two major types of wood available in the Swiss context (Lignum - Arguments Faveur du Bois, 2019).

### Structural Capacity

The wood micro-structure has an extremely high load-bearing capacity despite its low net weight (see Figure 1.3). Wood can support 14 times as much as steel, with far less manufacturing effort. Each stage of wood processing gives rise to a certain percentage of waste recovered as by-products (boards, squares, slats, wood energy). The size of waste depends on the diameter of the logs and the desired end sections. Several studies worldwide have identified small-diameter timbers' opportunity to be used as structural elements, requiring minimal processing and offering a high-market value to forest owners [28, 127, 180]. Raw wood fabrication requires highly skilled labour, as a result, sawing and planning timber still remains the general practice. Raw wood cannot be inspected in the same way as sawn wood, as it cannot be opened up to allow visual inspection of the wood, except of CT scanning.

Nevertheless, it has intrinsic advantages in fibre continuity. Knot defects are not relevant here comparing to sawn timber. Due to the growth of the tree, the grain in the trunk flows around the branches. There is no short-grain in a piece of raw wood. Thus raw wood is intrinsically stronger than sawn wood, but its properties are less well-defined [28]. The round wood is stronger because structural timber's strength is primarily governed by local fibre discontinuities around knots caused by sawing [180]. Sawing raw wood into a prismatic

## Chapter 1. Material Properties of Raw Wood

---

section cuts through the tree's grain while exposing the ends of the fibres gives a tree its strength. Round-wood also has a significantly higher cross-sectional area and section modulus than the largest sawn elements produced from them, as shown in Figure 1.3. According to the thesis of Aurimas Bukauskas [25, 26] the cross-section of a round timber has an area of 1.57 greater, and the moment of inertia is 2.35 times greater than the largest prismatic member derived from when considering perfect circular geometries. Finally, the regular section of raw trees is limited to a tree's taper, where the smallest end defines its largest section.

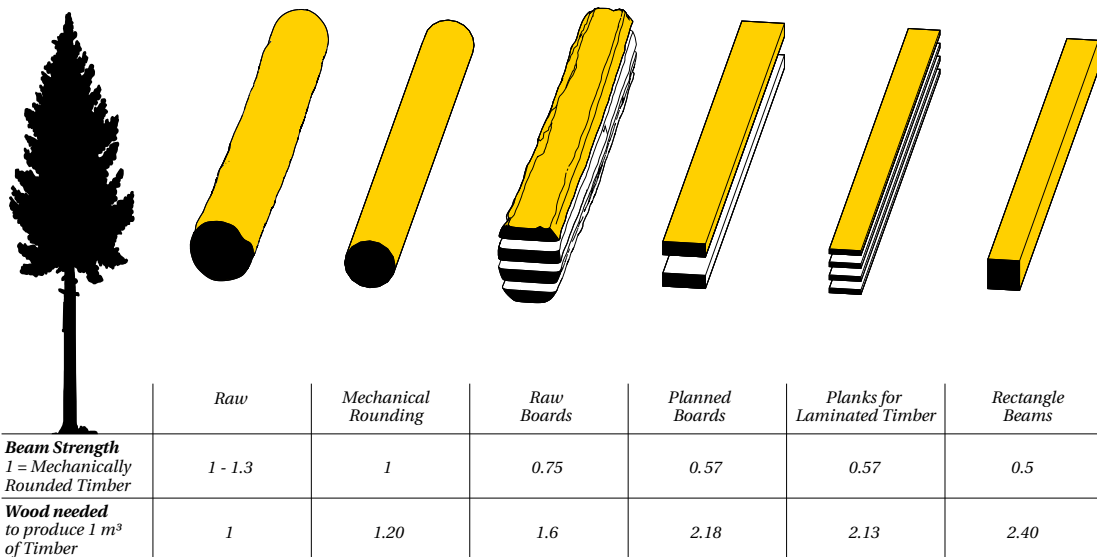


Figure 1.3 – Timber strength comparing to raw wood and processed timber (first line of the table), and number of trees needed to have the same volume of timber equal to the initial tree size (second line of the table, Lignum - Arguments Faveur du Bois, 2019).

## The Non-standard Production of Standardized Wood

Timber practices constitute an unnecessarily inefficient production circuit that moves from non-standard input (such as a tree) to standardised stock material (such as plywood or dimensional lumber and back to non-standard digital fabrication forms). Architectural complexity is often achieved through non-standard building components that are digitally defined and fabricated from standardised material [106, 144, 157]. Subtractive digital fabrication processes are commonly used to create complex components from homogenised wood products that have been glued together to ensure consistency [146]. While there are apparent reasons to standardise timber to ease fabrication and neglect fibre continuity, the non-standard building application might benefit from non-standard timber in its natural shape.

### Potential of Crooked Timber

The exploitation of bent and forked timber (see Figure 1.4) could reduce waste because such timber is not used in conventional construction [176]. The use of forks relates to an architectural effect on the natural occurrence of branch bifurcations and their implication in exposed structures, such as roof trusses. Such structural systems could be scaled from large pavilions to furniture, depending on a naturally grown tree radii. Most crooked timber or infested trees cannot be processed by regular sawmills and therefore are regarded as unsuitable for construction. Moreover, such timber is economically invaluable [189]. Crooked timber often ends up as firewood or perish without purpose while releasing carbon dioxide into the atmosphere. Currently, only around 35% of harvested timber is used in construction worldwide [126], when considering only straight tree trunks. Small-radii, curved or forked wood is discarded. If scanning and digital fabrication could be employed, such trees could constitute a valuable resource and present novel architectural and structural opportunities.



Figure 1.4 – Raw wood could be divided into three types by topological differences in shape (left): straight, bent (crooked) and bifurcated. Only central-axis and radial parameters are often used to work with irregular wood in CAD applications (right).

## 1.2 Swiss Context

Switzerland is covered in large mountain forests, and around 130 species of trees and shrubs are native to the country. Spruce is by far the most common tree species. More than a third of trees belong to this pine family. 10 million cubic metres of wood grow in the Swiss forests every year but only 5.2 million cubic metres are used in construction, energy, paper and wood-based composite production (see Figure 1.5). The timber industry mainly processes coniferous wood from spruce and fir. Deciduous wood only makes up 5% of production. About 60% of sawn timber comes from round and conical trunks. Forty percent of the residual timber is produced as a by-product in sawdust, wood shavings, wood chips, slabs and bark.

Per year, 3.04 million m<sup>3</sup> of wood is used for timber construction and wood-based products.

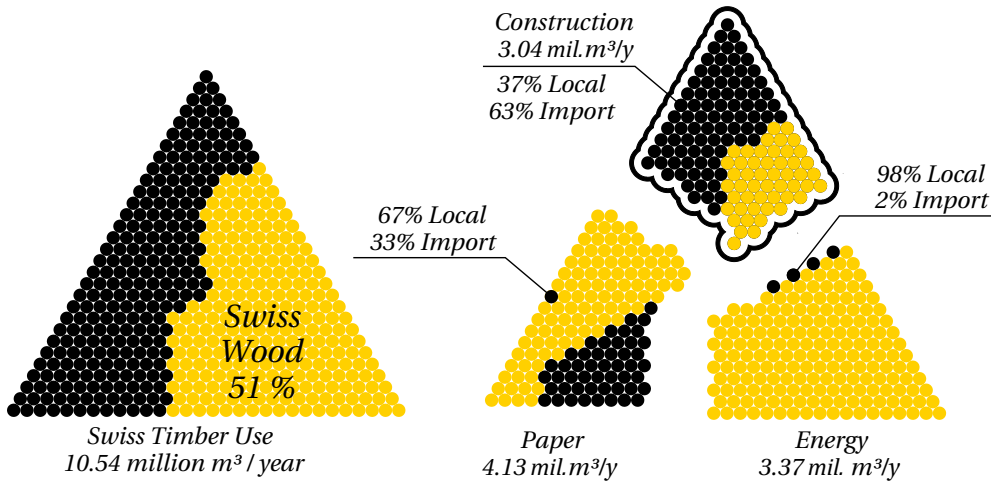


Figure 1.5 – Switzerland employs around 10 million cubic meters of wood per year. Around half of the timber is imported from the neighbour countries such as France, Austria, Germany (left figure, black dots). Timber use is divided into three parts (right): a) energy, b) paper industries, and c) construction. From the three parts, timber construction employs more than 63% of non-local wood, due to difficult mountain terrain. Lignum - Arguments Faveur du Bois, 2019.

More than 60% comes from abroad. The Swiss context is known for difficult mountain terrain, leading to timber import from neighbouring countries (see Figure 1.6). Timber harvested in the Swiss Alps relies on government subsidies, as cutting and selling no longer covers the labour costs. In addition to this, 15% of the annual harvest ( $0.72 \text{ million m}^3$ ) is exported in raw form for lower machining costs<sup>1 2</sup>. In other words, the timber is cut locally, and then is exported, and then gets sent back for Swiss construction as panels or regular lumber. In such a way, timber cost increase greatly without considering environmental issues caused by transportation, while relying on centralised post-processing factories abroad. As a consequence, in the past 10 years, the number of Swiss sawmills has fallen from around 600 to 220. The problem is two-fold: a) expensive harvesting process due to Alps, and b) the harvested timber is not exploited locally due to the lack of digital tools while relying on the manual processing techniques (see Figure 1.7).

<sup>1</sup><https://www.bafu.admin.ch/bafu/fr/home/themes/forets/publications-etudes/publications/annuaire-la-foret-et-le-bois-2020.html>

<sup>2</sup><https://www.bfh.ch/de/forschung/referenzprojekte/holzendverbrauch-schweiz/>

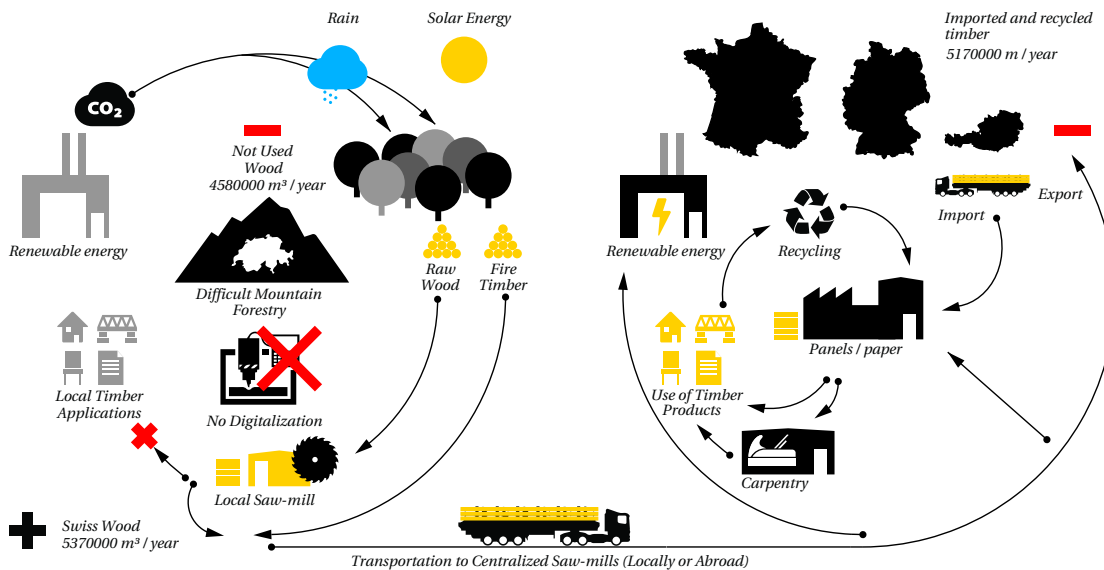


Figure 1.6 – Swiss mountain forestry has a three-level timber processing system: a) trees are harvested in the small mountain villages and minimally processed in the local saw mills, b) then timber is transported to a centralized saw mill for production of timber panels, glulams, wood products and paper, and c) raw-timber is largely exported, and the timber products are imported back.

The total Swiss timber use is divided into three categories: a) paper industry (4.13 million m<sup>3</sup>/year), b) energy (3.37 million m<sup>3</sup>/year), and c) construction and timber derived products (3.04 million m<sup>3</sup>/year). Import and local timber use vary greatly within these three parts: a) paper industry – 67% local and 33% import, b) energy industry – 98% local and 2% import, c) construction – 37% local and 63% import. The difference between import and local timber shows that crooked and small radius timber is largely employed for energy and paper industries that do not rely on import. The construction sector selects perfect straight wood, meaning that there is a potential to increase the local Swiss wood use by re-visiting timber that is unsuitable for construction. Consequently, an assumption is made that bent, bifurcation and small-radius timbers could be exploited for structural use rather than the raw biomass material for heating or cardboard.

## Chapter 1. Material Properties of Raw Wood

---



Figure 1.7 – Timber processing inventory in the local Swiss forest company Rossiniere. Wood-work is a labor-intensive process. The local processed timber is used locally only for decorative carpentry and small scale construction. For more information follow Appendix B.

## 2 Digital Fabrication Methods of Raw Wood

### 2.1 Scanning

Timber industries have been applying scanning methods to optimize tree growth and sawing techniques for straight timber. The industry is highly developed in terms of using advanced technology, such as CT scanning, 3D analysis, LIDAR and RADAR scanning, and customized sawing [7, 21, 35, 54, 58, 114, 125, 132, 152]. However, these techniques are only available at the scale of the saw mill or forest growth statistics. Since 2010 [44] there has been a growing number of experiments [7, 87, 104] in raw wood research that employ scanning techniques for structural form shaping with raw timber. The methods depend on an economic reasoning, SDK availability, scale, and the topology of a tree log, including small and large radii straight bent and bifurcated trees.

Environmental constraints and lumber processing costs demand a maximum quantity of every tree that enters a saw mill. One of the proven solutions is to employ laser surface and CT volumetric scanning. When the log is cut into semi-finished planks in the primary log optimization process, typically 3-4 scanners are mounted to capture the tree surface, while the logs are moving linearly on a thread-mill. The scan data is then interpreted in order to apply the most optimized cutting pattern. In the secondary plank optimization process, the scanning part is executed to get the maximum rectangular bounding area for each board. There are scanner models that take up to 3000 scans per second (LMI technologies). Speed of data acquisition is essential where the cutting process takes 70-300 planks per minute. The color scanning also helps identify defects such as knots, splits, rot, speck, beetle damage and leads to a so-called grade-based optimization.

The 3D scanning is necessary because of three points: a) each tree trunk is different (even straight), b) the design space has to consider these differences, and c) the timber fabrication requires to know the most accurate tree trunk position within the machining space. Therefore, it is necessary to collect the data about the real-world object (the tree) and possibly its appearance (the color). The collected data could reconstruct a 3D model or the low-level 3D representations, such as the central axis and radial parameters.

### Manual Measurement

Trees could be inspected, for a design, by manual measurement tools [104, 146, 175, 177]. The fabrication process could also be assisted by point-to-point measurement [94] or using Teach Pendant when XYZ coordinates are transferred to a digital model, e.g. 3 points could be taken to visualize a beam end.

### Markers and Tracking

Markers and positioning points could ease tree trunk fabrication if a 3d scan has already been performed. There are several possible solutions to position a log within a fabrication setup: (i) performing a second scan and aligning two clouds during design and then fabrication (ii) pre-drill dowel holes that matches machining setup [104] (iii) employ point tracking system i.e. (OptiTrack) [87]. The markers' location is determined by probing and matching reference features both found in the digital data-set and the actual raw woods. The marker system is a lightweight method that allows fast localization of the irregular tree trunks and 3D reorientation of the machining tool-path (see Figure 2.1).

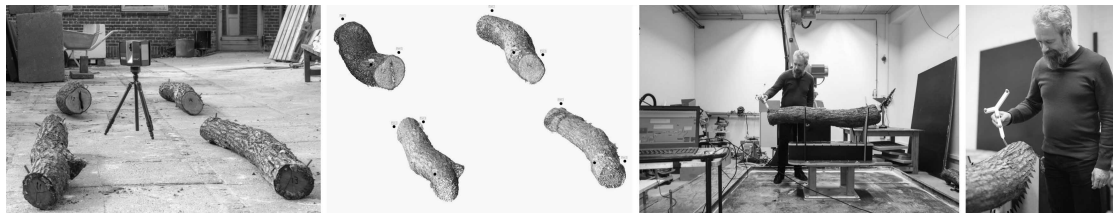


Figure 2.1 – Scanned logs are positioned in a fabrication setup using 3-point markers (Larsen, Agard [87] - Opti-track system).

### Photogrammetry

Photogrammetry is a recording method, measuring and interpreting photographic images to obtain a point cloud and a Mesh, usually with a texture data applied to Mesh vertex coordinates. The fundamental principle used by photogrammetry is triangulation. By taking photographs from at least two different locations, so-called “lines of sight” can be developed from each camera to get points on the object. These lines of sight are mathematically intersected to produce the 3-dimensional coordinates. Triangulation is also the principle used by theodolites for the coordinate measurement and it is how our eyes work together to perceive the depth of a space or object.

Digital models could be obtained by taking multiple photos with a relatively low-cost camera [175]. The downside of this method is that - it is a slow processing because of the manual process when taking multiple pictures and the long computation time (see Figure 2.2). However, it does not require expensive equipment by employing a standard camera or phone.

## 2.1. Scanning

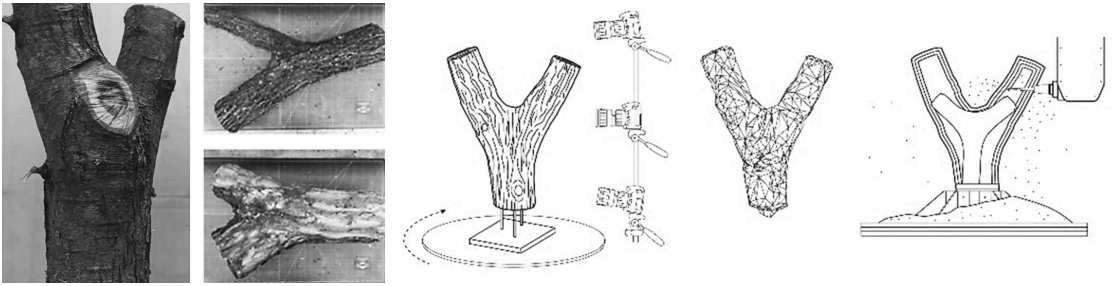


Figure 2.2 – Machining process of a tree fork to obtain a 3-valence connection element (project LIMB [175]).

Tree Fork Truss project [104] proposed a faster workflow by combining photographic images for a large set of forks and only scanning selected elements for the final design and fabrication. A photographic survey of 204 beech trees provided an approximate two-dimensional fork representations with enough detail to make informed decisions to cut trees. Following the harvesting of 25 trees, a second more detailed 3D-scan of each fork allowed the final truss configuration development. The 2D photographic survey could be relatively fast when tracing an outline and computing a central-axis [33]. A second longer scanning was needed to capture the pre-drilled holes for the fabrication and positioning (see Figure 2.3).

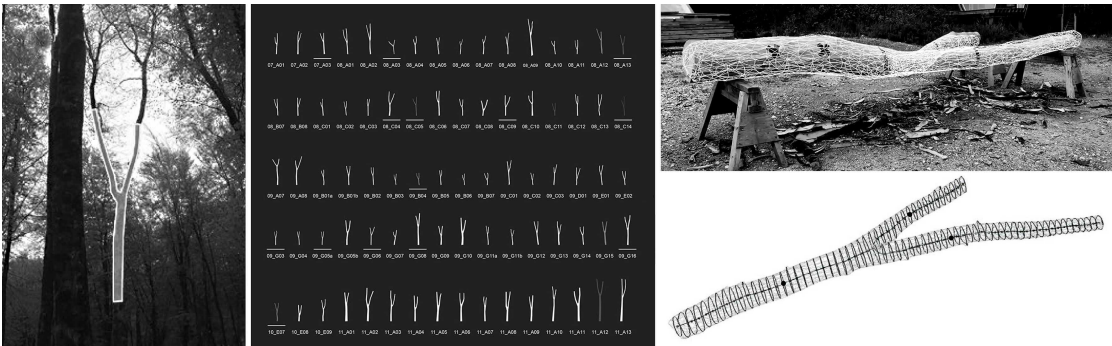


Figure 2.3 – A two stage scanning process: 2D photos were used for tracing an outline and a 2D skeletonization for a preliminary design stage of the fork selection (left), and the slower photogrammetry with the 3 reference points for the fabrication stage (right).

When a scanned object is relatively small (e.g. tree branches), it can be scanned using a rotary table, a camera, and ArUco markers. User manually rotates the table while the RGBD camera takes a series of images (50-100) [94]. This method is based on the existing open-source applications (truncated signed distance function (TSDF) Open3D or MeshLab) to create a point-cloud, mesh, and the remove the background. The following process is a skeleton extraction (see Figure 2.4). The skeleton is extracted from 2D Delaunay representation. Then, the central-axis is created by projecting the 2D skeleton to the mesh's top surface and shifting each point down by the local-radii. Finally, the whole shape of the branch is approximated as a generalized cylinder with circular cross-sections. This method works even if the Mesh is incomplete but applicable only to straight or bent beams.

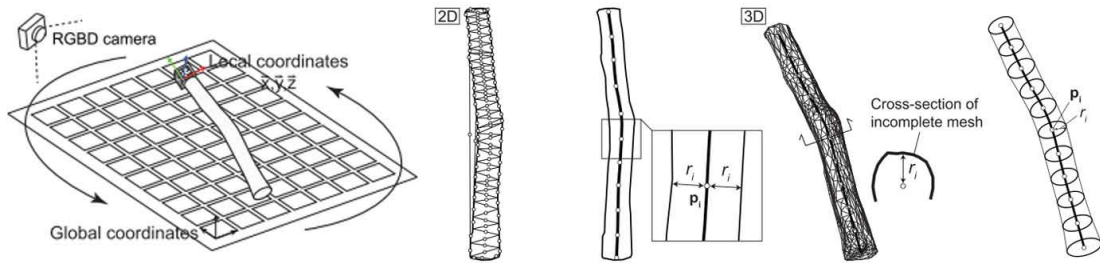


Figure 2.4 – A skeleton extraction based on 2D a Delaunay mesh Skeletonization, where a central-axis is projected to a 3D mesh [94].

Another approach employs a rotary system. The beam is rotated in small equal increments while multiple photos are taken by a camera [22]. Afterwards, the scanned geometry could be sectioned into a series of contour lines interpolated as circles and represented by a surface geometry. It is a low-tech DIY solution, but it helps to test the methodology with a minimal budget in the form of the architectural workshop and robotic training where a minimal number of raw wood beams can be fabricated for an educational use (see Figure 2.5).

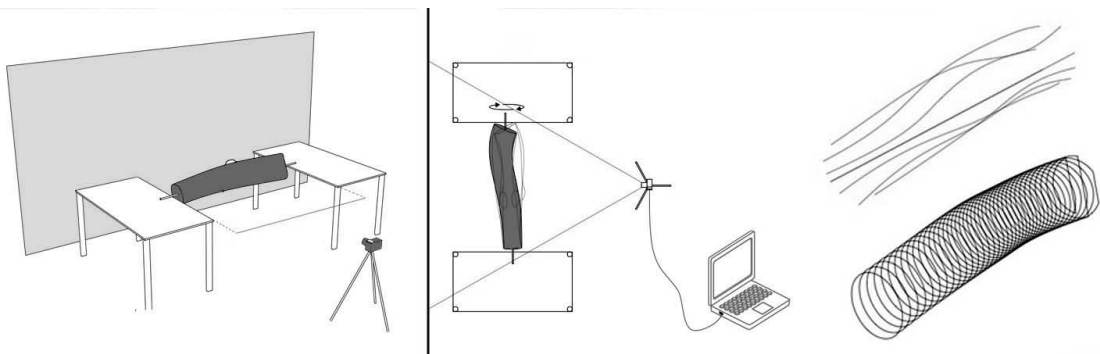


Figure 2.5 – A photogrammetry method for scanning a log while rotating it in small increments (*How to teach a robot to use a chainsaw?* | Robotic Fabrication Workshop @ IaaC | 2013 [22]).

### Structural Light Cameras

The structural light applications range from low-cost camera sensors (Kinect 360, Skanect 3D Scanning iPad Kit) to high-cost precise scanners (Artec). Structured light is the process of projecting a known pattern onto a scene. These patterns deform when striking surfaces for calculating the depth and surface information in the scene. One of the downsides of this type of scanner is that they are sensitive to the lighting conditions in a given environment. These sensors are also suitable for scanning trees, especially on a small scale, e.g. Conceptual Joining used Artec Eva structured light 3D scanner and Mesh with Artec Studio software [6]. Each fork had three markers on each flat end registered by the scanner as part of the texture. The mesh geometries were sectioned to obtain central axes by connecting co-parallel sections centres. These served as a geometric reference for matching the digital and the analogue models (see

Figure 2.6).

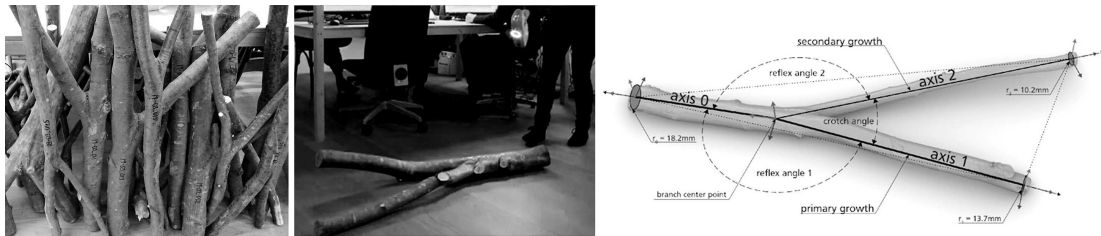


Figure 2.6 – The structural light scanner application for tree forks (Conceptual Joining [6]).

The key element in scanning applications, in general, is the software development kit (SDK). For instance, Kinect has found a way to academia [77, 177, 183, 189] and robotics (see Figure 2.7,2.8) since 2011. The software integration on windows computers was originally hacked, but Microsoft released an official free version due to an increasing user demand. The interest within users created a large community of open-source software applicable to architectural workflows, whereas most of the other tools are strictly licensed. It gave a possibility to incorporate depth sensing in existing applications with a relatively low cost and reliable software.

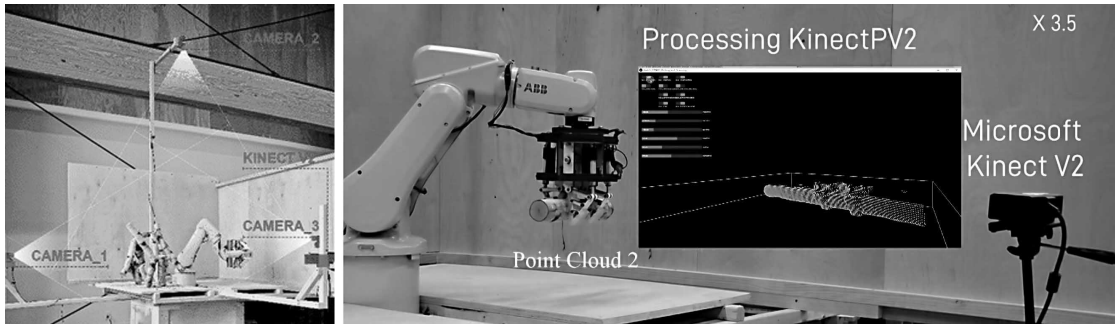


Figure 2.7 – Kinect application for estimating robot position for the assembly of irregular timber elements (RobArch 2018 Kaicong Wu [183]).



Figure 2.8 – Kinect scanning method applied outdoors and indoors. The point-clouds were sectioned and the sections were fit to circles to obtain the radii and the central-axis. (Biomass Boiler House - Design and Make, AA).

The Biomass Boiler House project at the Hooke Park tested the photographic record for a 2d curve extraction. However, the data was not precise enough for design and construction because most trees were curved in three dimensions. Instead, a Kinect gaming system sensor was used to 3D scan the trees and efficiently collect 3D geometric data. The scanning process

was executed by one person standing one or two meters away from the tree, rotating the scanner to capture the tree trunk (see Figure 2.8). The scanning positions were chosen to have a clear view of a trunk while avoiding overhead light coming through the canopy, as the Kinect sensor is sensitive to changing natural light. Therefore, further scans were made indoors. One hundred fifty-five trees were scanned in the forest and numbered, and another 110 trees were scanned indoors. The point-cloud alignment process was close to real-time when a scan was attached to the previous one after each iteration. Afterwards, the point cloud was meshed and sectioned to obtain radial parameters and central axes. A tree database was constructed using 3D models and a spreadsheet of tapering diameter, changing curvature, best sawing position, and maximum depth through physical and digital processes.

### Laser Scanning

Within the field of 3D object scanning, laser scanning (LIDAR) combines controlled steering of laser beams with a laser rangefinder. The most common form of laser rangefinder operates on the time of flight principle by sending a laser pulse in a narrow beam towards the object and measuring the time taken by the pulse to be reflected off the target and returned to the sender. Due to the high speed of light, this technique is not appropriate for high precision sub-millimetre measurements, where triangulation and other techniques are often used. By taking a distance measurement in every direction, the scanner rapidly captures the surface shape of objects, buildings and landscapes. Construction of a full 3D model involves combining multiple surface models obtained from different viewing angles, known as the point cloud registration process. This technology has already been successfully applied to scan parcels of forest, for example, in Kielder Water and Forest Park (UK) by ScanLAB [148] and a forest in Each Sussex by the Universal Assembly Unit. Also lower cost applications could be applied in fabrication process as shown in Figure 2.9.

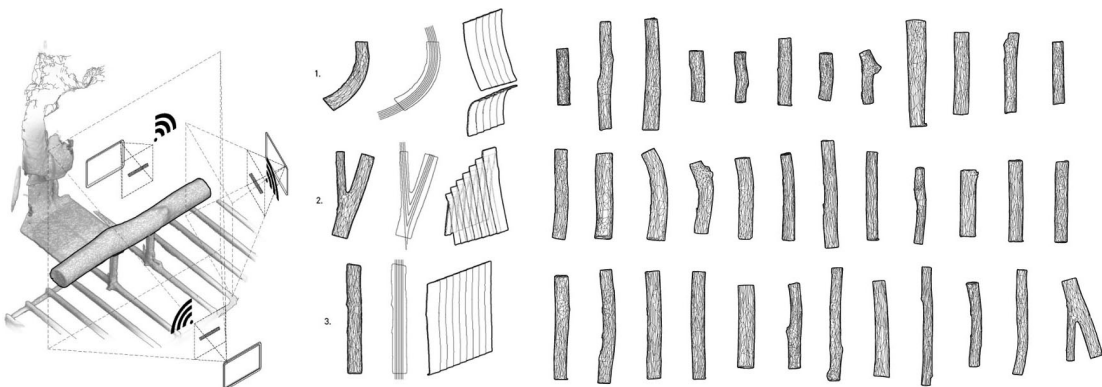


Figure 2.9 – Skanect 3D Scanning iPad Kit for robotic cutting (Zivkovic - Cornell University [189]).

The laser scanning could be used with a motion tracking system and the CAD application in Rhinoceros[138] together with custom made algorithms and plugins [87]. The digital

representation of a log was made by sectioning the point-cloud using the closest-point to plane method. Then projected points were ordered radially, and the boundary curve was constructed from the set of points. The surface representation of a log was made by connecting closed sections for NURBS. The centre points are connected sequentially to form the central-axis. The point-cloud processing output: a) central-axis, b) section curves, and c) a surface became the main parameters for fabrication and structural exploration (see Figure 2.10).

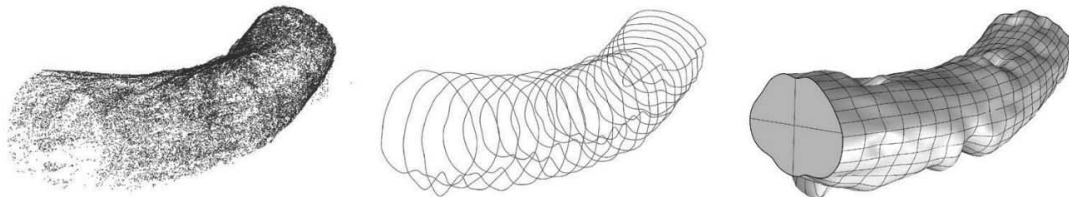


Figure 2.10 – Point-cloud processing of a tree laser scan (Larsen - Aarhus School of Architecture) [87].

### **Virtual Reality (VR)**

Virtual Reality (VR) applications are mostly used for guiding assembly sequence when projecting the digital models in real space. Additionally, it is possible to employ VR for tracing cutting outlines for manual cutting [6]. This was a low cost solution when digital fabrication was absent (see Figure 2.11). When using VR applications, a work-space and work-piece must be aligned together within the required tolerance to perform as much accurate fabrication as possible.



Figure 2.11 – Low cost virtual reality application for tracing cutting lines from a scanned model to physical one (Conceptual Joining [6]).

### **CT-Scans**

Modern saw mills employ advanced laser and CT scanning (see Figure 2.12). Scanning helps classify tree trunks, plan efficient sawing methods, and discard the ones that do not meet standards. The saw mill scanning data often have a full 3D representation of a log, including surface and interior volume, including tree knots. Additional information is also available, such as the type of wood, age, and the harvest location. This data could be shared in a web-based application to exploit disregarded trees, especially for a design use. These high-tech

## Chapter 2. Digital Fabrication Methods of Raw Wood

---

applications are much more optimized and advanced than previously mentioned but are hardly applicable in design-to-fabrication workflows due to the missing link between industry and structural design research with raw-timber due to the high cost and the data access. Furthermore, such data is lost when trees are processed into boards and rectangular beams, which is not the whole tree anymore. Lastly, such technology does not exist in the small scale saw mills due to the lack of collaboration between multiple small saw mills. Even if they can afford such an equipment they are too small in a larger Swiss context. Consequently, researchers are employing user-friendly scanning application focusing on the point-cloud processing rather than fast and robust industrial scanning for punctual single case studies.

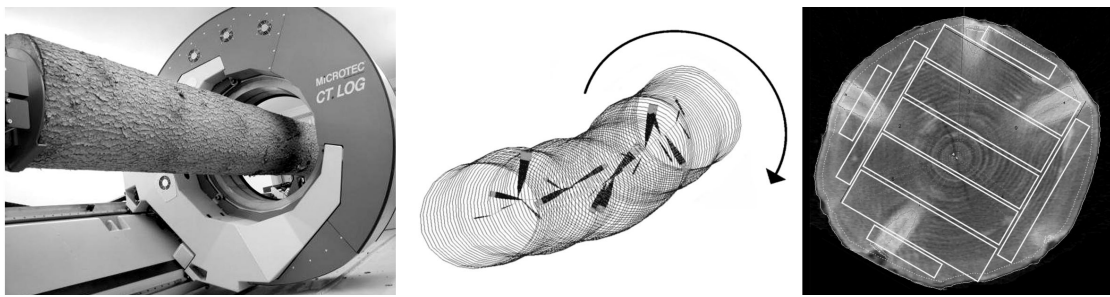


Figure 2.12 – CT-scanning to obtain the most optimal tree cutting pattern in a saw mill [58].

## 2.2 Connections

The most substantial reason for the renewed interest in raw wood structures seems to lie in manufacturing techniques. Newly developed digital tools are opening up unexpected possibilities for this material (see Figure 2.13), which, up until now, necessitated intricate manual skills, and were replaced by a more straight forward production methods. The new tools help draft geometrically complicated wooden joints that are no longer reliant on the elaborate manual techniques. Moreover, numerically-controlled machines (CNC and Robots) can mill every conceivable angle, to some extent, from a wooden element. Hence, the advancement in CAD-to-CAM application already enables design and fabrication for irregular timber shapes.

According to the Scanning chapter, raw wood has a standard minimal 3D representation: a) central-axis, and b) radial parameters along the axis of a tree. A connection geometry is positioned following this notation and subtracted using polygonal primitives. Such methodology could be called a Minimal Model for a faster digital representation and tool-path generation for wood-wood connections.

Raw wood connections could be classified by connection topology such as: a) side-to-side, b) top-to-side, c) top-to-top, and d) cross-halving. They often employ extra fasteners too. The following sections detail this grouping by reexamining existing projects made from irregular timber. While mechanical fasteners have become a standard practice for jointing timber assemblies due to their ease of use and predictable performance, research in robotic fabrication could explore the development of complex timber to timber connections inspired by the traditional Japanese joinery [167].

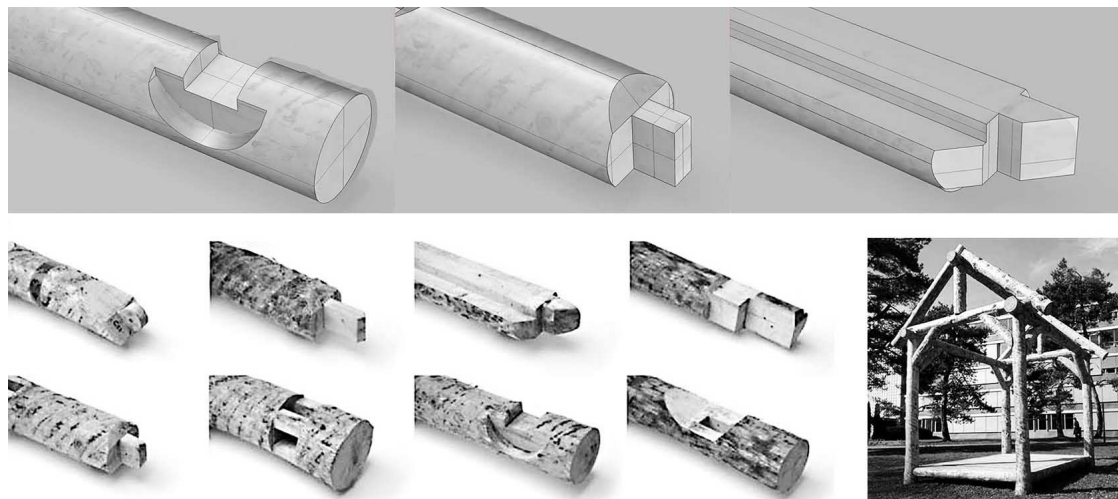


Figure 2.13 – Wood-wood connection in raw wood (7xCabin Constantinos Miltiadis and Tom Pawlofsky, CAAD, ETH Zurich [119]).

### Minimal Models

A common technique for defining joinery for irregular timbers is to create solid connection geometries; a pair of corresponding ‘subtraction volumes’ defined of each of the pair elements meeting at a given connection zone. In short, a joint is composed of a female and male element that must be machined from tree trunks. These subtraction volumes consist of geometric primitives, such as cuboids, cylinders, truncated cones and represents the wood material’s volume needed to be removed to obtain the connection surface[104].

The joinery volumes have to be scaled by a user-defined tolerance to compensate for the irregularity in the wood’s surface (see Figure 2.14). The fabrication tool-path has an extra cutting in the air to compensate for the inaccuracies between scanning and the digital 3D model. Another possibility would be to mill the whole round wood volume similar to the mechanical rounding procedure, but this takes an extended processing time [175]. Notably, the surface mesh or point-cloud data is not directly used to define the connection geometry. Consequently, only minimal information represents the connections both for the display and the fabrication.

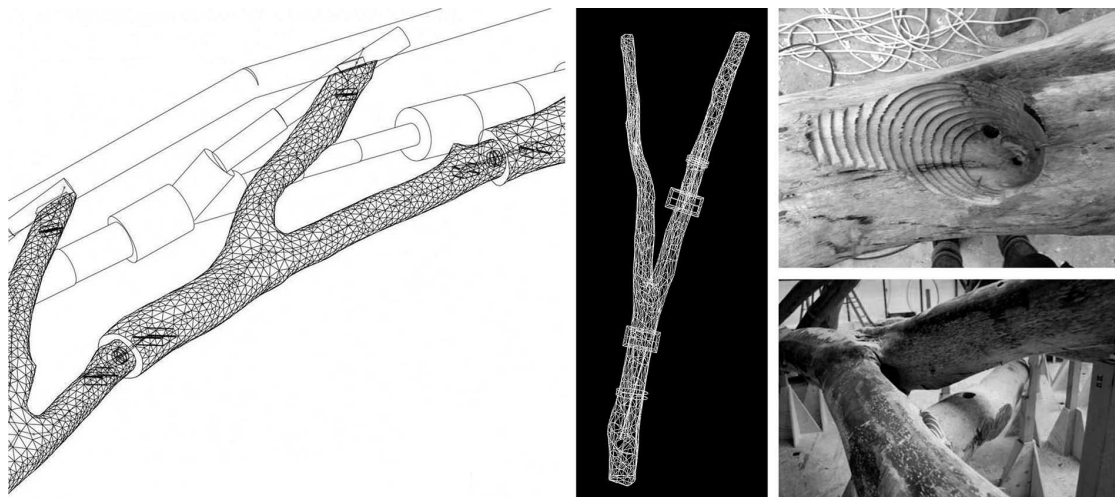


Figure 2.14 – Minimal solid representation of 3D scans are used for generating connections in irregular tree forks [146].

### Side-Side Joint

The side-to-side, also called end-to-end, joint is a connection following a grain orientation of wood. A scarf or a tenon-mortise joint is a classical connection that represents this category [104, 175]. These joints commonly have detachable fasteners such as dowels, keys, or bolts to reduce traction forces by compression and friction [6]. A scarf joint can have sub-types depending on the fabrication process, whether it is digital or manual. This type would only work when beams are near to a parallel orientation (see Figure 2.15). Overall, the side-side joints are used for extending parallel a beam length or form arches while relying on fasteners.



Figure 2.15 – End-end scarf joint exploration connected by a timber dowel and fabricated using an industrial robot (Conceptual Joining [6]).

### Top-side Joint

Top-to-side, also called side-to-end or T-joint, is often applied for in-plane nodes with a maximum available connection area. Depending on the assembly sequence, these joints may have sub-categories of a finger, a feather or a tenon-mortise. These joints could be applied for truss systems, Nexorades or Zollinger structures (see Figure 2.16). This connection type is often used when the connection zone is larger than 2/3 of a section [29]. Otherwise, it is possible to reduce beams eccentricities using bent crooked timber [87].

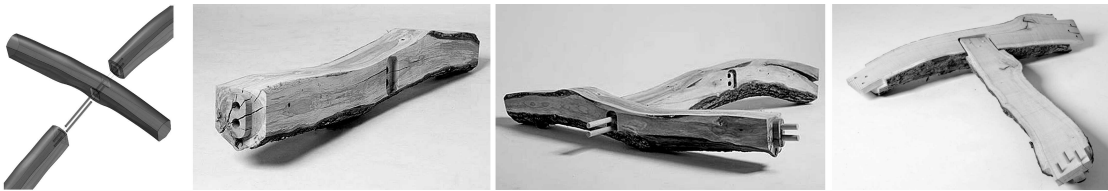


Figure 2.16 – T-joints connected using dowels (Larsen - Aarhus School of Architecture [87]).

### Top-top Joint

Top-to-top connection is a type of wood in which beams are flattened from longitudinal sides and stacked together. The same principle applies to vertical walls and slabs. The top-top joints follow a traditional cabin construction [177] that could be connected using packers placed along beam sides, and wood wedges could be used where large deviations occur between each beam. This principle is also interpreted in a free-form wall system exploiting bent wood at the AA Design and Make Boiler House as seen in Figure 2.17.



Figure 2.17 – Crooked timber connection using keys, wedges, packers and screws [177]).

### Cross Joint

The cross joints could be used for doubly curved discrete grid-shells, reciprocal structures [177], and planar assemblies, e.g. walls and slabs [185]. The geometries of cross joints are calculated at the intersection nodes of beam axes. The axes give the orientation of the joint by the local curve tangent. Each joint has to be customised to the skeleton intersection angle and the local radius. The cutting method often employs milling, and saw-blade processes (see Figure 2.18). Conical cross-lap joints ensure the insertion freedom and, at the same time does not block the timber assembly. Consequently, the joint can be tightened by the additional fasteners such as dowels, screws, or bar elements.

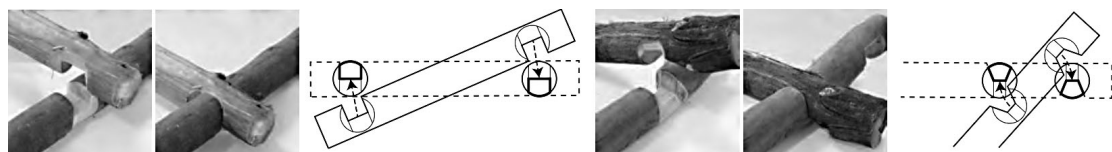


Figure 2.18 – Cuts of the orthogonal joint limit the assembly sequence, while the angled joints do not restrict the insertion. (Larsson - University of Tokyo [94]).

### Combined Joints

The combined joints category describes multi-valence timber connections, e.g. end-to-end and side-to-end meeting in one node. This joint is still a pair-wise connection with subtractive cuts located at the same intersection point. This method is commonly used by Japanese carpenters working with timber frame structures made from round section wood<sup>1</sup>. The digital fabrication methods allows to employ these joinery methods without the highly skilled craftsmanship when using robotic fabrication (see Figure 2.5).



Figure 2.19 – A joint combining a scarf and tenon-mortise connections in one node. The joint is fabricated using a robotic chain-saw (How to teach a robot to use a chainsaw? | Robotic Fabrication Workshop @ IaaC | 2013 [22]).

---

<sup>1</sup>Takenaka Carpentry Tools Museum

### Fasteners

Raw wood structures require additional fasteners ranging from timber dowels, screws, textile threads [79] to engineered metal plates. The thesis preference is to avoid the latter to rely mostly on wood-wood connections. The connections strategy is to maximise the transfer of forces through timber-to-timber bearing and to use additional elements to interlock elements by blocking the assembly sequence. For example, the plain scarf joints relies only on extra fasteners because wood-wood connections can only partially block the insertion. Each beam's end could have predrilled holes for timber dowels, metal screw, or dowel-nut fasteners [175]. The Tree Fork Truss project relies on metallic connectors for side-side and conic top-side joints. The ends of the beams are tied together using pair of steel bolts to transfer compression forces evenly. The top-side joint applies an oblique through-bolted mortise. The tenon connection employs planar 'seat' surfaces milled for smaller reinforced timber truss members and screwed together [146]. Furthermore, raw wood structures are similar to Bamboo system considering the round section. Hence, thread fasteners 2.20 could be equally used for small-radii timber similar to vegetal rods [79]. There is a broader range of metal connectors usually employed for beam systems [26]. The research question asks whether it is possible to use timber joints for at least pair-wise connections. Consequently, these examples focus a hybrid fastener and wood-wood connections.

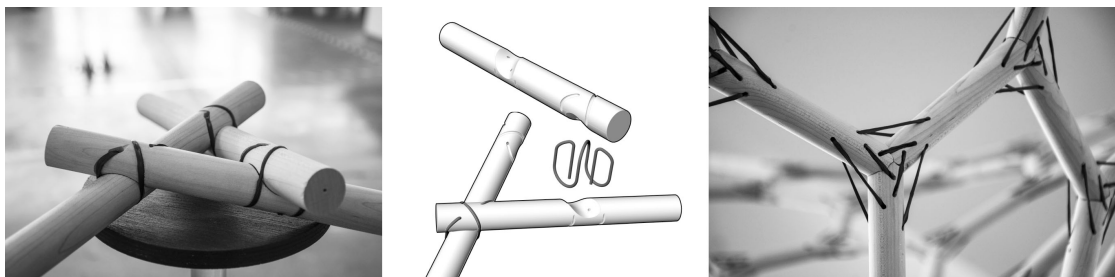


Figure 2.20 – Fibrous Timber Joints workshop in Smart Geometry 2018 by Dominga Garufi, Hans Jakob, Tobias Schwinn, Dylan Wood.

### Algorithmic Modelling of Wood-wood Joints

The discussed joinery types are categorised based on local observations noted between raw-timber projects. There is no standard algorithm or system that could help draft timber joinery for irregular woods. The joints are developed based on individual case studies only. The separated models lead to a time-intensive modelling process and manual tool-path generation. The absence of a strategic joinery algorithm does not allow reusing the proposed processes for other cases or building further research. The examples show the narrow scope of the wood-wood connection explorations. Consequently, it is necessary to advance on automatic connection joinery generation to ease both the CAD drafting process and to ensure safety during robotic CAM fabrication.

## 2.3 Digital Fabrication

Digital fabrication of raw wood is distinguished by two primary motives: a) to develop timber to timber connections rooted in carpentry traditions, and b) to explore performative manufacturing through analogue between robotic trajectories and human motion. This process is also related to a close collaboration between craftspeople, designers, engineers, roboteers and foresters by sharing knowledge within their specific domains [167].

Rules of digital fabrication emerge from the forms needed to be produced by each cutting tool. For example, a Japanese carpenter can create relatively complex joints from a series of planar cuts due to their pull-saw plane. Each cut in digital fabrication is governed by tool-head dimensions and machine reach-ability, as well as the size of components and joints, while a digital fabrication tool, e.g. CNC or robot, allows each saw to approach the work-piece in ways a human operator may not manage. The saw may still struggle through the cut due to their blades' geometric characteristics and kinematic motion limitations. Consequently, the hand-crafted and digital craft becomes a vital component of each research investigation.

### Manual Fabrication Informed by Digital Models

The Boiler House [177] demonstrates a non-digital fabrication process informed by digital models. There are five processes involved in the prefabrication: a) milling, b) chamfer cutting, c) drip cutting, d) relief grooving and e) debarking (see Figure 2.21).



Figure 2.21 – Fabrication process of the crooked round beams: bottom and top side flattening, edge chamfer, relief grooving, drip cutting and debarking (Biomass Boiler House [177]).

A mobile, modified band saw/chain-saw is designed to allow free movement for the curved top and bottom cuts. Additionally, a relief cut is designed to pre-release the pressure that reduces the wood's shrinking and seasoning. Drip cutting is needed to control the drying process by creating a cut along the beam using a disk saw. De-barking is required to prevent the tree's bark from catching water and nursing micro-organisms that rot logs. This methodology shows

that it is possible to transfer digital models through well-equipped work-shop tools that are not numerically controlled but instead rely on a craftsmanship skills-set.

#### Industrial Robot Arm

Industrial robot arms are the most common tools for raw wood cutting as it allows customized workflows to combine different cutting and vision tools. There are two possible approaches for fabricating an irregular tree object: (i) scanning before fabrication with marker placement for precise positioning [104] and (ii) scanning during fabrication to align the tool-path of an unknown object position in space. The first method rely on markers such as pre-drilled holes or point markers [87] that are picked up in the 3D-scanning process. They can be incorporated into the digital modelling processes and ultimately transferred back to the physical realm by being used as the supporting points when the fork component is mounted in the robot cell (see Figure 2.22).

Timber mounting setup seems to be an obvious and simple object to make. However, the design of a jig could help limit or even decalibrate the machining process. A good design of the setup follows a fluent fabrication process. If the complete surface milling is needed, the fixation has to be as minimal as possible (see Figure 2.31). While this allows maximum cutting area, the more extended parts could vibrate. Another method employs dowel and belt systems (see Figure 2.22) limiting the cutting area but resulting in a more stable and robust solution. An adjustable ‘trolley’ could be moved in 2-axis longitudinally, acting analogously to a 7th-axis rail and enabling the robot to access the various parts of the tree for fabrication.



Figure 2.22 – Robotic cutting using a 3-point positioning method, captured during the prior scanning process [146].

Raw wood cutting may require a set of customized tools atypical to traditional CNC machining, e.g. chain-saw cutting (see Figure 2.23). Equipping a robotic arm with an analogy tool means implementing the potential offered by traditional techniques. It helps to materialize the complexity of digital space derived from the lack of homogeneity of the material and its tolerances [189]. These workflows rely on skillful robotic integrators who can adapt stationary wood-working tools in timber work-shops, e.g. band-saw for automated robotic manufacturing typically mounted via Schunk adapters [87]. Traditional tools and techniques are hijacked, re-invented and applied as innovative processes for architecture. In converting these tools into end-effectors, their performance is altered. Consequently, through rigorous physical

## Chapter 2. Digital Fabrication Methods of Raw Wood

---

testing, the raw wood design strategies could ensure the digital transfer of the wood-working tradition [167].

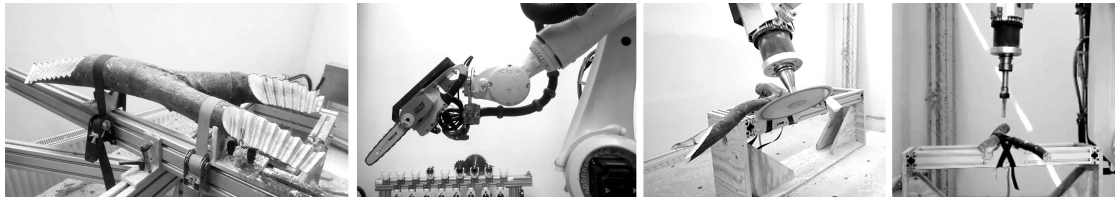


Figure 2.23 – The customized robotic workflow using a combination of a chain-saw, milling and saw-blade to find the most optimal fabrication method for the end-end connections (Conceptual Joining [6]).

The machining process of a chain-saw offers long cuts with nearly scrap-free results [119]. Most of such tools started as non-industrial timber applications in small-scale design, e.g. furniture, by integrating robotic tool-path applications in CAD/CAM software for architects and designers as shown in Figure 2.24.

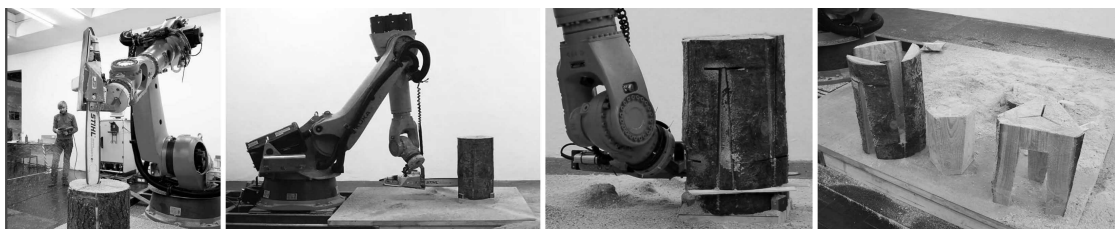


Figure 2.24 – Chain-saw robotic cutting for small scale design experiments that served as an art performance where stools were sold to the audience (7xStool Tom Pawlofsky, [119]).

Building on top of this knowledge, these experiments are often scaled up to timber frame structures at a scale of architectural work-shops within an academic environment. With a priority given to the gesture of cutting, timber's anisotropic nature may be neglected (see Figure 2.25). Such investigations would be rarely possible in the industry, as they do not necessarily bring an immediate profit, or they may take a long time without satisfactory results for future automation.



Figure 2.25 – The chainsaw application is applied for a round wood joinery experiments in the Robotic Fabrication Workshop at IaaC [119] .

Nevertheless, cultivating and implementing radical and innovative architectural production modes creates a new potential for prototyping and designing complex timber structures. In a human operator's hands, the chain-saw becomes a vigilant act of averaging out tool vibrations, whereas the robot produces imprecise cuts due to static movements resulting from the violent vibrations. The robotic fabrication may employ such a tool-set throughout resistance evaluation and adjustment of cutting speeds. It is necessary to note that the chain-saw was found to resonate up to 4 mm due to the arm's inflexibility and lack of damping [167]. These experiments may require human and robot collaboration where the unfinished timber needs to be finalized using hand-tools (see Figure 2.26).



Figure 2.26 – Chainsaw and bandsaw robotic movements, AA Design and Make [167].

A band-saw cutting is necessary for large timber biomass removal or curved cutting (see Figure 2.28). The device is similar to a hot-wire cutting method. It is composed from a large frame with two rotary elements. The saw could be broken fast due to torque and has to be replaced several times during prototyping. The band-saw end effector could employ a standard band-saw, reinforced with a welded steel frame, and mounted on the robot. The process allows for a high material efficiency due to the machining method as the band-saw has the smallest possible kerf of any mechanical woodcutting method. The technique is also explicitly not "subtractive", but trans-formative [77] (see Figure 2.29). The geometry generation methods could reconfigure a timber work-piece that is bent in one direction into a double curved surface. The custom band saw end-effector with a 25 mm blade could also be used for cutting raw wood into planks [189]. A robot can cut irregular tree logs into naturally curved boards of various shapes and varying thicknesses. The rest of the process stays the same: a) logs are positioned on a custom-built log-mounting system and b) then scanned in place to determine their position relative to the robot. The slicing process is relatively swift, with the robot moving at a cutting speed of an approximately 10 mm per second. The robotically-carved timber boards can be assembled into double-curvature surfaces by adjusting the cut thickness (see Figure 2.30). The curved boards or "lamellas" could also be cut using helical cuts [66]. Differently from the band-saw cutting method, a milling process is used for a large volume removal. This proposal concerns an attempt to bend lumber from a manufacturing processing using a collaborative robot (Robotmob-IMaxPro) that can move on a track. The robot can mill long linear elements using a linear movement. (see Figure 2.27).

## Chapter 2. Digital Fabrication Methods of Raw Wood

---



Figure 2.27 – Milling helical cuts while moving on a linear track (IMaxPro [66]).



Figure 2.28 – Band-saw cutting to obtain flat and curved sides of a beam (Larsen - Aarhus School of Architecture [87]).



Figure 2.29 – Band-saw board stripe cutting to form a double curved surface (Johns - IAAC [77]).

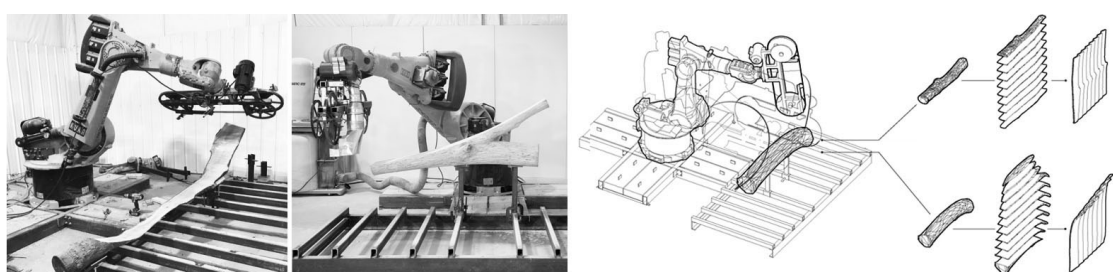


Figure 2.30 – Band-saw cutting for straight and curved planks (Zivkovic - Cornell University [189]).

#### CNC - 5-axis

The CNC machining is a rarer fabrication method for cutting raw wood because of its standardized use for timber plates, rectangular beams or glulams. The LIMB project [175] used a 5-axis CNC router to cut tree crotches to a custom timber shape. The design intent is to produce standardized nodal elements that can be joined quickly to connective strut elements. Using the CNC router, exact final angular and linear dimensions could be precisely attained within milling and cutting processes. The surface of volume milling has to be avoided as much as possible as the LIMB project required a 2-hour milling for each fork. Contrary, there are better applications for the local joinery cutting [146] to reduce the fabrication time. Finally, the machined parts have to be sealed to delay cracking and drying (see Figure 2.31).



Figure 2.31 – CNC machining process from a raw tree to a connection node (time required: 2 hours per one fork), project LIMB [175].

#### CNC - 3-axis

3-axis CNC cutting may be applied for simple design models that employ a 2D geometry representation with a shear transformation on a XY-plane. These machining applications are relatively low-cost compared to robots and the 5-axis CNC. However, this method is highly limited only to the milling process that can be slow. For example, a simple scarf joint may require multiple passes until a satisfactory result is achieved (see Figure 2.32) while it would take a few cuts using an automated saw-blade system. Such experiments show that the 5-axis cutting is necessary for the fabrication of most of the raw wood joints. However, several examples are employing such methodology because of the limited budget for research experiments.



Figure 2.32 – 3-axis CNC machining of a small scale tree branch, manually referenced for the machining setup (Conceptual Joining [6]).

Machining setup is another issue commonly addressed in the raw wood fabrication workflows because each raw wood shape is different within its shape. Moreover, the round surfaces do not have any reference points, unlike regular rectangular timber beams. The positioning solution ranges from pre-drilling reference points [146], Opti-Track system, point-cloud alignment [87] to audio-visual guided fabrication using ArUco markers. The latter employ manual positioning of a branch while trying to reach an approximate pitch and roll rotation. This setup also shows the difficulty in 2.5 axis machining because the branch has to be re-positioned for each joint fabricated within the same beam (see Figure 2.33).

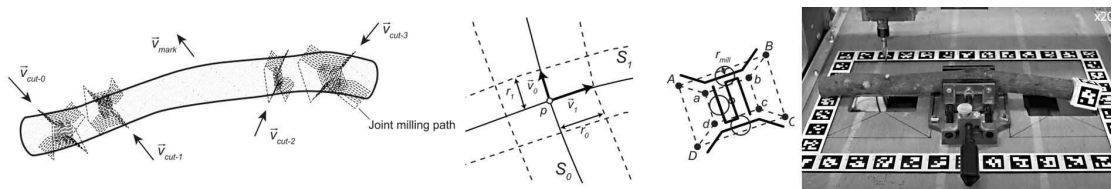


Figure 2.33 – An audio-visual guidance for the positioning of a tree branch within a 3 axis machining setup ((Larsson - University of Tokyo [94])).

## 2.4 Differences between Research and Industrial Applications

There is a difference between industrial applications and research for several reasons: a) scale of economic resources, b) large team working on one complex problem versus a single researcher, c) open-source applications versus closed commercial methods. The most vital point of research is the possibility to share (collaborate), and to build one's work on top of the current state-of-the-art. Existing industrial solutions (scanning+robotic cutting) for raw wood is not open-source and must be purchased for a specific robotic integration. It leads to methodology development by building research on the current state-of-the-art and research collaborations to challenge the current industrial methods.

Commercial practices employ raw wood based on economic reasoning: fast fabrication and cheap material. There is a lack of interest in a) local circular economies, b) sustainable solutions, and c) architectural design. Curved, Forked and small-radius trees are not considered as part of the industrial chain too. Companies employ only large straight raw wood fabrication, whether it is mechanically rounded or naturally grown. Enterprises such as Unilog / TTT, FEEL, WholeTrees, Balmer Systems and Mobic SA employ standardized and customized fabrication for mostly straight raw wood used for common timber products without facing the challenge to exploit low-value timber.

A steep learning curve needs to be considered to challenge this complex problem. It consists of 3 parts: a) scanning for design and machining, b) automatic joinery generation for unique timber elements, and c) fabrication for cutting free-form elements using a robotic arm. Furthermore, it is necessary to achieve an equal or similar technological level to other research institutes, meaning the robotic installation, calibration, hardware control, and overall

workflow development takes a significant amount of time. Afterwards, a design methodology could be tested by technical experiments and architectural case studies.

In summary, industrial companies exploit straight timber, while researchers consider irregular and small-radii timber as a potential timber product for bespoke timber structures. Current timber joinery algorithms need to be explored further because there are no raw wood fabrication methods available in commercial software. Finally, research must develop a level of control and understanding to customize digital tools to bridge architectural design methods and technology to scan and cut a tree.

## 2.5 Stock Assignment

The assignment problem of tree trunks is a fundamental combinatorial optimization problem. The number of trees must be assigned to only one design target. Any beam could be assigned to any target curve; however the assignment has a cost depending on how well the beam fits, and depending on the curvature, length, radii and fork parameters. If all solutions are tested, the search space becomes n-factorial. Therefore, alternative methods are often proposed. For example, a meta-heuristic process could be implemented to find an appropriate solution through partial search. Evolutionary Solver Galapagos [141] is used to assign the forks locations sequentially based on a local sorting of geometric similarity in Tree Fork Truss project [146]. Alternatively, combinatoric optimization using Hungarian algorithm could be applied for a Nedorade structure [94]. These methods are detailed in the following subsections.

### Genetic Algorithms

Genetic algorithms could be combined with user interfaces to explore and breed the design outputs. Within a genetic algorithm's cyclic structure, such an approach incorporates parametric geometry generation, simulation for performance evaluation, and the ability to sort and compare a wide range of solutions based on single or multiple objectives. The results can be visually compared by teams of designers across a graphic web interface that includes the potential for human interaction. For example, ParaGen [174] application is employed to allow designers to explore the LIMB project's solution space. The fork sorting is based on the smallest bifurcation angle, and the assignment rule followed a notation of SRSS (Square Root of Sums of Square) of angle differences between the digital and real joint [175]. Another method proposes a 2D axial sorting according to an axial curvature, and an iterative surface fitting method to form continuous curves [177]. The fitting stock curves to a predefined surface does not give good results due to the curvature differences between the given form and the available pieces. The curve-end tangent fitting produces many discrete combinations, but these curves do not form a continuous surface. Therefore, a combined strategy is proposed considering both goals in an iterative process. The process first identifies critical sections of a surface, and then the assignment is started to find the other suitable tree segments. Similar beams help to reduce the search when only one tree is used from each of a given section.

### **Clustering**

Grouping method is proposed by applying a clustering algorithm [6] to reduce the variability of parts. A clustering method groups the forks' catalogue in several types according to geometric similarities, e.g. dimensions of each branch and its average crotch angle. Besides clustering geometries, the algorithm also returns one "proto-part" for each cluster, generated as the average of the geometric features of the parts contained in the respective cluster. These "proto-parts" are then used to generate and aggregate structure applying a plane-to-plane transformation, according to the predefined connectivity rules [140].

### **Combinatoric Optimization**

The assignment of timber beams could be made by minimizing the sum of cost values considering how well a central axis fits digital analogue axes by employing the Hungarian Algorithm [94]. The goal is to match branches to target curves by searching for every branch's best pose to every target and calculating the cost as the difference between them. Two criteria could be used for the matching routine: (i) the curves' directions should be aligned and (ii) the strongest curvatures should lie in the same plane. This match results in (i) the intersection point between curves, and (ii) a plane in the strongest curvature of the branch. The differences between a skeleton and the target curve could be evaluated at several points on the target curve. The cost for every pair of target curves and branches is computed to obtain a matrix to search for the lowest costs for the possible alignments. The assignment may result in misalignment between target design and stock. Therefore, a force-guided relaxation could be employed to adjust the positions and orientations of branches to ensure the connection area.

### **Manual Assignment**

Such design frameworks must have a well-defined and narrow search space to produce valuable results, and it is advisable to start the problem formulation by manual modelling process (digital or physical) to understand the rule-set of assignment [104]. The overall stock fitting workflow starts from an intended design that could have several variations. For instance, a truss system connection nodes might differ depending on the connecting beam angles, or the global surface might vary depending on crooked beam curvature. Then a selection of elements from the stock is made. Finally, the intended design is adapted based on the tree trunk selection. If the assigned elements do not fully match the design intention, a dynamic relaxation could be performed to reduce axial eccentricities. Hence, the overall stock design process often relies on an initial sketch that must be flexible enough, or close enough to the final result to perform the optimization algorithms.

# **3 Architectural Design Methods using Raw Wood**

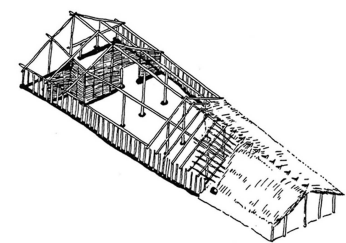
## **3.1 Historical Record**

Minimally processed timber has been used as a load-bearing element in structures since at least as early as the Neolithic period [53]. Numerous examples of architecture by pre-industrial societies worldwide show the variety and ingenuity with which cultures have taken advantage of timber's inherent structural characteristics to create buildings, bridges, and fortifications. Particularly notable examples are the actively-bent longhouse frames of the Iroquois [86], the grid shell-like Fale (thatched hut) of pre-colonial Samoa and Tonga [15], the log-type churches of pre-industrial Russia and Europe and their half-lap joinery [47], and the timber arch bridges of Song-dynasty China [188] also known as Nexorades. Whole-timber was also used on a massive scale during industrialization in forested regions worldwide. Also, raw wood was used in the building of bridges and various temporary structures that expanded in road and railway networks of the Pacific Northwest of the United States. As shown in Figure 3.1, engineers in these areas used abundantly available timber as combined foundation piles and above-ground load-bearing elements, rapidly erecting large bridges and viaducts at low-cost [78].

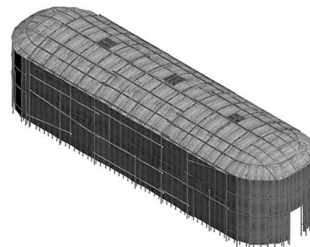
Historical precedents of the irregular tree use in wood structures could be found in both 17th-century framing for naval vessels [14, 117], and joinery in timber barn construction. In need of non-linear components, shipbuilders selected appropriate trees based on the geometric form of wood and their fibre direction's strength. Boat builders could construct stronger vessels [101] by aligning the grains of tree branches that grew in response to specific external loads. The historical record (see Figure 3.2) shows that the craftsmanship of ships and building was tightly intertwined. For example, the cupola of churches followed the construction of ship hulls [103]. These structures offered joinery following the grain direction and topology of trees (forks, bent and straight elements), side-by-side connected boards and beams [81], and forming side-end connection [37]. The irregularity of trees was explored to build vaulted structures by stacking elements or constructing frame-structures using wood-wood connections inherent in the traditional shipbuilding techniques.

## Chapter 3. Architectural Design Methods using Raw Wood

---



The Reconstruction of the Danubian Neolithic House [Foundation2013]



Neolithic Settlements [Kvetina2013].



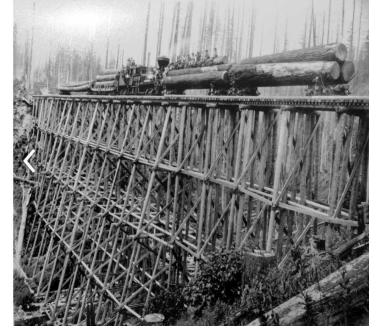
From Tongan meeting house to Samoan chapel [Barnes2008].



Historic Wooden Architecture in Europe and Russia [Khodakovskiy2015]

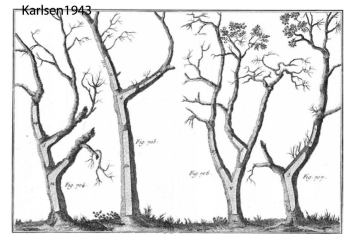


China's unique woven timber arch bridges [Zhou 2018]

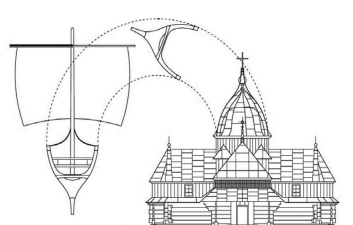


Cedar River Trestle Bridge [Kinsley1925]

Figure 3.1 – Historical record of the straight raw wood use in building construction.



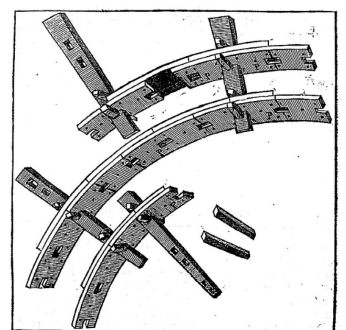
Encyclopédie méthodique: Marine. Panckoucke. 1786 [Encyclopédie1786]



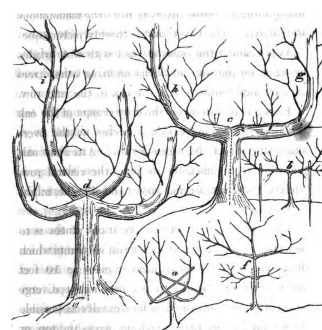
Wooden Domes. History and Modern Times. [Misztal2017]



Brunnen Family XiX c. Turtmannthal, Valais. [Brunnen]



Illustrations de Nouvelles inventions pour bien bastir et a petits frais. [Delorme1561]



On Naval Timber and Arboriculture. [Matthew1831]



Kurs dieriewiannych konstrukcij cz. I i II [Karlsen1943]

Figure 3.2 – Historical record of the raw wood use including straight, forked and bent beams.

### 3.2. Applications using Straight Wood

Later developments of inexpensive timber fasteners and mechanization of timber processing led to straight timber use only. While commercial applications focus on simple linear repetitive prefabricated systems, there is an emerging type of structures based on bent and forked raw wood. The topology difference of trees widens the scope of applicability of locally sawn wood by embracing their inherent qualities. Crooked wood exploration led to new structural applications absent in structures from straight timber. Accordingly, the following classification follows the raw wood topology.

## 3.2 Applications using Straight Wood

### Slab and Wall

A slab made from raw wood follows a design principle of stacking beams side-by-side. The method dates back to a primitive hut [142], driven by an economic reason to produce low-cost structural settlements for mass production (see Figure 3.3). Beams could be joined together using timber joints (grooves), keys and tensioned by cables [16]. Additionally, slab and walls could be used in standardized timber construction for the mid-rise buildings [17]. Such a system could be made from a relatively small radii tree varying 15-20 cm in diameter, de-barked, untreated with a water content of not more than 15%. Additionally, composite applications are employing half-cut round-wood in combination with steel connectors [182]. A wooden floor also requires a joisting and decking to ensure horizontal bracing [30]. Furthermore, there are several composite applications of raw wood, and concrete [68, 151]. In addition to this, several studies focused on bridge decks made from low-cost timber [24, 121, 139]. Lastly, there are multiple raw wood and timber plates applications, including patents [118, 165], and commercial products such as Loggo. Thus, slabs and walls made from freshly cut trees have to integrate more extensive detailing by largely transforming timber natural form into regularized construction elements while considering the current construction requirements.

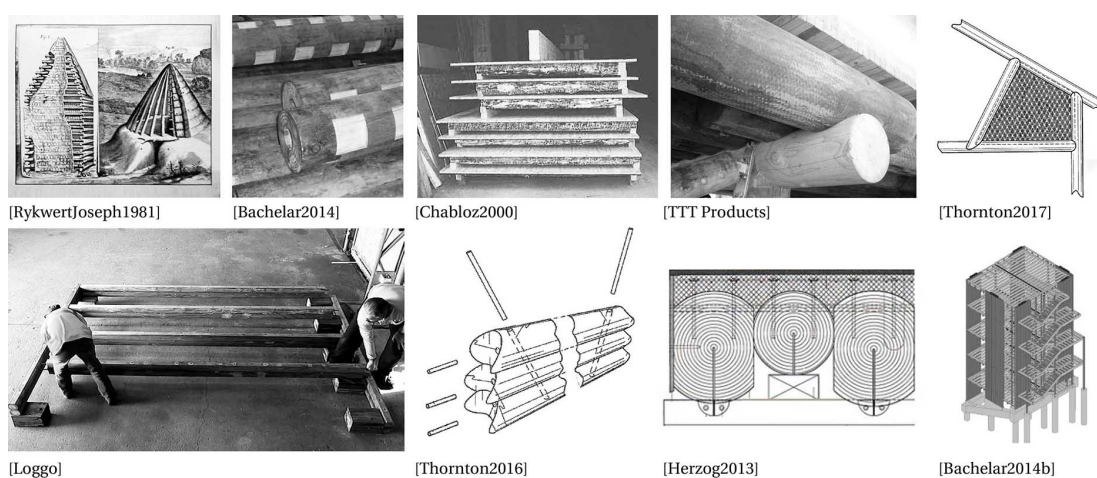


Figure 3.3 – Existing slab systems are mainly focused for the mass production market.

## Chapter 3. Architectural Design Methods using Raw Wood

### Frames

The timber frame buildings are formed using small-radii trees, known as tree thinning for a low-rise small-scale housing. The tradition focuses on a harvested timber topology, and local carpentry knowledge [88]. These structures are made from naturally curved trees, split down its length with the two mirroring halves joined at the peak, called “crucks”. Pairs of crucks are then joined together to form a primitive frame. The addition of a collar or tie beam forms the A shape, giving the cruck frame its strength and stability. Raw wood thinning is a plentiful and inexpensive resource in many parts of the world, generally destined for the low-grade applications such as pulping, board production or fuel but could be applied for small-scale frame structures as well [97]. Raw wood thinning is commonly used for bending active frame structures in research [28, 79] and practice<sup>1</sup>. Industrial applications rely on mechanical fasteners that could be employed with minimal carpentry knowledge. Furthermore, steel connectors are used to join mechanically rounded timbers [109] to design portal frame structures for the mass prefabricated building systems. TTT Products Ltd developed the technology to lathe 15 m long poles into Unilog - up to 480 mm in diameter - that are joined using Sleeve connectors rolled from 3-4 mm Steel. AA Hooke Park developed a Tension joint made of a steel rod embedded in epoxy and placed into the timber's stepped drilled hole. Hence, the construction methods require good carpentry skills to benefit from locally sourced timber and to develop an industrial methodology to unify timber and apply industrial connection methods taken from traditional steel structures.



Figure 3.4 – Raw wood frame structures constructed using joints that varies from industrialized metal connectors to wood-wood connections.

<sup>1</sup><http://richardkroekerdesign.com/pictou-landing-health-center.html>

### 3.2. Applications using Straight Wood

#### Truss

Most raw wood truss systems relies on steel connections<sup>2,3,4</sup> because of complex nodes when multiple beams meet at the same point (valence larger than two)[36, 45, 48, 72, 73, 91, 180, 187]. A tree trunk is used as a linear beam element interconnected side-to-end. Trusses show a structural advantage of raw wood by exploiting a maximum use of timber biomass. In general, the design of the easily fabricated metal connectors is emphasized to assemble many similar beam elements, even though the sustainability and ease of manufacturing are questionable. The wooden trusses are applied in bridge structures as well [4, 181]. Another option would be to form a Vierendeel truss to avoid the complex metal connectors [104]. Additionally, there are methods to connect multiple timbers to form tree-shaped columns [25, 36]. Other techniques focus on hybrid timber, and steel connections [62] to ease the fabrication and assembly. Minimal steel connectors were also used in the Lausanne observation tower by Julius Natterer [111]. Therefore, it is hardly possible to employ only wood-wood connections for large-span structures made from raw timber considering the multi-valence truss nodes (see Figure 3.5).

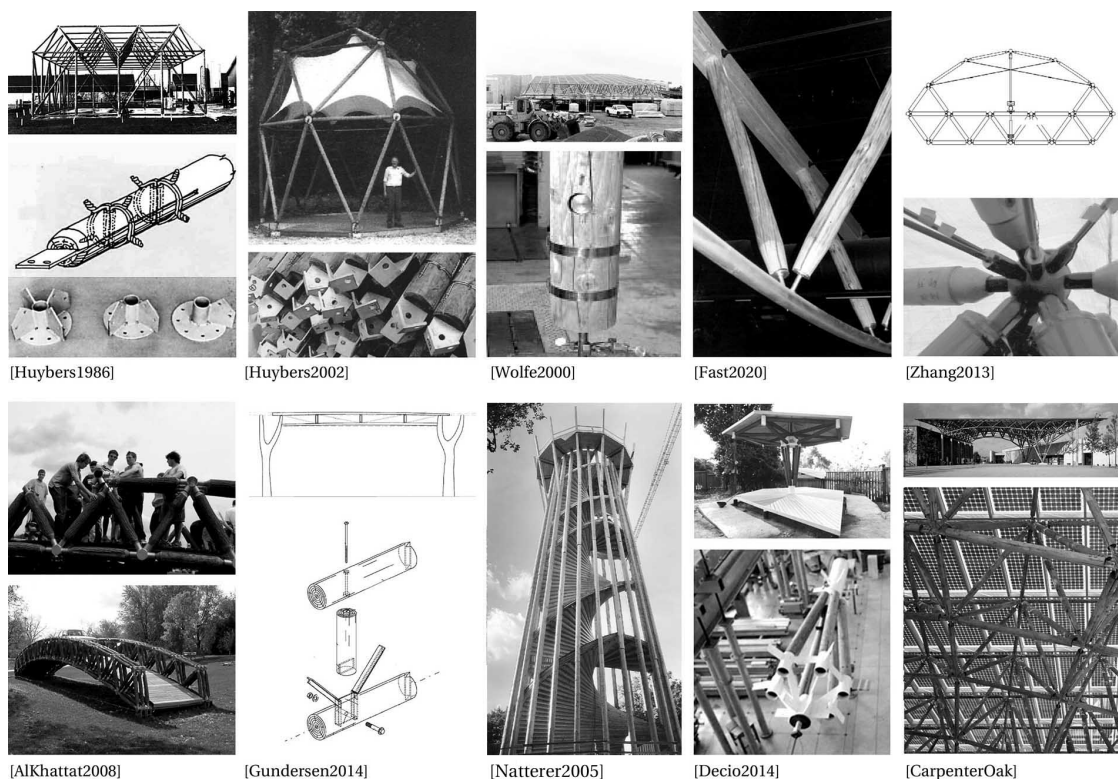


Figure 3.5 – Trusses from raw wood are mainly composed from steel connectors and mechanically rounded timber.

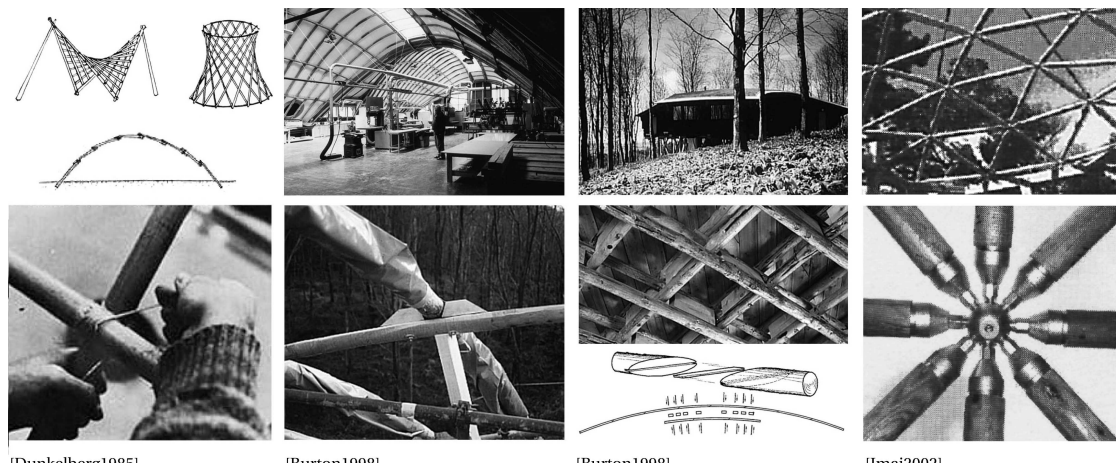
<sup>2</sup><https://wholetrees.com/portfolio-item/festival-foods-grocery-store/>

<sup>3</sup><https://www.nattererbcn.com/index.php/tuerme>

<sup>4</sup><https://carpenteroak.com/projects/solar-canopy-the-earth-centre/>

### Grid-shells

There are two distinct topologies of grid-shells applied in raw wood: a) nodal systems similar to trusses and b) bending-active structures. There are applications both in roofs of single and double-layer grid-shells [28, 57, 74]. The bending-active structures are highly inspired by Bamboo structures, also known as Vegetal Rods [79]. Particular details have to be developed due to variability in cross-section, as the dimensions at any particular node point cannot be known precisely. A grid-shell connection was proposed, which uses a fixed wedge, an adjustable wedge, and a clamping strap [28]. This joint accommodates the shell's accurate geometry, the unknown cross-section of the arch members, and the need to transfer force through the joint. It was found that bending raw trees has a relatively small curvature limit - they break over far enough at the top, in the crown of grid-shell arch. A solution was made for slicing timbers at the base to distribute the stress of bending. Another consideration is the roof cover of grid-shells that must have flexibility in their design to adapt to differences in raw wood. The most labor-intensive part of such grid-shells is the membrane and detailing of windows and doors. This work requires skilled carpenters and well-defined digital fabrication workflow. Another point of raw wood grid-shells is the continuity of timbers. Westminster Lodge's project employs a scarf joint with a tongue to achieve a reliable and straightforward timber joint (see Figure 3.6). In addition to this, blocking pieces were used to generate a shear connection between the top and bottom layers. Past and current Hooke Park examples broke the ground for new applications in raw wood and show that it is possible to develop a cost-effective and low-tech joinery solutions for the unique building topologies. It is not possible to predict every peculiarity of the natural material, but it constitutes that small-radii construction is feasible.



[Dunkelberg1985]

[Burton1998]

[Burton1998]

[Imai2002]

Figure 3.6 – Grid-shells are made from small-radii raw wood varying from the bending-active structures to nodal systems.

#### Nexorades

Nexorade structures (Reciprocal) from whole timber date back to the ancient Chinese construction method of woven bridges such as Rainbow Bridge. In Nexorades, beam elements mutually support each other as a load-bearing system. The configuration of reciprocal frames simplifies the construction system because only two members are connected at each node, instead of multiple beams such as space-frames or trusses. As a result, the fabrication of such nodes is more easily manufactured due to the low-valence connectivity. Beam elements are often identical or similar in length, and cross-section is achieved by cutting timber joinery to remove the raw wood variability.

The reciprocal framework is controlled by several parameters: eccentricity, engagement length, rotational direction, cross-section, length of a bar, and excess length. The geometrical definition of such structures has recursive behaviour in the overall structure and its final form. The smaller the radius of that window, the higher the curvature is. The bar thickness directly influences the eccentricity, while the length of an element influences the density of the structure. If higher curvature is needed, it typically leads to shorter members. Additionally, the elements need to have an excess length to form a cross-lap joint that can also affect the structural behaviour.

There are several reasons why reciprocal structures reappeared in the raw wood construction. Firstly, sustainability awareness leads to rediscovering raw wood and to re-examining the past historical examples, instead of preserving the modern material such as steel and concrete. Secondly, numeric fabrication helps to cut custom traditional timber joints without the slow and highly skilled carpenter knowledge. Thirdly, simple wooden elements can encourage ideas for cost-effective free-form structures. They are also potentially interesting where the construction speed is required, and geographical or logistical conditions are challenging. Moreover, Nexorades employ short elements that could re-employ hard wood that has little value in the current timber construction. Furthermore, reciprocal patterns have aesthetical advantage due to various possible ornamental patterns.

Since Nexorades have only one type of joint, the fabrication of beam elements could be automated. The technology to cut elements varies from hand-crafted timber joints fastened by threads or steel bars, to robotic and CNC manufacturing. Since the raw wood variability requires cutting into a timber section, the design process is less restricted than elements in equal sections. For instance, beams have an interval of maximum allowed section removal rather than one possible position. Besides Platonic objects and planar or circular tilings, no theoretical results have been found for form-finding of Nexorades because the non-linear solvers do not provide certainty about their output besides a minimal understanding, considering the surface curvature, beam size, and arrangement properties using translation or rotation methods. Furthermore, Nexorades are not structurally efficient as free-form space-frames or grid-shells due to a low node valence and structural redundancy, but they have simple connection details.

### Chapter 3. Architectural Design Methods using Raw Wood

Tetsuro Kurokawa began using cedar, a cypress solid-wood tree trunks in so-called skeleton log construction, allowing the erection of wide-spanning structures using short raw wood members. The construction technique requires a low degree of processing with minor residual wood because the timbers were only debarked. The digital fabrication led to multiple different raw wood Nexorade applications: a) the 2D arch bridge [38], b) circular array of linear elements<sup>5</sup> or fans [164] forming a dome and c) tessellated surfaces<sup>6,7</sup> (see Figure 3.7). Hence, Nexorades can be utilized to erect an extensive range of constructions, stretching from bridges and polygonal roof structures to large hall roofs inspired by historical examples [8, 23, 26, 27], while only relying on pair-wise connections.



Figure 3.7 – Nexorade applications varying from the 2D arch, joint-free art installations to small-scale dome structures.

<sup>5</sup><https://www.timber-workshop.com/work/lake-bunyonyi-timber-frame>

<sup>6</sup><http://www.rinusroelofs.nl/structure/dome-bp/dome-bp-00.html>

<sup>7</sup><http://www.urbancampsitemsterdam.com/2017/installaties/oscar-sanders-stacking-sticks/>

## 3.3 Applications using Forks

Applications of tree-forks require a new digital survey, design, fabrication tools and interpretation of the traditional carpentry methods. Forks or branches are not used in conventional production. However, they give unique qualities as connection elements. Claus Mattheck at the University of Karlsruhe carried out extensive physical testing of the behaviour and strength of natural forked tree sections [100]. More extensive research was carried out on structural, and fracture capacity of tree bifurcations in hazel [115, 153, 154]. This research studied the toughening mechanism of tree forks through the critical joint between branches.

For architectural application, the splits of fibres in a crotch could be exploited as a joinery element, allowing structure to be assembled following the parallel to fibre orientation. The following research studies use tree bifurcations to take advantage of a joint's structural benefit with a single piece of wood that purposely grew under natural forces. While a tree fork has a structural advantage over beams connected with external fasteners, it imposes a structural topology limited by an angle between two branches. Consequently, tree forks' applications have a specific structural and architectural vocabulary based on the available stock of tree crotches.

Jonathan Enns [44] proposes a triangulated column system "NatureFrame", in which a pedestal of multiples rolled veneer posts could be joined in one node. The design of the structure follows a selection of branching parts closest to the intended proposal. Trees are digitally dissected topologically before any cuts are made to the living trees. The geometric representation of the discrete tree parts was simplified, providing quantitative readouts such as dimensions, angles, volumes, axes, and radii that are grouped into a digital catalogue (see Figure 3.8).

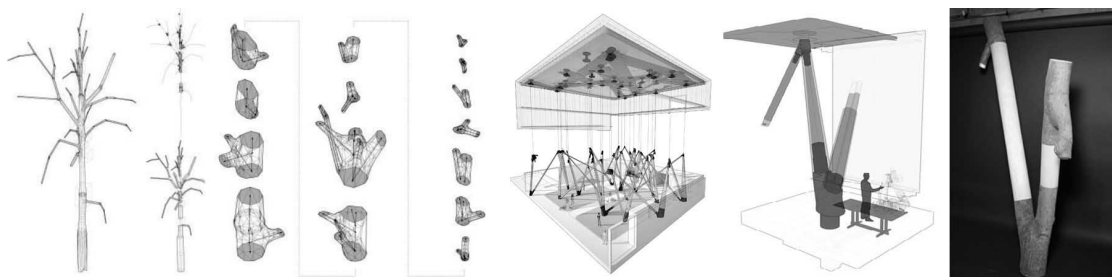


Figure 3.8 – NatureFrame concept proposal for exploiting tree crotches by Jonathan Enns.

Tree forks could also form 3-valence grids. For example, hexagonal lattice structures could be composed of straight linear beam elements attached to forks by wooden dowels, and screws [166, 175, 176]. Four design methods are proposed for using forks: a spatially optimized parametric branching nested structure, a parametric hexagonal organic dome with multiple angular facets, a three-way triangulated columnar structure, and a two-way triangulated frame reminiscent of the traditional timber framing (see Figure 3.9). The LIMB project was realized to

### Chapter 3. Architectural Design Methods using Raw Wood

---

explore the potential use of natural tree bifurcations as a new joinery method in a heavy timber construction. The placement of forks was based on the angular dimensions and dynamic inventory-constrained form-finding. The process selects the available crotch geometries into the design geometry through optimization to minimize the geometric discrepancies of the intended design. The global design framework applied the following design strategy: a) a hex topology grid selection, b) relaxation of the grid to find an optimal compression shell, c) assignment of the crotches and minimization of the difference between the target and fork geometries, and e) structural analysis. The physical prototypes relied on a long machining process to shape timbers to the desired 3D model and remove visual discrepancies.

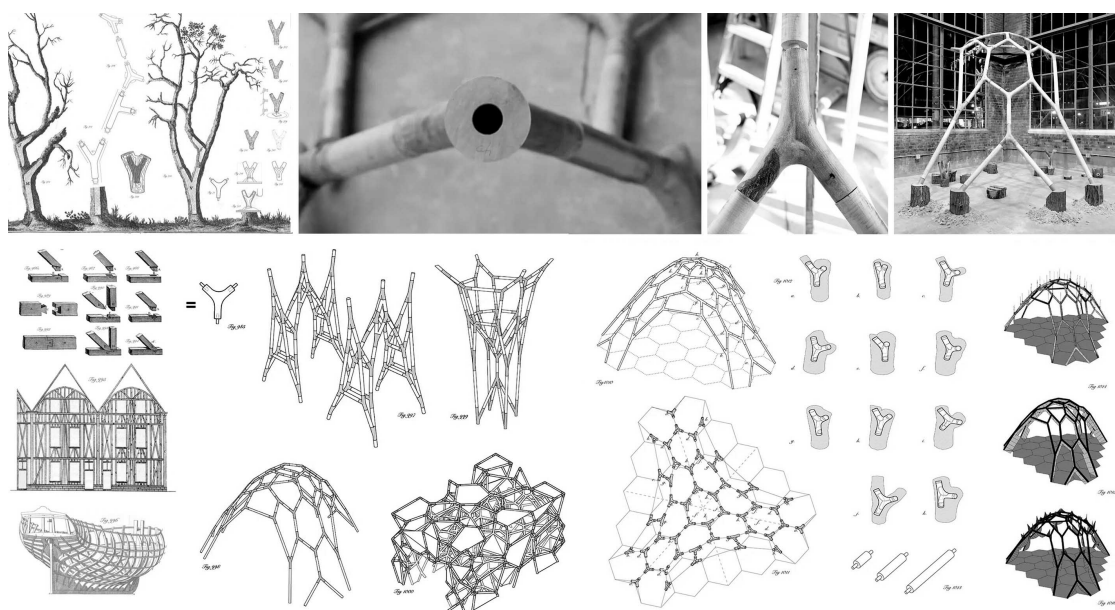


Figure 3.9 – Hexagonal frame system made from tree crotches that are machined to round sections - Limb project [175].

One of the most known contemporary examples of branches application is the tree fork truss (wood-chip barn) made by Design and Make studio in AA, London [104, 146]. The design methodology is based on four key strategies: a) the development of a precise referencing system to ensure consistent placement of each component independent of its distinctive features (three dowel holes for scanning and fabrication), b) the photographic and photogrammetry techniques deployed to identify and 3D scan appropriate tree-forms to build a database of available geometries, c) the meta-heuristic evolutionary optimization of each discrete component placement within the structurally determined arch form, and d) the strategies employed in the automatic tool-path generation for the connection fabrication to ensure the overall dimensional precision independent of the local irregularity (see Figure 3.10). The application employs trees in their natural form with a minimal fabrication applied only at the connection node.

### 3.3. Applications using Forks

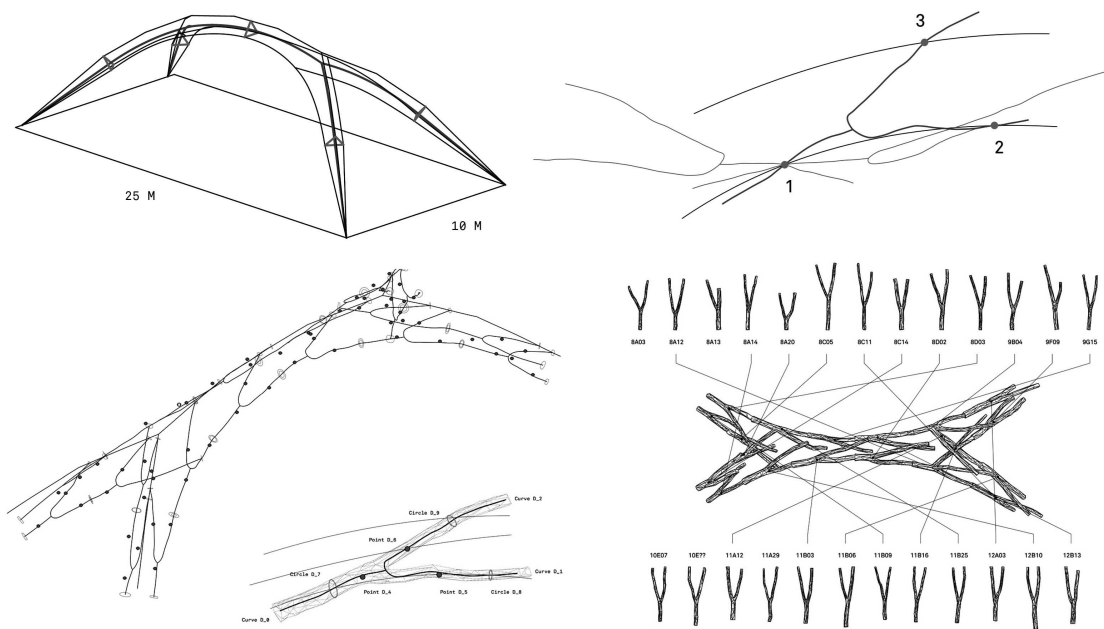


Figure 3.10 – Tree Fork Truss (AA Design&Make wood chip barn) was based on a structural Vierendeel arch system, where a fork is placed using an iterative genetic algorithm based on a 3 point branch placement [104].

The branching of a tree trunk, e.g. Hornbeam, could also be used as a T shape for a column-slab bracing [99]. These T Shapes do not necessarily have to be two-dimensional. Instead, they could create branching frame structures (see Figure 3.11). Hard-wood applications, such as oak, do not yield extensive application possibilities in the same way that relatively straight mono-culture spruce forests do. Nevertheless, they could have a topological advantage due to bending and forking, resulting in unique building topologies.

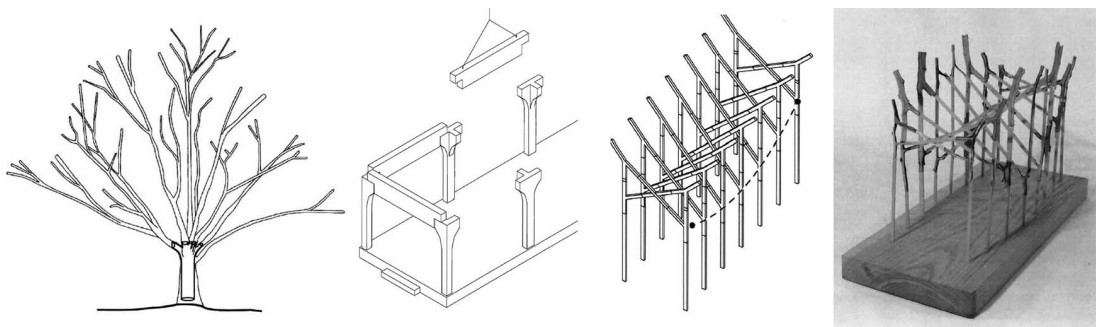


Figure 3.11 – Design explorations of tree forks applied for a slab-column and truss system [99].

A Conceptual Joining team proposed another strategy to explore the design and performative potential of a specific set of unique elements and the relative emerging formations, rather than relying on a predetermined design, for which elements have to be adapted [6]. The design and

### Chapter 3. Architectural Design Methods using Raw Wood

---

manufacturing process is articulated in different steps: a) 3D scanning of branches and automated features extraction from the scanned Meshes, b) clustering of the scanned geometries according to geometric features, and generation of 'proto-parts' as averages between clustered branches, c) generation of design structures using recursive aggregation of the generated proto-branches, d) replacement of "proto-branches" with scanned geometries, according to specific design and performative parameters, e) compensation of structure gaps using a force-based relaxation of the whole model, and f) automated joinery generation and post-processing for fabrication (see Figure 3.12). The project is considered as a 3D art installation and structural exploration of small-radii tree crotches.

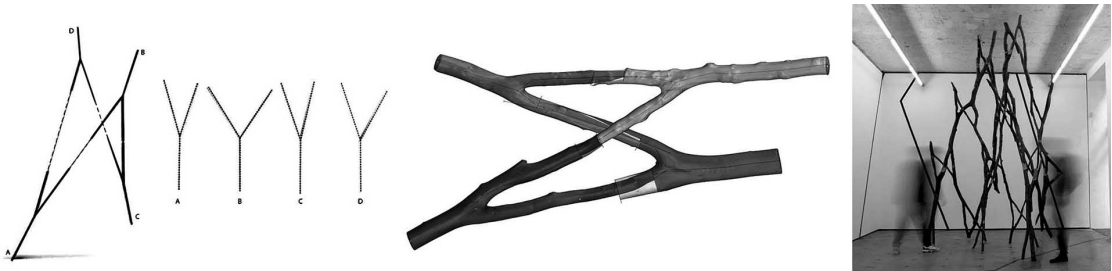


Figure 3.12 – Design methodology based on tetrahedral cell aggregation in a 3D grid (Conceptual Joining [6]).

Besides simple truss structures (WholeTrees), the fork applications have been applied only in the research applications relying on recent developments in digital workflows, using scanning and robotic fabrication. The novel tools help develop design methods with irregular elements, whereas industrial applications only focus on the use of straight beams. These examples also manifest an idea of exploring the timber of minimal value with a particular architectural language coming from the appearance of elements. The overall workflow needed to be developed for the tree forks, such as scanning and robotic cuttings, shows the broader use of irregular materials (not necessarily timber) that are not needed to be unified into equal shapes to have a value in construction.

### 3.4 Applications using Crooked Curved Wood

The bending of wood is formed due to reaction wood [149]. Trees form reaction-wood when their growth deflects from the vertical axis below one or two degrees. The most straightforward example is the tree branches that have deflection due to bifurcation. They are also often curved due to a mountain terrain, constant wind or sun directions. There is a difference in the micro-structure between the soft and hard-woods (see Figure 3.13). In hard-wood, reaction wood is called tension-wood because it is formed on the opposite side of the tree central-axis, whereas the reaction wood in soft-wood is formed on the opposite side and called the compression-wood. The bentwood has no economic value because saw-mills cannot process them. Several research studies demonstrate the advantage of bending for free-form structures following a tree trunk's natural curvature.



Figure 3.13 – Reaction-wood formation in the crooked, bent tree trunks [149].

Experiments with crooked wood often aim at curved beam fitting to a larger curve or surface. The fitting of the logs in a larger constellation is a negotiation between an available stock material and design intent. Bent logs could form a "lamella" roof following a NURBS surface [87]. The grid-shell, inspired from the Zollinger system, could be formed by first subdividing the geometry into curved segments and matching the lengths of the tree trunks in the stock. The next step is to pair each curve with a pre-scanned beam. The curvature comparison is made between stock elements central-axes for the most suitable selection. Then a log is oriented towards the master surface and rotated to match the surface iso-curve. Normal and tangent vectors are used for matching the two geometries. A ruled surface is made to describe how a log needs to be divided length-wise or trimmed to fit the target curve's size and orientation. The final steps are a joinery and tool-path implementation to connect the structural members physically. The result is a structure where the available stock matches the overall design as much as possible (see Figure 3.14).

Similar research is conducted when applying bent branches for reciprocal structures [94]. The system is most suitable for DIY applications, furniture, and small architectural structures. A workflow is proposed that maps a set of scanned branches to a Nexorade pattern. The best-fitting branches are assigned to the target curves of the structural pattern. The assignment

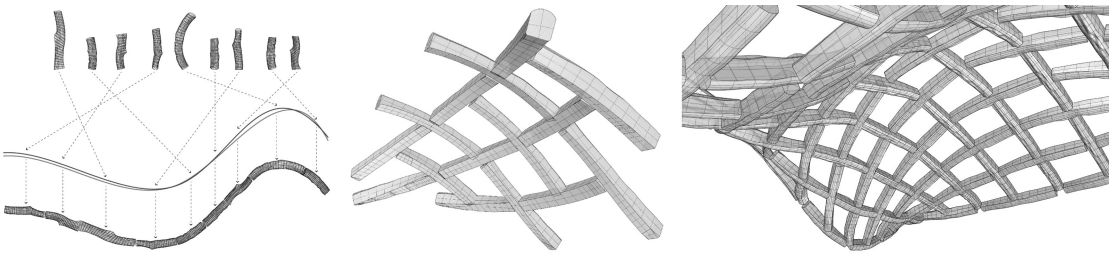


Figure 3.14 – Grid-shell inspired by the Zollinger roof system from the crooked-bent-wood (Aarhus School of Architecture) [87]).

process is optimized by employing dynamic relaxation by attracting the central beam axis within a given distance. Afterwards, half-lap joints are assigned at each intersection node of branches. An audio-visual positioning guides human fabrication and a 3-axis computer numerical control (CNC). The fabrication setup has a precision within 1 cm due to the low-cost methodology. Nevertheless, this work has a key contribution for the matching methodology between the scanned branches and target curves (see Figure 3.15).



Figure 3.15 – Design workflow of the reciprocal structure made from small radius branches (Human-in-the-loop, The University of Tokyo [94]).

A stacking method could form a curved surface that is sectioned along the Z-Axis [177]. The construction method is known from the traditional wood cabin assemblies when beams are flattened at two sides and stacked together. Side connections could be made by giving a profile to the flattened side or joined using additional fasteners such as screws, wedges, packers or dowels. Identifying an area of trees with naturally grown curvature could lead to an idea that a variant of traditional log-cabin construction could be developed using curved elements to generate a material-inspired free-form wall system. This methodology includes the following steps: a) low-cost scanning (Kinect), b) feature extraction (central-axis, taper, radii), c) curve-to-surface iterative fitting method, and d) semi-digital fabrication method (see Figure 3.16).

Another method was used for the facade cladding system such as Ashes Cabin [189] that questions whether irregular and natural wood geometries can be used to create surface structures from bent planks. Architecturally, the bentwood are strategically assembled to create window openings, framed views, awnings, door handles and entrances (see Figure 3.17). The project utilizes both straight and curved logs to reduce waste and exploit irregular trees.

### 3.4. Applications using Crooked Curved Wood

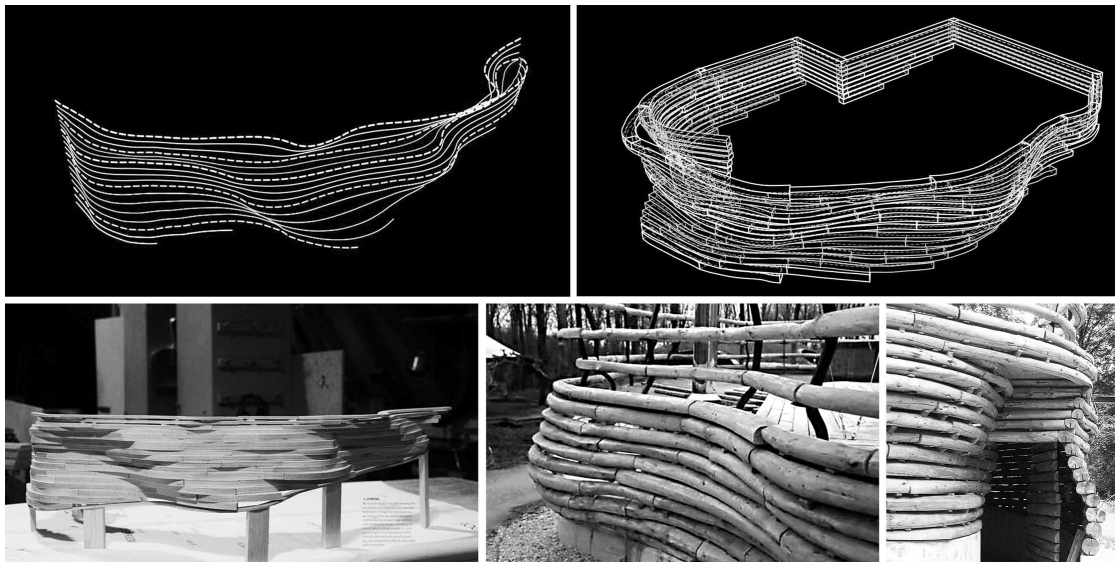


Figure 3.16 – Vertically stacking of raw beams with natural curvature following the tangential and surface fitting methods (Biomass Boiler House - Design and Make Studio, AA [183]).

From the ten selected ash trees, 45 smaller logs were cut, catalogued, and matched to the envelope of the initial cabin design. The research team proposes the following workflow: a) selecting and harvesting available ash trees, b) 3D scanning (Skanect 3D Scanning iPad Kit), c) slicing logs into boards, and d) assembling the boards to a variety of surface conditions. Three surface-layering conditions were developed: (i) planar surfaces based on straight log geometries (ii) curved surfaces based on curved logs, and (iii) double-curved surfaces based on curved or straight logs.



Figure 3.17 – Facade system using band-saw curved cuts (Ashes Cabin) [189].

These research projects show potential in low-value curved timber that is similar to tree forks. The natural curvature allows free-form structures that are typically not possible when using straight timber. The curved fibre direction's inherent qualities reflect on the architectural language found by matching a stock of trees while re-iterating the design target using the scanning and digital fabrication techniques.



## 4 Research Motivation

### 4.1 Two Challenges: Architectural Design and Fabrication

The processing of wood in its natural form presents two challenges: the first one is a technical scanning-to-fabrication challenge, and the second one is an architectural CAD modelling challenge [87]. The first challenge consists of methods needed to handle the raw timber between the digital and physical space. The second challenge investigates an architectural potential of raw wood in construction employing wood-wood connections. The natural form of timber cannot be precisely known due to precision of a scanner, rules imposed by cutting tools and CAD modelling processes requiring as minimal 3D representation as possible for a fast computation. Nevertheless, low resolution referencing systems can be used to ensure the construction precision and link digital design modelling with the material that exhibits complex irregularities.

#### 4.1.1 Challenge 1 - Building Better Models for the Digital Joint Design

The aim of the thesis is to develop an algorithm for using wood-wood connections in whole timber assemblies built upon previous IBOIS, EPFL research. It is also acknowledged that raw timber requires a combination of external fasteners with timber joints. Research studies are analyzed to understand whether any existing tools could be used for the non-standard joinery. An assumption is made that most of the projects are developed as unique case studies and there is no common, collaborative tool that could ease CAD modelling using raw timbers. Even though there are many researchers working on the empirical studies, as is discussed in the literature review, there are no guidelines or digital tools for design-to-fabrication workflows for the integral mechanical attachment of raw woods.

The re-examined raw wood design workflows offer a solution for one building type that is highly constrained by the stock based form-finding process. The reusability and applicability of the methods question how the raw wood could be transferred for less computationally intensive (more common) design use. The steep learning curve using hard coded geometries,

genetic solvers, customized fabrication setups distance the usual architectural practices. At the same time, large timber fabricators do not use crooked timber and employ only straight raw wood (MobicSA). Even in such a situation, the design methodology is concentrated in the timber companies that also impose a low architectural quality. These two confronting situations co-exist without dialogue because raw wood research is a relatively new field, and sharing the know-how is hardly possible even when an industrial collaboration is enabled. Thus, the current situation raises a question of how high-tech research and high-tech industries could be brought together into the less computationally intensive architectural practices?

Fabian Scheurer (Design-to-Production) questions a larger timber design context by saying that “We need to build better models instead of novel geometries” (see Figure 4.1). The author emphasizes the gap between architectural 2D and 3D drafting methods for timber buildings. Furthermore, timber construction companies often have rigid and specialized fabrication techniques. These professionals are not always eager to adapt or change their working standards. As a result, the design intent is influenced by the construction methods, that need to be considered early on in the design phase. More importantly, there is a need to question his/her working standards, willing to learn and develop better models to consider the digital design chain for timber construction. Consequently, the research asks how to develop a raw-timber design workflow that could link low-level CAD design with high-level CAM fabrication techniques.

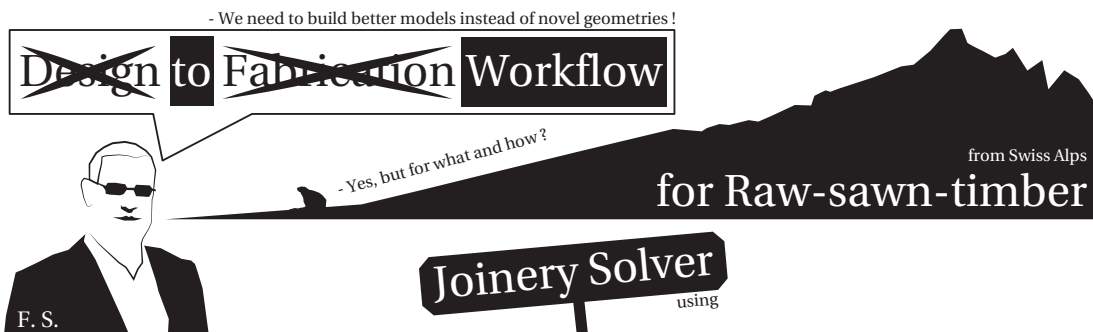


Figure 4.1 – Thesis title explanation focusing on building better design-to-fabrication models inspired by the work of Fabian Scheurer. The modelling framework, called Joinery Solver, focus on connection modelling automation giving a particular focus to raw-sawn-timber.

### 4.1.2 Challenge 2 - Scanning-to-Fabrication

There is a research gap between large centralized timber companies that embrace the mass pre-fabrication technology to develop repetitive, non-customized solutions fast in comparison to the local Swiss forestry where digitalization is absent. Industrial collaborations with the publicly and privately owned Swiss forest in Rossiniere and the robotic company ImaxPro helped to clarify this problem after visiting the two distinct practices employing the same raw wood material.

Additionally, there is a research gap between experimental raw wood experiments and the automated industrial applications. The following methods have to be implemented to be at least minimally competitive with the large centralized timber companies: a) scanning techniques in terms of point cloud processing to link CAD modelling interfaces with physical machining strategies, and b) robotic tool-path optimization for raw wood fabrication and joinery methods. Industrial applications rely on fast and automated profit-driven methods, whereas the research environments could afford slower manual methods. The more advance architectural raw research could take advantage from the industrial optimization strategies to minimize the manual operations. There are two primary problems that have to be solved: a) raw timber scans referencing and transformation into low-poly CAD models using slightly automated and mostly manual methods, and b) tool-path preparation for wood-wood connections is often time-consuming, non-error prone and secure.

Redundancy, repetition and lack of documentation of existing raw wood workflows makes a similar research difficult to begin. Industrial solutions are rarely available and research methods are lost once the research or a project is finished. As a result, the same or similar methods need to be developed in parallel to the existing ones only to reach a similar level of technology. The workflows behind the case studies are not shared, making raw wood research laborious to start before a researcher could bring an additional value to this field. Consequently, there is a primary focus to develop open-source tools to be able to use the work outside the research context.

## 4.2 Small Radius Timber

Small radius timber (diameter is less than 30 cm) and crooked wood (see Figure 4.2) is available for the research study due to collaboration with Swiss publicly owned forests: Rossiniere and Lausanne. Such raw wood construction could serve as a low-cost and low-impact building system, providing profit to the local forestry companies. There are several important considerations for the Swiss forestry context:

- rugged mountain terrain influences the tree harvesting method compared to relatively simple flat terrains in the rest of Europe
- spruce, a relatively straight timber species, populates the Swiss alps and only the lower part, that is larger than 30 cm, is used for construction
- tree forks often break when a tree falls down a mountain slope
- curved reaction wood is only found at the bottom of a tree (0.5 – 1 m length)
- it is challenging to replace unique pre-fabricated crooked timbers because there are no two trees alike.
- current architectural needs aim at the pre-fabrication imposing straight timber use

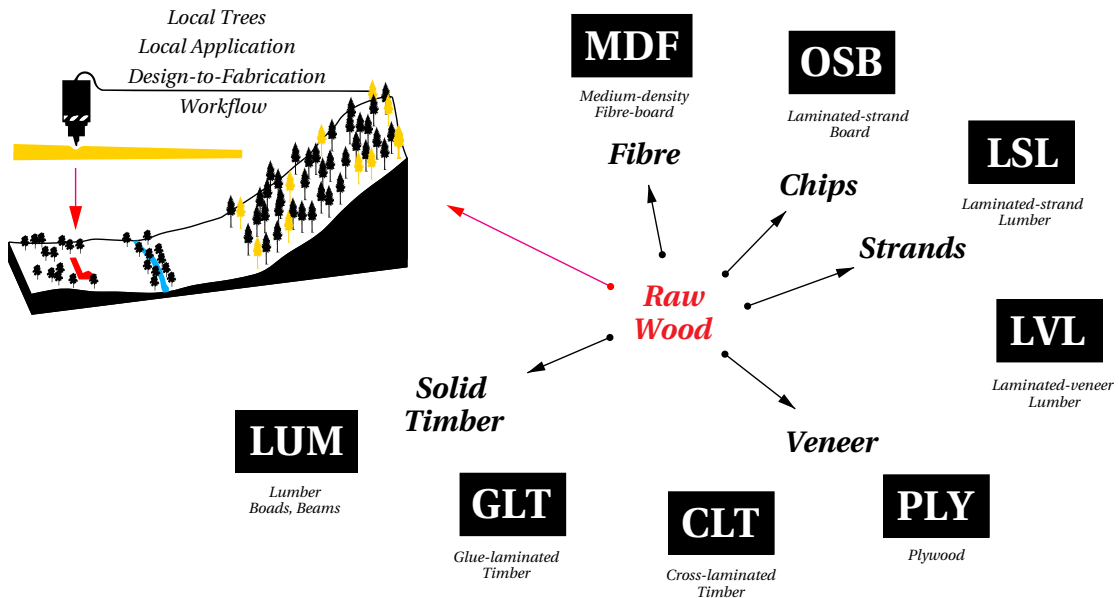


Figure 4.2 – In a larger context, the research employs solid lumber within the local Swiss forestry context. If it is possible to embrace the digital fabrication technology e.g. robotic cutting, there will be a chance to build with local wood, instead of relying on large centralized companies. Moreover, it would help to exploit crooked and small-radii timber that has a great architectural and structural potential that is not exploited by the current industry.

### 4.3 Motivation and Overview of the Proposed Workflow

Several main objectives prevent wider adoption of raw wood as a structural material: (a) complex and costly connection, (b) material-constrained design process, and (c) absence of digital tools applicable for the irregular trees and lack of automation in construction (see Figure 4.3). These points form one interconnected design-to-fabrication framework.

It is challenging to design a structural connection where multiple members meet in one node. The proposed design methods employ pair-wise connections only that could highly simplify the joinery modelling and fabrication. However, raw wood explorations are often based on single case studies without developing methods applicable outside their context. A joinery algorithm has to be developed for raw wood to ease the drafting process of wood-wood connections. Structural explorations should not be restricted by the hard-coded design processes and the automated joinery could assist the design modelling techniques.

Also, it is necessary to follow an available tree stock. The raw wood methodology constitutes a paradigm shift in the design, starting from an element rather than a global form. Each time an architectural study starts, timbers must be scanned or measured. Automation is needed to create a tree stock fast to be competitive with engineered timber products. An architectural project in raw wood starts from the available tree stock and capitalizes on its idiosyncrasies.

### 4.3. Motivation and Overview of the Proposed Workflow

This reciprocal design process fosters synergies and feedback between material, fabrication, digital form, and full-scale construction.

Robotic fabrication has to be employed to machine timber joinery. The shape of timber and its position within a machining setup differs for each timber. In addition, the fabrication setup must be stable enough to obtain precise results while allowing a robot's maximum reachability. Machining methods and tools differ from regular sized wood as well. The joinery algorithms and tool path generation need to be interconnected to work with variable geometry while imposing main principles observed in raw wood fabrication.

Fully leveraging the opportunity gap between the physical materiality of the wood and its digital design parameters remains one of the most challenging research aspects. Consequently, an automated workflow is proposed to intertwine pair-wise wood joinery, scanning and robotic fabrication to enable timber design in its natural raw form.

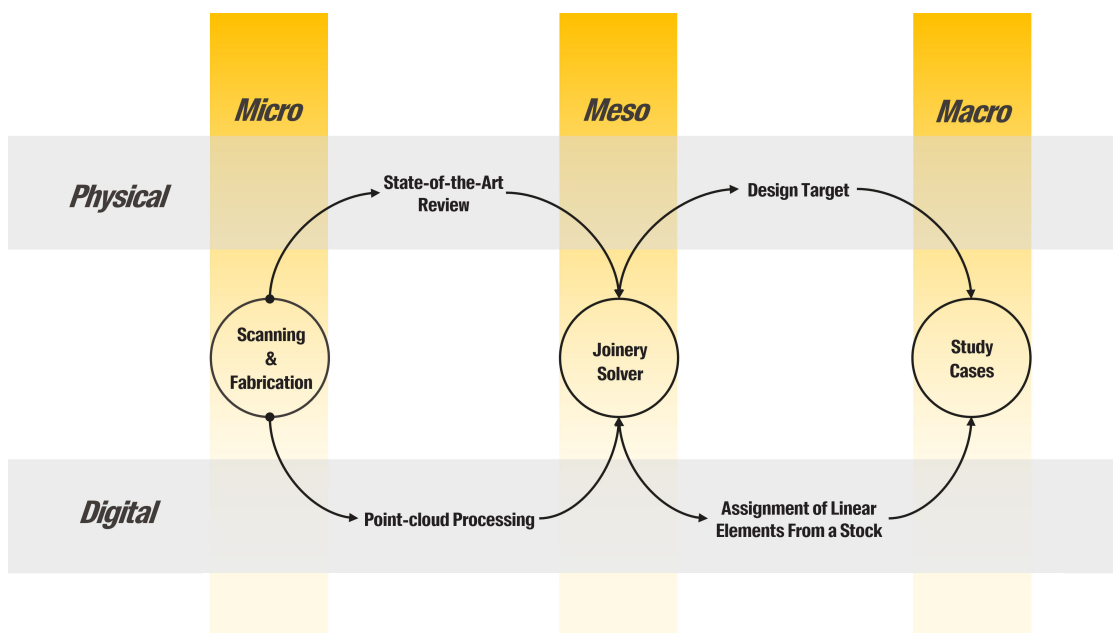


Figure 4.3 – The thesis is framed within three scales: a) Micro-scanning and fabrication automation, b) Meso-joinery generation to ease design process with raw wood to apply to c) Macro-design methods demonstrators.

## 4.4 Thesis Structure

The thesis framework is developed in two main parts: a) Part II - Methodology, b) Part III - Demonstrators. Separate technical tests, such as tree forks; visits to publicly owned forest Rossiniere; and software frameworks are discussed in the Appendix. Following is the thesis structure:

### **Part II - Methodology**

#### **Joinery Solver - Chapter 5**

---

- Representation of the data-structures for the Joinery Solver (Appendix C - NGon).
- Fast and robust connection area and node detection within the proposed model.
- Joinery topological library.
- Solve 2D Polygon and 3D Mesh Boolean problem for a joint visualization.

#### **Scanning - Chapter 6**

---

- Physical setup, calibration and software development for the Faro Focus S 150 laser scanner and the industrial robot arm ABB IRB6400R (Appendix C - FaroSharp).
- Pointcloud processing framework: a) skeletonization of tree scans, b) tool-path alignment and c) point-cloud processing library (Appendix C - Cockroach).

#### **Robotic Fabrication - Chapter 7**

---

- Physical setups for fabrication using CNC and the industrial robot.
- Tool-path planning based on the robot reachability and comparison to the G-Code control (Appendix C C - IBOIS-CNC, OpenNest).
- Fabrication integration using pairs of polygons.

### **Part III - Demonstrators**

#### **Side-side Joints for Shell Structures - Chapter 8**

---

- Modelling framework for shell structures.
- Surface discretization methods for doubly curved surfaces.
- Prototypes in sawn and raw timber.

### **Raw wood Cross-lap and Side-end Joints for Nexorades - Chapter 9**

---

- Examining existing methods of Nexorades and applying these techniques to raw wood.
- Mesh subdivision and tiling system for generating a linear Nexorade pattern.
- Joinery types in Nexorades.
- Stock based assignment problem.

### **Part IV - Appendices**

#### **Timber joinery and Teaching - Chapter A**

---

- Technical test: multi-valence joint.
- Technical test: truss from tree forks.
- Technical test: Nexorade fabrication using CNC.

#### **Rossiniere Forestry - Chapter B**

---

- Visit 1 - understanding the level of digitalization in Rossiniere.
- Visit 2 - available timber resources in the local foresteries.
- Visit 3 - forest harvesting method in Swiss Alps.

#### **Software Frameworks - Chapter C**

---

- NGon - Joinery Solver and Polygonal Mesh Processing methods.
- OpenNest - Nesting 2D Planar Polygons.
- Cockroach - PointCloud Processing methods.
- FaroSharp - FaroFocus S 150 laser scanner automation.
- IBOIS-CNC - Tool path automation for CNC machining.



## **Methodology Part II**



# Foreword of Methodology

Three parts are developed for the design-to-fabrication workflow: a) wood joinery generation, b) laser-scanning, and c) robotic fabrication (see Figure 4.4). The methodology starts from the Joinery Solver chapter to understand how wood-wood connections could be used in raw wood. The solver considers curved and bifurcated trees. The output of this workflow could be used both for visualization and fabrication because the joinery application links a data-structure for cutting and display. The second chapter is based on laser scanning and point-cloud processing. There are two main objectives: a) obtain a tree stock, and b) align a work object (a tree) within a machining setup. There are several ways the point clouds are used for fabrication: a) employing markers to get a position and orientation of a tree trunk, b) aligning two scans by a point-cloud registration, or (c) using Skeletonization. The fabrication chapter compares the developments for CNC and robotic fabrications. The fixation method of raw wood is explained in further detail, ranging from timber setups to mechanical steel systems. The robotic method is chosen for testing the link between scanning and cutting. Lastly, robotic tool-path planning is automated to ensure the robot tool-path reachability.

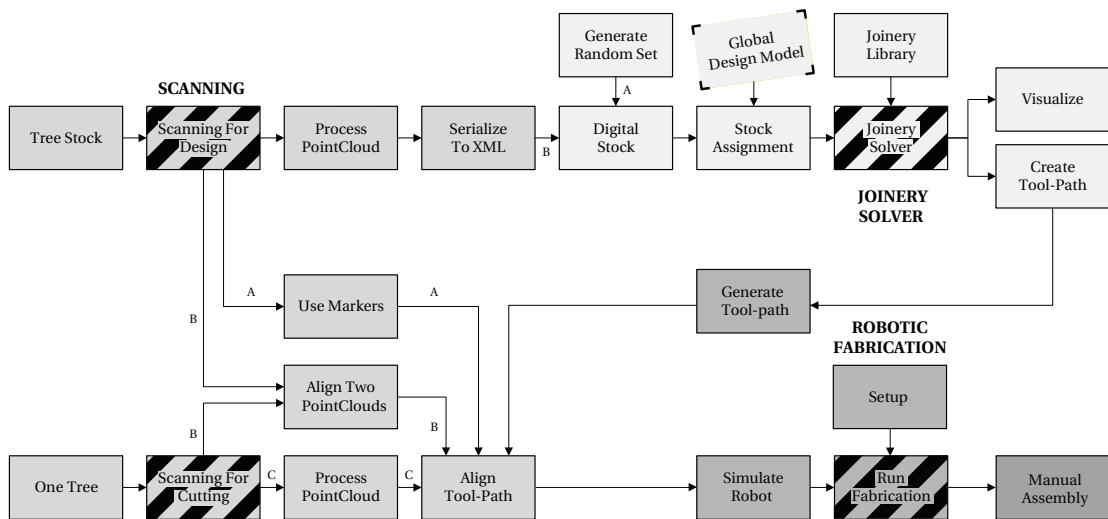


Figure 4.4 – Thesis methodology: a) Joinery Solver, b) Scanning, c) Robotic fabrication.



# 5 Joinery Solver

## 5.1 Foreword

This chapter is based on:

P. Vestartas and Y. Weinand. Joinery Solver for Whole Timber Structures. *WCTE2020, Santiago, Chile, August 24-27, 2020.* infoscience.epfl.ch/record/281960.

This chapter presents an algorithm aiming at geometry generation for pair-wise wood-wood connections (see Figure 5.1). The method is based on a collision detection using the following methods: face-to-face, curve-to-curve, face-to-plane, mesh-to-mesh. The 3D models are represented by minimal shapes using a hybrid model of polygons and curve axis. The joinery generation methods are based on a Unit-Tile Change-of-basis transformation following an assembly graph. From the linear algebra, the rule of the Change-of-basis says that it is possible to transform one coordinate system to another even if the second one is non-orthogonal. The first coordinate system represents a joint drawn on an XY plane and the other system is equal to a joint location in a structure. The technique is subdivided into several connection types: a) cross, b) side-side, c) top-side, d) top-top, e) custom-cuts (see Figure 5.3). Lastly, the algorithm considers flat and rectilinear fabrication methods.

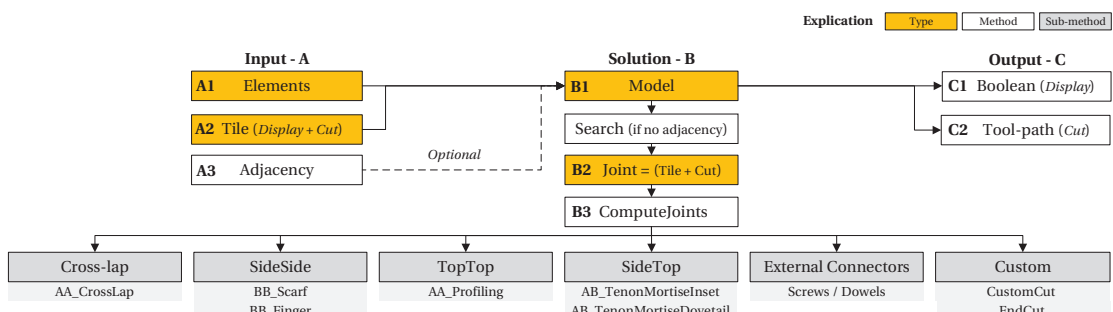


Figure 5.1 – Data-types and methods used in the Joinery Solver.

## Chapter 5. Joinery Solver

---

The overall workflow includes the following steps: a) creation of a timber element, b) a connection zone search, c) a transformation of a joint, d) a 3D visualization, e) and a tool-path generation. First, the user specifies a series of timber elements. Second, connection zones are identified using the R-Tree data-structure [63] and an oriented bounding-box collision. Third, joinery Tiles are selected, from the joinery library. Fourth, the joint geometry is computed. The method proposes two alternatives to visualize timber joints using a polygon intersection [9] and Mesh Boolean Difference [161] methods. The algorithm is designed for robotic and CNC fabrication. The methods are assessed using an industrial robot arm and a 5-axis CNC machine. The data structures and algorithms are made using the RhinoCommon geometry library for Rhino3D [138]. The workflow is open-sourced, including example files [168].

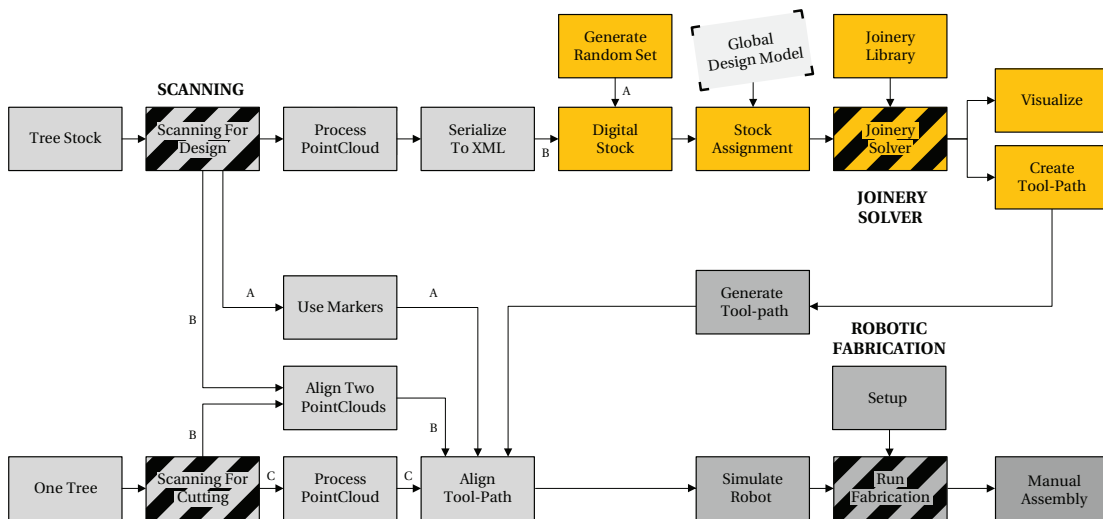


Figure 5.2 – The Joinery workflow focus on wood-wood joinery generation.

---

The Joinery Solver chapter is structured as follows:

- Section 5.2 introduces existing joinery methods and explains why the Joinery Solver is developed.
- Section 5.3 describes data-structures of the algorithm:
  - Element - minimal model and collection of joint cuts
  - Joint = indexing + Tiles. Tile = female + male Cuts.
  - Cut - tool-path integration
- Section 5.4 describes search methods to identify the connection zones.
- Section 5.5 details following joinery types (see Figure (5.3)):
  - A - Side-Side, B - Top-Side, C - Cross
- Section 5.6 explains 2D Polygon and 3D Boolean methods for a joint display.
- Section 5.7 summarizes the efficiency of the proposed method.

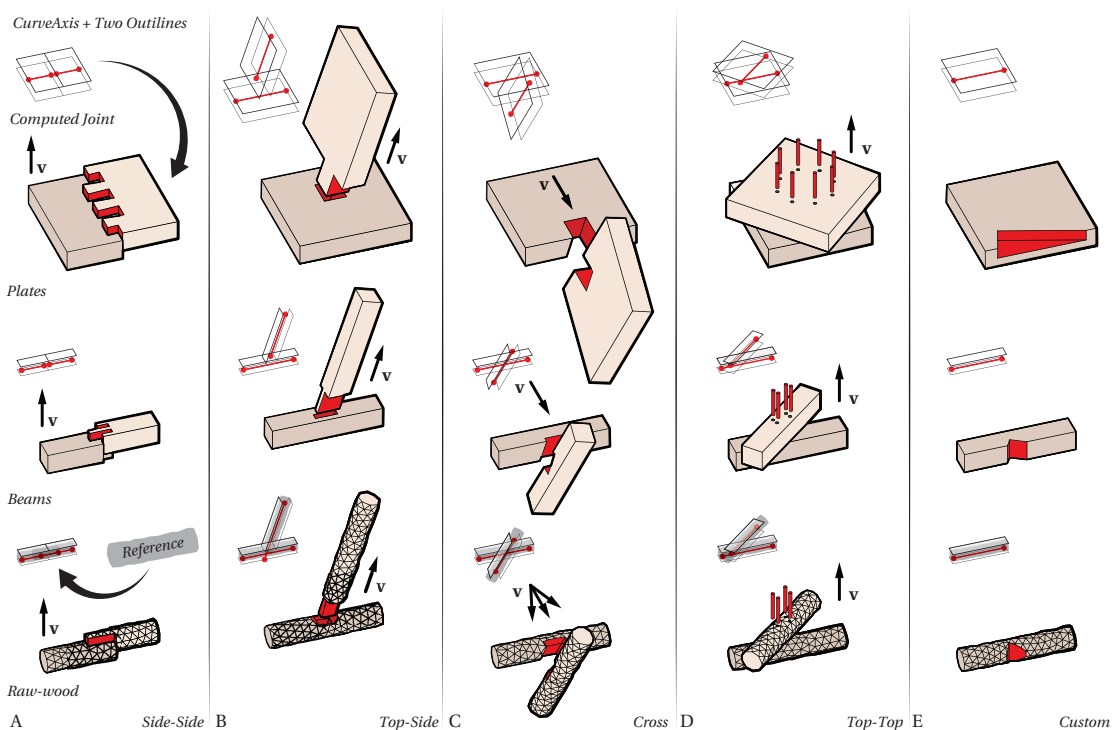


Figure 5.3 – Joinery Solver connection types using a curve-axis and pair-polygon model.

## 5.2 Introduction

**Existing Methods** Joinery is divided into two categories: a) external fasteners such as screws, dowels, keys or 3D printed nodes, and b) integral joints such as wood-wood connections with curved or planar contact zones. Connections allow discretizing a 2D or 3D shape to simple parts that are specific to a particular material fabrication technique. Even though joinery is admired for assembly, structural performance and aesthetic quality, drawing integral mechanical attachments remain a time-consuming and challenging practice. Joinery belongs to an extensive research context such as a) the shape decomposition [5, 11, 13, 32, 41], b) the structures from self-supporting and interlocking blocks [3, 42, 50, 55, 80, 85], c) the models from planar interlocking cardboard facets [34, 69], d) the surface discretization techniques for small scale furniture and toys using plate-edge connections [2, 18, 31, 67, 70], e) the nodal systems [76, 96], LEGO [61, 83], and f) the wood-working practices in carpentry and furniture [49, 155].

The current research belongs to the larger group of architectural applications in timber construction such as a) timber beams [10, 46, 94, 159], b) engineered timber-plates [112, 131, 173] and c) raw wood structures [6, 146, 176]. There are two distinct application models: a) economy driven mass-prefabrication for identical timber elements using customized robotic systems, and b) unique architectural research projects addressing the complexities of structural shaping. Large architectural projects often employ interlocking connections by manual modelling

## Chapter 5. Joinery Solver

---

decisions, commonly applied to one case study. Mass customization is often discussed as a possible combination of both systems [82, 84] but still lacks flexible implementations for the CAD practices in architecture.

Joinery frameworks for architectural design are divided into two categories: a) linear elements such as rectangle section beams and glulams [108, 158], and b) flat polygonal elements such as engineered timber plates [12, 135]. Furthermore, raw wood have no specific design tool readily available, making it challenging to apply this material in practice resulting in the highly customized workflows [104, 174].

The contribution to this timber joinery field is an algorithm that can generate joints for plates and beams, regardless of a timber shape, whether it is regular or irregular. The joints are identified using a collision-based search. The linear and polygonal elements share similar properties considering local joinery geometry. Even though these materials are different in a global structural behavior, both types can take advantage from each other at the micro-scale of the joint modelling. Consequently, the contribution allows joinery generation applicable for raw wood, regular beams and plates.

**Problem Statement** The necessity to develop the Joinery Solver algorithm is initiated from the involvement in the research of the timber-plate structures [112, 113, 131, 169, 173] that continued with linear beam elements both in rectangular and irregular sections [170, 172]. In this context, only pair-wise connections are employed that stores a three-level information: a) a connectivity-graph to track the assembly information, b) a 3D shape joint shape for the display, and c) a tool-path for the digital manufacturing. There was a re-occurring problem within multiple case-studies: each time a new parametric model is hard-coded for a specific project, it could hardly be re-used in the other projects. Also, specific elements such as boundary edges, foundations or custom details often have to be modelled manually. An observation is made that the intertwined model of a global shape and the local joinery makes the re-usability of the joinery algorithms difficult.

**Application Requirements** A separation of the micro joinery model from the macro shape model into two independent algorithms is taken as a primary idea. In practice, a design shape is highly likely to change depending on structural and architectural constraints, whereas the joinery remains similar or must be extended based on the new joint implementations. To prove this method viable, the workflow has to identify connection zones and nodes using a fast, robust and scalable method if the initial adjacency graph is absent. The joint detection is needed, when there is no information about a joint type and its location. Furthermore, it is necessary to solve numerous face-to-face and curve-to-curve intersections due to the slow quadratic iteration ( $O(N^2)$ ) comparing to the joinery generation using a single Mesh graph. Additionally, it is necessary to provide an extendable software interface to add new types of timber joints that were not used in the past. Moreover, the geometrical generation of wood-wood joints is closely linked with fabrication methods such as CNC machining or

industrial robotic cutting that must be considered together with the 3D modelling techniques. Lastly, these are the principal algorithm design requirements: a) re-usability of the joinery methods for more than one case-study, b) development of a joinery library c) automatic wood-wood connection generation, d) ensuring fabrication constraints and safety, e) interconnect linear elements (beams) with planar elements (plates), f) propose an alternative fast graph construction method instead of using a pre-defined graph data-structure such as the Mesh, g) integrate joinery algorithm into the common CAD modelling environment, and h) employ minimal models for a fast computation.

### 5.3 Data-structures

#### Element - Minimal Model and Collection of Joint Cuts

**Element Data-structure** Element is a data-structure that represents a timber object in its minimal geometrical description. Timber elements have several categories: a) timber-plate, b) straight or curved rectangular beams, c) raw wood. The research scope is continuously demanding to shift between a) current research in raw-sawn-timber, b) a collaboration with IBOIS, EPFL researchers in timber plates, and c) teaching using different timber elements. This experience poses a question: is it possible to reuse joinery geometry algorithms when the shape of timber changes?

Additionally, the Element representation has to be as minimal as possible to perform fast computation methods such as a) detection of connection zones, b) joint geometry generation, and c) a joint volume subtraction from a timber shape. There are two known low-resolution models: a) a polygonal model defined by a group of top and bottom outlines [136], b) axis-plane representation for curved and straight beams [160]. A hybrid model could take advantage of the two systems (see Figure 5.5). The polygonal plate representation enables face-to-face searches while skeleton models help define joints when elements are intersecting.

Furthermore, an Element is defined from a local joint scale instead of its global appearance because connections share similar geometrical machining properties. A joint geometry follows a shape of a tool such as milling, drilling, flat-circular saw-blade, lathe, chainsaw as demonstrated in Figure 5.4. Machining tools constrain timber connections to rectilinear, orthogonal, and oblique cuts. As a consequence, timber joints are drawn in a unit cube that are aligned to connection zones (see Figure 5.7). In this instance, one plate edge joint is similar to a beam connection since both are rectilinear. Hence, the element data structure is described as a collection of many rectilinear joints.

To summarize an element description, there are three main parts: a) collection of rectilinear joints (Cuts) b) reference to the original shape of a timber element (triangular mesh), c) minimal model representing a shape of a timber element (planar Polylines + Axis direction).

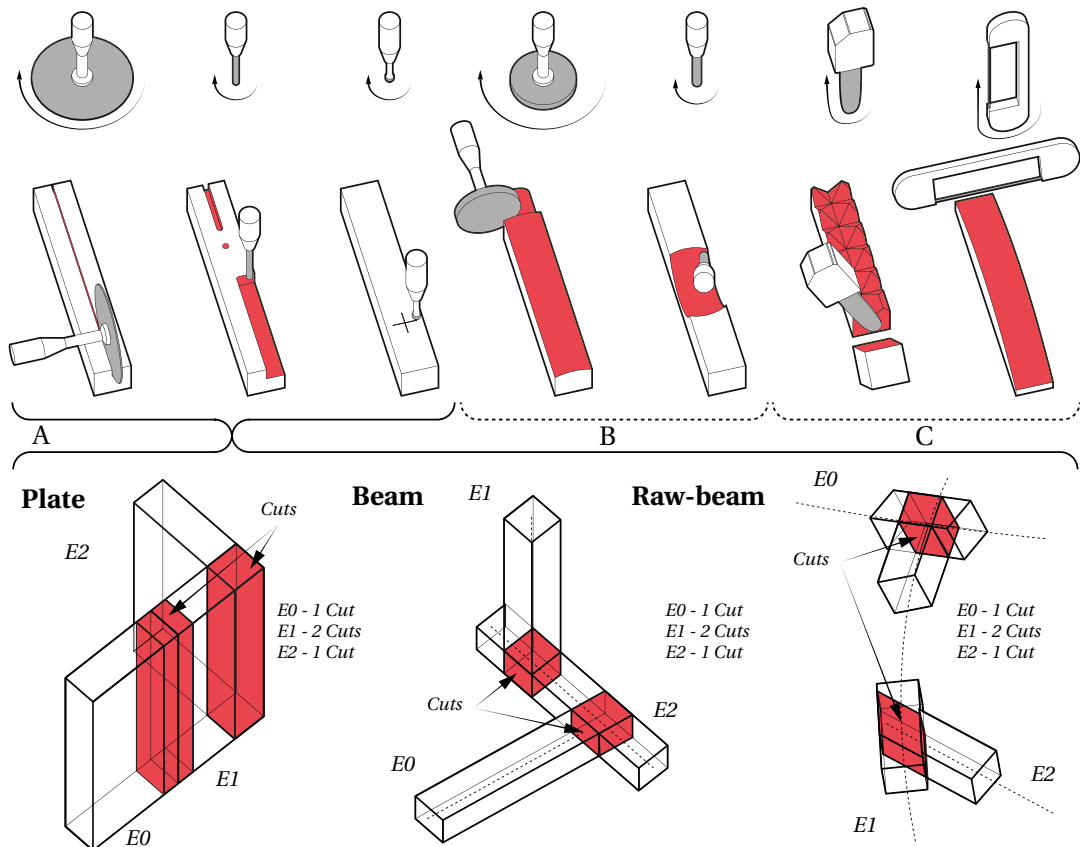


Figure 5.4 – Element data-structure is represented by a minimal timber shape with cutting volumes. The idea is derived from cutting tools (a). The description does not include cases for large surfacing areas (b) or custom-tailored tools such as robotic chain-saw or band-saw (c).

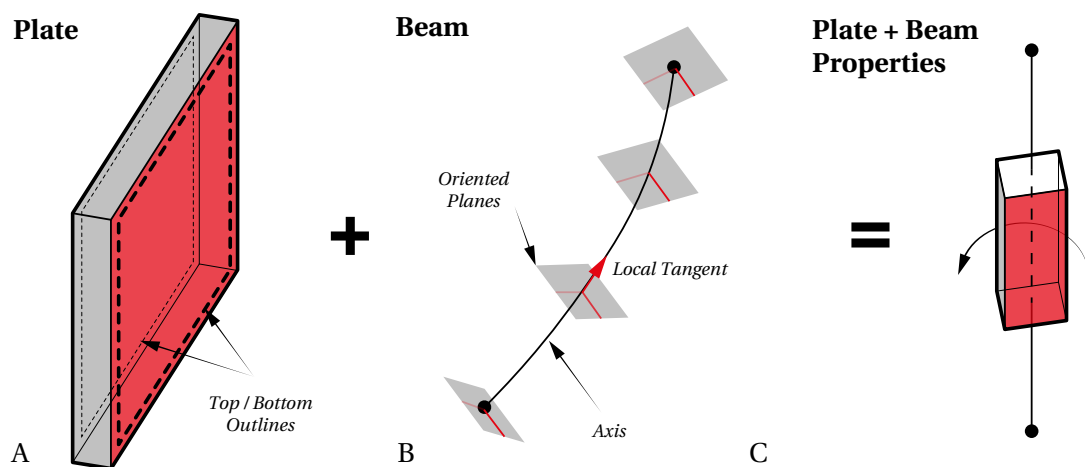


Figure 5.5 – A hybrid model (c) takes advantage of the two systems: Face model (a), and Axis-Plane model (b). The first one helps to detect face joints, whereas the second model helps to detect joints when objects are intersecting or have eccentricities.

**Element Grouping** Elements can form groups, often named as components, modules, or clusters. The groups of elements form a model or are nested in the larger hierarchies. For example, a tree trunk could contain three circular beams forming a tree fork, and a truss system may contain both straight and forked elements [176]. Box elements that contain individual timber-plate elements could also form a two-layer timber plate structure [136]. Furthermore, curved beams could form large modules and the modules are grouped into building envelopes [179]. As a result, the application has to reflect on such tree structures and find a correct indexing logic. Additionally, the element grouping require a reference to one shared object. For the timber-plates, the representation is equal to an input object - a list of top and bottom outlines. For a straight, bent or bifurcated beam, it is necessary to have one shared geometry per one group to perform the Mesh Boolean operations, where a collection of outlines are constructed around the connection nodes (see Figure 5.6).

The overall hierarchy is represented by one sorted list. The key of an element has as a string of indexer "x;y0;y1;...;yn", where "x" integer is pointing to an item id in a global list, and "y" shows grouping order, whether it is one group or groups of assemblies. The main reason for using a single sorted list over nested lists of lists is the joinery computation. Most of the time, it is necessary to solve joints element-by-element, and grouping is used only to compute the assembly order. In addition, indexing helps to skip joints for adding connections within a group. For instance, three beam elements cannot have any connections that form one tree fork. The element insertion order of the sorted list follows the Key-comparer method while iterating over a Path with fewer integers by incrementally comparing each index with the next one. When both keys are equal, a priority is given to the smaller list length. In such a way, it is possible to work with elements one by one and keep the track of grouping.

#### Joint = Undirected Graph + Tiles. Tile = Female + Male Cuts

**Digital Joint Representation** Joinery is represented by a drafting system utilizing a unit-cube and a series of orthogonal projections inspired by woodworking techniques [49]. In a 3D structure a joint is oriented to a connection zone using three transformations: a) a change of basis, b) a scale, and c) a plane-to-plane transformations. The connection zone, in a 3D structure and the unit-cube, is represented by a pair of rectangles to construct three vectors for the change of basis transformation (see Figure 5.7). A joint is drawn using a series of machining cuts to have an equal representation in fabrication and visualization. Additionally, the joint data-structure tracks adjacency information between the pairs of elements. The cuts are also represented by the pairs of polygons to define the tool-path. A pair of female and male cuts is named as a Tile. The algorithm has to identify which element is male and female to distribute correct cuts to each element from a Tile. Hence, the algorithm has a three-level hierarchy: a) "Joint" that contains indexing information, b) "Tiles" that contains c) female and male "Cuts". The Tile and the Joint types are not represented by the same classes because a Tile has no information about the element-to-element adjacency and can be reused through-out many similar joints for a faster computation (see Figure 5.12).

## Chapter 5. Joinery Solver

---

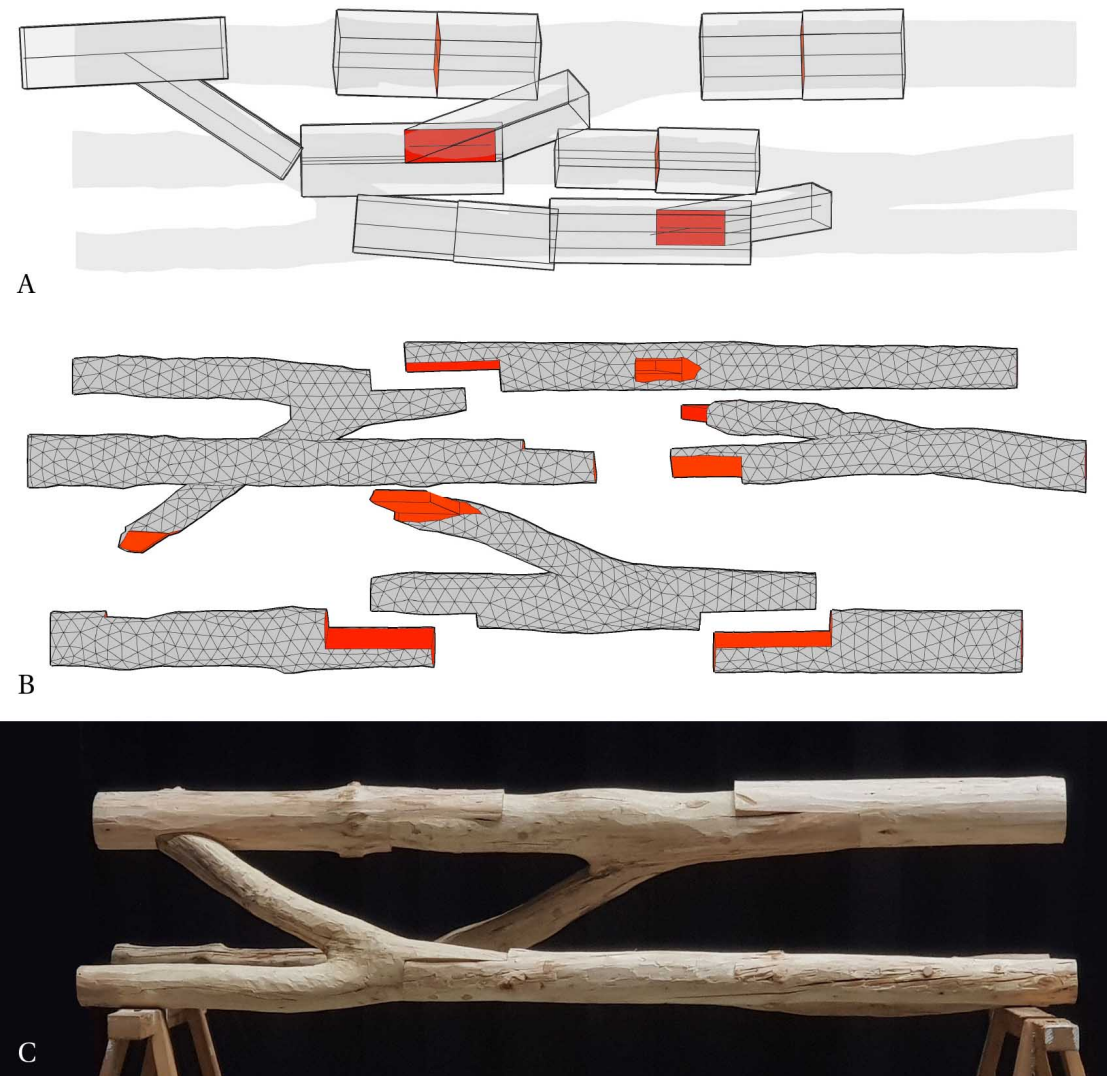


Figure 5.6 – Grouping of elements (a) and the reference Mesh – irregular tree trunks (b) for the fabrication of the tree truss (c).

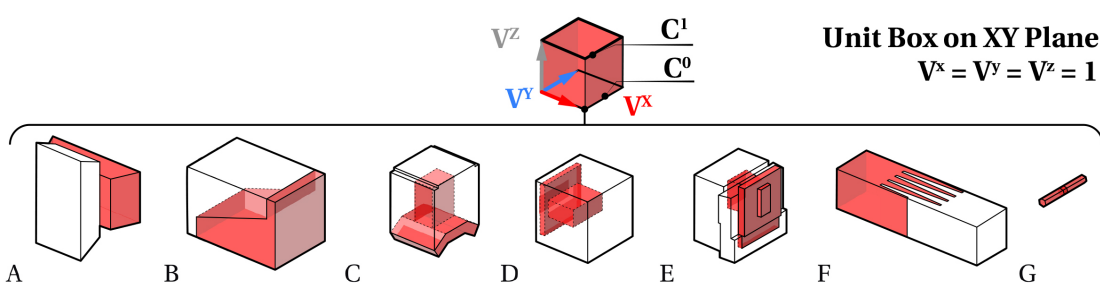


Figure 5.7 – Unit Box Tile and a series of geometrical descriptions for: a) Cross-halving, b) Scarf, c) Tenon-Mortise, d) Tenon-Mortise-Inset, e) Dovetail, f) Finger, and g) Dowels.

**Joint Data-Structure** Joinery solver employs an undirected-graph to track element-to-element adjacency. A vertex in a graph is a timber element, and the edge is a joint (see Figure 5.8). The dual of the graph represents the joint graph. A graph allows computing the assembly sequence, insertion angles and query element neighbors. Hence, the primary goal of a Joint is to track adjacency information such as: a) the element indexing, b) edges, and c) axis parameters. The adjacency can already suggest what type of joint is possible to apply for a pair of elements. For example, two beams can be connected: a) side-to-side, b) side-to-top, c) top-to-top, or d) cross. Moreover, the joint data-type contains the 3D information for: a) the joint-area if elements are positioned side-by-side, b) joint lines when elements are intersecting, c) joint-volumes represented by a pair of four-sided polygons to define boundaries of a connection. The joint-area and joint-lines are used for the connection zone visualization (see Figure 5.8 A), whereas the joint volume is computed at a later stage for the change of basis transformation to orient a joint from a XY plane.

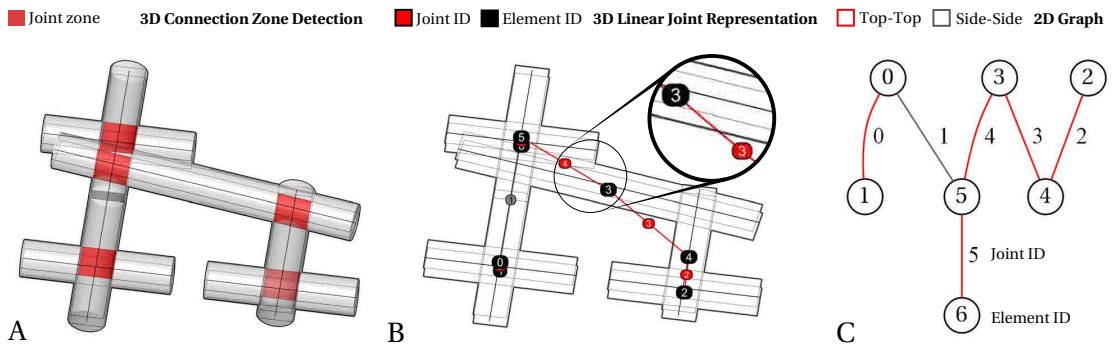


Figure 5.8 – Connection areas can be represented as a) polygons or as eccentricities between element axes. The Joint data-structure stores adjacency between elements shown in b) 3D graph and c) 2D graph.

**Tile Data-Structure** The Joint contains a list of Tiles that represents groups of female and male cuts. While the Joint stores the adjacency, the Tile reserves the geometry of a connection (see Figure 5.7). The topology of a joint may differ, but the joinery volume stays the same. Every connection in the proposed Joinery Solver points to a pair of objects. As a result, it is necessary to track geometrical information for both elements at once, and then distribute the cuts to individual elements using the Tile data-structure. Tile only contains the geometry information that is reused within multiple self-similar elements. The geometrical information is stored in two arrays of Cuts. One array is used for female cuts and the second one for male cuts. Tile has also indexing information to track the name of a Tile and its parameters. Furthermore, there is a series of functions that help to compute Tiles from the given joint parameters. For example, a user might need to automatically control a joint's length and area. The Tile stores these parameters due to two scenarios: a) the Tile is copied and transformed within self-similar beams, b) the Tile is rebuilt for each element if, for instance, tenons are computed depending on an edge length. Lastly, the Tile stores closed Mesh volumes to perform Polyline or Mesh Boolean Intersection.

## Chapter 5. Joinery Solver

---

**Tile Transformation** The Joinery Solver is based on a change of basis transformation to swap the coordinate system of a joint polygon as demonstrated in Figure 5.9. Joints are oriented from the XY plane to the joint area using the two additional transformations (see Figure 5.10): a) plane-to-plane, and b) translation. The change of basis transformation could be applied using two rectangular bounding polygons. The two rectangles are the only input for the three required transformations that constructs the three transformation axes (see Figure 5.11). Since the Tile type contains a series of Cuts, there is no need to create a new tool-path for fabrication. Fabrication pipeline will take advantage of this setup by directly using deformed outlines for the 6-axis robotic machining. The Tile tool-path ensures safety because one confirmed tool-path is the same in all cases within the same joint category.

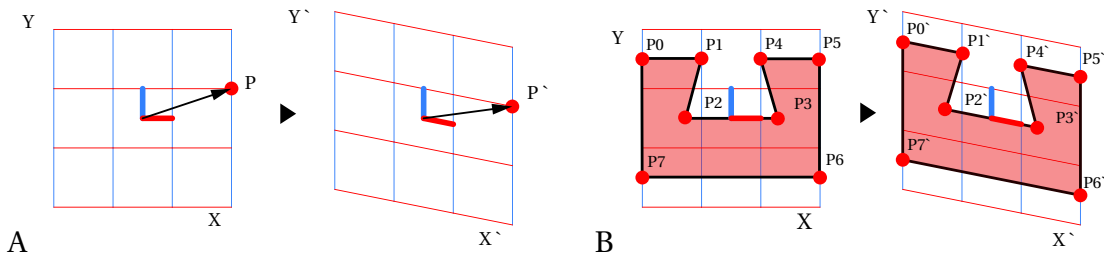


Figure 5.9 – Change of basis transformation applied to a) a point, and b) a dovetail outline. The same process is valid for 3D operations.

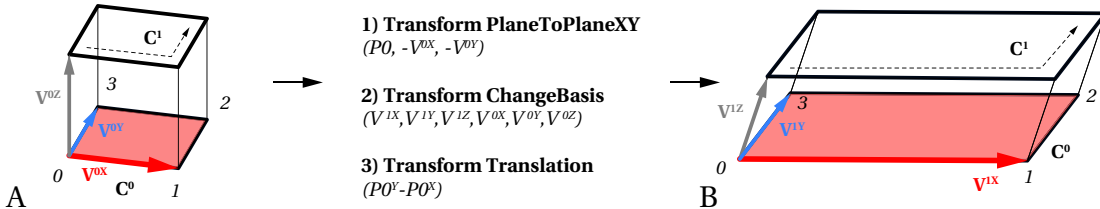


Figure 5.10 – Tile transformation from the Unit Tile to the 3D joint area, using the three transformations: plane-to-plane, change-basis, and translation.

### Cut Data-Structure

Cut data structure stores information about the tool-path generation and cutting volumes. For visualization purposes, cut is only a pair of polygons (see Figure 5.11), but for machining, there is a range of possibilities derived from the robotic and CNC testing (ABB 6400 IRB, 5-axis CNC Maka). For example, a joint may require milling, sawblade, drilling, engraving, and other types of tools for fabrication. The control of these tools differ from one to the other in many ways: a) TCP (Tool-Center-Point) b) the size and shape of a tool, b) the movement according to the center of a tool (milling) versus movement by the edge of a tool (sawblade), c) a notch specification, d) the interpolation of passes, and other properties. Consequently, a Cut is used as a base class to generate the tool-paths and track information for Boolean Difference methods. The Cut data-structure is further detailed in the Robotic Fabrication chapter 7. To summarize, Cut is a volume that needs to be removed from a female or a male element. Cut is

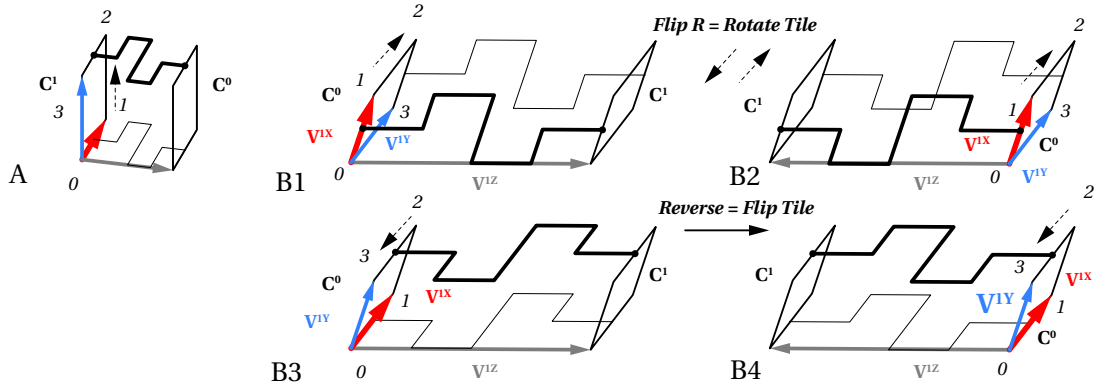


Figure 5.11 – The geometric principle behind the joinery generation is the change of basis transformation of the joint polygons (a). The user has to track the correct orientation of a tile (b1-b2-b3-b4) when using such a method.

a data type to store properties for tool-path generation so that Cut-derived classes could apply tool-specific machining methods. Since all cuts are described as pairs of polylines, there is an equal relation between a joint visualization and its tool-path output.

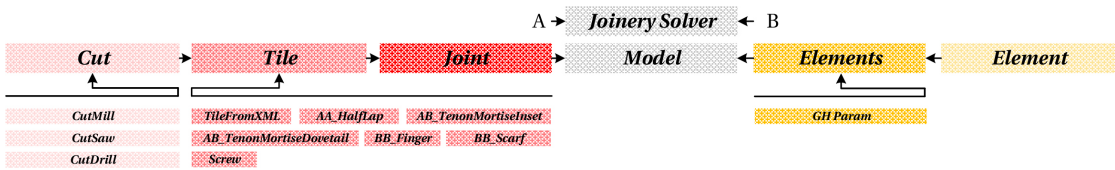


Figure 5.12 – Data-structures of the Joinery Solver: a) Joints and b) Elements. Each of those data structures contains the sub-structure: a) Joint, Tile, Cut, and b) a list of Elements.

## 5.4 Search Methods for Connection Zones

Connection zone detection is needed: a) to identify where a joint is located, (b) category of a joint, and (c) indices of elements connected by a joint (adjacency). The detected connection areas are indexed by color to have a visual feedback of a joint type. The search can be costly due to  $O(n^2)$  element-to-element iteration without considering the number of parts at each element. Therefore, an efficient R-Tree Bounding-Box search [63] is applied to check if a pair of objects are colliding within their bounding-boxes. Each bounding-box is inflated to avoid floating point errors when boxes are touching side by side (see Figure 5.13 A). Additionally, collisions between aligned bounding-boxes are checked because the RTree method can only identify collision pairs within world-aligned bounding-boxes. Then the algorithm performs a more accurate search. Four intersection methods are applied: (a) Curve-to-Curve, (b) Face-to-Face, (c) Plane-to-Face, (d) Mesh-to-Mesh (see Figure 5.13), depending on a connection type. Besides R-Tree search, it is possible to apply AABB, BSP, Octree, K-DTree, or Spatial-hash search. The R-Tree is chosen due to the existing implementation in the RhinoCommon library[138].

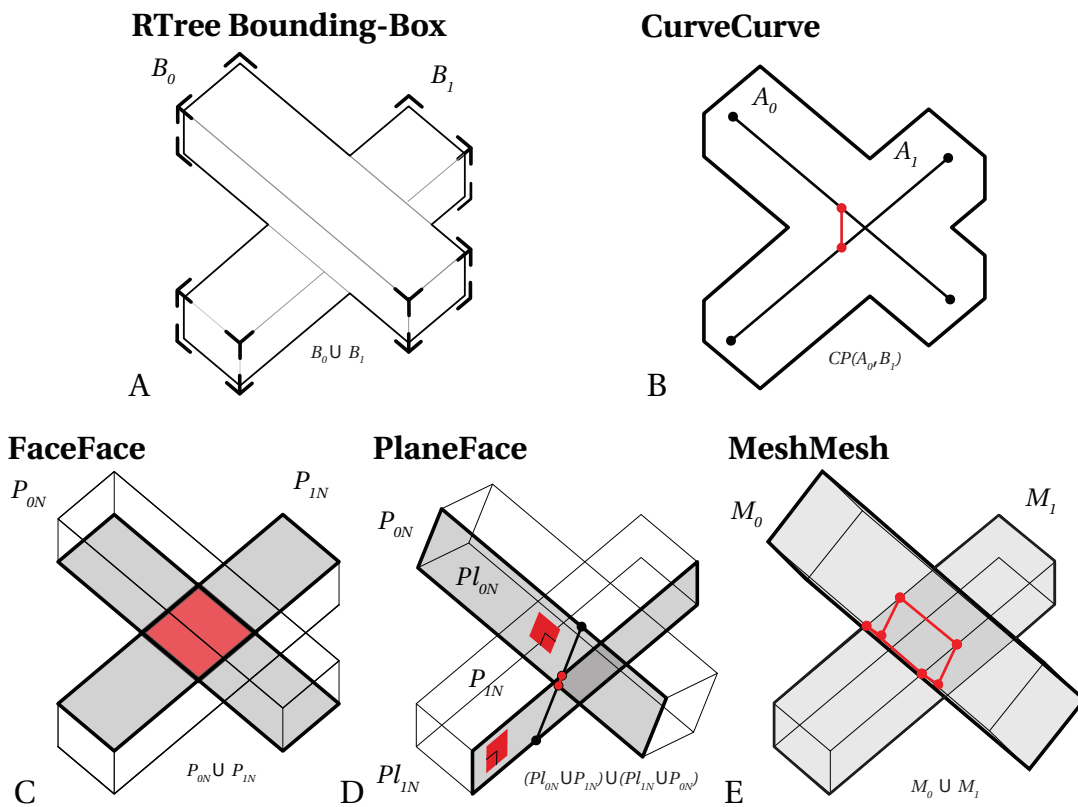


Figure 5.13 – Search methods. RTree search is applied as the first step for all the elements (a). The Curve-Curve intersection helps to define elements when only curves are given (b). The joint areas are identified by the Face-to-Face intersection (c), Plane-to-Face (d), Mesh-to-Mesh (e). Depending on connection type the last three methods could be performed all together or only one of them.

### Curve-to-Curve

The curve-curve search method is performed to define an element type around linear elements (see Figure 5.14). The curve closest points are found using the curve proximity method [138] that indicates the closest parameters on each curve (see Figure 5.13 B). From the axial intersection it is possible to derive the following connection types: a) end-to-end, b) cross, or c) side-to-top. This method's detailed study is described in the first version of the Joinery Solver, including straight and curved axes [171]. The function also considers local radii to define a size of an element at the connection zone. The method measures if curves at the closest eccentricity point are parallel within a given tolerance (see Figure 5.14 A) or non-parallel (see Figure 5.14 B). In the non-parallel case, elements may cross each other (see Figure 5.14 B1-B2), or form a side-to-top joint. By measuring how close the eccentricity point is positioned to the middle point between the two axes, it is possible to identify whether the element has to form the cross or side-to-top joint. After this method is performed, an additional Face-to-Face, Plane-to-Face, and Mesh-to-Mesh have to be computed to identify the connection zone topology.

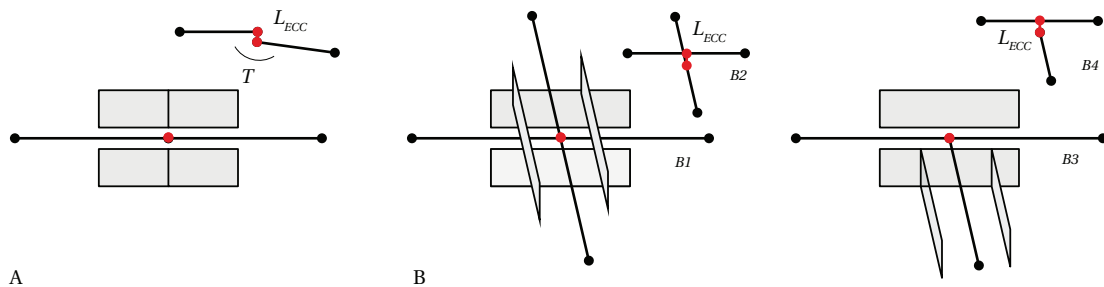


Figure 5.14 – Curve-to-Curve search method for the following types: a) side-to-side, b) cross, and c) side-to-top. The curves could cross (b1-b2) or stop at one end (b3-b4).

### Face-to-Face

The face-to-face method searches for the co-planar element's faces. The co-planarity is validated in two steps: a) planes Z-Axes, derived from the closed polylines, are pointing in the same or opposite direction, and b) a distance between the planes is close to zero. This operation is  $O(n^2)$  because of the search between current and all the neighbor element outlines. Then, a 2D Boolean intersection method [9] is performed (see Figure 5.13). There are three possible configurations: A) side-to-side, B) top-to-top, C) side-to-top. Side-to-side and side-to-top have an additional direction property  $L_{JAC}$  that is necessary to give an orientation to a joint, including the non-symmetrical or locally coupled joints. In contrast, the top-to-top case could only employ extra fasteners, such as screws or dowels. This procedure takes half of the time in relation to the overall search, including the RTree method. If the intersection is valid, a) there are no triangular faces, and b) small segments are compared to the minimal touching face, then an assumption is made that there must be a connection. Finally, a joint object is created pointing to the element edge and face indices, joint areas, and types.

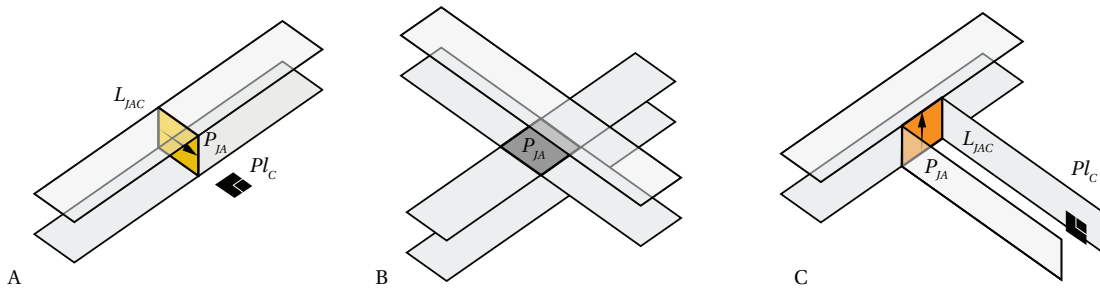


Figure 5.15 – Face-to-Face search: a) side-to-side, b) top-to-top, c) side-to-top. Joint orientation ( $L_{JAC}$ ) by intersecting the central plane of the element ( $Pl_C$ ) with a polygon ( $P_{JA}$ ).

### Plane-to-Face

The Plane-to-Face intersections are computed using the top and bottom outlines and their respective planes (see Figure 5.16 A). There are four possible intersection combinations from a total of four polygons, and their planes resulting in four lines. Then intersection lines have to be oriented to one direction (see Figure 5.16 B) to create the bounding volume (see Figure 5.16 C). Afterwards, a maximum bounding volume must be found by projecting all the intersection line points to the centre line, where the centre line is an average of the two corner lines (see Figure 5.16 D). Then the centre-line is adjusted to the maximum length by projecting all the initial lines endpoints to the centre line (see Figure 5.16 E). Hence, the most extended line's orthogonal planes form the maximum bounding volume using the line-plane intersection (see Figure 5.16 F). This search method outputs a Joint that contains a list of properties, pointing to element indices (adjacency), joint areas, and types. Lastly, the joint object is appended to the overall connection list in the Model data-structure.

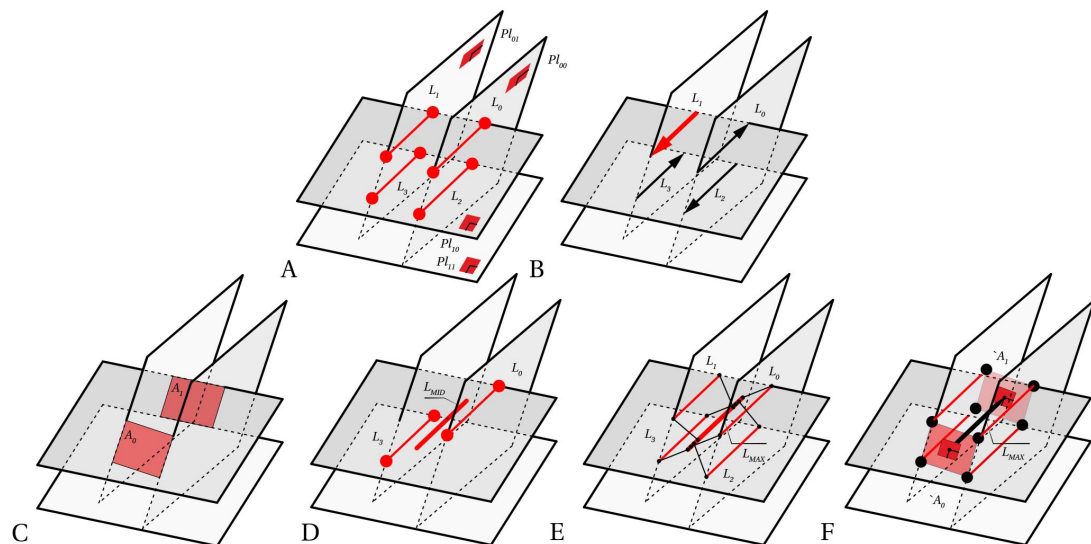


Figure 5.16 – Plane-to-Face search: a) two pairs of faces, b) Plane-to-Curve intersection for 4 combinations, c) intersection area, d) centre line from diagonals, and e) the bounding area.

### Mesh-to-Mesh

The Mesh-to-Mesh method employs a triangular mesh intersection between two elements (see Figure 5.17). The Mesh-to-Mesh search aims to cut one volume from the another Mesh. This method finds intersection lines between two closed objects (see Figure 5.17 A). If there are no intersection lines or if they are co-planar, the collision is not valid. An assumption is made that it is possible to compute a minimal bounding-box using each element's centre face plane and the intersection lines. The box is computed two times – one for the first element, and two for the other element, using their respective central planes. The bounding-box with a longer edge from the smallest box edges is considered the cutting volume (see Figure 5.17 B). A pair of rectangles is then extracted from a box where the first rectangle lies within the intersection lines (see Figure 5.17 C). These two rectangles define the cutting area for the Tile change of basis transformation. When the pair of rectangles is computed, the joint is added to the joints list for the further computation.

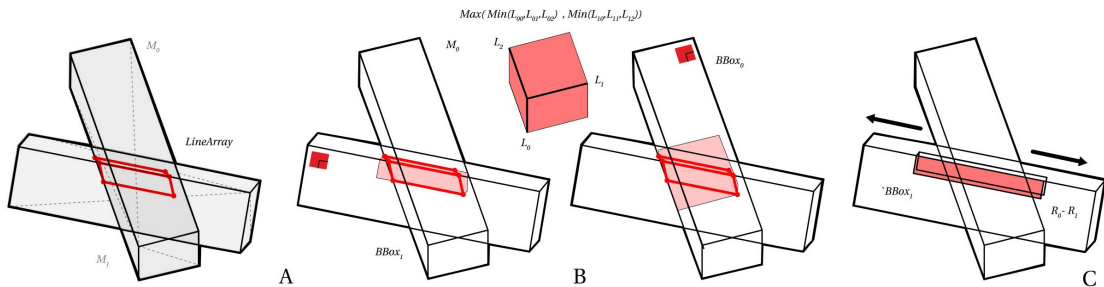


Figure 5.17 – Mesh-to-mesh search: a) Mesh intersection result is a series of lines, b) then a bounding-box is computed for each pair of elements, and c) one of the two boxes is selected and extended.

## 5.5 Connection Types in a Model

The joints that are found in the search methods are stored in the Model data-structure together with the sorted list of Elements and Tiles. The type of a search method depends on a Tile category. For example, if the user would like to compute a cross joint then only the plane-to-face search is performed in the Model. Elements that are stored in the Model, initially do not have any adjacency information about the neighbors. The Search methods help to identify connectivity between elements and a joint type. Secondly, the Model's methods redirects geometry generation of a connection based on a found type, such as a) cross, b) side-to-side, or c) side-to-top. Thirdly, Boolean operations are computed based on the oriented Tile geometry. Finally, the user can see the output information, such as a) initial elements with joints (oriented tiles), b) a graph (Joint List) to show the adjacency, and c) a tool-path (Cuts). The following chapters explain the connection topologies by examples of each joint type.

### Side-to-Side Topology

**Side-to-Side - Algorithm Definition** The side-to-side connection is a joint that shares a surface formed between the top and bottom outlines (see Figure 5.18). Structures, such as slabs, vaults, and walls, belong to this category. Several conditions need to be considered: a) elements are rotated in the contact zone; or b) they are in-plane (see Figure 5.19).

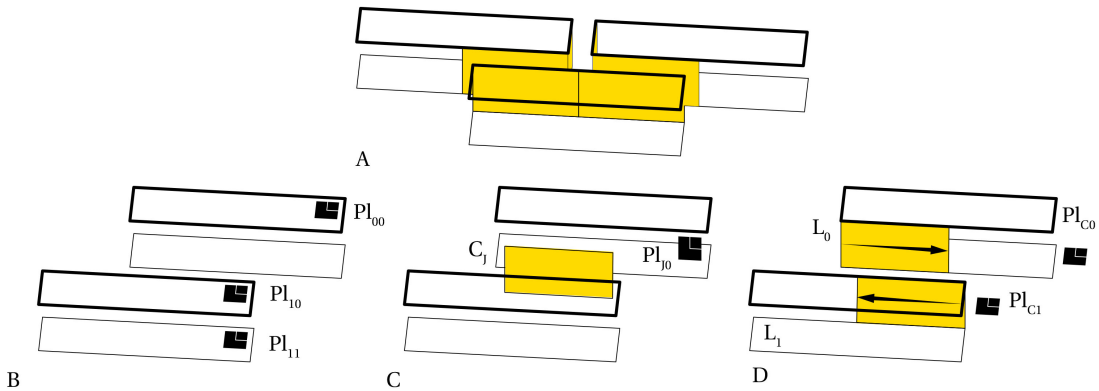


Figure 5.18 – Side connection generation: a) connection area, b) top and bottom planes, c) connection area plane, and d) connection area directions.

The rotated option is based a boundary rectangle method (see Figure 5.19). The solver uses a pair of rectangles to generate a joint. As a result, a plane is needed to define the boundary from the intersection zone. Firstly, the plane is created from an approximate normal contact zone by averaging the cross-products of the joinery area polygon vertices (see Figure 5.19 A). The X-Axis of the connection area plane is aligned to an average normal of adjacent elements. Secondly, the aligned bounding box is computed around the contact area corner points (see Figure 5.19 B). Thirdly, the bounding area is extended, depending on the distance values given by the user. The depth of the connection is chosen depending on the thickness of adjacent elements (see Figure 5.19 C). Finally, Tiles are transformed into the connection area and assigned to the corresponding elements (see Figure 5.19 D).

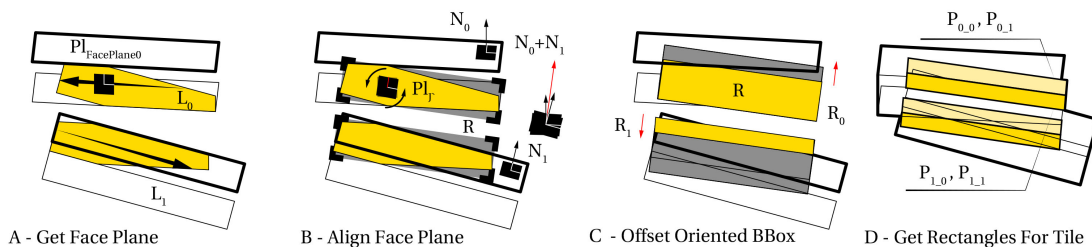


Figure 5.19 – Side-side connection in rotation: a) connection-zone, b) bounding-area generation, c) offset bounding area by element thickness, d) create polygons for Tile mapping.

When elements are in a parallel orientation (see Figure 5.20 A  $L_0$  and  $L_1$ ), there are two distinct sub-categories: a) out-of-plane b) in-plane (see Figure 5.20 F), based on Dihedral angle. The

Dihedral angle is a value between two faces of an element's top or bottom outlines (see Figure 5.20 C). In-plane joints can be hardly machined below the limit of thirty degrees and lose structural integrity due to the loss of contact zone. Afterward, it is necessary to compute a pair of rectangles for the change of basis orientation (see Figure 5.20 D). The pair rectangles differ for in-plane and out-of-plane joints. In both cases, a single Tile is oriented twice to adapt to two orientations of an element. The Figure 5.20 D (bottom) shows the intersection between end-planes and an array of four planes: a) the current element top plane, b) the offset side plane, c) the current element bottom plane, and d) the offset side plane in the opposite direction. The same process is repeated for the next element with its respective top and bottom planes. The out-of-plane pair of rectangles are computed using the same end-planes, and differently to the in-plane case, pairs of planes from both elements. The bounding rectangles must be shifted one time in the neighbor element side to have a correct Tile orientation (see Figure 5.20 E).

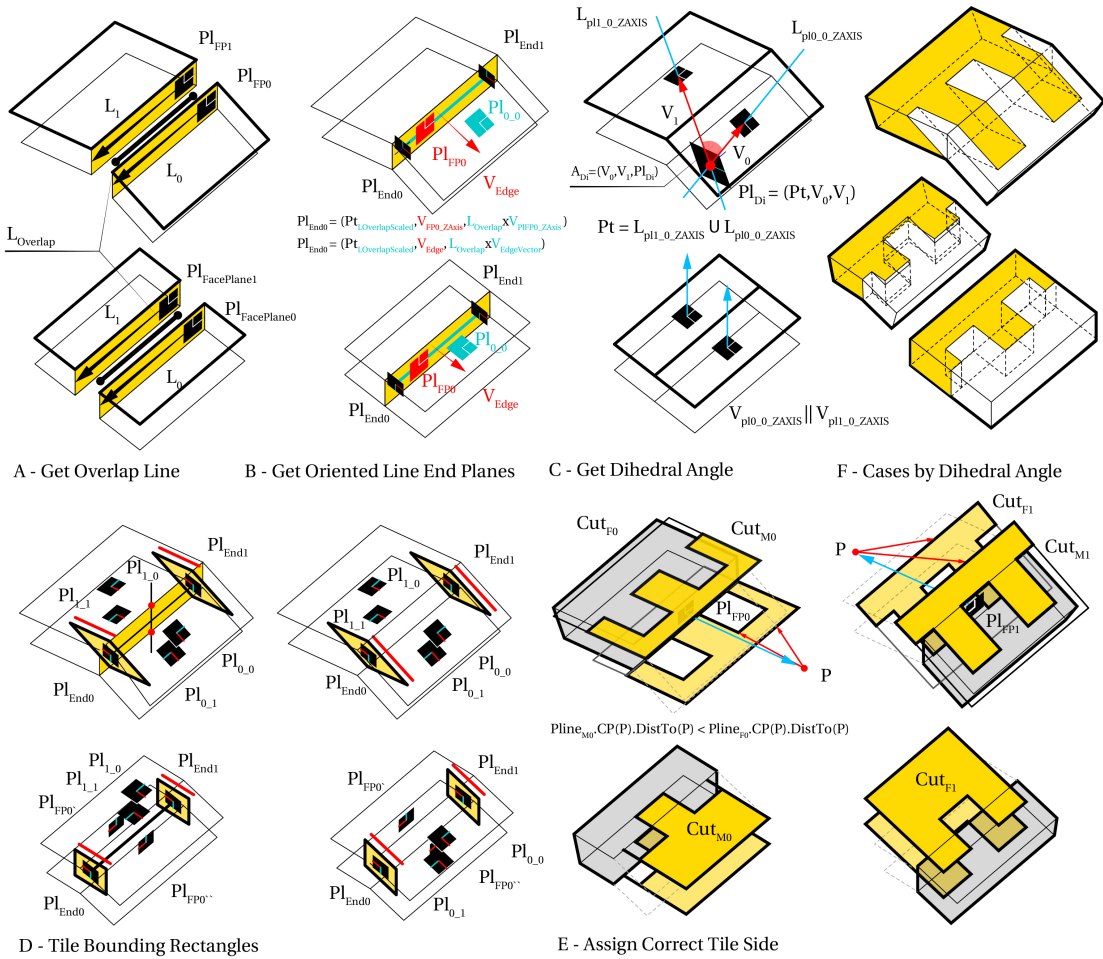


Figure 5.20 – In-plane (bottom row) and out-of-plane joints (top row) generation: a) get the overlap line, b) get the oriented line end planes, c) measure the Dihedral angle, d) bounding rectangles used for change of basis transformation, and e) assigned to the male and female elements.

Face-to-Face connection zones are also applicable to raw wood joinery. For example, a raw wood beam can be connected in a) a parallel orientation (see Figure 5.21 A), b) a 2D oblique angle (see Figure 5.21 B) or c) a 3D shifted angle (see Figure 5.21 C). The intersection between the two cylinders might not be evident since tree trunks vary from beam to beam. Therefore, a simplification is taken to have the polygonal element representation with a reference object. Depending on the design, the Face-to-Face area must be extended to fully overlap with the reference object.

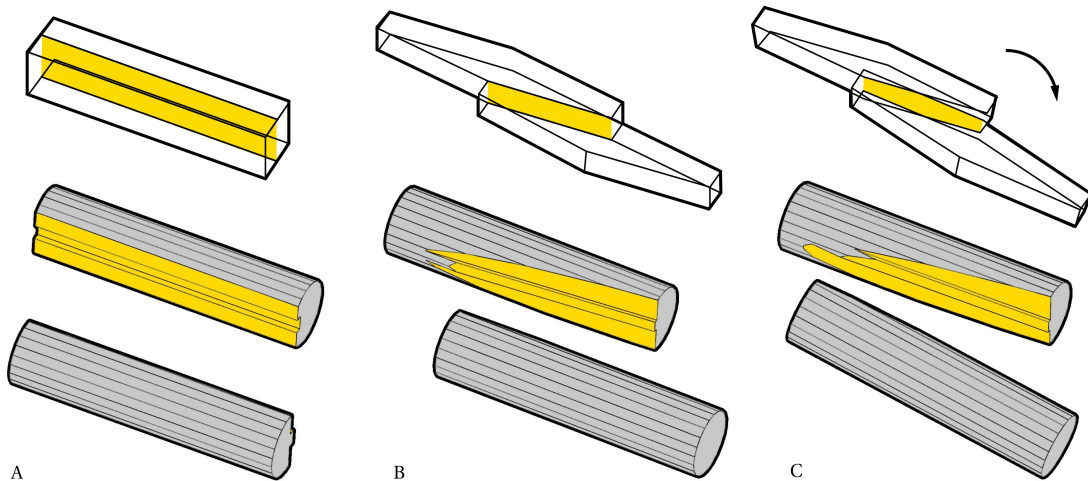


Figure 5.21 – Minimal polygonal geometries (top) and reference objects as a triangle Mesh for: a) the parallel case, b) the single rotation, and c) the two rotations.

**Side-to-Side - Stacking** The side connections for solid lumber have to be as simple as possible because the surfacing of large contact zones is a relatively slow process. The machining operation suggests the design of a joint – grooves along the contact zone or a series of external connectors, such as dowels (see Figure 5.22 B-C). Both systems can be used together since the first option blocks one translation vector, while dowels could interlock the other direction (see Figure 5.22 C). The beams can be interlocked sequentially using angled dowels as shown in Figure 5.23 . The proportions of one single tenon could be changed as well as the number of grooves. This technique is commonly used for flat slab or wall systems since the curved and discretized surfaces might contain only a partial connection zone seen in the larger assembly. The larger-scale studies employ solid lumber in the form of bricks that are stacked side by side (see Figure 5.24 and 5.25).

The algorithm is tested within a series of models that contain planarized elements, including a) a shell, b) a flat slab and c) a stacked wall [169]. The top surfacing is necessary if the structure is used as a floor. The top surfacing falls into a custom cut category because a connection zone concept cannot describe it. Slab systems in raw wood are usually combined with additional material, such as concrete or several sub-structure layers [139] to obtain a flat walkable area or to avoid the extra material removal.

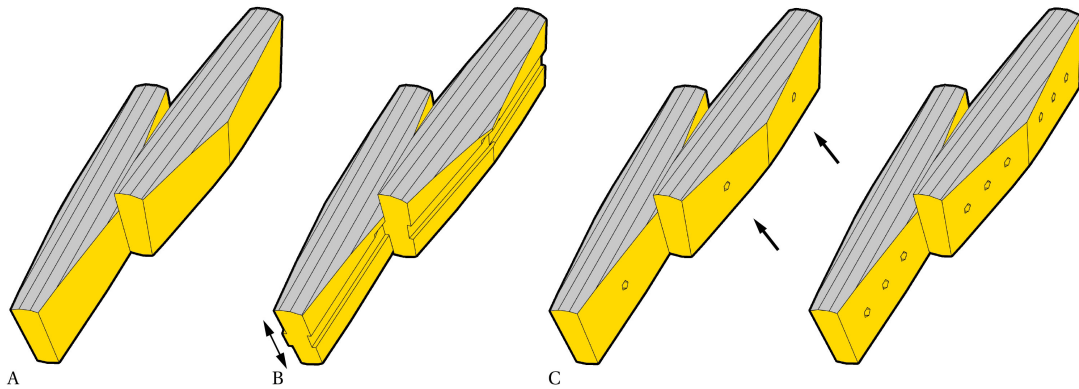


Figure 5.22 – Side connection sub-categories: a) surfacing, b) grooving, c) oblique fasteners.



Figure 5.23 – Side-to-side connection using wooden 10 mm in radius dowels.

The same principle applies to a regular linear array of timber and other tessellations, such as a hexagonal pattern 5.25). If linear elements map a curved surface, in this case, raw woods, they could hardly have a regular equilateral tiling. Panelization of double-curved surfaces often requires close to circular elements to avoid eccentricities between elements [124]. The connection area and curvature of a surface have a direct relation – beams must be oriented in the lower direction of a surface (see Figure 5.25 A), instead of the higher curvature resulting in eccentricities (see Figure 5.25 B). As opposed to the timber plate fabrication, raw woods must be mounted and strapped one at a time, meaning that the time for cutting and fixing each timber increases linearly, therefore the tiling density is a compromise between the fabrication constrains, surface curvature and the dimensions of a tree trunk.

## Chapter 5. Joinery Solver

---

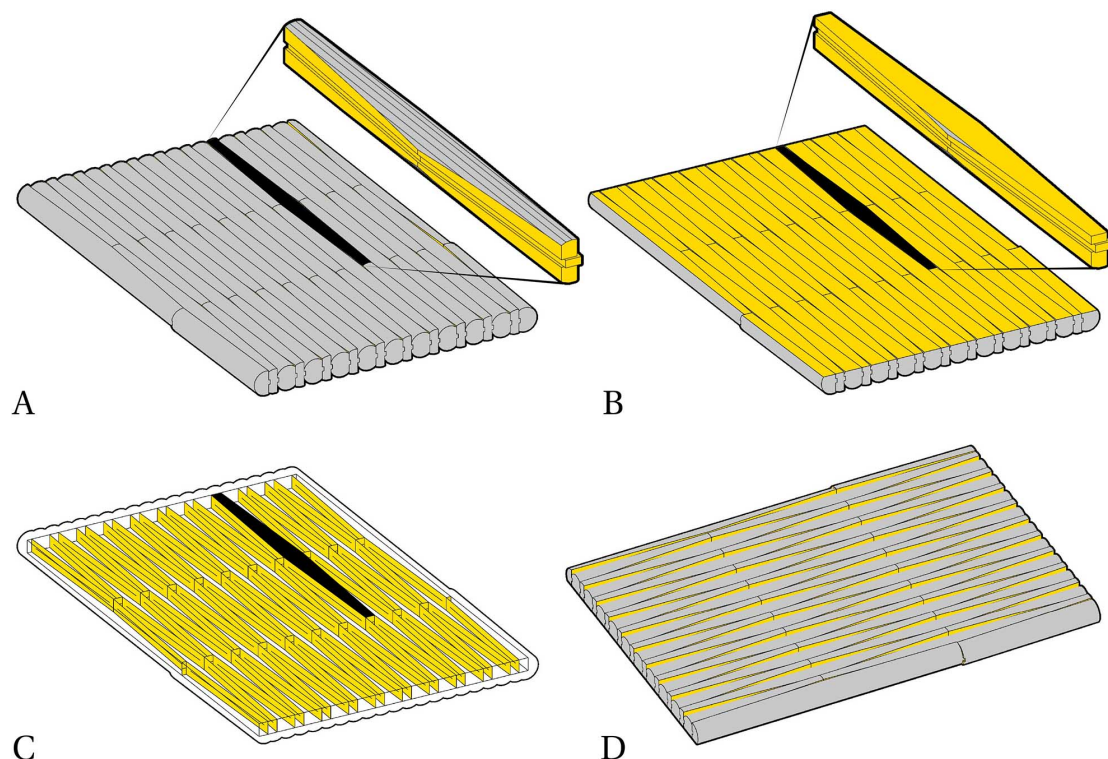


Figure 5.24 – Stacking timber linearly to form a) a slab/wall system, b) flat cut from, c) hexagon elements, and d) the bottom part of the slab.

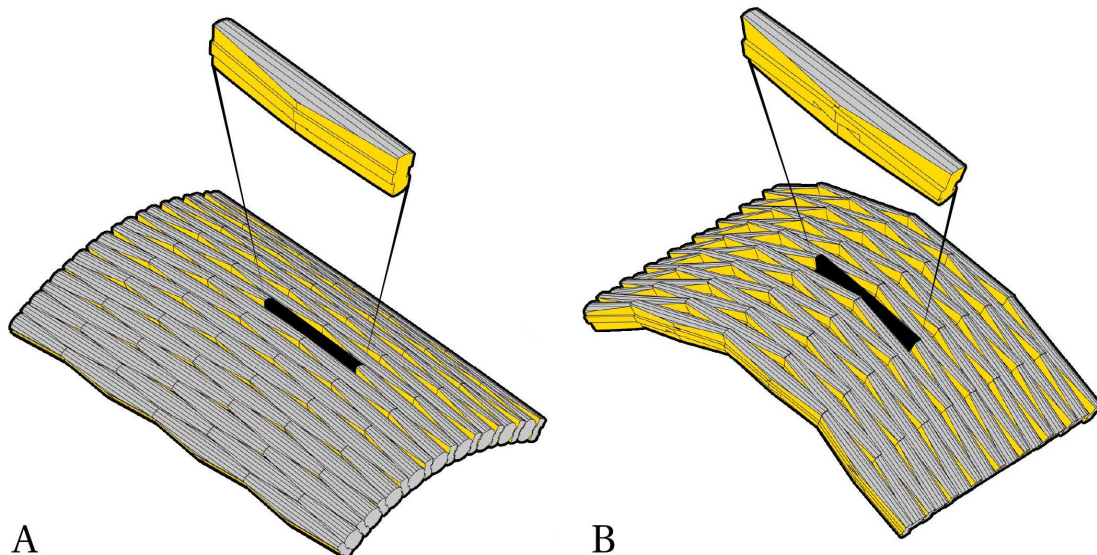


Figure 5.25 – Curved surfaces: a) curvature along shorter width of a beam, b) longer edge of a beam.

**Side-to-Side - Physical Connections Tests** Technical tests helped to understand the joinery type needed to connect a pair of timbers side-by-side [169]. The side connection prototypes were the first ones that inspired the development of the joinery algorithm because of the following reasons: a) the necessity to automate the manual modelling process of timber joints, b) including tool-path generation, c) joint visualization, and d) reuse of the workflow for similar case studies. The tool-path safety is the primary goal because cutting raw wood is more complicated than machining timber plates. Fabrication of timber plates is mainly a 2D problem: the CNC cutting motor must stay above one plane that is restricted by a maximum rotation of the CNC table. In contrast, free-form lumber must be lifted in the air, fixed to a specially designed rig, and cut without a collision. The manual preparation of the tool paths frequently resulted in minor accidents due to human error when preparing tool paths, requiring constant monitoring to stop the cutting at the right time. In this case, there is no reference plane, and the cutting motor must always point outwards the work-piece. In the short term, manual preparation for cutting several timber pieces can be faster than developing the Joinery Solver because many issues need to be thought of and physical experiments have to be performed beforehand. In the long term, the same methodology could be re-applied for both visualization and cutting. The following physical tests were performed: a) the hexagonal bricks with dowels, b) the longitudinal Finger joint, c) the short-end Finger joint, and d) the perpendicular-to-grain Finger joint (see Figure 5.26).



Figure 5.26 – Technical tests for the side connections: a) surfacing and dowels, b) longitudinal, c) short-end, and d) perpendicular-to-grain Finger joint.

**Side-to-Side - Frames** The side-to-side connection belongs to another large group of short-end connections. Scarf, Tenon-Mortise, Miter, with or without additional fasteners. The most common application of this joint is the elongation of straight beams if a longer span of timber is needed. A relatively minimal shift is possible to maintain the contact zone for the angled cases as shown in Figure 5.27. The short-end wood-wood joints are relatively strong in compression but weak in traction. Therefore, they require additional fasteners, ranging from timber keys, metallic bolts, cross-dowel-nut connectors to metallic plates [26]. Several models were machined to test the simple scarf joint using robotic milling (see Figure 5.28). The wooden dowels block the Scarf joint by drilling holes in an oblique angle. Two dowels are positioned at the centre of a connection node. In such a way, they have the maximum connection area. The joint was rigid enough within the prototype scale, and for larger assemblies, additional keys and fasteners would be necessary.

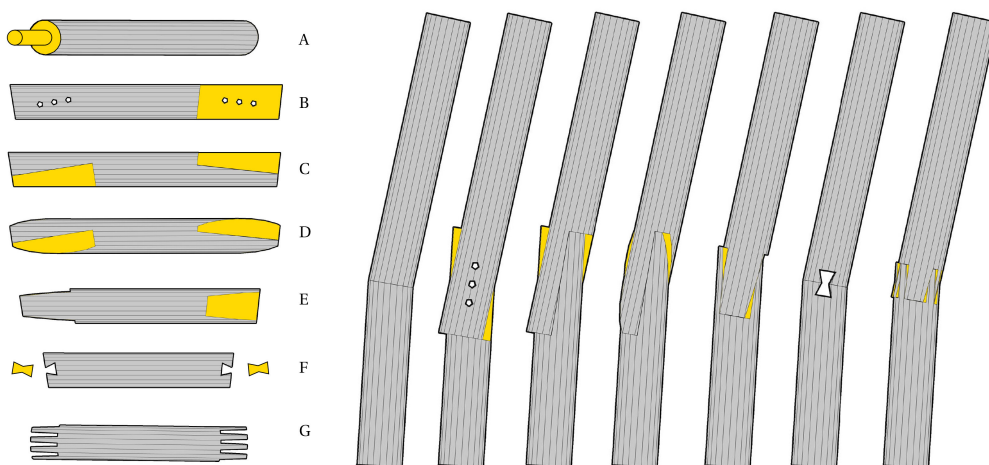


Figure 5.27 – Short-end connections for a round section: a) Miter + round dowel, b) Scarf, c) Double-scarf, d) Double-scarf-angled, e) Finger, f) Butterfly-keys, and g) Feather.



Figure 5.28 – Plain Scarf joint (a) connected using two dowels (b). Dowels are inclined to block the timber assembly. The joint depends solely on external connectors.

The short-end connections would benefit the most when using crooked wood (see Figure 5.29). The connection could be detected by intersecting each tree trunk's centre axis (see Figure 5.29). The tangent at the intersection point determines the orientation of the node (marked in yellow). The rectangle direction is computed using an average of the two tangent axes. The main benefit of using bent raw wood is the maximum overlap of the two timbers because they are close to a parallel orientation in the connection node.

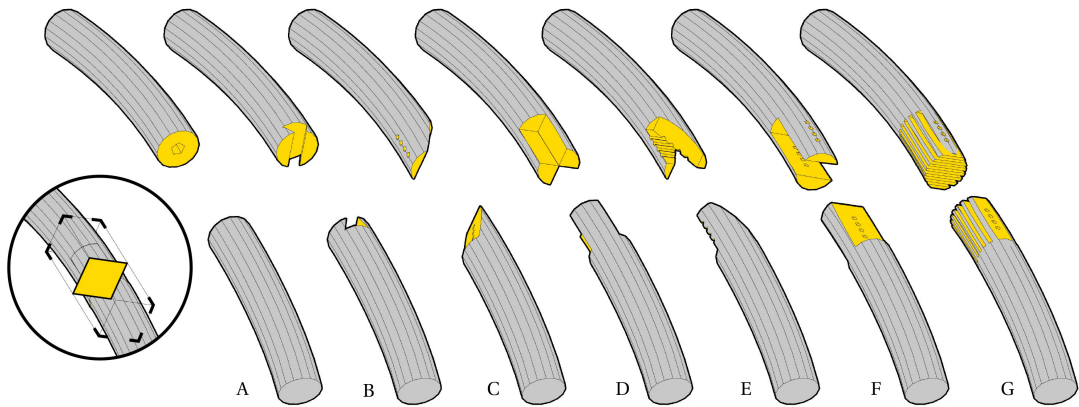


Figure 5.29 – Side-to-side short-end joint for the round section using a crooked timber : a) Miter, b) Butterfly-key, c) Scarf, d) Double-scarf, e) Double-Angle-scarf, f) Finger, and g) Feather.

The Scarf joint was re-employed in a prototype from forks (see Figure 5.30). In this case, relatively small tree forks were used for a Vierendeel truss acting as a three-valence joints whose ends had to be elongated using straight raw woods. A plain scarf joint connects two flat planes, meeting at a close to a parallel angle of the beam axes. The plain scarf was chosen for several reasons: a) the fastest and simplest fabrication method, b) an aesthetically simple joint, and c) the ease of assembly. The tree fork prototype served as an experiment to understand how one can accurately position a rough timber in the machining setup, then precisely fabricate the tenon-mortise and scarf joints. In total, three forks and four straight beams were cut to build a triangle Vierendeel truss. This fabrication experiment also shows that it is necessary to combine tool-path with joint geometry generation because only one joint Tile had to be solved before cutting started, whereas the rest of the tool-path, from the similar joints, is generated automatically. For more extensive experiments, when applying the same joint type, external connectors have to be studied in more detail.

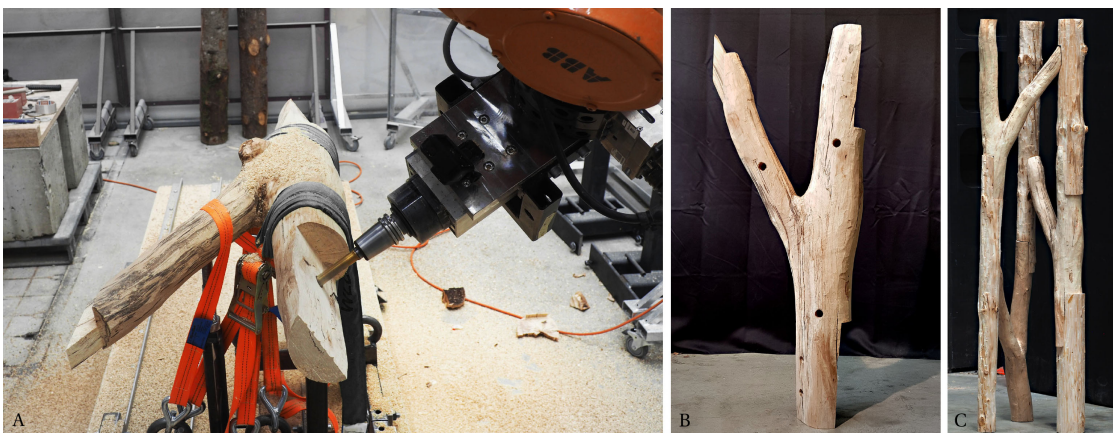


Figure 5.30 – Fabrication of the Scarf joint (a) and the tree fork after it is demounted from the fabrication rig (b) and the assembled prototype (c).

**Side-to-Side - Extension of the method to Timber Plates** Side connections could be applied to a timber plate structure when two elements share one side face without any rotation. Sub-categories, such as dovetails and snap-fit joints, start from the finger joint specification (see Figure 5.31). The finger joints have an angle constraint derived from the CNC fabrication – sharp oblique angles below thirty degrees are hardly possible. It is feasible to overcome this constraint by employing saw-blade or perpendicular-milling, but are hardly used in practice. The finger joints — a) in-plane, b) out-of-plane — look similar in shape, but they require a different geometry generation method. The exploration of plate geometries within the proposed Joinery Solver is needed because the research focused on locally sawn-timber, including timber boards and irregular beams. Furthermore, the global joinery development is highly inspired by previous research in timber plates [131] that helped to understand the plate-outline methodology and extend this approach to the beam-like elements. The structures of timber plates have a significant advantage in fabrication, comparing to beam elements because only a 2D contour has to be cut. Furthermore, multiple elements can be machined at once. The joint generation is simpler than the previously mentioned wood-working joints as it can be described as a 2D problem – a 2D contour needs to be inserted into a side of a plate. Consequently, 3D BRep or Mesh Boolean methods are not needed when relying on the fast polygon intersection (see Chapter 5.6).

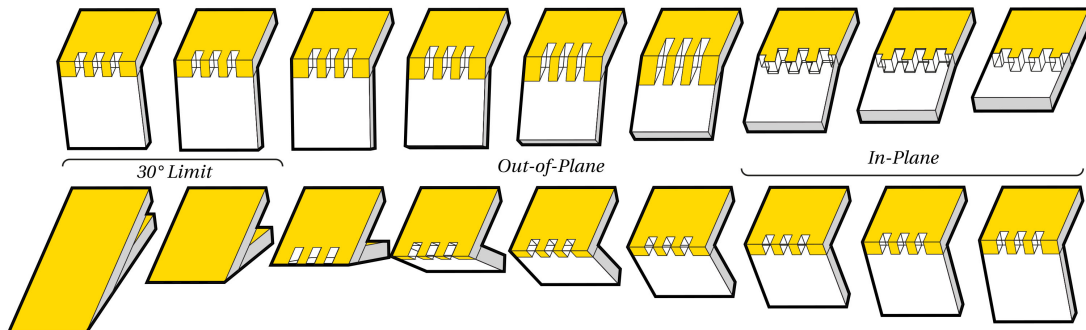


Figure 5.31 – Finger joint application for timber plates within a 30-degree limit.

The Joinery Solver can change the angle of the finger joints by specifying an edge direction using a list of lines provided by the user (see Figure 5.32 A). The angle joints are necessary for the assembly sequence. In some cases, orthogonal joints could not be inserted without changing the joint direction (see Figure 5.32 B-C-D). The oblique joints are possible due to the 5-axis CNC machining. Furthermore, the change of an angle is generally applied to cross-laminated timber. The tenons break easily in solid lumber if not oriented parallel to the wood grain orientation. The Joinery Solver could apply different types of joints in one element by detecting each plate's Dihedral angle and the user specification of the input Tiles. The current implementation of Tiles have methods for tenons, keys, dovetails (see Figure 5.32 D).

## 5.5. Connection Types in a Model

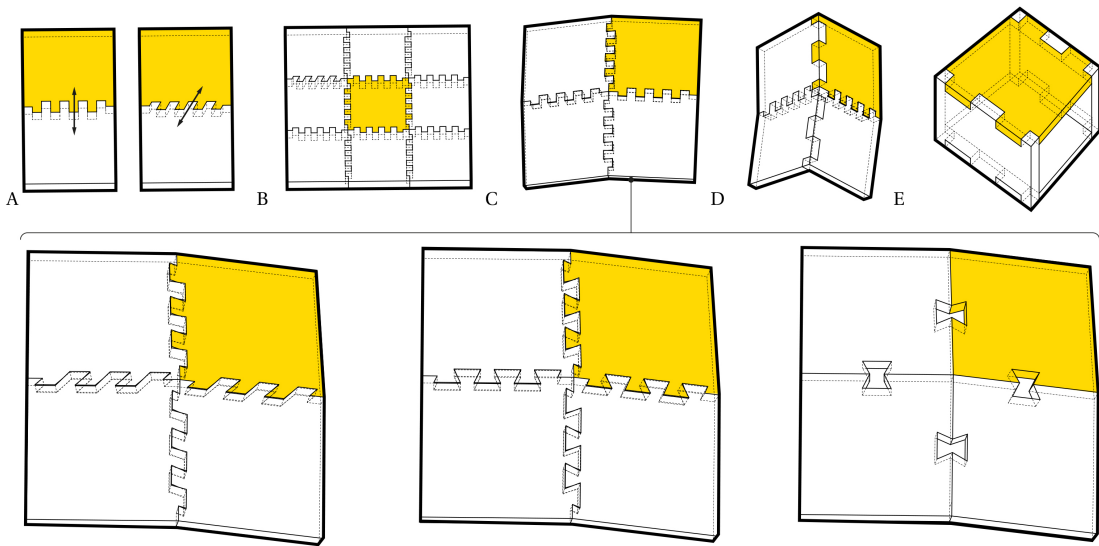


Figure 5.32 – Test models for the development of the Joinery Solver: a) Finger joint perpendicular to an edge and inclined, b) joinery within multiple edges, c) multiple in-plane Finger joints from the user specified Tiles, d) mixed in-plane and out-of-plane Finger Joints, and e) out-of-plane Finger joints.

Finger joints are usually combined with the Miter joint to ease the assembly. They are used for geometries that have nodes with a higher valence of three. Meshes with a higher valence than three could be hardly extruded using planar facets, except for simple cases, such as Platonic solids, where the hybrid Miter-Finger joint could be employed (see Figure 5.33). The Miter joint option, together with other properties, such as the division of an edge and the angle of each tenon, could be controlled by the user interface.

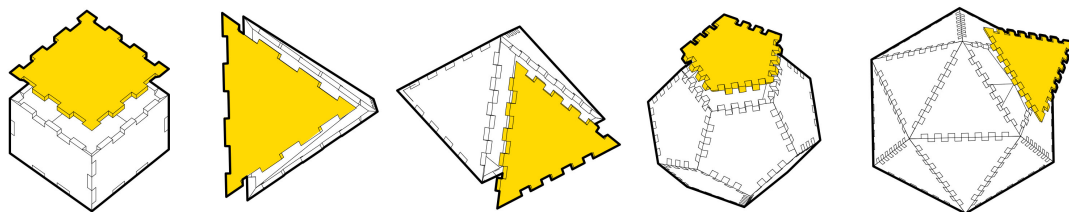


Figure 5.33 – Finger joints applied to platonic solids using Miter joints for the higher than the valence of three.

One Tile could be reused within self-similar edges without measuring edge length or Tiles could be rebuilt per each edge, depending on its length (see Figure 5.34). The first method is faster because the Tile data structure needs to be duplicated once, while the latter needs to be recomputed. The computation time is not evident within plate structures because geometry generation is applied for polygons only. Whereas beam-like geometry results in a slower execution speed as solid Meshes are duplicated or recomputed at each node. This notion of rebuilding a Tile versus copying helped for the fabrication too. The Tile change of basis transformation often results in skewed geometric shapes. However, milling these geometries

## Chapter 5. Joinery Solver

---

would not have a valid result because the flat tool must always stay oriented perpendicular to a plane. For beam elements, each pair of polygons are always projected to form an orthogonal tool-path after the change of basis transformation. There is no such projection in the plate structures because CNC machining can cut joints with a milling tool moving in an oblique angle.

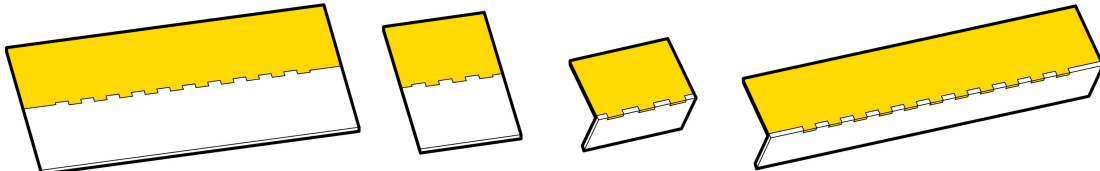


Figure 5.34 – Tiles with a varying number of finger joints per edge.

The full design process could be seen in Figure 5.35. Firstly, the connection areas are identified (see Figure 5.35 A). The middle line within each connection rectangle marks the direction of a joint. It also shows that all plates are parallel between each other. The edge line is also used as a guide to form a joint plane together with adjacent element base-planes. Secondly, joints are oriented to a connection area and are rebuilt depending on the user's edge division value (see Figure 5.35 B). Tile outlines must lie within the plate top and bottom outlines to perform the boolean operation within an element and the joints. Thirdly, joints are merged with outlines and meshed for preview (see Figure 5.35 C). The fabrication model does not require meshing because outlines are directly used for CNC cutting. A larger number of examples applicable to timber plates could be seen in Figure 5.36 and the physical experiments are illustrated in Figure 5.37.

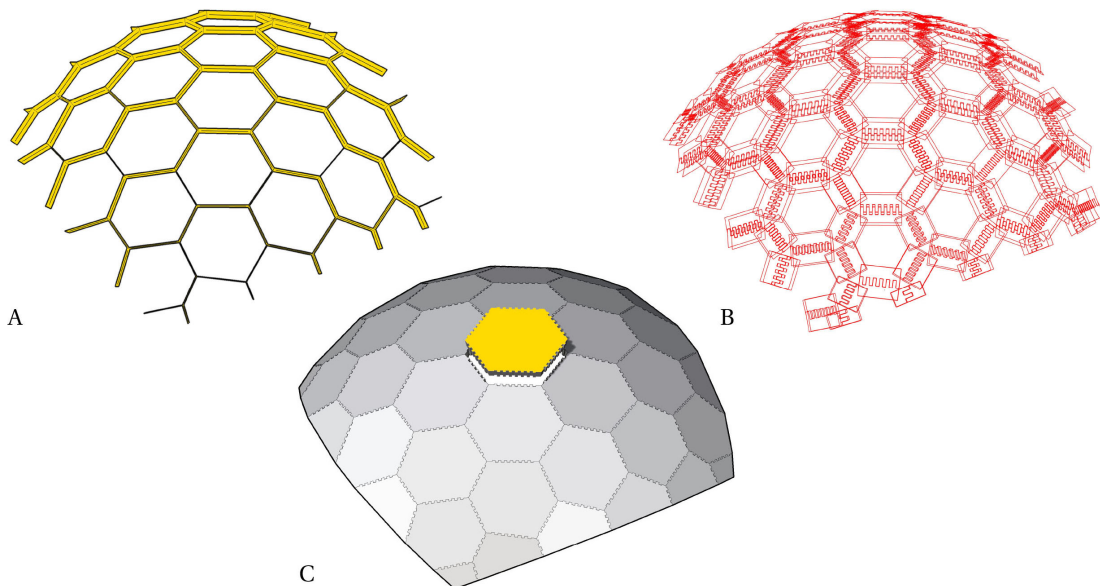


Figure 5.35 – Finger joint application for a planarized hexagonal shell: a) the connection area, b) the oriented Tiles, c) the result of the merged Plate outlines with the joint polygons.

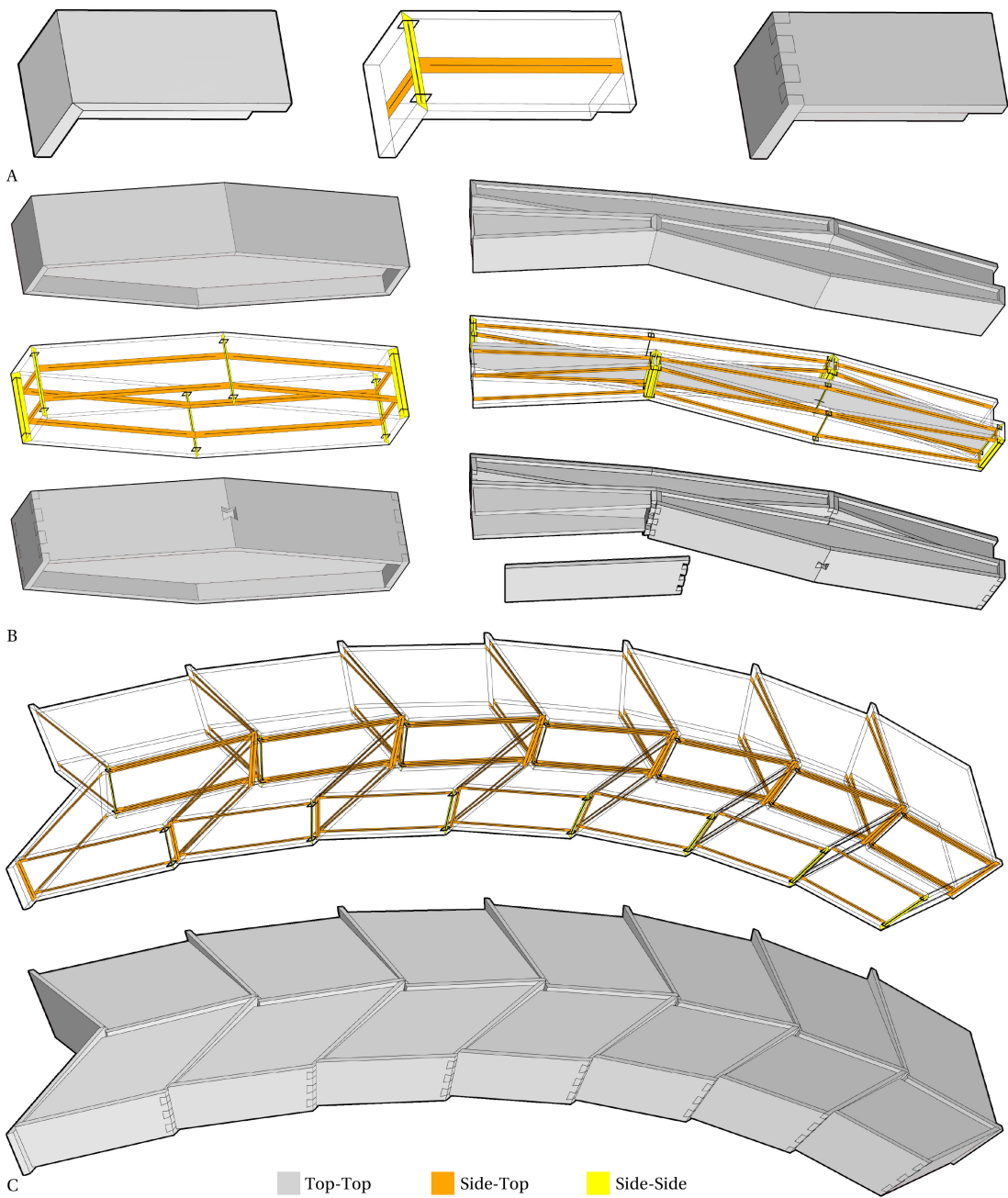


Figure 5.36 – Overlap face detection. Figures show all three types of detectable area: Grey colour – top-to-top, Orange colour – side-to-top, Yellow colour - side-to-side. Since the chapter describes only the side-to-side connections, only these joints are generated: a) single out-of-plane corner, b) hexagonal boxes with a butterfly-key and the out-of-plane Finger joint, c) multiple Dovetail joints within the side-to-side connection zone. Black rectangles mark the volume where a joint Tile is oriented.

## Chapter 5. Joinery Solver

---



Figure 5.37 – Side-to-side joint application in raw wood (a) and timber boards (b). The raw wood elements were flattened from three sides (a1), and the butterfly-keys were inserted (a2) into the milled half-key cuts (a3). Dovetail joints were applied to a collection of wooden boards as well(b1), to form the hexagonal boxes (b2) and the cross-laminated timber example using out-of-plane and in-plane joints (b3).

### Side-to-Top Topology

Joints, such as Tenon-Mortise, Ari-Kake, Half-Tenon, Bisector, Snap-fit could be represented by interconnecting a side of one element with the top outline the second one. In beams, it could be understood as an end of a curve interconnected with another curve at its center. For plate elements, the side face is connected with the top face of a neighbor plate. The algorithm definition follows the face detection method by identifying which side of an element belongs to the female and the male part of a Tile. The mortise must be assigned to the female element and tenon to the male element. Unlike the previously mentioned methods, the Tile orientation is essential in this topology (see Figure 5.38).

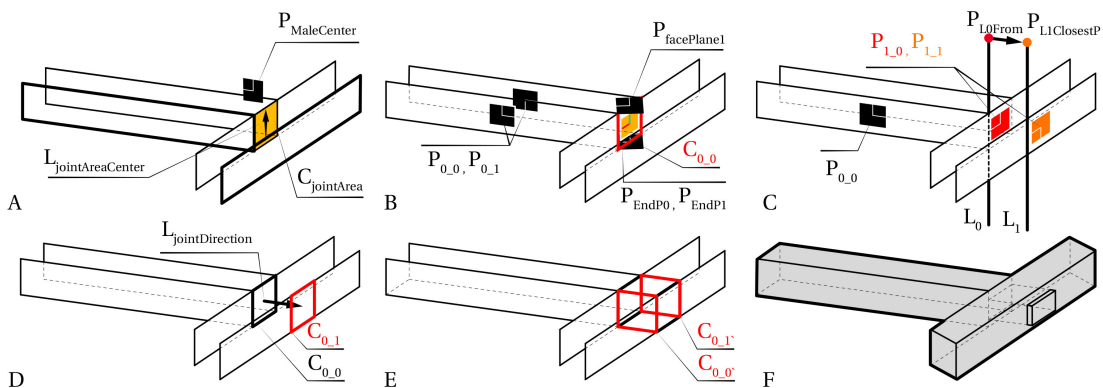


Figure 5.38 – Side-to-Top connection: a) joint area polygon is intersected with male element center plane to get a center Line, b) formation of the rectangle boundary, c) direction of a joint; the direction is the closest distance between the lines, d) rectangle boundary is moved by the plane, e) rectangle boundary is rotated to get the bounding rectangles and f) the joint geometry.

Joinery generation depends on the following steps: a) the joint-area-line detection, b) the boundary-rectangle computation, c) the offset vector, d) the joint boundary, and e) its reorientation to perform f) the change of basis transformation of a Tile (see Figure 5.38). Firstly, the joint line is computed by the intersection of the middle male plane with the joint area polygon (see Figure 5.38 A). Secondly, a rectangle is computed by the intersection of the joint-area-plane and the four other planes: a) the male plane top, b) the joint line start plane, c) the male plane bottom, and d) the joint line end plane (see Figure 5.38 B). Thirdly, the direction of a joint is computed by intersecting the top-male plane with the joint-area plane and its opposite plane. The result of these two intersections are the two lines. The direction between the first line start point to the second line the closest point defines the joint direction (see Figure 5.38 C). Then, the boundary rectangle is moved by the joint direction (see Figure 5.38 D). The rectangles must be rebuilt so that their faces match the male element top and bottom outlines (see Figure 5.38 E). Finally, the joint Tile is oriented to the boundary rectangles to generate the shape of the timber joint (see Figure 5.38 F).

## Chapter 5. Joinery Solver

---

The connection method depends on the element orientation. If the male element is rotated ninety degrees relative to the neighbor (see Figure 5.38 C), the joint direction changes as well (see Figure 5.39 C). This can be used as an advantage when a joint has to be generated in an orthogonal direction. There are several possibilities why the orthogonal joint is needed: a) the assembly sequence requires such a joint orientation, b) the oblique wooden joints lose integrity, meaning they can be easily disassembled, thus requiring a perpendicular joint, or c) if the fabrication is constrained by the orthogonal cuts. Suppose a user needs a different orientation, e.g. parallel to a male beam element. In that case, it is possible to adjust the joint's direction by inputting a list of lines positioned at the outline edges (see Figure 5.39 D (bottom)). The joint rectangle (red polylines) can be extended or reduced if, for example, a space must be left between corners of a plate or a joint must be enlarged to compensate for the irregularities of raw wood. The next geometry generation sequence is the same as discussed before, but it results in two angled cases (see Figure 5.39 F). As a consequence, the element's orientation is essential to the joinery generation method. Consequently, the alignment of elements is necessary to consider due to machining and the joint's topology. Different angle cases and applicability for beam and plate elements are shown in the Figure 5.40.

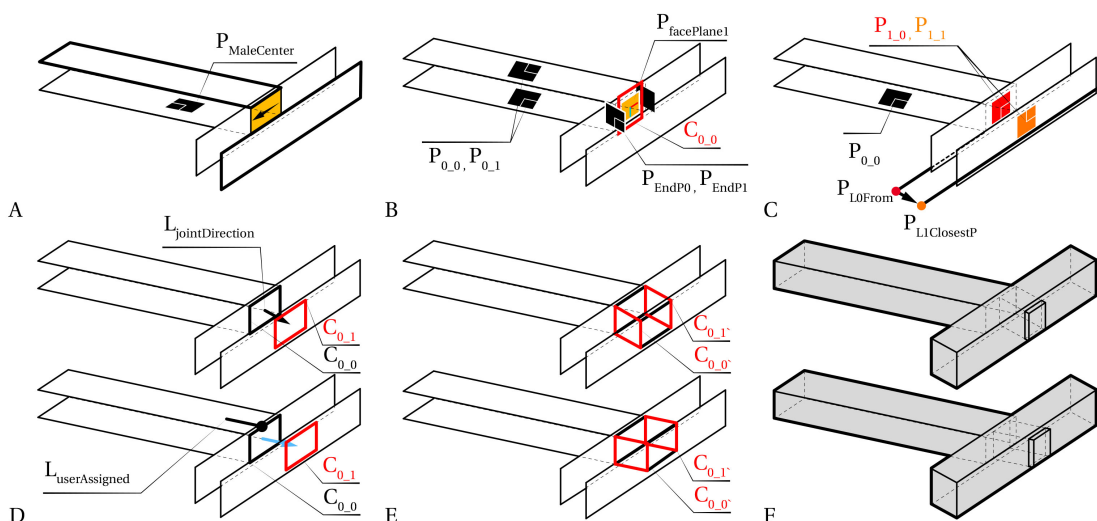


Figure 5.39 – Direction of a joint depends on the orientation of elements: a) joint line and b) area, c) perpendicular orientation, d) can be used as-is or adjusted, e) shift of rectangles, f) resultant of the geometric operations.

Tenon-mortise is one of the most often used joints in the side-to-top category. The connection looks similar to timber plate joint (see Figure 5.41 A-D) but requires an entirely different machining process in frame structures: a) plates can be cut parallel to a machining table, b) whereas a beam tool-path may require spindle movements in planes parallel to joint surfaces. The joints in beam elements are often scaled down from the beam axis (see Figure 5.41 C (red color)) to accommodate enough connection area around the joint. Otherwise, the female element would be split in half, unless the half extended tenon is used. This issue points to the material constraints – linear elements are used in fixed widths or diameters that

## 5.5. Connection Types in a Model

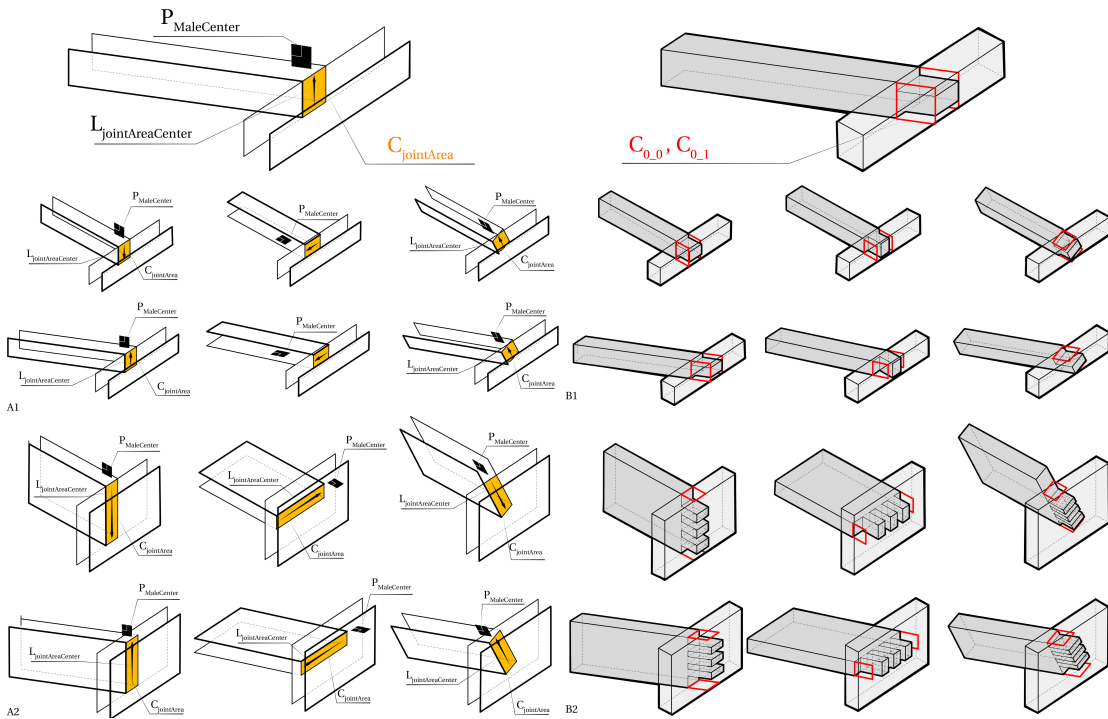


Figure 5.40 – The side-top method is applied on rectangle beam elements (a1) and timber plates (a2). The joinery generation contains the same a pair of rectangles in beam elements (b1) and plate elements (b2). Other joints can be assigned to a rectilinear volume as well.

shape the timber joint's proportions. Whereas the plate position could be changed by moving elements from an edge to gain a more extensive zone around joints (see the difference in mortises in Figure 5.41 A-B). Raw wood requires additional cuts (see Figure 5.41 D) due to the unpredictable wood characteristics, such as bisector cuts or surfacing due to knots or surface imperfections. Lastly, the tenon is slightly inserted into a female element to gain a rectangular surface area.

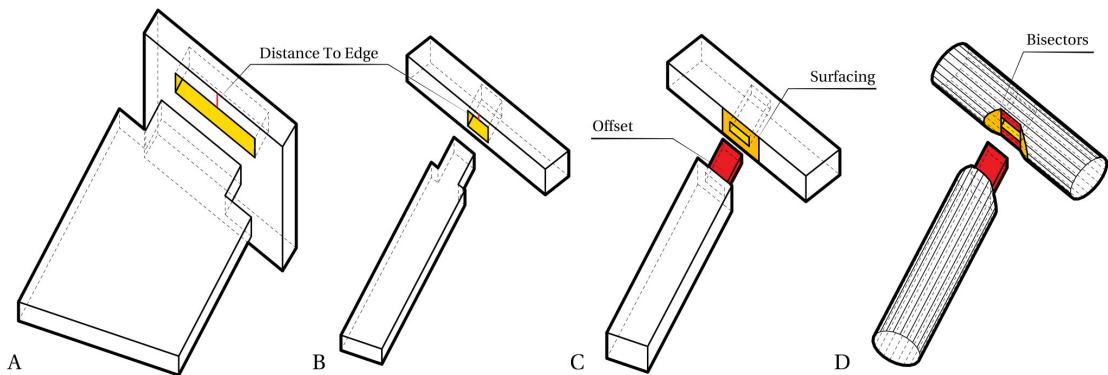


Figure 5.41 – Difference between single tenon a) in plates, b) timber planks , c) regular rectangle beams, and d) raw wood with bisector cuts.

## Chapter 5. Joinery Solver

---

A physical model in raw wood was made to test the Joinery Solver and the Tile tool-path generation (see Figures 5.42, 5.44). The comparison between plates and raw wood beams shows a gradual difference in the shape of a joint imposed by timber irregularities and the rectilinear machining. To speed the machining process, the joint is fabricated on a single beam then cut in half to check the tolerance of the robotic cutting (see Figure 5.42 D-C).



Figure 5.42 – Tenon-mortise joint from raw wood: a) tenon, b) mortise with rounded edges due to the milling-tool, c) assembled joint, and d) the fabrication rig, e-f) assembly of the two elements. Timber was then cut in half to test the assembly.

Angled tenon-mortise joints have angle limits. The sharper the insertion angle, the harder it is to fabricate the tenon-mortise connection. In the fork prototype (see Figure 5.43), the fabrication limit is thirty degrees, meaning the 18 mm diameter and 11 cm length milling tool could not cut sharper angles within the thickness of 15-20 cm diameter beams. Besides that, tenons with sharper angles can be disassembled easier because the insertion of an element does not follow one direction but rather has an additional rotation freedom (see Figure 5.43 D). The second contact surface has little effect. There are several solutions to this issue: a) the joint can be fabricated in a perpendicular direction, b) instead of using partial tenon, a through-tenon joint would have more substantial integrity, c) additional elements could lock the joint, and c) instead of a single tenon, two tenons would fix the rotation problem.



Figure 5.43 – Tenon-mortise and forks: a-b) assembly, c) the prototype composed of four straight beams and three forks, and d) the observed rotation moment.



Figure 5.44 – Tenon mortise fabrication using the minimal milling process.

**Side-to-Top - Joint Orientation** The orientation of a joint has to be controlled for the connections that do not have self-symmetry, e.g. half tenon-mortise 5.46). The wrong orientation of the joint would reverse the assembly order and the fabrication tool-paths. In the Joinery Solver, the orientation depends on the joint-area-centre line that is generated

from the intersection of the male-element-centre plane and the joint-area (see Figure 5.45 A1-A2). The joint-area polygon is generated from the intersection of the male side outline and female top or bottom outlines, meaning that the winding of original elements influences the joint-area polygon turn and, consequently, the joint-centre-line direction. The Figure 5.40 shows multiple cases where the direction differs depending on the joint and polygon winding. To control this behavior, when non-symmetrical joints are used, two pre-processing steps are taken: a) the user has to specify an orientation axis that helps to shift the polygons towards the given axis and b) at the side-to-top generation method, the joint-area-centre-line segments have to be oriented based on the re-ordered outlines. A joint-area-centre-line is intersected with the female side outline. The first intersection point must be the closest to the start of the polyline. The detailed study of the multiple half-dovetail joints is shown in Figure 5.45 D1-D3, where all-female outlines' are oriented upwards. A physical model was machined to show the necessity to control this feature (see Figure 5.46).

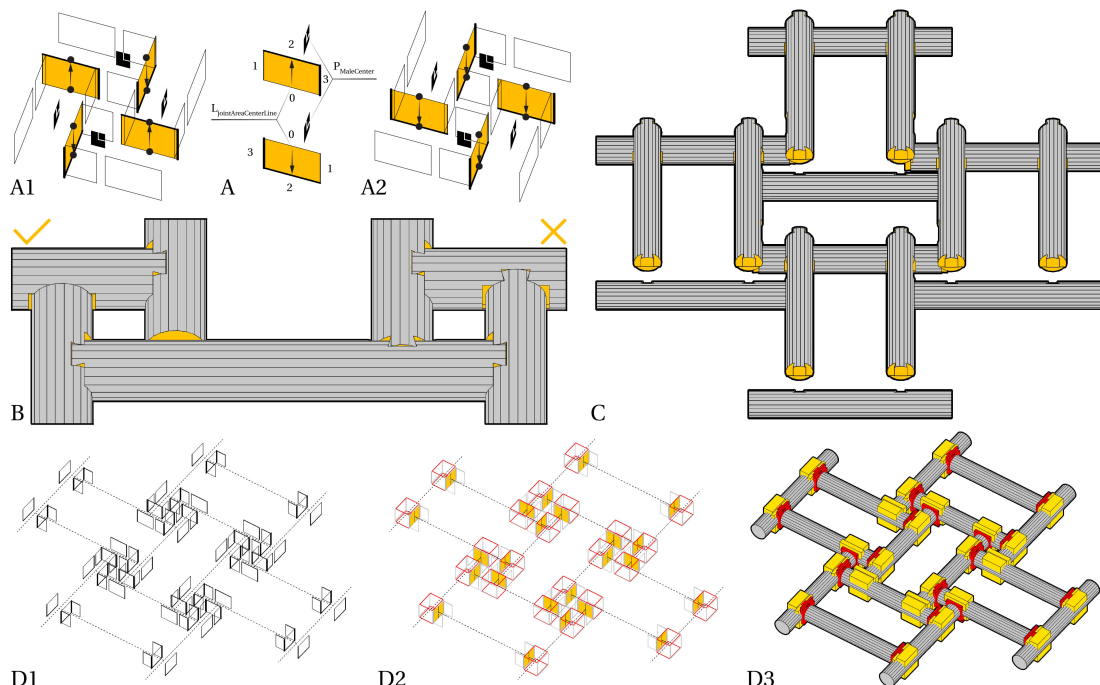


Figure 5.45 – Half-dovetails: a) the outlines are oriented by the female outline winding order (a1 – correct direction, a2 – not possible to assemble) b) the 3D model reflects the cases a1 and a2, c) the larger assembly. The sequence: d1) orient the female outlines, d2) align the intersection lines by red rectangles, d3) male (yellow) and female (red) cutouts.

Tenon-mortise joints have a rigid assembly comparing to the other raw wood joints, meaning that connecting surfaces of a joint interlocks the structures without additional fasteners. Each element must be inserted using one direction to have a collision-free assembly. The single insertion vector gives a structural integrity, but it can also limit an assembly of a larger structure. Another alternative is proposed by employing the Bisector cuts to explore an assembly that is not limited by one insertion vector (see Figure 5.47). Similar to the side-side connections, this



Figure 5.46 – Half-dovetails: a) single element, b) assembly of two elements, c) and closed element, which is impossible to assemble without gradually rotating each adjacent element.

joint is dependent on the strength of fasteners. A physical model was made to test this idea by cutting small radius tree trunks (see Figure 5.47 C). The assembly was locked by two dowels, connected to a pair of timbers. Within the small connector zone, even with long timber dowels, the beam has a rotation moment. Therefore, panels are added by surfacing one side of a beam. After this prototype is made, a dowel-nut connection was proposed to ensure a more rigid connection within members (see Figure 5.47 A), when the addition of panels is not an option. Hence, the side-to-top connection is tightly connected with the assembly sequence varying from Tenon-Mortise, Half-Dovetail to Bisector joints. The joints have to be analyzed in terms of a joint topology, the larger assembly scale, and the overall insertion sequence.

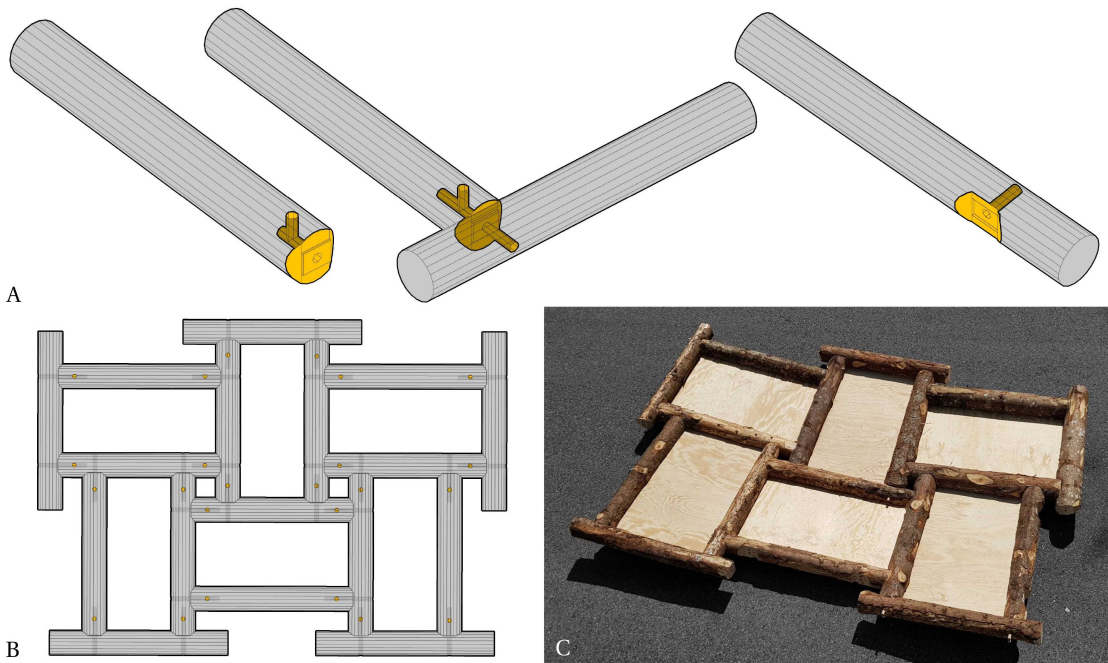


Figure 5.47 – Joint with a) a dowel-nut connector, b) a larger assembly, and c) the prototype.

**Side-to-Top - Extension method to Timbers Plates** The side-to-top joint is also applicable for timber plate structures. There are three observed differences between beam elements and plates: a) beams mostly have one joint at the end whereas plates can distribute many joints along an edge, b) beam joint digital geometry must be cut out from a reference shape, whereas plate geometry computation lies within a pair of outlines, c) the beam connection can be used only for the two ends a tree trunk, whereas plates have the whole the contour. The plates have an option to change the angle depending on the user's given direction. Geometrically, there is no fixed orientation besides wood grain orientation, which is hardly considered by architectural projects and usually understood as uniform.

In the Joinery Solver, all joints are oriented perpendicular to an edge (see Figure 5.48 A). It is also possible to assign to each outline edge a different insertion direction or have one common orientation throughout the whole element (see Figure 5.48 B). These options apply both for beams and plates. The solver also measures the angle between the perpendicular edge vector and the newly defined orientation. If the angle is bigger than the maximum angle of fabrication, the joint geometry generation is skipped (see Figure 5.48 B short sides of the top plate).

Besides timber joints, extra fasteners could be used by subdividing joint-area-line edges. A more detailed study for extra fasteners was developed for Nabucco Opera where screws were used to connect multiple components into a spiral assembly (see Figure 5.48 C). Real project cases allow testing the algorithm in terms of scalability and implement new features that are necessary to go from a digital model to a prototype. The algorithm is tested to understand its limitations by starting not from the rules of the tool but rather from the designer's creativity that could help develop the algorithm further. For example, the user employs several joints within one element, such as a combination between screws and tenon-mortises (see Figure 5.48 D). In the same example, the top-to-top joints fasteners were used twice, which was not considered before as an option: a) 20 mm dowels for the component alignment that is positioned close to the center of a plane, and b) the screws that are offset by a half of the timber plate along the whole contour.

Another case study is taken as the Annen project [136] to explore the multi-valence edge joints and test the scalability of the algorithm. During this test, the fast R-Tree search broke because the hash function for checking visited elements was insufficient for the unique 23 040 000 element pair identification (see Figure 5.50). The issue is resolved by implementing a more robust identifier for face-edge pairs to avoid duplicates when searching for a connection area (see Figure 5.49 F). This specific structure has a unique three-valence joint that connects two side-to-top joints (see Figure 5.49 A). Two main points must be considered at this case: a) the angled tenon cannot intersect (see Figure 5.49 B), b) when elements are rotated, it is hardly possible to predict the intersection zone (see Figure 5.49 C). The global Joinery Solver was designed by considering pair-wise connections only which is applicable for this multi-valence case. This case study helps to implement the additional features by coupling two side joints (see Figure 5.50 D). The user must input adjacency information to identify the two pair of

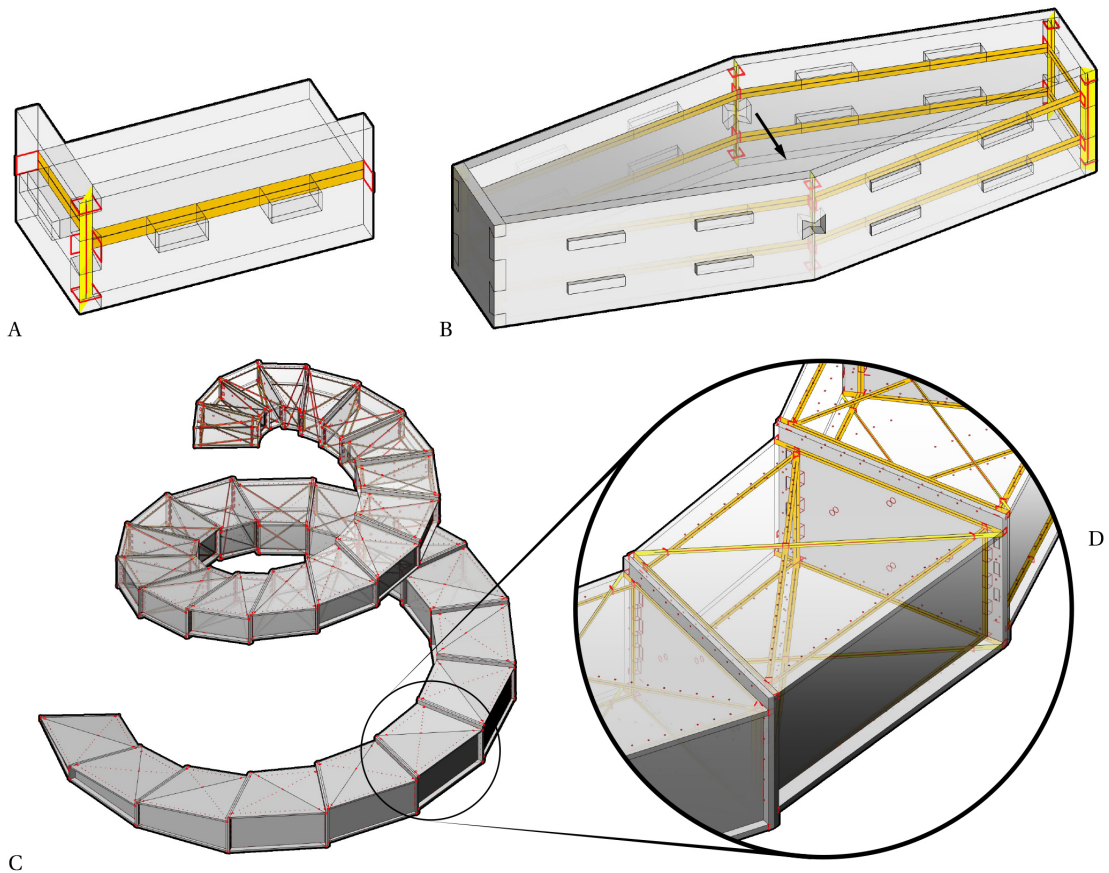


Figure 5.48 – Side-top connection applied for timber planes: a) single corner b) axis-aligned joints, c) a large scale application using both fasteners and timber joints, and d) two types of fasteners per each pair of elements.

elements. Then an average line is computed from the two side-to-top joint-are-lines. Then, a plane is computed on the average line considering the average edge vector that results in an even distribution of tenons (see Figure 5.50 E). The same process is applied for the rest of the 14 box components (see Figure 5.49 F) and then the full project (see Figure 5.50).

Additionally, the project requires two different connections: a) tenon-mortise for top and bottom plates, b) dovetails for the corner connections. Initially, all joint Tiles are assigned to the all possible connection areas. In this case, some side-to-top connection zones must stay empty to enable the assembly sequence. The issue is resolved by applying a string identifier to all top and bottom plates outlines as "AB\_TenonMortise" and all vertical plates as "BB\_Finger" (see Figure 5.49 G). The orientation of the boxes were assigned per each element. Overall, these examples show the need to study existing projects to help develop the Joinery Solver as a versatile tool rather than a generic algorithm.

## Chapter 5. Joinery Solver

---

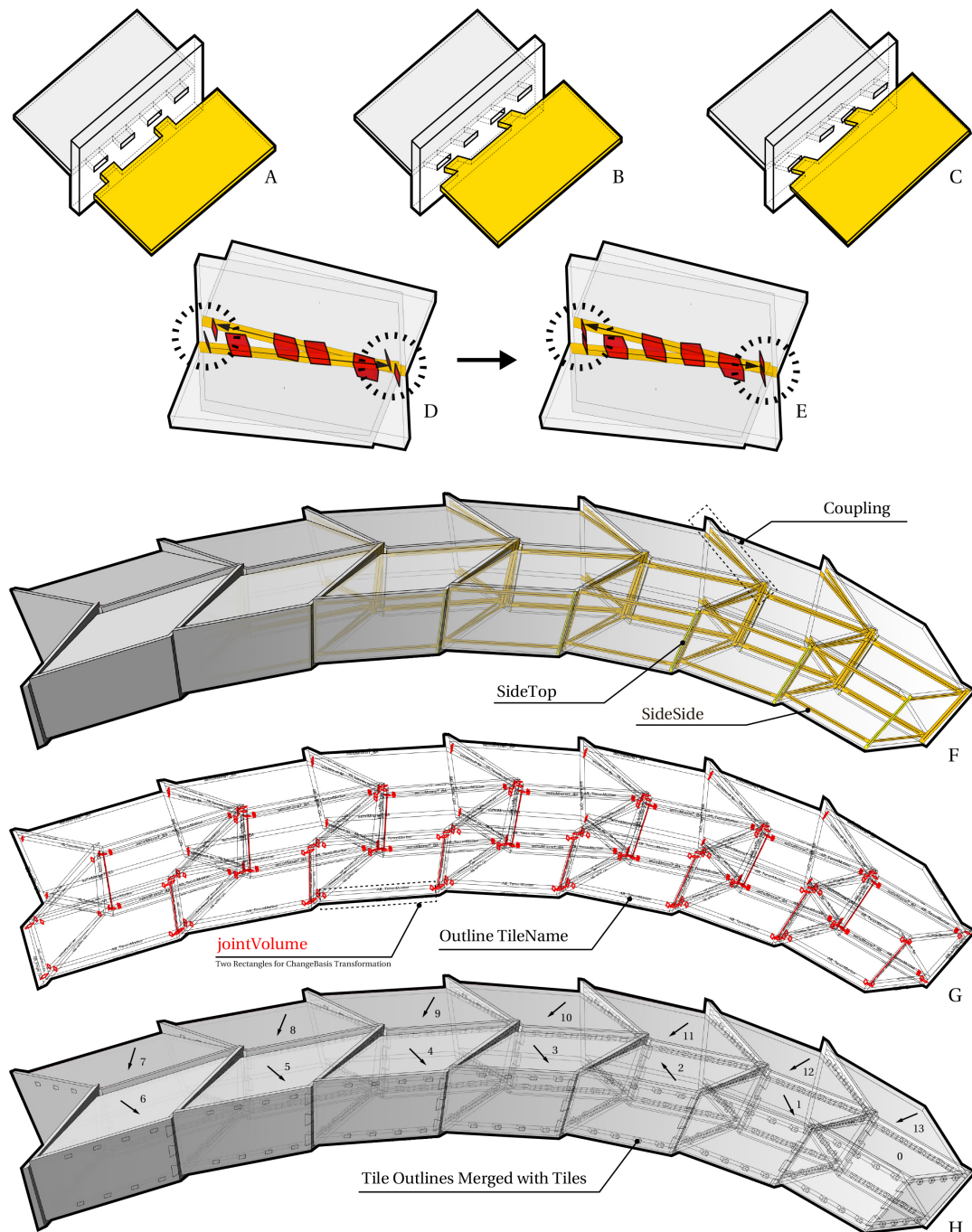


Figure 5.49 – The three-valence finger joint composed of the two side-top connections: a) the parallel case, b) the oblique option, c) the rotated possibility where d) joints are not aligned and the added feature to, e) align the tenons. Larger assembly: f) the multiple connection areas, g) the pairs of boundary volumes represented as pairs of rectangles, and h) the generated side-to-top and side-to-side joints.

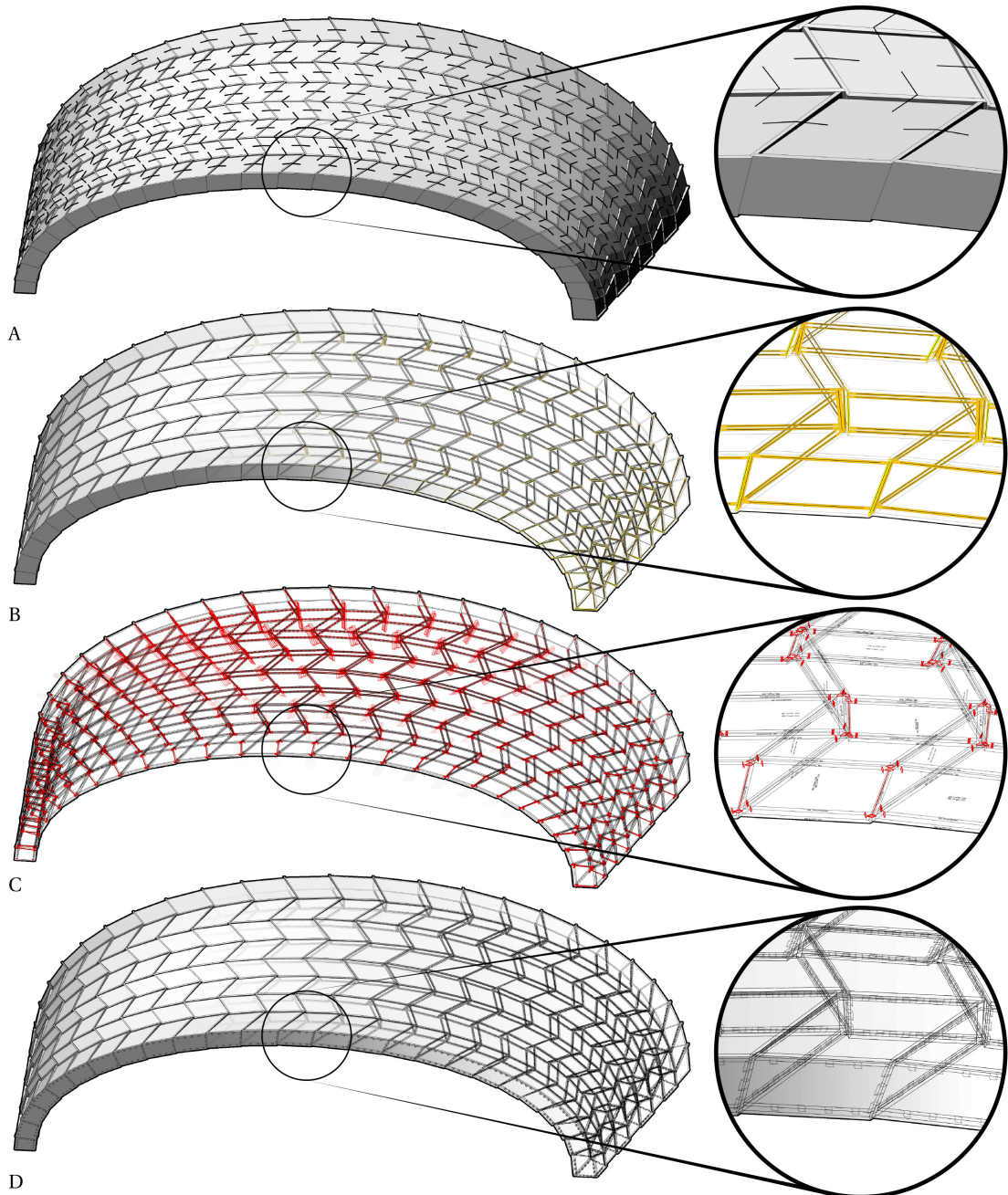


Figure 5.50 – Large scale test using eight hundred plates as a reference from the Annen project [136]. Joinery Solver requires several inputs: a) the coupling of two side-to-top joints, b) the sides are identified using the R-Tree search and the oriented-bounding-boxes, c) the joint volume is generated as a pair of rectangles, and d) joinery Tiles are oriented to the connection zones that are merged with the plate polygon outlines.

### Cross Topology

There are several cross joint topologies due to a) the assembly sequence and b) the shape of timber elements. Simple half-cuts are used for timber plates and beams in rectangular sections, utilizing the three contact zones per element (see Figure 5.51 C1). Furthermore, angle cuts are employed due to a non-linear assembly sequence (see Figure 5.53). However, these joints only have one contact surface (see Figure 5.51 C2). When a structure contains curved or irregular timbers, such as raw wood, conical cuts are needed. The joint becomes more complicated because of the additional side cuts (see Figure 5.51 C3-C4). There are two options to cut the conical cuts: a) using an extended conical Tile that is composed of six milling operations (see Figure 5.51 C1), or b) employing a conical Tile that looks simpler but machining takes nine cuts, adding the additional constraint of reachability within a robot or CNC machining space (see Figure 5.51 C3). Finally, the algorithm splits a tile into the female and male parts by assignment to the corresponding elements.

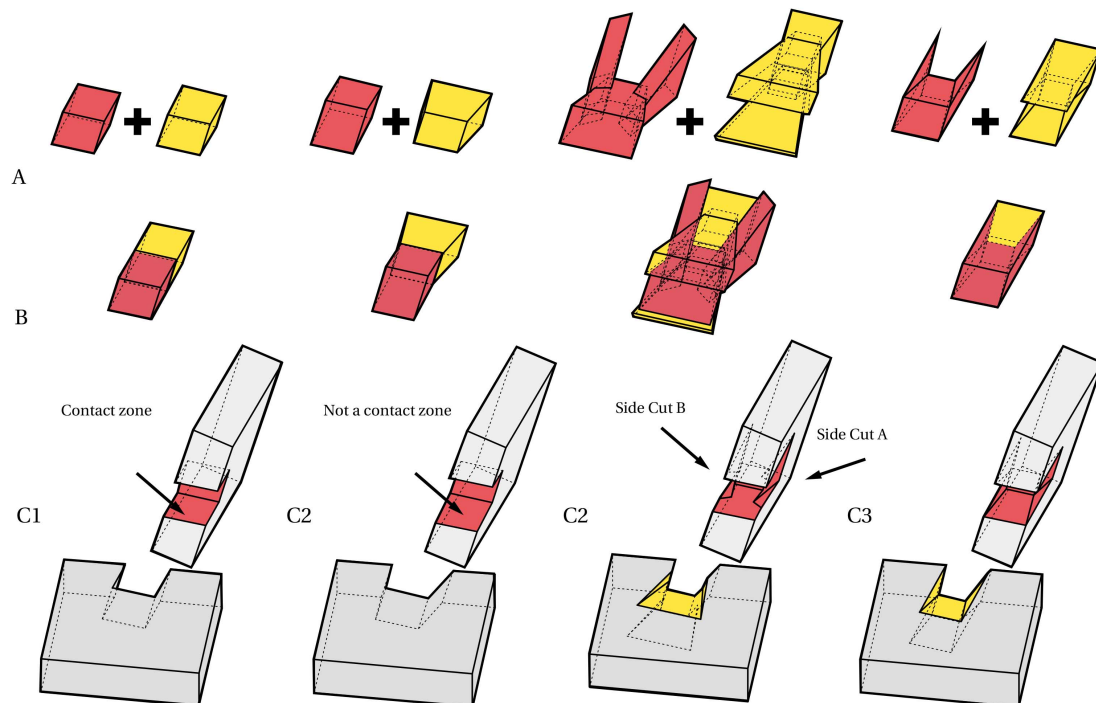


Figure 5.51 – Cross joint Tiles: a) rectilinear cuts, b) angled half cuts, c) extended conical cuts for the six side milling, and d) the conical cuts for the nine side fabrication.

The cross joints, in beam structures, have little resistance to bending forces because the section of an element is reduced. When a structure forms the out-of-plane joints, so-called Nedorades, it is possible to minimize the connection zone using constraint based solvers. It is preferred to keep at least 2/3 of a section to obtain a better structural integrity of a wood-wood connection [29]. The cross joint often has extra connectors, such as ropes, cables, scaffolding couplers, screws, bolts, or dowels to prevent elements from slipping away from each other.

The connection is not sufficient to interlock two members on its own. The most efficient use of the joint is when two elements rest on top of each other because they avoid the material removal from the section. In this form, the load-bearing capacity is limited by the potential shearing resistance of the timbers. However, there is little rotation resistance in such a case and in raw wood subtractive cutting operation is necessary due to the irregularities of trees.

Structures with an orthogonal beam arrangement could be assembled without introducing additional cuts, while curved assemblies employ conical cuts to insert the timbers without a risk of collision. There is a broad range of possible cross joint applications within timber structures: a) timber plates (see Figure 5.52), b) regular rectangular beams (see Figure 5.54), c) raw wood (see Figure 5.55). Additionally, the assembly sequence may not follow one insertion vector per one element. Elements have to be rotated in place due to the reciprocal pattern (see Figure 5.53). It means that existing beams have to be lifted or rotated together with the previously assembled elements that need to be re-inserted in the structure. When the assembly is finished, each node must be tightened to ensure an overall structural rigidity (see Figure 5.57).

Several changes are suggested to improve the cross joint. Multiple layers of timber can ensure a better connection rigidity and gain a greater cross-section [171]. Over time, weak connections using bolts and other fasteners could also lead to sagging, similar to Zollinger systems [163]. Less sustainable glulam production refines the weaker lamella construction in floor or roof systems. Even such highly engineered timber structures require additional fasteners [159]. Besides, there are suggestions to avoid using the cross joint by changing it to side-to-end joint to obtain a shell-like behavior, similar to the Zollinger system [123]. The advancements are tightly connected to digital fabrication, such as CNC and robotic fabrication for quad tessellated surfaces [59].

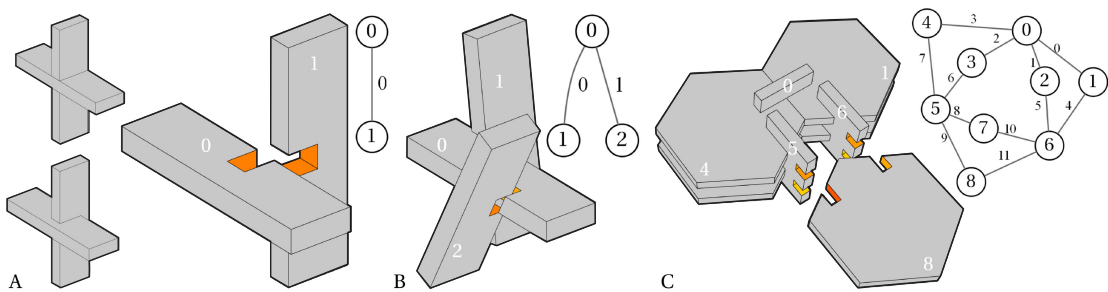


Figure 5.52 – Elements and their corresponding connectivity graphs: a) a complete and a partial overlap in an orthogonal case, b) two joints in one element, and c) the simultaneous insertion of one element to multiple parts.

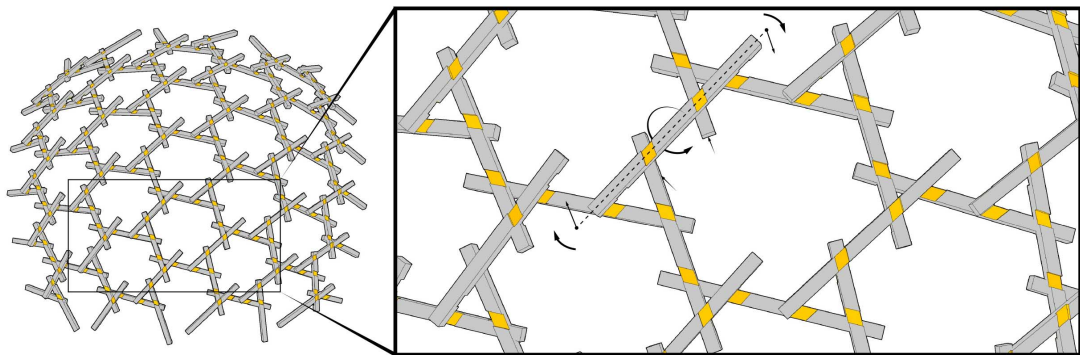


Figure 5.53 – Assembly sequence requires translation and rotation to insert elements.

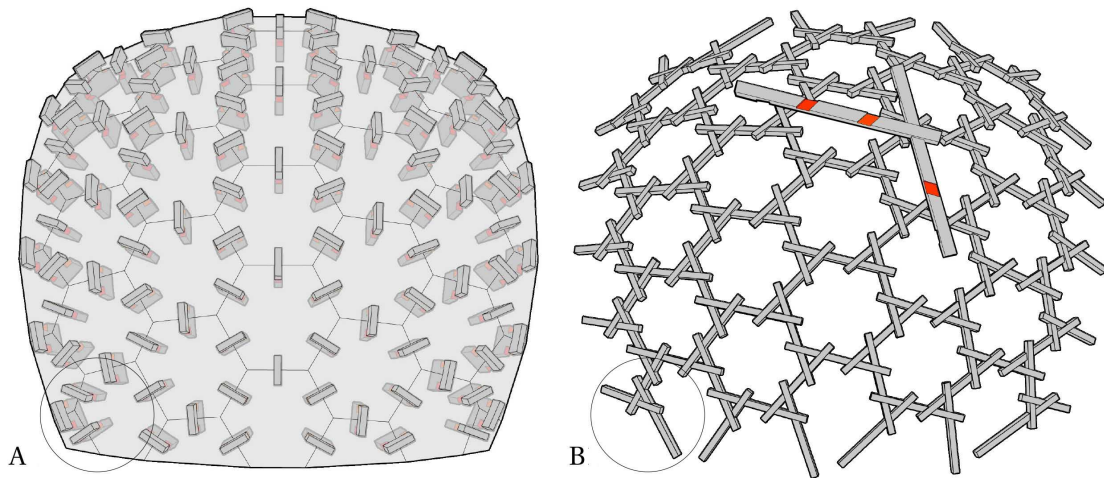


Figure 5.54 – Comparison within cross joint application in a) timber plates, and b) beams.

**Cross-joint - Conical Cuts** There are a few parameters that controls the conical cross joints. The simplest example is to widen an angle of a joint (see Figure 5.55 A). However, such an option has one contact area. Hence, it is necessary to create the conical cuts from both sides of a joint to insert members freely and obtain the contact area (see Figure 5.55 B). Furthermore, the joint geometry can be used for round-sections and bent elements. Depending on a fabrication method, there are two sub-categories of conical joints: a) the conical joint with extended oblique cuts (see Figure 5.55 B), and b) the conical joint that requires nine cuts instead of six (see Figure 5.55 C). The side cuts are relevant to the round sections because they already have a minimal contact area due to the cylindrical volume (see Figure 5.56 B1-B2 and C1-C2). The bisector cuts require the longer machining time and the larger robot reachability, but they are critical for a collision-free assembly. The 6 cuts can be machined using milling, while the 9 cuts (see Figure 5.55) are commonly cut using a combination of a saw-blade and milling. Finally, joints can be adapted to a variety of angles for non-orthogonal cases (see Figure 5.57 C) and fasteners (see Figure 5.57 A-B).

## 5.5. Connection Types in a Model

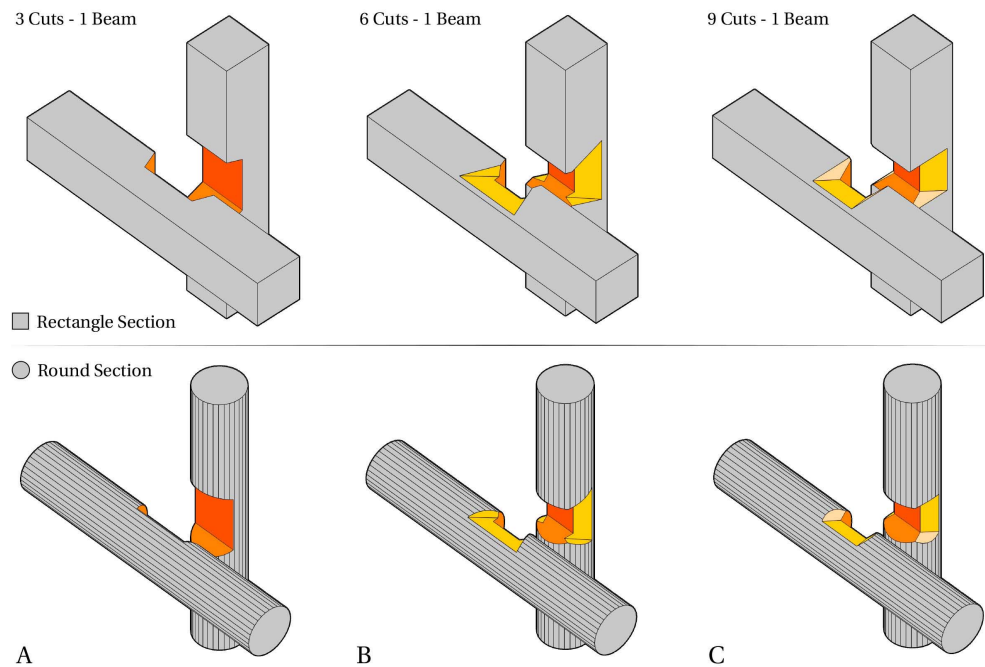


Figure 5.55 – Comparison between the rectangle and round sections: a) beams have one contact zone and 3 cuts per 1 beam, b) Conical extended cuts with 6 cuts, and c) 9 cuts.

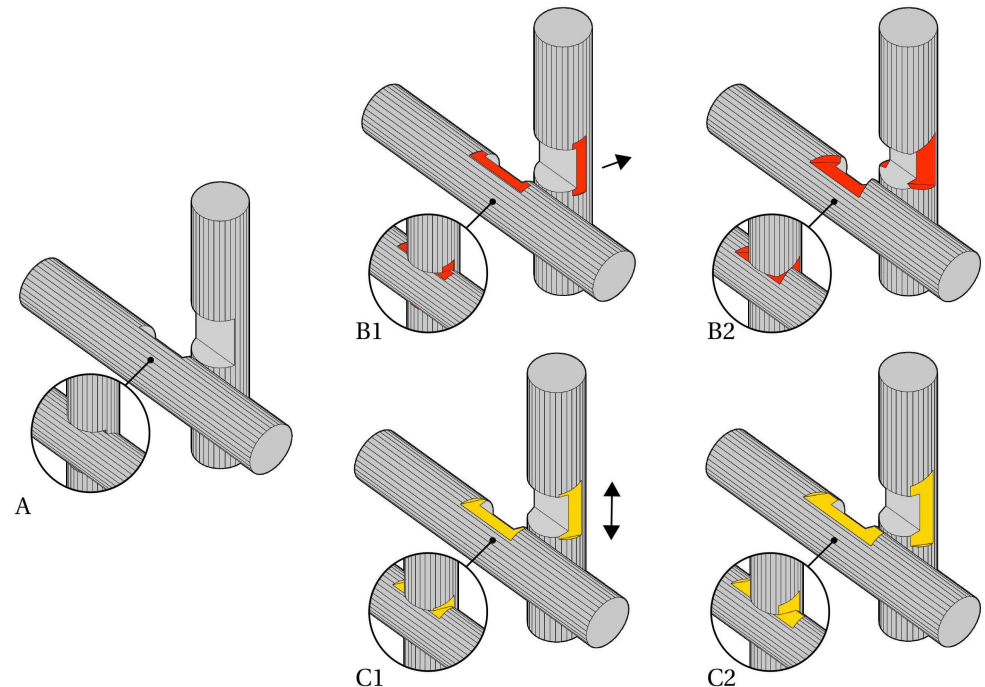


Figure 5.56 – Side cut properties. Angle cuts (a) have only one contact surface. Control of horizontal (b1-b2) and vertical (c1-c2) extension cuts.

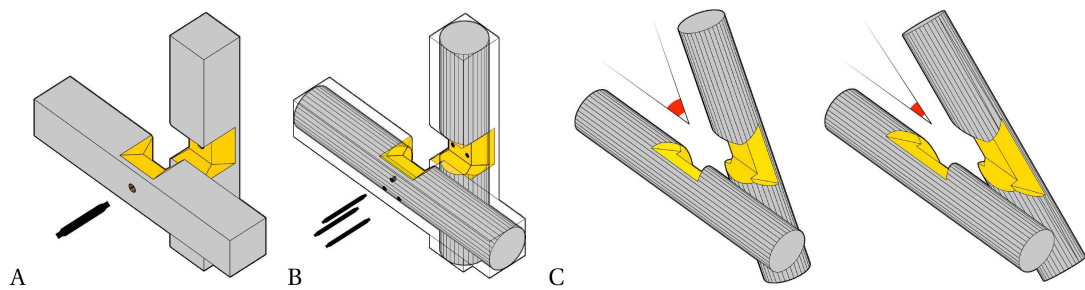


Figure 5.57 – Additional fasteners for a) rectangular or b) round sections. Joinery Solver also considers c) angled cases.

**Cross-joint - Bending and Irregular Elements** The cross joints could be used for irregular raw wood [94, 171] and bent elements [159]. In this case, joint volumes are constructed on an approximate intersection between central axes of beams, considering their local radii (see Figure 5.58). When axes are not physically touching, the intersection-line is taken between the two closest curves, so-called eccentricities. The connection volume is computed in the same way as discussed in the previous sections (see Figure 5.58).

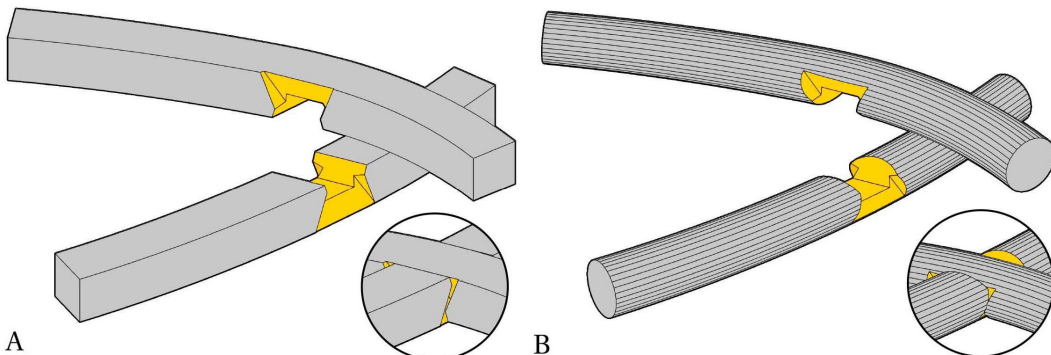


Figure 5.58 – Cross joint within a bent shape: a) regular cross-section and, b) round section.

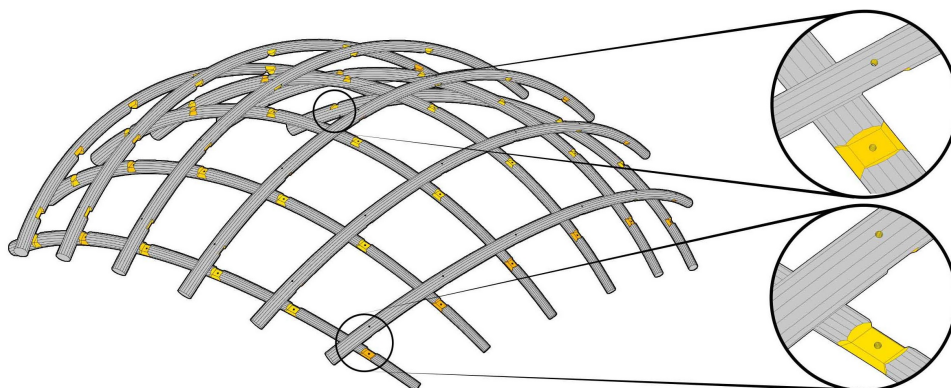


Figure 5.59 – Multiple cross-conical joints for bent elements.

**Cross-joint - Study Case of Seiwa Bunraku Theater** The cross joint could be applied for reciprocal structures. The insertion order of reciprocal structures follows rotation vectors rather than translation (see Figure 5.60 C). Seiwa Bunraku Theater, designed by Kazuhiro Ishii, is taken as an example. The structure is a flat planar grillage for a walkway ceiling made from the relatively short rectangular elements. In the original project, the structure contains only flat cuts similar to Figure 5.55. These cuts are manually adjusted, including additional side cuts for a rotational assembly. The overall section of three timbers exceeds 1 meter in-depth and is held by metallic elements to fix the nodes. To learn from this historical example, the structure was replicated in the lab and detailed in the Appendix A. Elements were assembled one by one while rotating the current and adjacent elements (see Figure 5.60 C). Finally, timbers were blocked using additional fasteners.

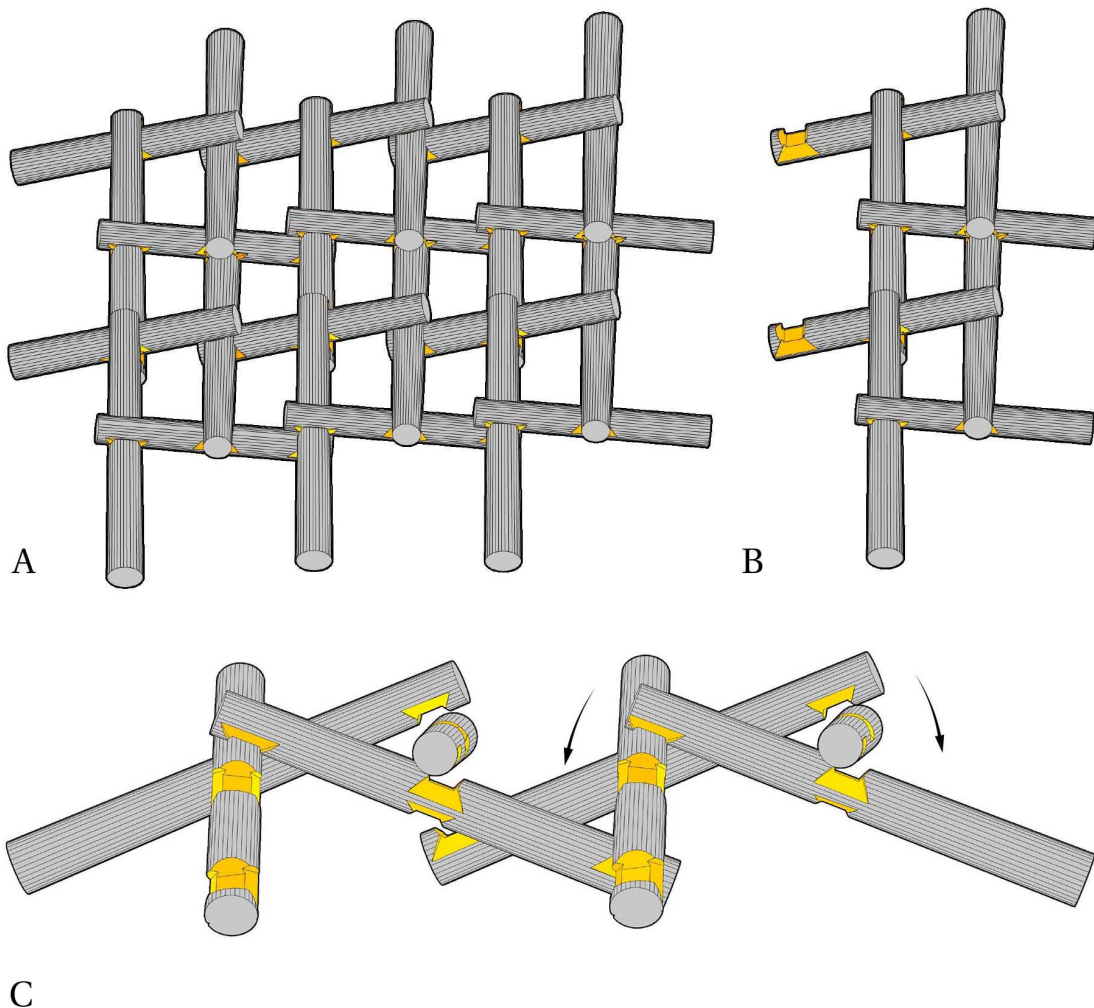


Figure 5.60 – The cross joint in the flat Reciprocal structure inspired by the Seiwa Bunraku Theater (Kazuhiro Ishii) (a). The prototype (b) is assembled using while rotating beams (c). The Theater was replicated by making a physical prototype and is discussed in the Appendix A.

**Cross-joint - Study case of a Two-Layer System** The second study case explores the cross joint by introducing a two-layer system. The aim is to increase the static height of the structure. Beams are inserted using one insertion vector per element. The prototype employs a quad grid that is divided in U and V directions, where one direction is positioned on top of the first one. Two models were machined to check the tool-path generation using the industrial robot arm ABB IRB 6400R. The smaller model contains eight elements (see Figure 5.61 B), while the larger structure is four times bigger, employing twenty-four beams and forty-eight cross joints (see Figure 5.61 A). The structure also contains unique details for the beam ends for a connection to the floor and the boundary cuts. The Joinery Solver has a separate category for custom joints allowing to consider boundary and foundation fabrication in one tool path. The smaller structure was first assembled on the ground and then lifted onto the base. The structure was matched with the timber stock, meaning that elements were assigned to the structure by measuring timber lengths and radii within the best overall fit. Hungarian algorithm is used to solve the assignment problem. The larger prototype was assembled on the ground, then disassembled and beam by beam constructed again in a vertical orientation.

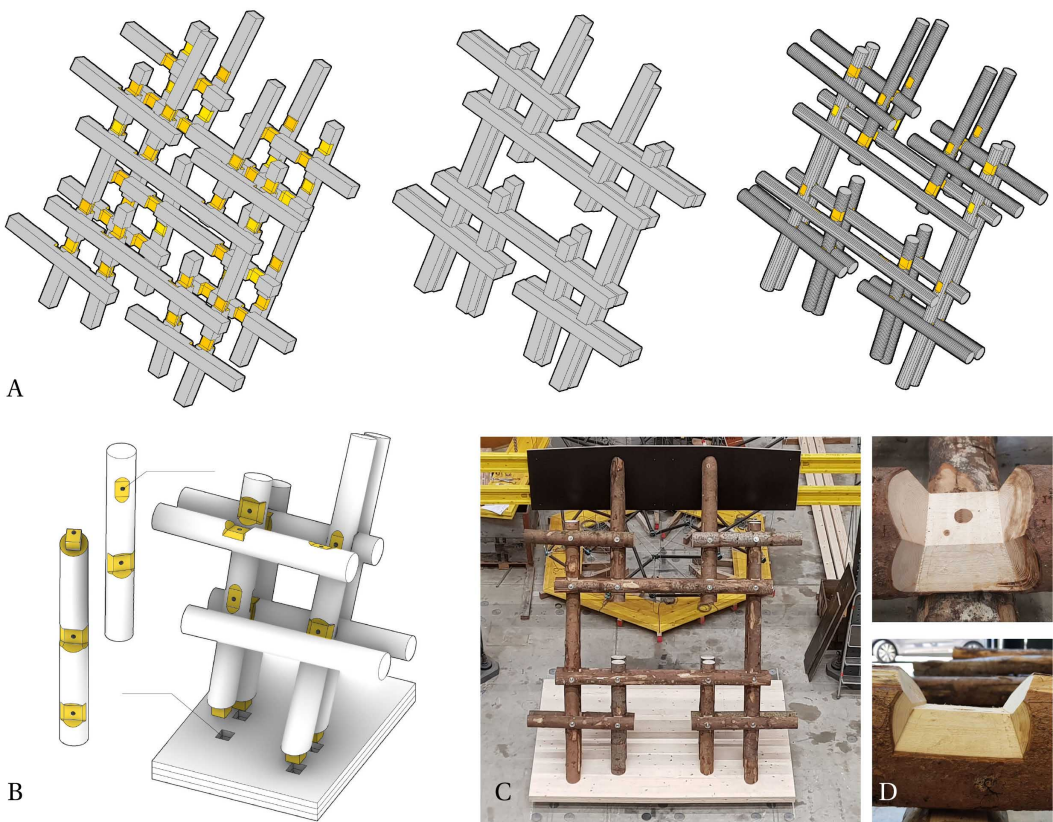


Figure 5.61 – The cross joint for the two-layer reciprocal prototype (c) using conical joints on both sides of a beam (d). The algorithm is applicable both for regular rectangular beams and raw wood with irregularities (a).

**Cross-joint - Single Layer Study Cases within Different Timber Elements** A series of digital prototypes were tested during the development of the algorithm. The user does not typically consider how a joint needs to be drafted, focusing on a global shape rather than on the small scale joinery. The analysis of existing study cases helps to implement new joints and understand the scalability of the proposed methodology as demonstrated in Figure 5.62.

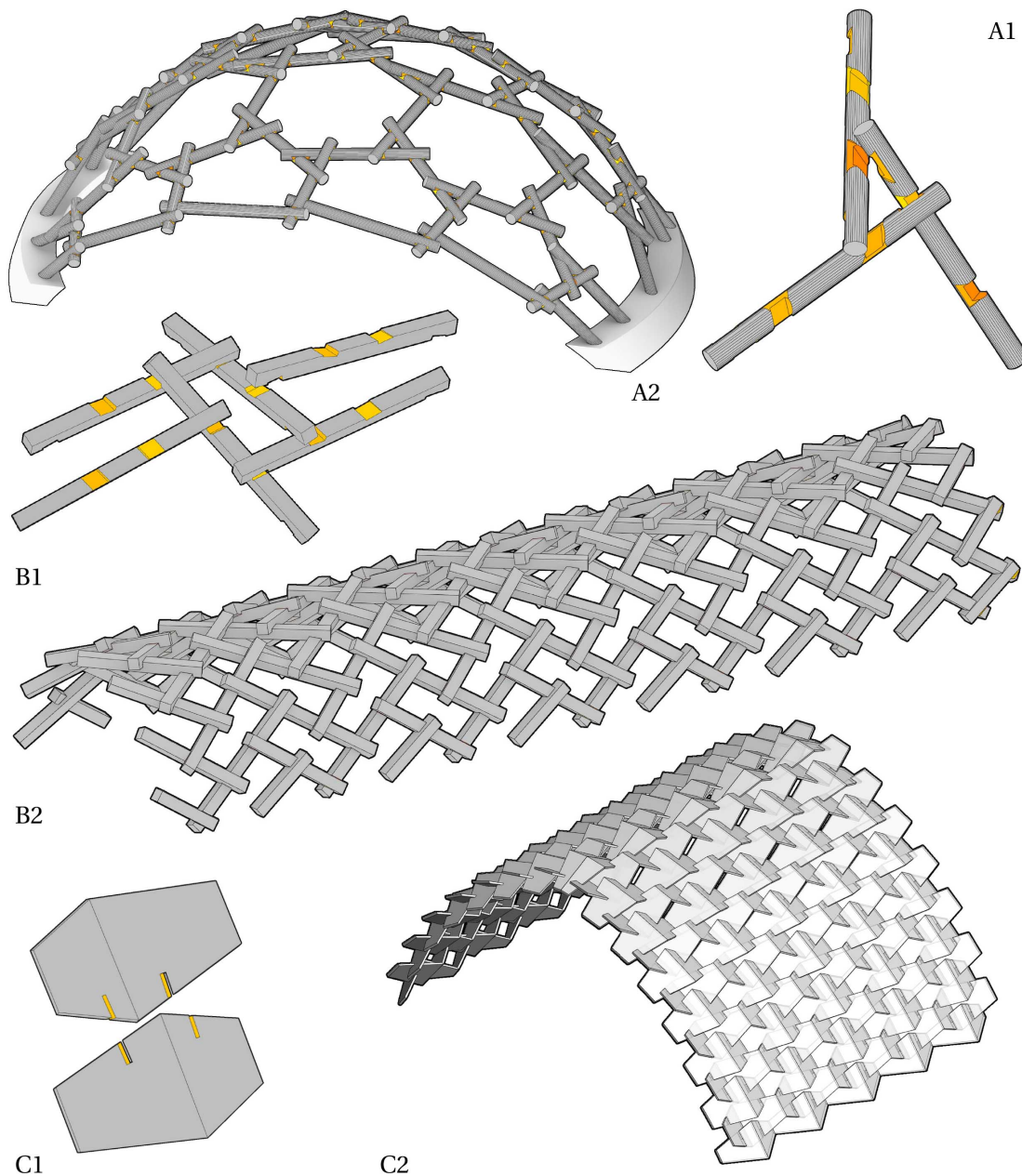


Figure 5.62 – Single layer hexagonal reciprocal structure (a), structure replicating the Iseya town-house roof in Kawagoe, Tokyo by Noboru Moriyama (b) and timber structure by Sina Nabaei (IBOIS, EPFL) (c).

**Cross-joint - Joinery Physical Tests** Several cross-lap joints were fabricated (see Figure 5.63). Most of the samples contain extra fasteners ranging from wooden dowels and metallic bars to threads. The cutting timber joint in raw wood requires surfacing and approximation to compensate for the irregularities, such as knots, bark, curvature, and wood taper. If there is no surfacing (see Figure 5.63 A), then there is no contact area. Before developing the conical joint for raw wood (see Figure 5.63 I), single perpendicular cuts were made (see Figure 5.63 D,E,F,G). These joints have one connection surface, but the side cuts do not give any benefit. The introduction of Bisector cuts (see Figure 5.63 H) helped to approximate the node geometry. Finally, timbers are interlocked using external fasteners (see Figure 5.63 B,C).



Figure 5.63 – Cross joinery: a) Dowel, b) Metallic-thread, c) Ropes for tightening the connection, d) Flat-cut, e) perpendicular-to-grain Tenon-mortise joint, f) Tenon-mortise with an extra timber connector, g) parallel-to-grain Finger, h) Bisector, and i) Conical.

The joints give a specific aesthetic value besides the structural quality. For example, the metallic thread is a less sustainable solution, but hardly visible in comparison with the rope fastener. In conclusion, the approximation is necessary for modelling joints using raw wood, and it is necessary to provide the maximum contact area that is blocked using additional fasteners.

## 5.6 Boolean Methods for 2D Polyline and 3D Solid Meshes

The Boolean operations have to be used for visualization of timber joints. The physical process of subtracting joints from an element using CNC or robotic fabrication is similar to the digital model representation. 3D solid volumes have to be subtracted from an element to merge the joint within the timber element. Boolean operations, including 2D polygons and 3D meshes, are used for numerous higher-level algorithms, such as the calculation of Booleans, Offsets, Mesh Repair, Minkowski sums, and Meshing geometries with defects. All these methods share a basic need – the partition of a 2D or 3D space into a set of topologically well-formed cells to separate the interior part of geometry from the exterior. The partition into cells, or mesh arrangements, has been subject to extensive research and seen as a complex yet computationally intensive problem, which often constitutes the biggest bottleneck for higher-level algorithms, including the design of joints. The Boolean Difference method is neither trivial, nor errorless, and there are only a few robust and fast algorithms. Four methods were implemented during the development of the Joinery Solver: a) display of cutting volumes within an element to avoid the Boolean operation, b) 2D polyline merge method for flat elements, such as plates, using line-line intersections, c) 3D Mesh Boolean Difference [161], d) 3D BRep Boolean Difference operation (RhinoCommon) (see Figure 5.64). The four methods are written from the fastest to the slowest and the least robust: a) real-time, b) less than a second for 1000 elements, but applicable only to timber plates, c) 20-100 ms for one beam element, considering this is the most robust method for Meshes (CGAL), d) 500-1000 ms for one solid element and is most likely to produce incorrect results. The metric varies depending on an element's and joint's complexity.

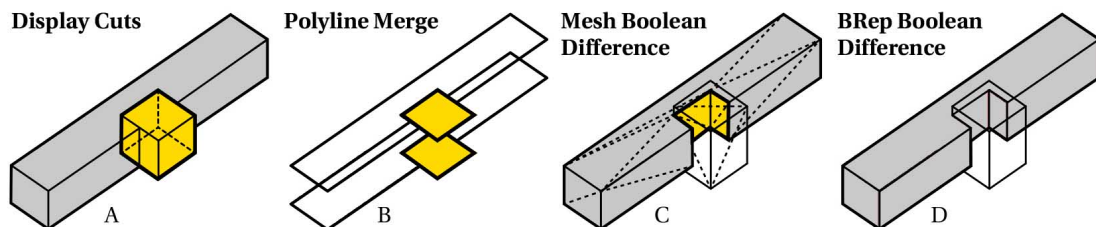


Figure 5.64 – Method of a timber joint visualization: a) display of the cutting volumes, b) 2D polyline merge method, c) 3D Mesh Boolean Difference [161], d) 3D BRep Boolean Difference operation [138].

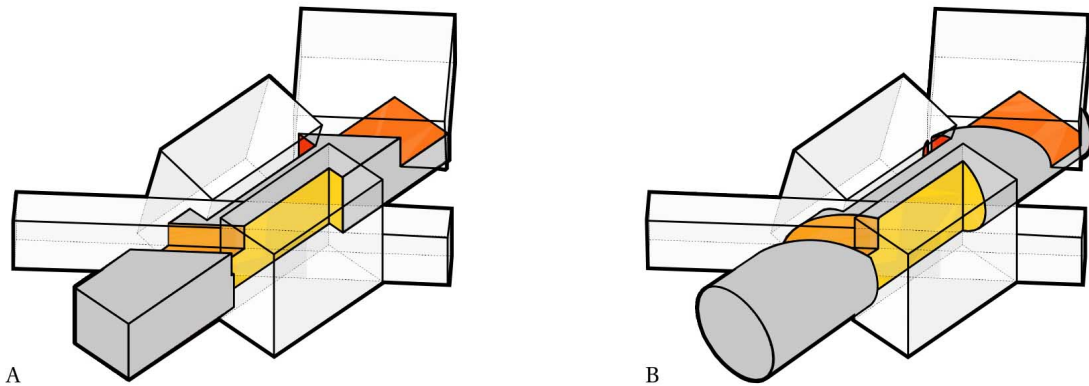


Figure 5.65 – Mesh Boolean difference method: A) rectangle beam, B) round beam. The algorithm tracks mesh face information from the initial cutting elements (yellow-to-red colors).

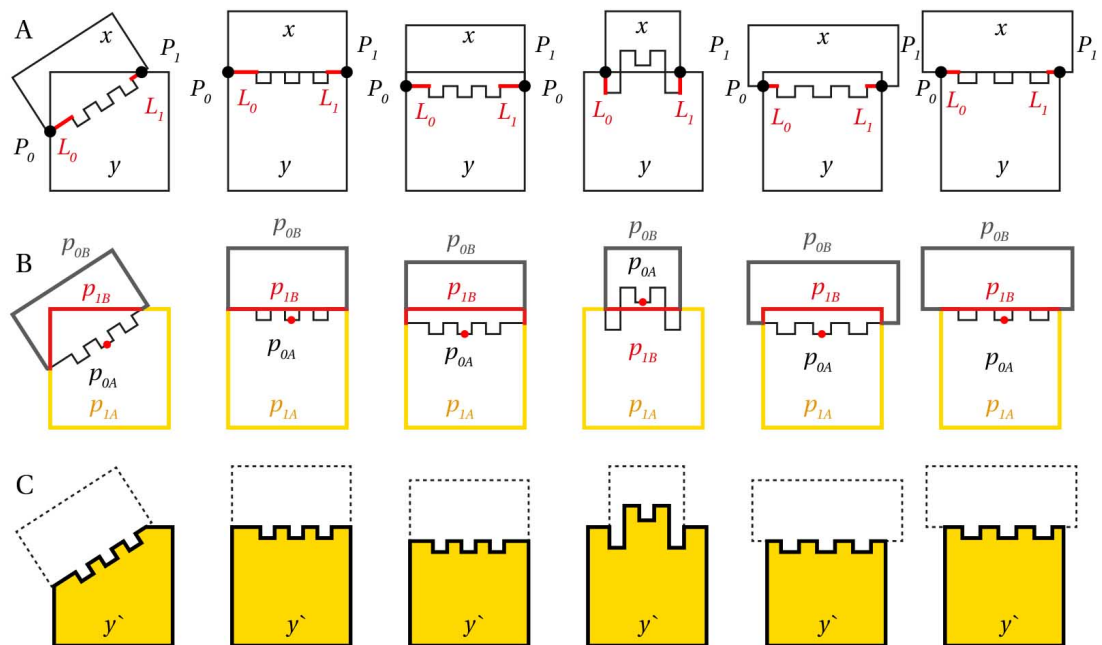


Figure 5.66 – 2D polygonal merge method: a) detection of intersection points, b) selection of the correct outline part to be replaced by the joint outline part, c) the joint outline is merged with the element outlines.

## 5.7 Conclusion

### Outlook of the Joinery Solver performance

The collision search methods (curve-to-curve, face-to-face, plane-to-face, mesh-to-mesh) takes most of the computation time to identify the right element due to the costly geometrical comparison. Besides this, there is only a minor difference between the R-Tree search and models that employ Mesh based graph models. The connection zones are identified close to

$O(\log MN)$  in a runtime. For this comparison, the Joinery Solver employs an optional graph input for tracking neighbors within pairs of elements. Usually, this method is needed when the algorithm has to be optimized for one case study, and the significant performance is required. Besides this, the local search takes a significantly longer time, even if the adjacency is given. However, the search speed is not equal to a design and debugging speed. Timber structures often contain a self-similar large amount of elements. Understanding the global joinery behavior and fabrication methods is often performed with only a dozen less or a few hundred elements. In such cases, the algorithm runs within less than 200 ms for 100-200 elements, excluding Mesh Boolean Difference method (1.5 sec for simple rectangle or cylindrical elements using CGAL library), or Polyline Intersection (80 ms), which is sufficient and responsive enough for the research scope. Usually, the testing process takes a longer time than the finalization of the entire project. As a consequence, the priority is given to choose between the joinery types instead of designing the shape of a structure that can be generated after the valid assembly method is chosen.

### **Conclusion of the Joinery Solver**

The proposed method shows that it is possible to automate the local joinery generation, considering timber fabrication methods proven by physical tests. The Joinery Solver is able to identify connection types and generate wood-wood connections based on the predetermined joint shapes. The application also allows the implementation of the new connection types and is not limited by the given models. The aim is to understand a common logic within pair-wise connections and categorize joints without avoiding their possible specificity. The analysis of existing built projects, pavilions, and physical tests shapes the algorithm. Every timber project is unique in its details. The challenge is to have a system where multiple different structures could co-exist within the same interface. The solution to this problem is the joinery generation at the smallest scale of the connection nodes.

From the architectural point of view, the local joint conditions already suggest possible structural applications. For example, raw-wood connections suggests the design of the following structures: frame systems, Nedorades, post and beam structures, flat and spatial trusses, single and double-layer grid shells. The stacking of beams results in slab and wall systems either straight or following a tree shape. Additionally, the Joinery Solver demonstrates that it is possible to employ similar modelling strategies using different types of timber elements. The joint similarity is based on the machining methods that have no prior definition of an element shape that is being cut. In contrast, the tools inform the shape of a joint. The Joinery Algorithm could also be understood as an archive of previous projects that helped arrive at its current state. In conclusion, the macro scale of a timber structure is kept as a design process for the user of the application, and the micro joint scale is automated.

### **Divergence between Plates and Beams**

The developed methods demonstrate the joinery methodology of plates and raw beams. Therefore it is necessary to discuss where they diverge from more standardized workflows in the current production and building industries and share similar specifications. For example, at the connection zone, the joinery geometry generation method is equal. However, the topology of plate structures and raw woods result in different classes of structures. For example, plates are used for segmented timber arches, shells, and folded structures, whereas raw woods are more used for frames, trusses, Nexorades, and grid shells. Another example of walls and slabs can be built using fewer connections while employing panels, whereas beams must have additional subtractive post-processing to interconnect elements one by one to cover a similar surface area. Currently, the robotic fabrication of raw timber is more economically viable than glue-laminated timber, and they have added value towards decarbonization, but they also impose specific aesthetical qualities that are subject to design needs. Lastly, the frame systems built from linear elements must be covered using, e.g. panels, facade elements, or membranes. The so-called structural skins and facades in relation to raw wood must be considered too. Enclosures may not necessarily have only wood-wood connections and can be specific to individual structural morphology, such as roof tiling. Consequently, hybrid frame and plate structures are proposed for the joinery solver to strengthen the structures by additional bracing and covering the linear elements.

# 6 Scanning

---

This chapter is based on:

P. Vestartas and Y. Weinand. Laser Scanning with Industrial Robot Arm for raw wood Fabrication. *ISARC2020, Kitakyushu, Japan, October 27-28, 2020.* p. 773-780, 2020.  
DOI: 10.22260/ISARC2020/0107.

---

## 6.1 Foreword

The Scanning chapter presents an integration of laser scanning and point-cloud processing for robotic raw wood fabrication (see Figure 6.1). There are two main parts: a) Faro Focus S 150 hardware and software implementation to the robot controller, b) point-cloud processing algorithms for a scanned tree library and a tree trunk alignment within a fabrication setup. The workflow results in an open-source library called Cockroach [116], applicable not only to solve the current research problem but also for fabrication-aware point-cloud processing and architectural applications when scanning is used. The findings compare the scanning method based on calibration, the time needed to communicate between the robot controller, and the application's accuracy. The results show that it is possible to perform robotic cutting and scanning interchangeably in one automated workflow.

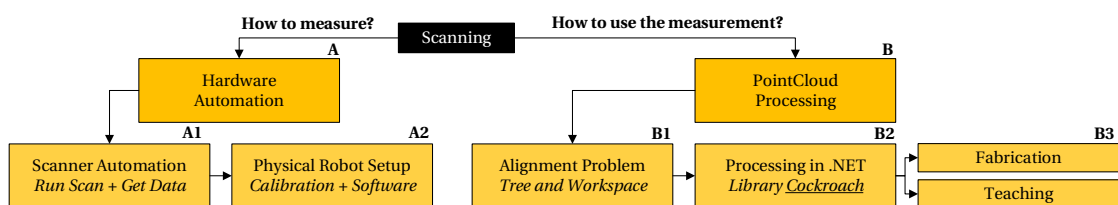


Figure 6.1 – Scanning workflow: a) scanner automation b) point-cloud processing.

## Chapter 6. Scanning

---

The integration of the Scanning chapter in the overall methodology is seen in Figure 6.2. The fabrication starts by geometric acquisition of a tree stock as an input for the Joinery solver. The robotic fabrication is linked with scanning using three point-cloud alignment methods a) markers, b) cloud-to-cloud registration, and c) skeletonization to know the position and orientation of a tree trunk in relation to the robot.

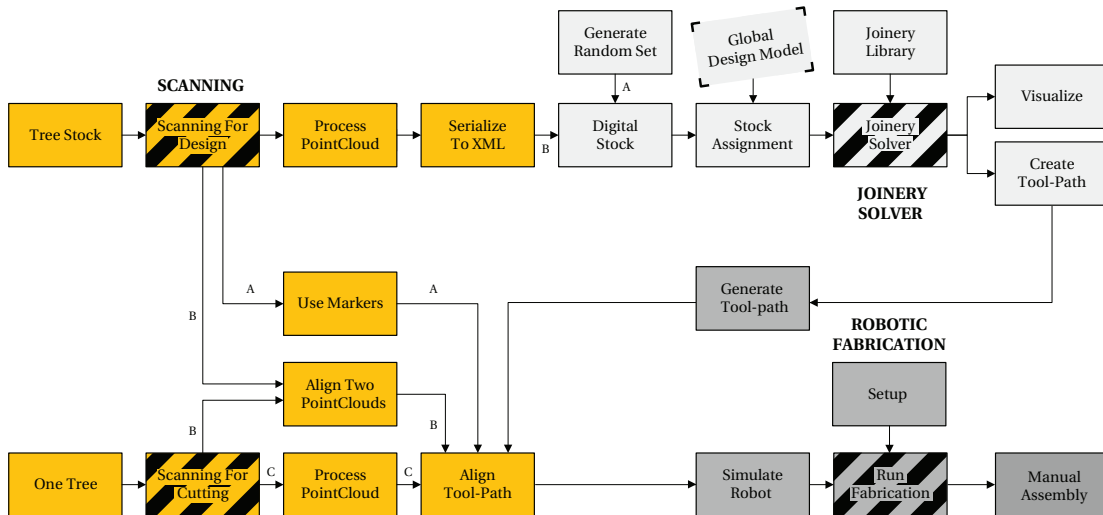


Figure 6.2 – The scanning method integration in the overall design-to-fabrication workflow.

---

The Scanning chapter is structured as follows:

- Section 6.2 introduces the types of objects that are scanned, the state-of-the-art algorithms for point-cloud processing, calibration methods and the contribution of this study.
- Section 6.3 Laser scanner Faro Focus S150 hardware and software integration with the industrial robot arm ABB IRB 6400R
  - Objective of the robotic scanning
  - Setup and control of the robotic scanning
  - Scanner and robot calibration
- Section 6.4 Point-cloud processing for raw wood fabrication.
  - Objective of Point-cloud processing for tree scans
  - Skeletonization to obtain minimal radial parameters
  - Cloud-to-cloud registration for a tree alignment from a digital stock
  - Point-cloud processing framework - Cockroach
- Section 6.5 summarizes the efficiency of the proposed methods.

## 6.2 Introduction

### Scanning Differences in Saw-mills and Architectural Design Workflows in Raw wood

The majority of timber construction projects employ standardized engineered products, and timber is rarely seen anymore as a naturally grown construction material. Timbers are glue-laminated to span large distances, cross-laminated to make timber joints regardless of its orientation. Engineered timber products such as panels, boards, and square beams define the vocabulary of timber research [26, 130]. However, these techniques could be enriched by timber with as little transformation as possible. Today, raw wood research shows the potential in whole timber structures by exploiting robotic arms, computer-vision, cutting and assembly techniques to adapt to the natural characteristics such as bending, bifurcation and taper [104, 146, 175].

The scanning methods for timber are applied in sawmills, ranging from fast laser scanners [150, 162] to volumetric CT scans [7, 21, 132]. In the industrial context, geometry acquisition is used to optimize the cutting pattern of trees into boards, identify timber knots and disregard crooked timber. The process is designed to get the most profit from timber without defects. The methods are often well structured using a digital database to track the maximum use of material, age, species, and the location where the wood is harvested from [87]. The so-called stock of wood and its properties is already present in larger centralized companies. The problem is that such data is only available for the sawmill companies' and is neither transferred for design use nor for digital fabrication. Also, scans are only captured for sawing optimization and the processed lumber no longer resembles the initial tree. There are only limited research and development applications (ImaxPro) regarding raw wood cutting that are not open-source or applicable for wood irregularities.

This situation is changing in architectural research starting from AA Hooke Park since the introduction of robotic cutting. The numerical cutting demonstrated a direct relation between CAD software and automated machining. The physical experiments in raw wood helped change the notion that only standardized timber could be employed. This shift is in close relation to scanning methods. The primary goal of scanning is a measurement tool that automates the manual process needed to get numerical values about timber length, radius, surface characteristics. The scanning gives a vision to the blind industrial fabrication machines and informs design decisions. The most common techniques are marker detection and tracking devices, photogrammetry, camera sensors, laser scanning, virtual reality applications, and volumetric scanning.

Hardware automation is only the first step, but what is lacking the most is Point-Cloud processing tools. Without such methods, the scans have little value besides visualization. Point-Cloud processing libraries such as Open3D [188], Cilantro [186], CGAL [161] are written in the lower level languages C++ and are not brought for higher-level languages such as C# or Python. Architects, engineers and roboticists often have little knowledge of these existing methods

because they are trained to employ CAD visual interfaces. The steep learning curve distances designers and engineers from fabricators and computer scientists. At the same time, developers in the Computer Science field have little interest in timber fabrication practices. One of the critical goals, besides fabrication workflow, is the development of an interface that bridges the point-cloud processing tools with a CAD environment (Rhino3D) in a form of a .NET library written in a cross-platform language C# PInvoke to call the robust and fast C++ point-cloud processing methods [116].

### Raw wood Fabrication Problem - Position, Shape, Topology

There are two reasons why scanning is necessary for raw wood fabrication: a) positioning a tree-trunk within a fabrication setup (see Figure 6.3A), b) create a digital stock of timber and employ the tree library for a design, (see Figure 6.3 B). The placement of a tree and radial-parameters vary within the fabrication setup (see Figure 6.3 C). Only radial parameters, central-axis and topology (straight/curve/branched) are analyzed in the design context, and natural characteristics are excluded, such as bark, cracks and knots. Furthermore, design of timber connections must consider the unpredictability of wood by using the simplified minimal models.

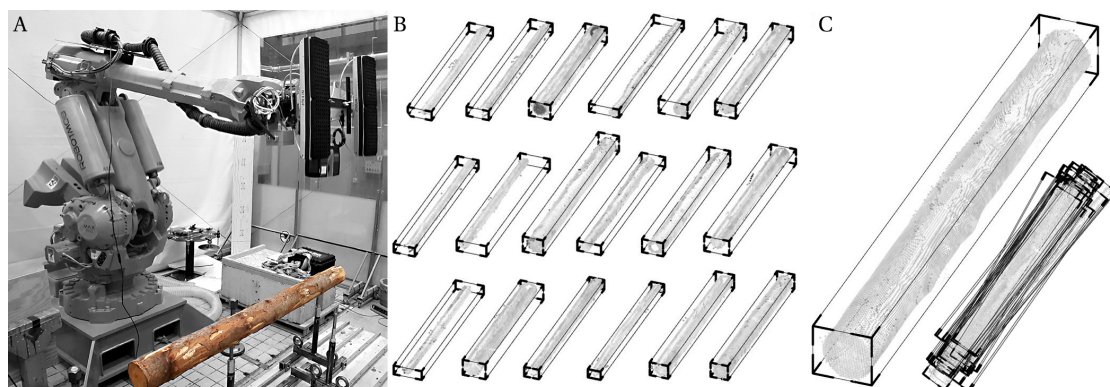


Figure 6.3 – Scanning method: a) a group of scans are collected using a laser scanner and a robotic arm, b) point-clouds of trees, and c) the variability of tree placement within the setup.

The digital stock of timber could be obtained by scanning groups of trees, as seen in Figure 6.4. It is possible to apply a static scanning method when trees are laid on the ground in large groups. Then point clouds are processed using the registration software and then the individual scans of tree trunks are extracted. The point-cloud processing could be applied to find a tree central-axis and radial-parameters. Then a point-cloud file is discarded, and only geometrical features are written for storage, such as XML or TXT files (see Figure 6.4) C. The similar process is applied to scan a tree stock gathered from three publicly owned forests: Rossiniere, Chavornay, Lausanne. The files serve as a digital library that helps develop a structural system from a set of processed tree scans called the stock. This data could also be used during the fabrication stage.

## 6.2. Introduction



Figure 6.4 – Collection of a tree stock: a) multiple tree scans, b) ground removal and clustering into individual elements, and c) the deviation from the uniform cylindrical geometry.

### Context and Setup

The tree harvesting process is assisted by a collaboration with mountain forestry in Rossiniere and Lausanne (see Figure 6.5). The Spruce trees are harvested in the Swiss Alps using a cable system due to the difficult mountain conditions, then brought to a temporary processing site where trees are cut to 5 meters length for the transportation and saw-mill processing (see Figure 6.6). Timber that is not used in saw-mills, for example such as small-radius crooked timber is brought to EPFL and scanned for structural design use. The small-radius timber is mostly left rotten in the forest or sold as fuel. Therefore it has a low economic value. For research, this material is sufficient enough for small-scale prototypes since it takes time to fabricate large wood elements with CNC or robotic application installed for education use.

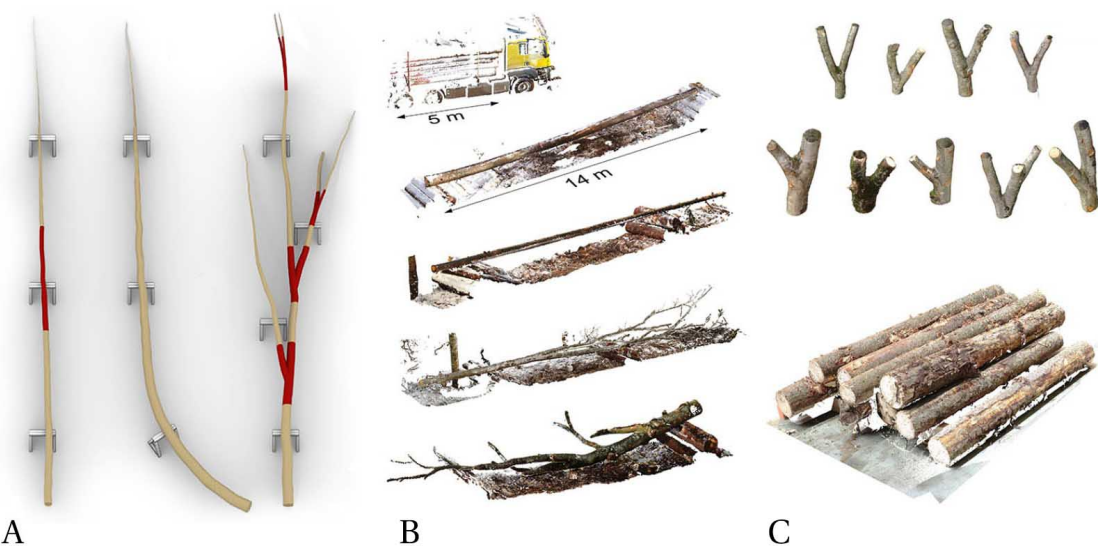


Figure 6.5 – Scans taken from the publicly owned mountain forest in Rossiniere: a) the intent to find straight, crooked and forked tree topologies, b) harvested trees, and c) trees brought to EPFL for fabrication.

The research employs ABB IRB6400R<sup>1</sup> industrial robot arm and Faro Focus S150<sup>2</sup> stationary laser scanner. The scanning is an integral part of a design-to-fabrication system, including the laser-scanning and the joinery solver. The objective is to scan the raw wood for a design and fabrication using an automatic tool-changer to perform different tasks interchangeably, such as scanning, vacuum-grip, and cutting. The scanning alignment of crooked trees is made within the machining setup. Also, geometry acquisition is needed for design by means of a digital stock. The scanned trees are assigned to a digital model that could vary from tree shapes. The selection process is guided using a Hungarian algorithm<sup>3</sup>. Afterwards, the timber joints are created using the Joinery Solver. Consequently, the fabrication tool-paths are oriented to machining space and the timber elements are assembled manually.

<sup>1</sup><https://library.e.abb.com/public/d9b91046c343c6fdc1257b1300574b6f/lRB%206400R.pdf>

<sup>2</sup><https://www.faro.com/en/Products/Hardware/Focus-Laser-Scanners>

<sup>3</sup>[urlhttps://github.com/vivet/HungarianAlgorithm](https://github.com/vivet/HungarianAlgorithm)



Figure 6.6 – Tree harvesting and scanning processes: a) trees are cut manually and brought to a temporary site by a mountain cable, b) selection of tree forks, c) trees are cut in a few large pieces, d) forks are brought to IBOIS, and e) then scanned (fabrication rig was not developed at that time).

## Chapter 6. Scanning

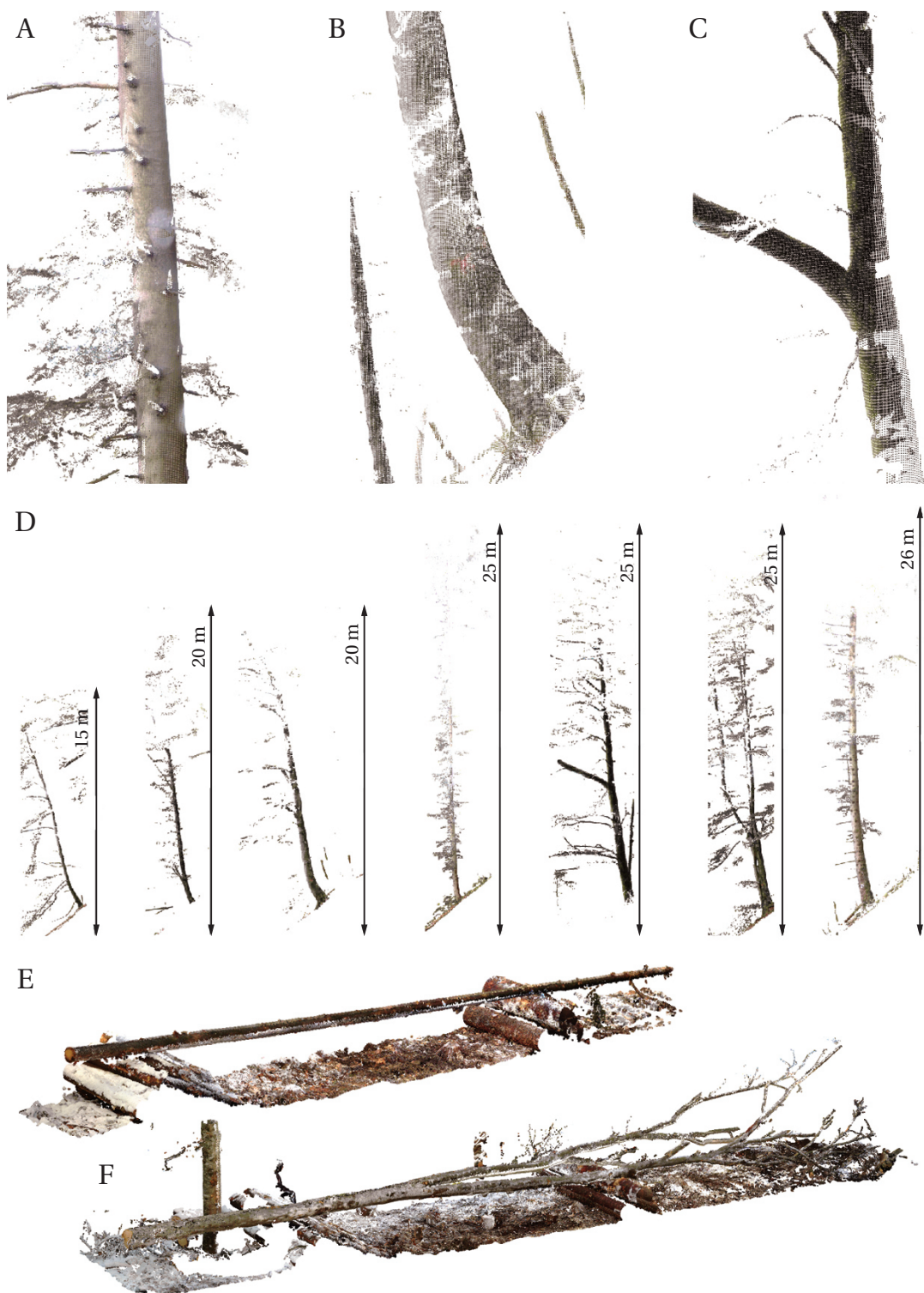


Figure 6.7 – Scans from the mountain forest in Rossiniere: a) straight trees, b) the reaction wood close to the base of a tree, c) bifurcation, d) total length of a few selected trees, and e) the scans of trees after cutting, showing major topologies of the straight tree trunks and sharp bifurcation.

## 6.3 Laser Scanner and Industrial Robot Arm Synchronization

### Objective of Robotic Scanning

Often scans are aligned using the slow cloud-to-cloud or target based alignment because the scanner's orientation is unknown. The proposed workflow helps to use the robot as a cloud-to-cloud registration tool. When the scanner's position is known - the TCF (Tool Center Frame) is used to transform scans from a base plane to the target plane (see Figure 6.8). The precision of the scan depends on the tolerance of the chosen calibration method.

The Faro scanner is connected to a computer via wi-fi or the Ethernet cable. A series of methods are performed to send the scanner parameters, perform a scan, and retrieve the scan file. Point clouds are also cropped to an approximate log position depending on the user input. If the robot environment is unknown, the Peek method performs one scan, then loads it to Unity software for a preview. This step is needed because, initially, it is not known where the workpiece is located. It also helps to avoid a collision between the robot and existing objects within the workspace. When the scanning is finished, it is known that the scanner is operational. For example, there is an electricity supply, the connection between devices works, data could be stored in a memory card, the environment is safe enough to move the robotic arm, and the user can approximately add the bounding-box values such as the height of the setup, the maximum width and length. The previous points belong to a checklist that is tested before the fabrication starts for many logs. Afterwards, the MultiScan operation could be run many times within the same setup. A series of scans are taken with the robot arm to have as much point-cloud coverage of the scanned object as possible (see Figure 6.8). When the checklist is tested, the overall workflow can be repeated automatically. This process is possible due to the calibration that helps to align multiple point clouds (see Figure 6.9) that are post-processed afterwards.

### Setup and Control of Robotic Scanning

The scanner is mounted on a vacuum gripper (see Figure 6.10 A) to perform a series of scans before the fabrication starts. The FaroCSharp<sup>4</sup> application can trigger the following methods: connection via wi-fi, synchronization of scanning parameters, start, pause and stop scanning, send and read the data. The scanner's field-of-view is 0°- 360°degree in the horizontal and -150°× 150°in a vertical rotation. The Faro laser scanner has an automation adapter that acts as a tool-holder. The custom U-Shape metal plate is added to mount the tool-holder to the robot gripper permanently (see Figure 6.10 B). The tool holder is temporarily bolted to the scanner. The scanner could be attached or detached from the robot by manually unscrewing one central bolt if, for instance, it has to be used temporary outside the research context. Lastly, the robot arm has a Schunk adapter to speed the mounting process to switch between the spindle, gripper and scanning tools (see Figure 6.11). Consequently, the scanner holder,

---

<sup>4</sup><https://github.com/petasvestartas/FaroCSharp>

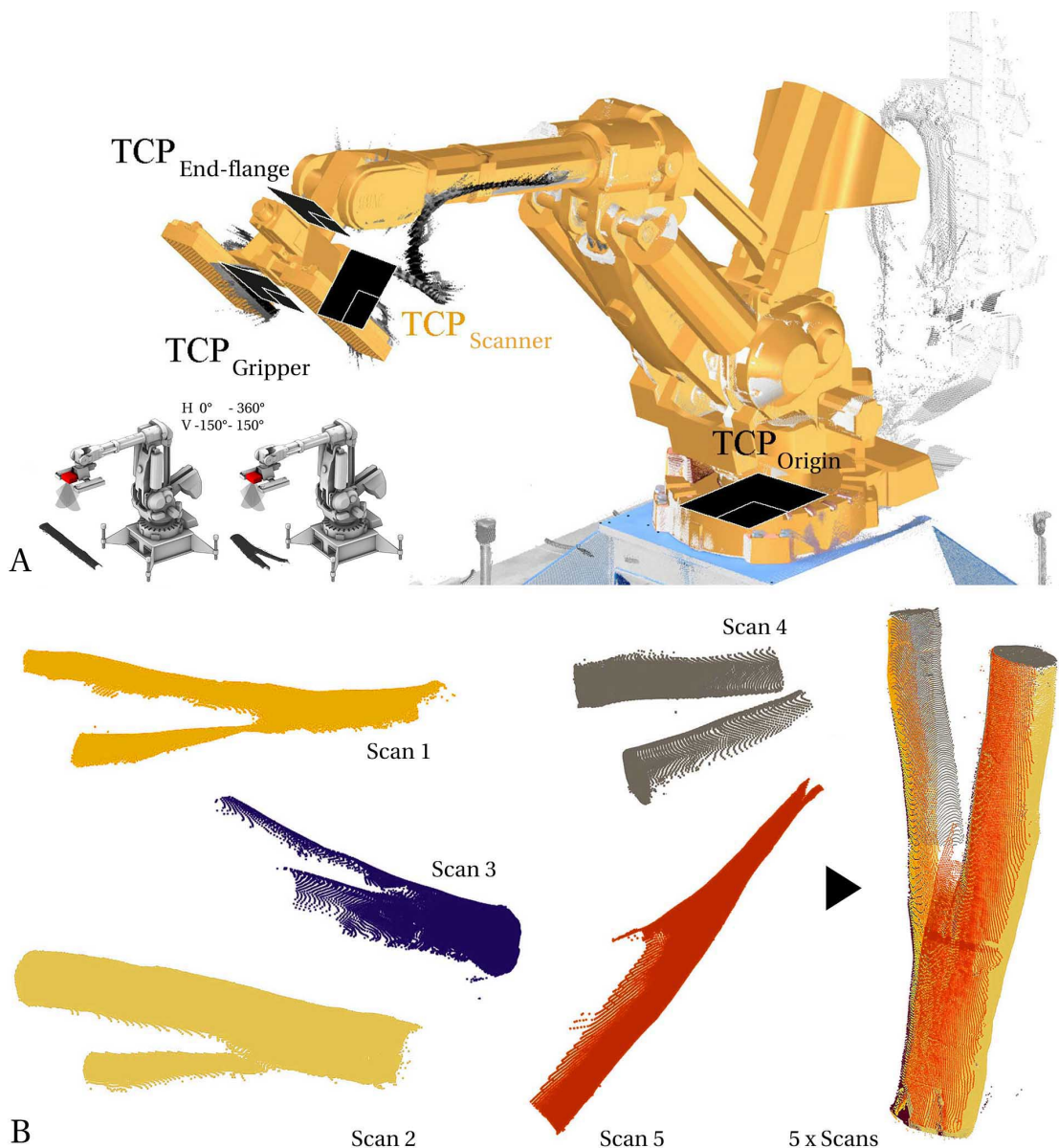


Figure 6.8 – Laser scanner is mounted on (a) the robot. The  $TCP_{Scanner}$  is not known. The scanner can capture a horizontal angle in the range of 360° and a vertical angle in the range from -150° to 150°. The scanner captures partial scans (b) that are aligned together.

tool-changer and the customized software allows controlling the scanner using the industrial robot arm.

The robot control is based on the software interoperability between the CAD/CAM application (Rhinoceros) and the cross-platform game engine (Unity). One software is utilized for the tool path generation based on the Joinery Solver, while the other is used to simulate the robot's movements physically. Each software has different coordinate systems that have to be

### 6.3. Laser Scanner and Industrial Robot Arm Synchronization

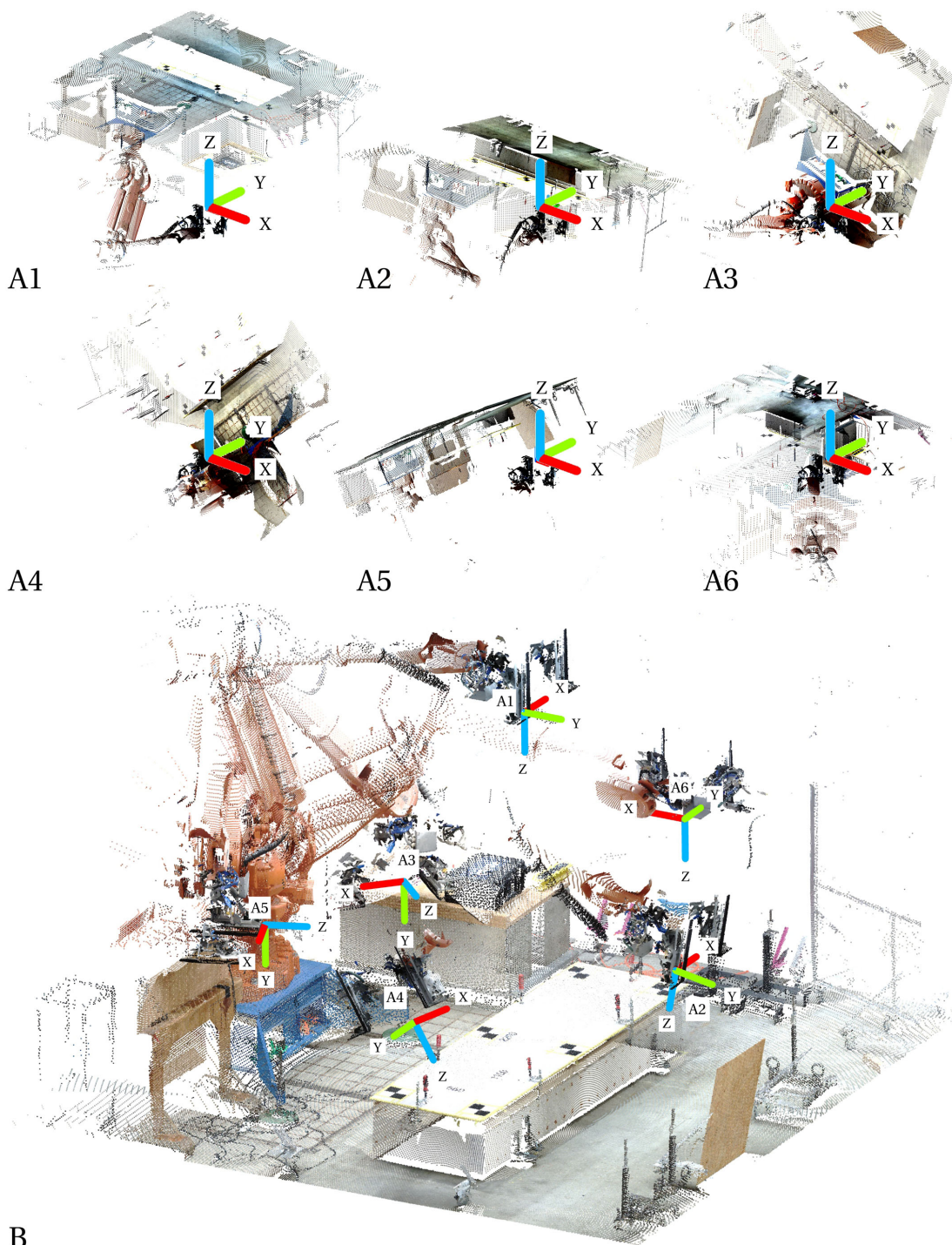


Figure 6.9 – Calibration process: first six scans are taken using six different robot poses a1-a6. The checkerboard targets seen in the scan are used for the scan alignment. Once the scans are aligned to the robot space (b) the six orientations are reused for the future scans.

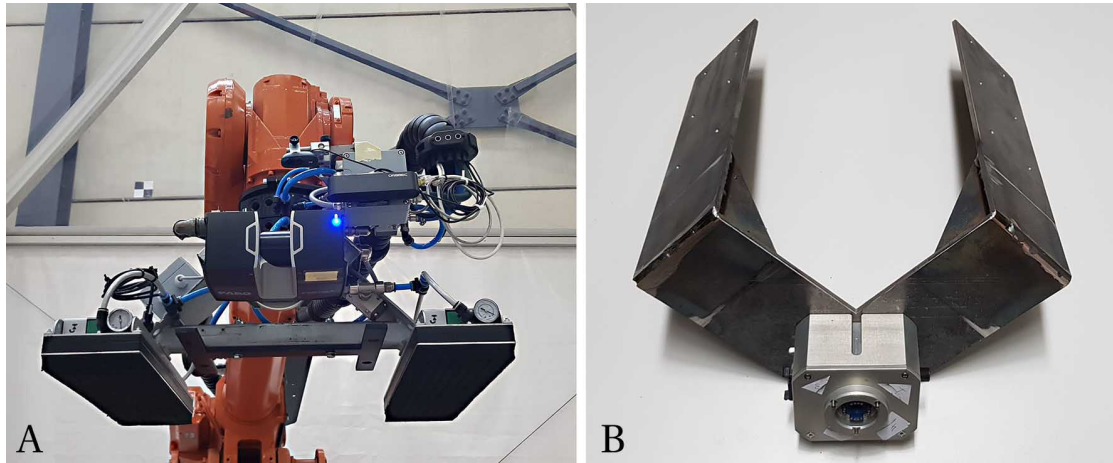


Figure 6.10 – The scanner is attached to the robotic arm (a) using a steel-plate holder (b).

matched to get an exact representation. The notation of rotation (Quaternion) and position (XYZ) is translated as following  $R_{ABCD}$  to  $R_{BDC-A}$  and  $T_{XYZ}$  to  $T_{XZY}$ . Each scan is triggered when the robot reaches a target, and then the next pose is taken when the scan is finished.

There are two scanning modes: a) the helical and b) stationary (see Figure 6.15). The stationary method is based on point scanning and sending data via wi-fi to a computer. In contrast, the helical mode could work continuously by sending signals from the robot controller to the laser scanner via a nine-pin cable. When the helical scan is performed, it is necessary to know the robot start, end position, and speed. Additionally, the robot could stop at small increments, trigger the scan, retrieve the signal data and convert the byte array to the point list. This method is also useful when a robot is placed on a linear track to gather a large scan in a shorter time than the stationary one. Consequently, the scanner gains a significant advantage by using known robots movements for the point-cloud registration.

### Scanner and Robot Calibration

The laser scanner has to be calibrated concerning the robot's end-axis to know its relative position at each scan. This process helps to avoid point-cloud processing and registration because the position of the scanner is already known in the robot world space (see Figure 6.12). The unknown (see equation 6.1) is a transformation matrix  $X$  of a scanner  $TCP_S$  that is relative to the end of the robot 6th axis  $TCP_R$ .

$$TCP_S = TCP_R + X \quad (6.1)$$

When the scanner is calibrated, a list of scan points  $P_i$  in a world-space is found by multiplying the rotation matrix  $XR_R^W$  and the translation matrix  $XT_R^W$  of the robot in the world space with points  $p_i$  that are positioned relative to the scanner rotation  $XR_S^R$  and position  $XT_S^R$  that is

### 6.3. Laser Scanner and Industrial Robot Arm Synchronization

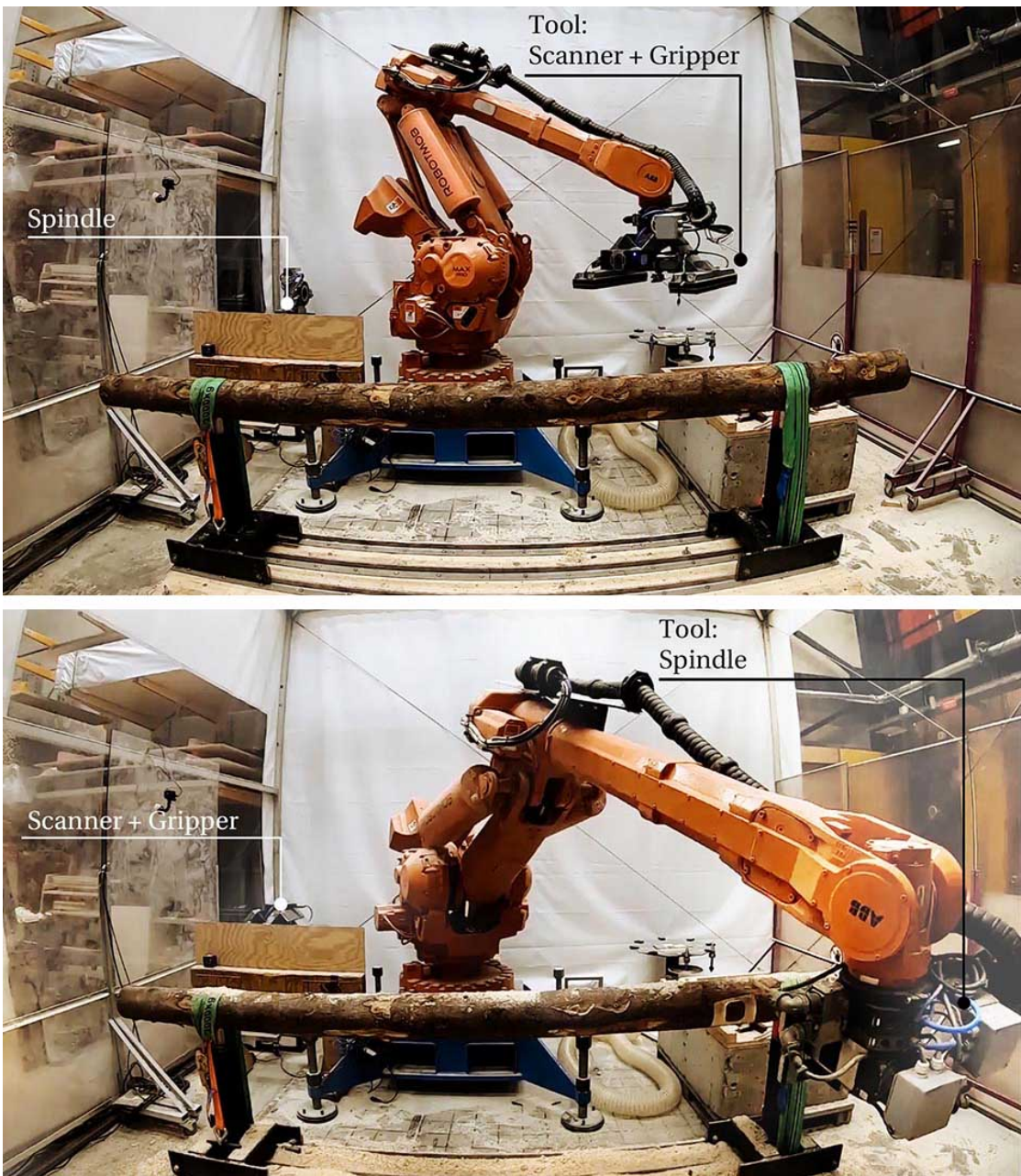


Figure 6.11 – Laser scanner is mounted on a vacuum gripper (a). When the scan is finished the tool is automatically changed to the spindle (b).

mounted on the robot arm, as described in the equation (see equation 6.2).

$$P_i = X R_R^W * (X R_S^R * p_i + X T_S^R) + X T_R^W \quad (6.2)$$

The calibration accuracy limits the alignment of scans (see equation 6.3). Several calibration

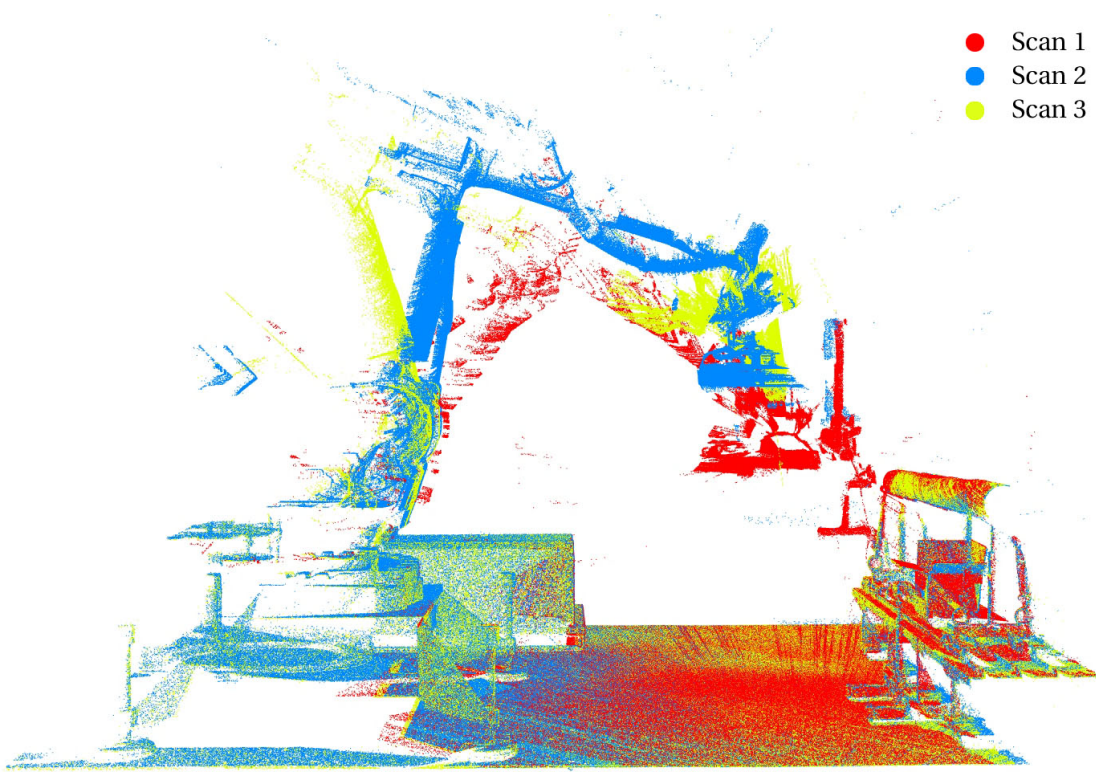


Figure 6.12 – The result of the calibration using Faro Focus S 150 laser scanner. Each color represents a separate scan.

methods are applied including: (a) the multi-scan registration on a sphere, (b) alignment to a robot base, (c) employing an external scanner device, (d) the sharp tool manual reference, and (e) the 4TCP method for the scanner holder measurement. The precision  $T$  of the scanning technique depends on the scanner tolerance  $T_S$  ( $\pm 0.1\text{-}0.5$ ), marker detection precision  $T_M$ , robot accuracy  $T_R$  ( $\pm 0.5\text{-}1.0$ ), and the calibration method precision  $T_C$  (see equation 6.3).

$$T = T_S + T_M + T_R + T_C \quad (6.3)$$

First calibration test is made by employing the Faro Arm (see Figure 6.13 D) to measure the end-flange of the robot and laser-scanner. The result is inaccurate and only gives an approximate position of the scanner. The imprecision varied between  $\pm 1.0\text{-}2.0$  cm in translation and  $\pm 1.0$  degree in an arbitrary rotation. While the Faro Arm is a precise measurement tool, the reflective surfaces and possible laser-scanner tilt in relation to the tool-holder could result in such a high inaccuracy.

A reference point calibration using an engraver tool and checkerboard markers proved to gain a sufficient tolerance. The robot is moved manually using the Teach Pendant to the centre of each target within several tries. The tolerance of manual measurement ranges between  $\pm 0.25\text{-}0.75$  mm. Then the robot is automatically moved to the highest reachable position based on

### 6.3. Laser Scanner and Industrial Robot Arm Synchronization



Figure 6.13 – Scanning a Faro Focus scanner using Faro Arm.

a given tool path. After the movement, the robot controller triggers the scan signal. When the scan is finished, the data is sent to the computer for the marker detection. The centers of the physical markers are measured multiple times per each point to increase the precision and the target location that are detected by the Faro Scene software. The same procedure is tested first using 4, then 6 and 12 markers to increase the tolerance. The resulting precision is between  $\pm 1.5\text{--}2.0$  mm that is good enough for detecting the raw wood trunk position for the manufacturing of timber joints.

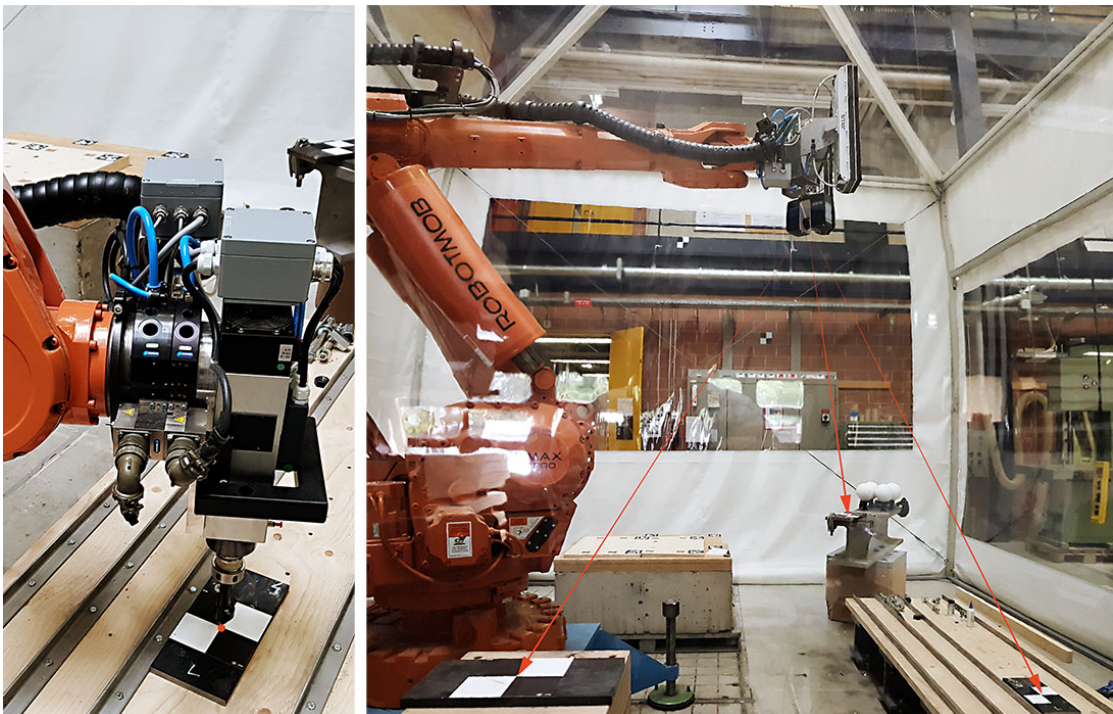


Figure 6.14 – Targets are measured by the sharp-tool and captured by the laser-scanner.

The trial and error process of the scanner calibration could be seen in Figure 6.16. The first

## Chapter 6. Scanning

tool-holder measurement method is the most imprecise (10-20 mm tolerance) and time-taking process. Sixteen robots poses are taken to get four corners of the tool-holder, then the centre point of the plane is moved by 135.5 mm in Z-Axis given by the scanner documentation. The second single-robot-base-scan method decreased the tolerance to 2-3 mm tolerance. The third method is based on multiple scanning methods - 9 scans per circle, within three circles that belongs to one sphere. The scans are aligned using Faro Scene software. Each group of 9 planes was fit to a circle used to define the translation vector between the end-flange TCP and the scanner TCP. All of the Faro planes are oriented from end-flange TCP to XY plane and averaged in their position and orientation. The fourth method is based on the hand-eye calibration using 4 TCP calibration. A sharp tool in the milling motor is used to calculate the rectangular marker position and orientation. Afterwards, the single marker is scanned to align scans to robotically measured points. The last method proved to be the simplest and accurate enough.

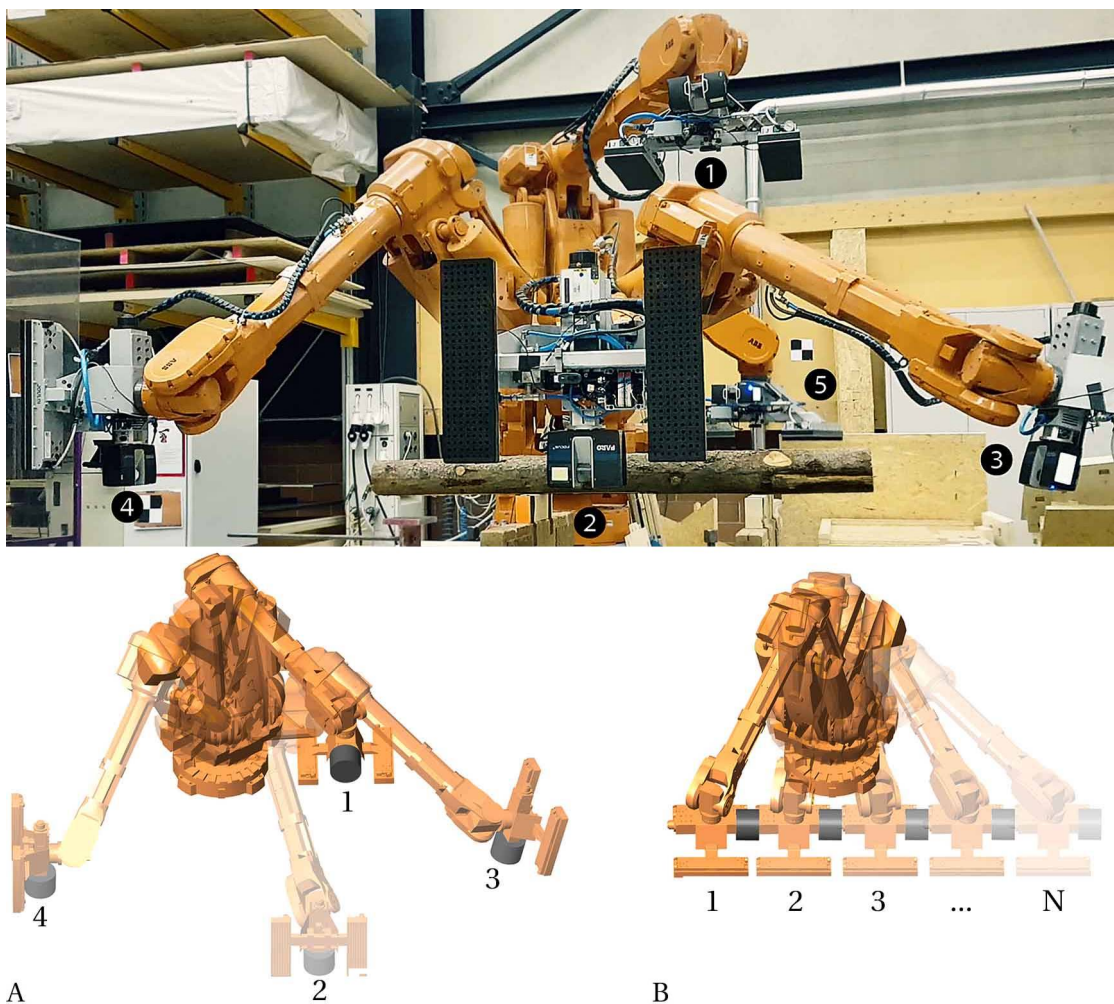


Figure 6.15 – Scanning types: a) the stationary mode when scans are taken one at a time, and b) the Helical mode when the scanner is running continuously without the vertical rotation.

### 6.3. Laser Scanner and Industrial Robot Arm Synchronization

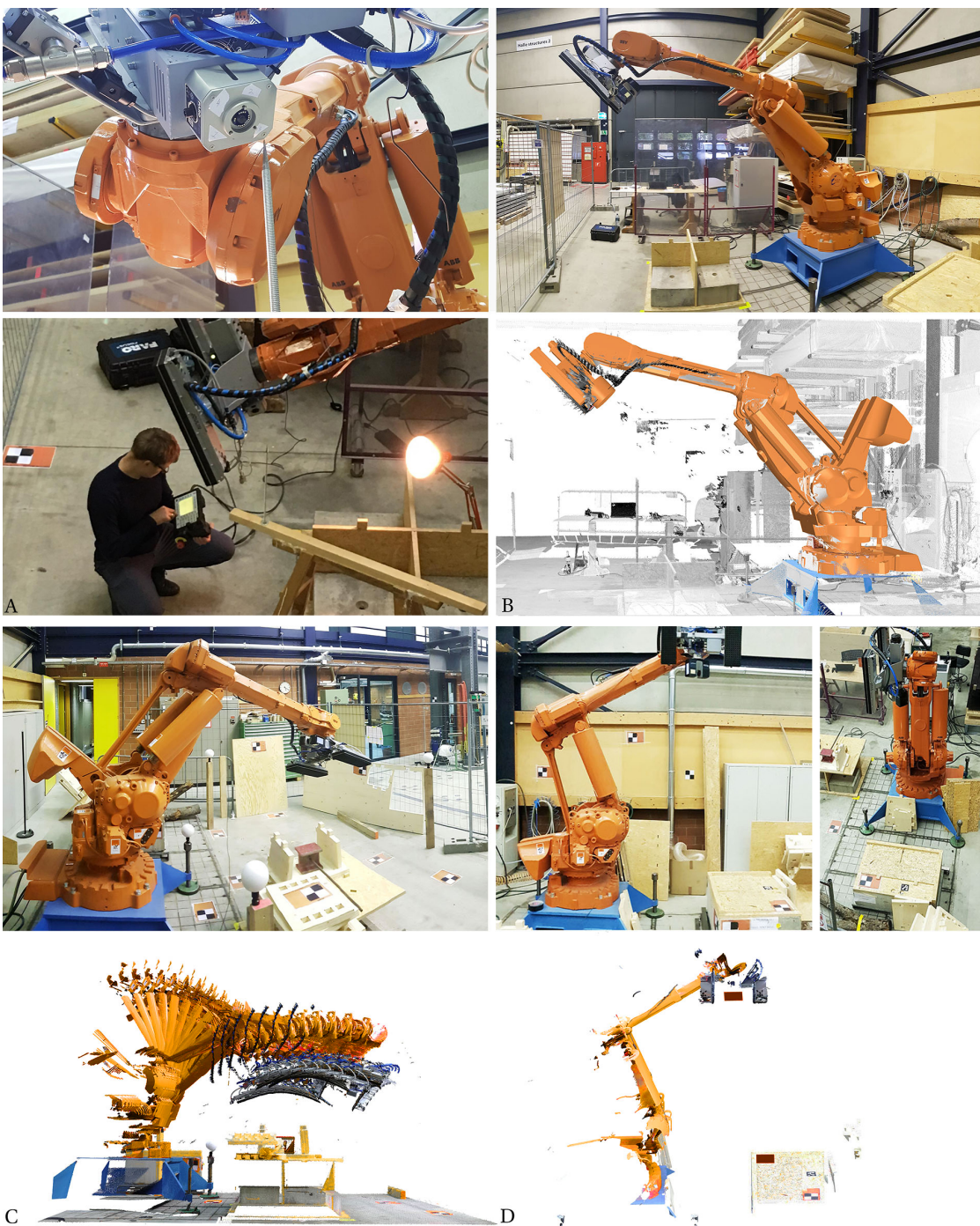


Figure 6.16 – Calibration method tested with ABB 6400 and Faro Focus S150: a) TCP calibration for the tool-holder (10-20 mm tolerance), b) alignment with the base (3-5 mm precision), c) 27 scans are aligned using Faro Scene targets on a sphere (2-3 mm precision), d) Alignment with a known work-object that was measured with the TCP method (2 mm precision).

## Chapter 6. Scanning

---

After performing all the different calibration methods resulting in the best 1-2 mm tolerance, the calibration was not in the expected range of precision for the Faro Focus scanner (normally less than 0.1 mm). There are several reasons for this, including:

- the rented robot is a relatively old machine that does not have the high precision anymore
- the scanner is mounted on a relatively big and heavy gripper. An assumption is made that the robot laser scanner's position might minimally change its orientation due to the heavy load
- each of the scans is taken at the maximum reachable position of the robot resulting in a backlash of the cantilevered arm

As a result, to validate these assumptions and propose a new method the four marker measurement method is performed. Instead of one TCP, multiple TCPs were used, each slightly different for the individual robot poses. In other words, each of the scan has a unique TCP. When this procedure is applied, the scans are aligned within the given tolerance of the scanner specifications ( $x < 1$  mm) (see Figure 6.17) in such a way the robot imprecision is removed. In conclusion, the scanner is aligned well and tested during the fabrication without any errors when understanding the cause of imprecision during the calibration process rooted in the robot movement and the mounted tool.

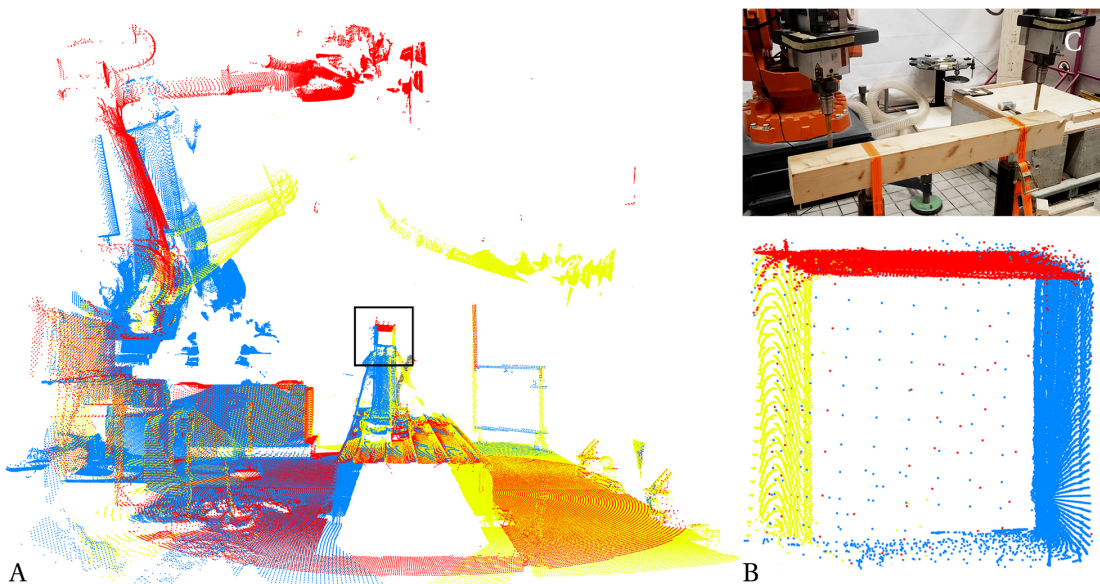


Figure 6.17 – Aligned scans based on the punctual calibration using multiple TCPs: a) aligned scans, b) detailed view, and the robot movement precisely along one edge of a rectangular beam.

## 6.4 Point-cloud Processing for Raw Wood Fabrication

### Objective of Point-cloud Processing for Tree Scans

The point-cloud processing methods are needed to know an approximate shape of a tree and its position within a machining setup. The simplest representation of this problem is a straight raw wood skeletonization (see Figure 6.18). For example, eight points could be taken from the flat-ends of a beam. However, the manual measurement might not be precise because a tree's actual centre axis might differ from the ends of a beam due to the curvature or twist. Besides that, this method is slow. Consequently, a series of techniques are developed to automate this process.

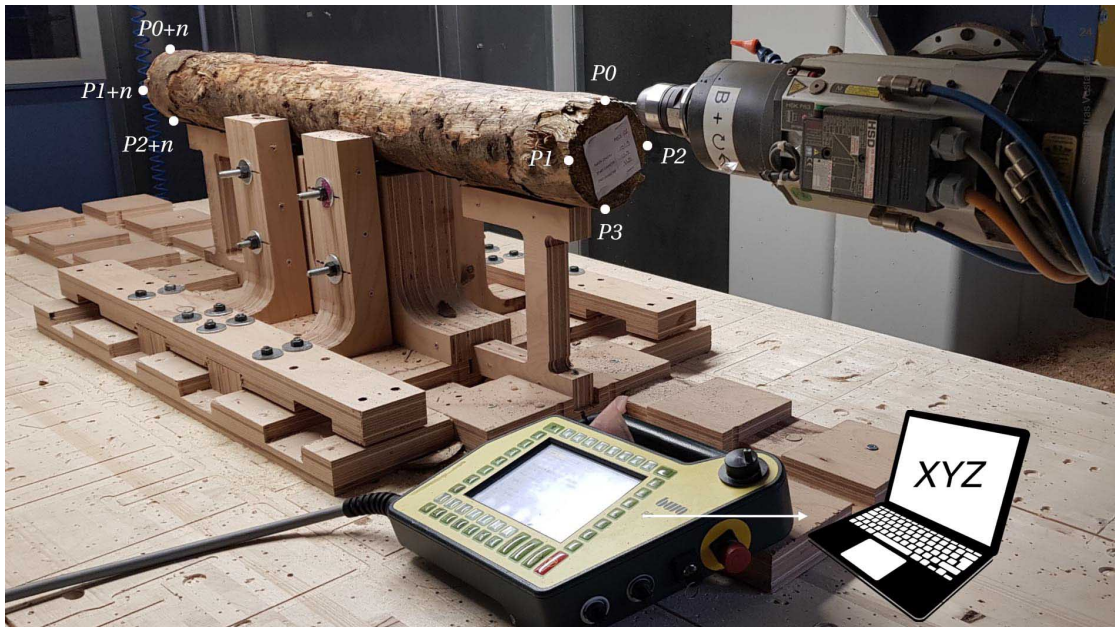


Figure 6.18 – Manually taking eight points from a straight tree-trunk using a Teach-pendant.

There are several existing methods that could be employed to automate this problem with a help of scanning: (a) QSM - modelling method that reconstructs quantitative structure models [60, 98, 128, 129], (b) MAT - Medial Axis Transform [120], (c) closed mesh reconstruction from a point-cloud and its skeletonization [1, 93], (d) image processing [95], point-cloud and (e) mesh sectioning [105, 110].

These methods are coupled with the previous robotic scanning subsection to obtain the minimal 3D representation of a tree. Three methods are developed to obtain the radial parameters of tree trunks, including (a) Flat-cut Sectioning, (b) Mesh-skeletonization, (c) Cylinder-fitting. While some of these methods are partially discussed in the before mentioned references, there is no open-source .NET<sup>5</sup> application available.

<sup>5</sup>.NET Framework is a software framework developed by Microsoft that runs primarily on Microsoft Windows.

## Chapter 6. Scanning

---

Afterwards, it is necessary to know where a tree trunk is in relation to the machining setup. It is possible to use the skeletonization methods as discussed previously. Also, a marker-less point-cloud alignment could be applied, if there is a pre-scanned digital tree stock.

These methods allowed to solve the shape acquisition and alignment problem. These algorithms opened new perspectives in point cloud processing also applicable to architectural applications. The extended framework is described in the last part of this sub-section.

### Skeletonization to Obtain Minimal Radial Parameters

**Flat-cut-sectioning** The first method is called Flat-cut-sectioning. The algorithm is developed thanks to contribution from Prof. Niels Martin Larsen[87]. The method is used for calculating central-axis and radial-parameters from straight or curved logs. The technique is based on the point-cloud sectioning when every beam has two flat-circular ends (see Figure 6.19). The workflow is divided into the following parts: get a minimal bounding-box of a point-cloud using PCA (Principal-Component-Analysis), get the two smallest planes of the bounding-box, find the closest-points within the two planes, perform RANSAC (RANdom-SAmple-Consensus) algorithm to identify the flat-cuts of the beam [52], interpolate planes from the RANSAC, cut the point-cloud by a closest-plane method, fit sections to circles, draw axis between circle centres, serialize the data to XML file. The method will fail if the robot cannot move far enough to obtain the flat cuts or the beam is not flat on both ends.

The Principal Component Analysis (PCA<sup>6</sup>) is used to calculate the bounding-box for the cropped point-cloud. Principal Component Analysis is a statistical procedure that uses an orthogonal transformation to convert a set of observations (here array of three coordinates of points) of possibly correlated variables into a set of values of linearly uncorrelated variables called principal components [43]. This transformation is defined in such a way that the first principal component has the most considerable possible variance (in this case, the X-Axis of a plane or bounding-box), and each succeeding component (Y-Axis and Z-Axis) in turn has the highest variance possible under the constraint that it is orthogonal to the preceding components. PCA is sensitive to the relative scaling of the original variables. A tree trunk's central axis is a centre-line between the two smallest face centres of the PCA bounding-box for the perfectly straight logs. However, a curved-beam requires a series of section cuts to identify the changes along the beam's axis. The following operations rely on a closest-point to the plane search.

The RANSAC [92] method is employed to identify two flat cuts of a beam. RANSAC is an abbreviation for "RANdom SAmple Consensus". It is an iterative method to estimate a mathematical model's parameters from a set of observed data that contains outliers. It is a non-deterministic algorithm because it produces a good result only with a certain probability, with this probability increasing as more iterations are allowed. The RANSAC method requires point-data that has more than half of inliers to get a satisfactory result. The inliers are points that lie on a

---

<sup>6</sup><http://accord-framework.net/>

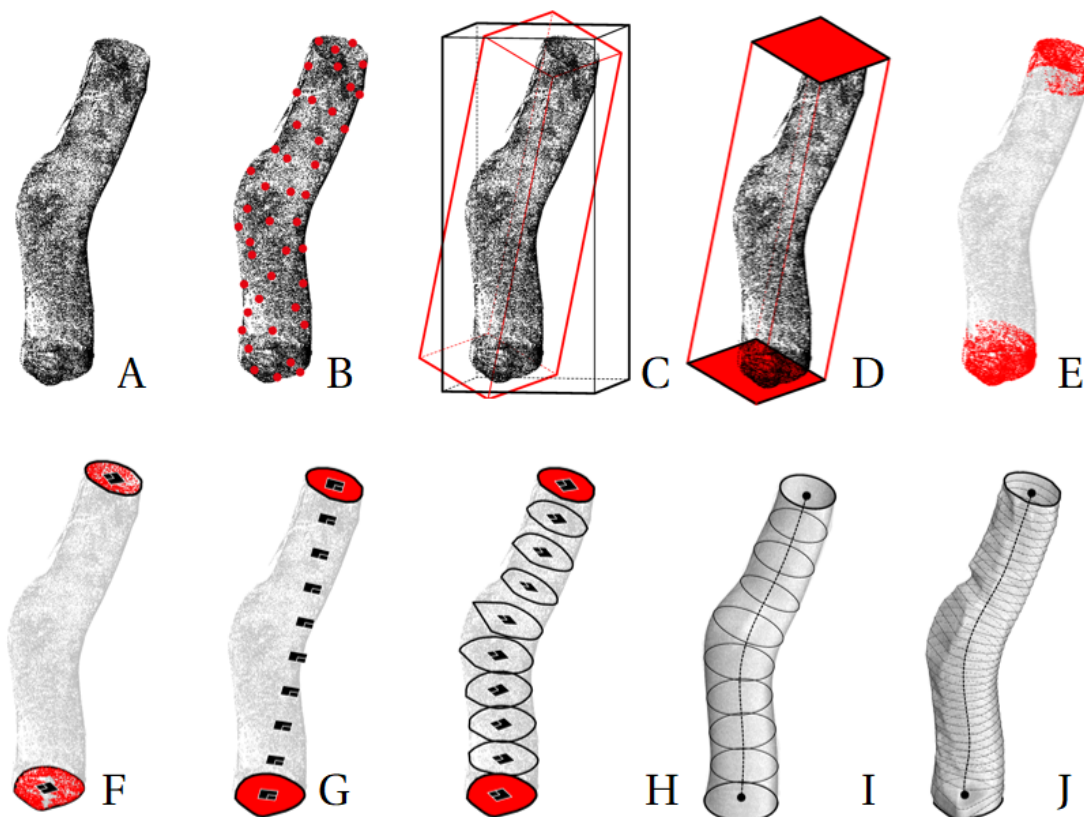


Figure 6.19 – Flat-cut Sectioning method: a) PointCloud, b) Sub-sampling, c) PCA, d) two smallest faces, e) closest points, f) RANSAC plane, g) interpolation, h) 2D Convex-hull, i) circle-fit, and j) surface representation.

plane of a flat cut of the beam and outliers are the rest of the data. The RANSAC input is taken from the closest-point method from the two smallest planes of the PCA bounding-box. The RANSAC gives a plane that is centred at the average point of the inliers.

When two planes are known at each end of the beam, one is projected to match the Z-Axis orientation. Then planes are interpolated, and the point-cloud is sectioned based on a closest-point to a plane function, as described in the Algorithm 1.

Sectioning is performed two times to fit the point array to a circle. One time for an approximate circle computation and the second with the noisy data removal (see Figure 6.20). The central-axis is computed by connecting the central points of circles. Often the section planes are parallel to the start and end plane. Therefore the sectioning is performed a second time by taking perpendicular planes of the axial-curve. This method is tested for a group of trees without an error (see Figure 6.21). The scanning procedure could be used for either fabrication or a tree library. Serialization is used to store the method results in the XML files. The stored data includes an axis point list and circle parameters (planes and radii). Finally, the PLY Writer

## Chapter 6. Scanning

---

and Reader is made to save point-clouds as separate files.

---

### Algorithm 1: PointCloudSection, Inputs: PointCloud, Plane, Tolerance

---

**Result:** PointCloudSection - Point Array

GetPlaneEquation(); // double array following notation:  $Ax+By+Cz+D=0$

GetPlaneDenominator(); //  $1/\text{Math.Sqrt}(e[0]*e[0]+e[1]*e[1]+e[2]*e[2])$

PointCloudSection; // Empty data type

**foreach**  $p$  in the PointCloud **do**

**if**  $(e[0] * p.X + e[1] * p.Y + e[2] * p.Z + e[3]) * d < \text{Tolerance}$  **then**

        CloudSection.Add( $p$ );

**end**

**end**

ProjectPointCloudSectionToPlane();

---

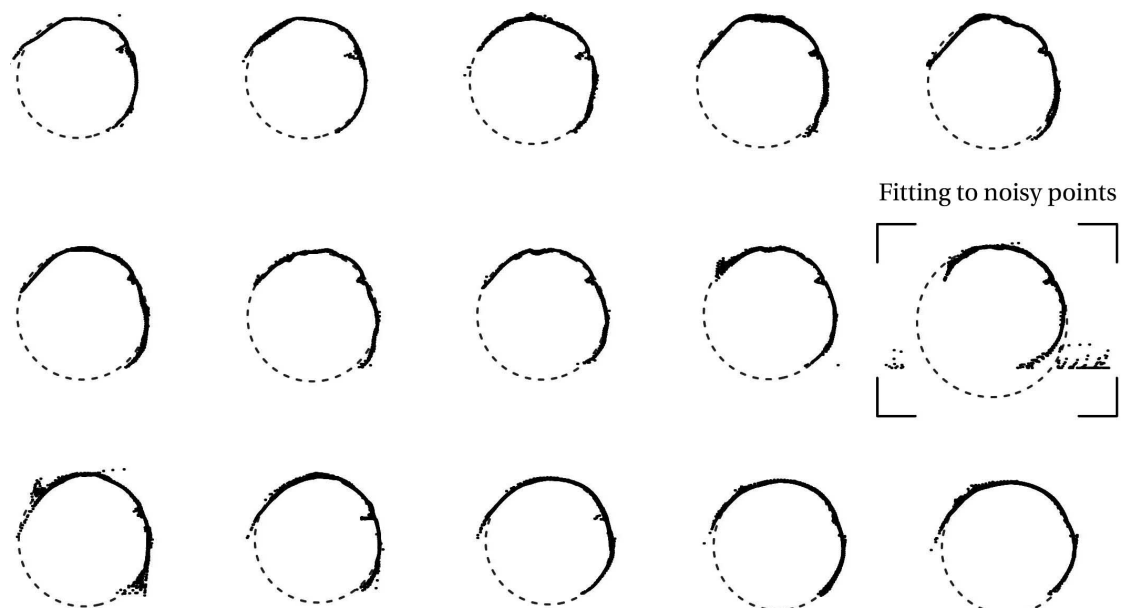


Figure 6.20 – Point-cloud sectioning using closest-point to a plane method, obtained from one beam. The circle-fit would not have good results if there are outliers (noise).

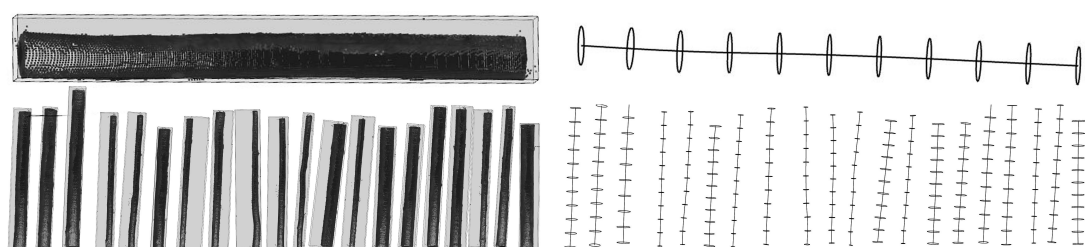


Figure 6.21 – Flat-cut sectioning: input (left) and result (right) .

**Mesh-skeletonization** The need to explore tree forks led to a search for the new methods. CGAL [161] skeletonization algorithm is implemented to test the closed Mesh skeletonization. The method is based on a surface reconstruction from a point-cloud [1], and the closed Mesh skeletonization [93]. Unlike the Flat-cut Sectioning method, it can be applied to the tree forks and bent or straight trees. Poisson surface reconstruction is chosen to retrieve a closed Mesh from points with normals. The normals are approximated by fitting points to a plane using a least-square method. A structured point array simplifies the normal estimation because the orientation point (scanner position) is already known. The local radii of a log are found by sectioning the Mesh by planes tangent to the skeleton-axis. The method is implemented as part of the robotic framework and tested within a series of bifurcated trees as seen in Figure 6.24.

Reconstructing 3D surfaces from points is a well-studied problem in computer graphics. It allows fitting scanned data, filling surface holes, and re-meshing the 3D models. The Poisson surface reconstruction allows reconstructing a surface based on an implicit function framework. The indicator function defined as value 1 for points inside the model and 0 - outside, and then obtain reconstructed mesh by extracting an iso-surface. The input for this function requires not only the point data-set but also the normals. When using a structured point array from the Faro laser scanner, it is possible to calculate normals fast because the orientation point is known as seen in Figure 6.22.

In this case, the normals are computed by taking the known neighbours points in a two-dimensional array (see Algorithm 2). If the point-cloud is not structured, the normals could be estimated using the Octree data-structure for the point-neighbourhood search, and Minimal-Spanning-Tree for orientation of the normal [161]. When normals are computed, their direction could point either inwards or outwards from a closed object. The normals have to be flipped as surface reconstruction will yield wrong results. Consequently, it is not enough to compute point-cloud normal because they must be a) oriented outwards a closed object and b) be consistently oriented concerning neighbours.

---

### **Algorithm 2:** PointCloudNormals, Inputs: PointList, ViewPoint, Tolerance

---

```

Result: PointCloudNormals
DeclareVectorArray;
foreach p in the PointList do
    GetNeighbourPoints(Tolerance);
    GetPlaneFromPoints();
    GetSignForNormal = (Plane.Normal * (ViewPoint - p) > 0 ;
    MultiplyNormalBySign();
    SetNormalToPlaneNormal();
end
```

---

After the Mesh reconstruction, the Mean Curvature Skeleton could be applied [1]. The classical application of the mean curvature flow is the surface fairing that could be taken as

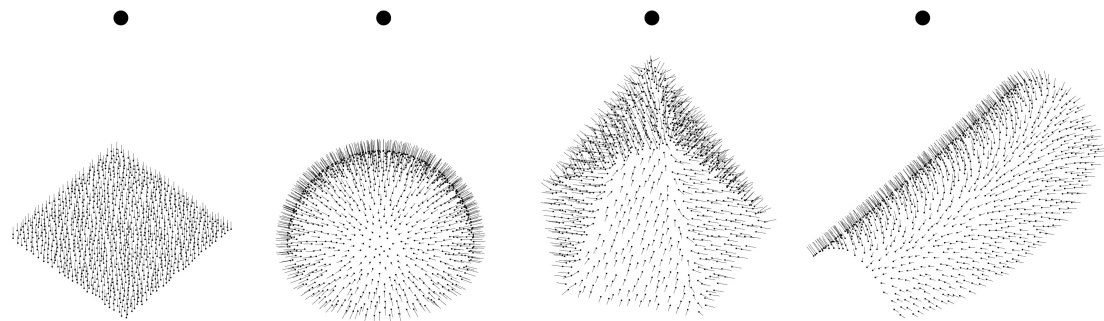


Figure 6.22 – Point-cloud normals obtained using the closest-point search and the fit to plane method when the scanner position is known (the black thick dot).

an advantage of its area minimization characteristic to get the curvature flow towards the extreme to collapse the input Mesh geometry and obtain a skeletal structure. The smoothed mesh is re-meshed at each iteration to obtain a stable, efficient computation and avoid the numerical instabilities. Finally, the Voronoi medial skeleton helps to obtain a central curve. This sequence of methods is applied for a fork skeletonization (see Figure 6.23). This method has been integrated into the Cockroach point-cloud processing framework (see Figure 6.24).

The proposed workflow works via C# interface when a point-cloud is saved as a PLY file. Then the Poisson surface reconstruction is performed, and C# - C++ wrapper calls the CGAL skeletonization method to retrieve the medial-axis of a closed mesh. When skeletonization is performed, the mesh is sectioned to obtain radial parameters. Similarly to the Flat-Cut Sectioning, the data is serialized using XML and PLY file formats. This process is also implemented in Unity, and Robot control interface (see Figure 6.23).

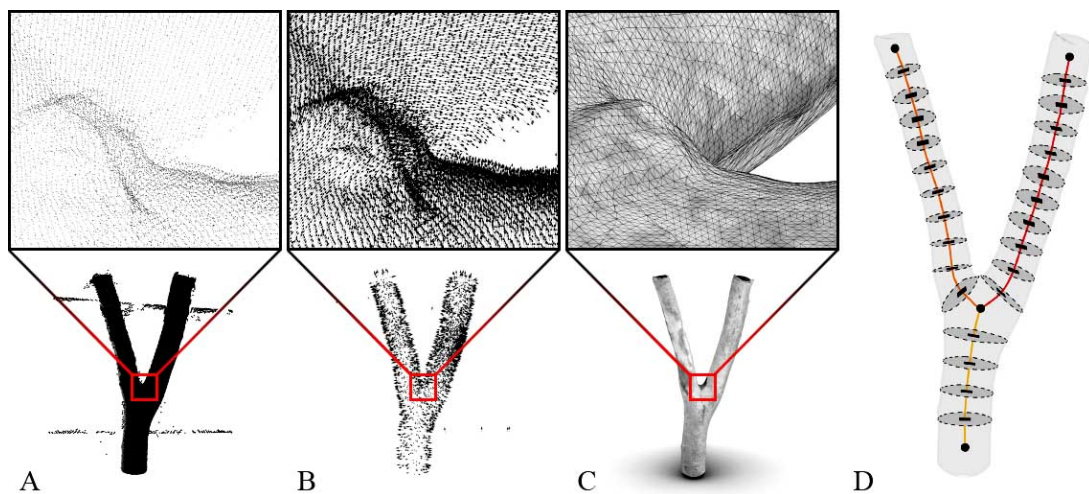


Figure 6.23 – Mesh Skeletonization: a) the point-cloud obtained from the laser scanner, b) estimation of the point-cloud normals (PCL), c) Mesh from the point-cloud (Poisson Surface Reconstruction), and d) Skeletonization (CGAL).

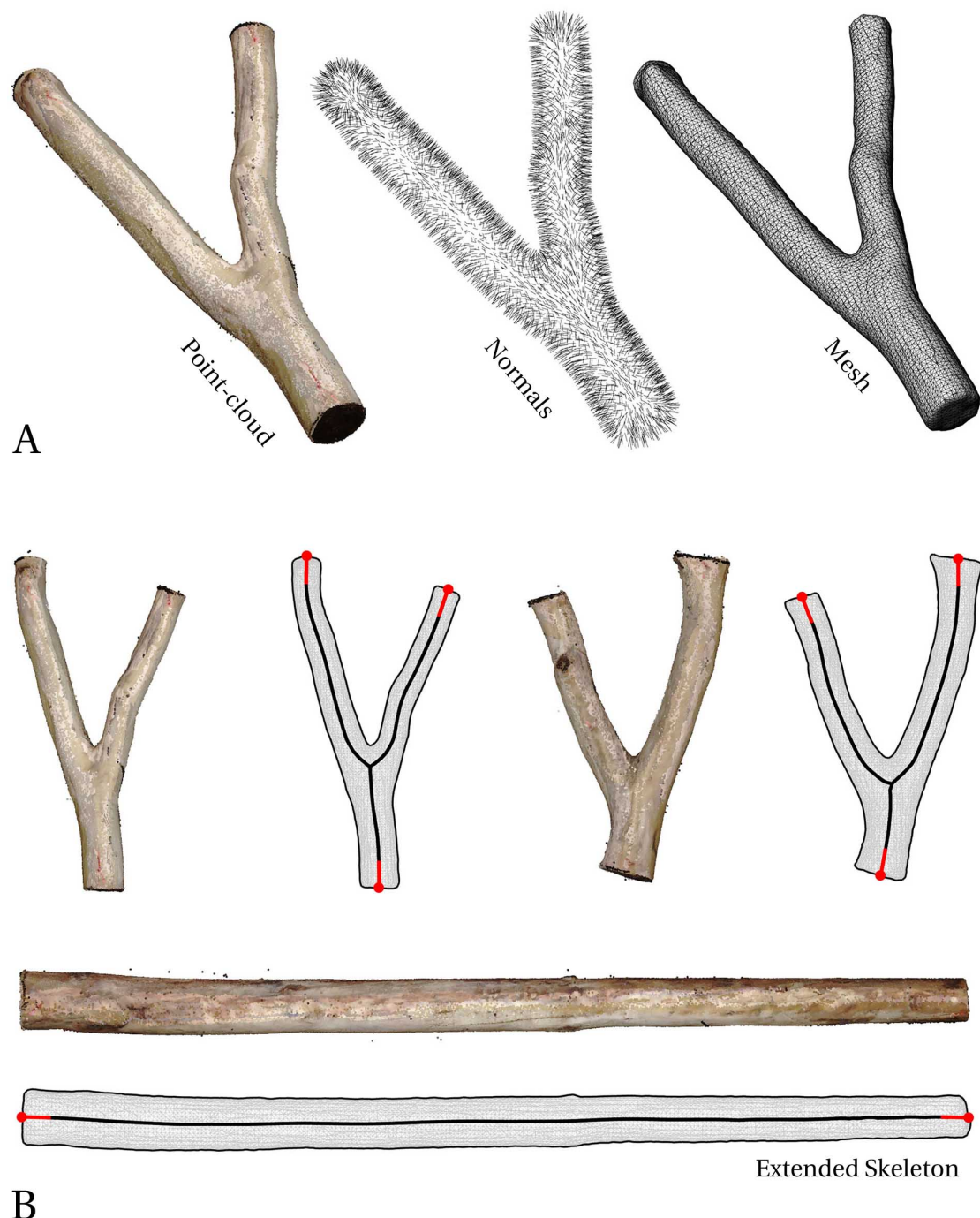


Figure 6.24 – Mesh Skeletonization integration in Cockroach plug-in: a) cropped point-cloud with computed and oriented normals to perform the Poisson Surface Reconstruction, B) Mesh Skeletonization with extended lines due to the Mesh contraction (red lines). The Mesh Skeletonization is based on a curvature flow in a Mesh smoothing algorithm. The higher resolution of the Mesh, the better the result is.

**Cylinder-fit** The Mesh-skeletonization requires a complete point-cloud that could fail when multiple trees are scanned. The last method is developed to get a skeleton from incomplete scans. The method employs a cylinder fitting of the point-cloud. The list of points is projected to a 2D plane to approximate an outline of the point-cloud using the Marching Squares algorithm<sup>7</sup>. Afterwards, the axis is extracted from a 2D curve using the Zhang-Suen thinning algorithm<sup>8</sup>. Then the axis is projected to the initial list of points to measure the local radii of axial points. Consequently, cylinders are fit along each line of the axis. The method was tested for both bent and bifurcated beams that contained noise from scanning and external objects such as straps of the fabrication setup and robot parts (see Figure 6.25).

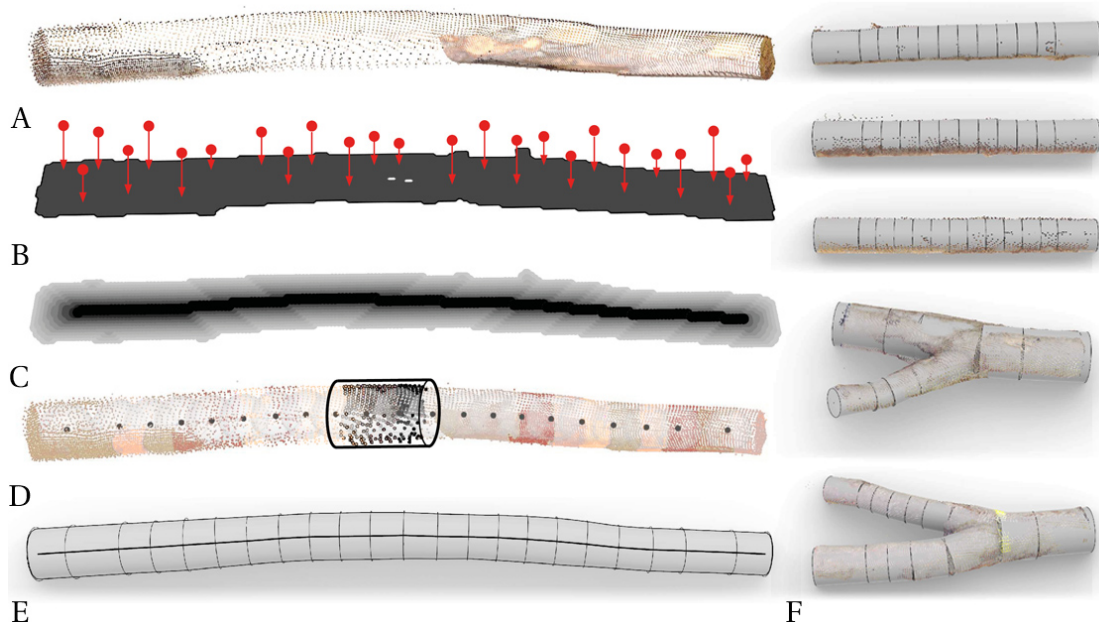


Figure 6.25 – Cylinder-fit Skeletonization: a) Point-cloud, b) projection, c) 2D Thinning, d) cylinder-fit, e) radial parameters, and f) the application in straight, curved and forked trees.

The Cylinder-fitting proved to be the most suitable method both for the fabrication and tree-stock collection. The algorithm is simplified by considering the raw wood elements as the 2D objects. Most of tree-trunks have a significant bending in one direction and rarely twist in both directions. A tree trunk could be segmented into cylinders, neglecting its smooth representation because it is not treated in fabrication or design. The skeletonization could be performed faster in 2D and then be projected back to 3D without relying on the third-party libraries.

The 2D skeletonization requires a closed outline obtained from a list of points either by the image edge detection filters or by the 2D meshing process. It is recommended to clean a point-cloud beforehand to reduce the noise from the scanning, such as Statistical Outlier

<sup>7</sup><https://catlikecoding.com/unity/tutorials/marching-squares/>

<sup>8</sup>[https://rosettacode.org/wiki/Zhang-Suen\\_thinning\\_algorithm](https://rosettacode.org/wiki/Zhang-Suen_thinning_algorithm)

Removal (SOR)<sup>9</sup>. Each point-cloud is oriented to a base plane using the Principal Component Analysis (bounding-box) already discussed in the Flat-cut sectioning method. The point-cloud is scaled to a uniform unit scale to fit a fixed rectangular area representing the 2D Bitmap. The variability of a data set could be seen in Figure 6.26.

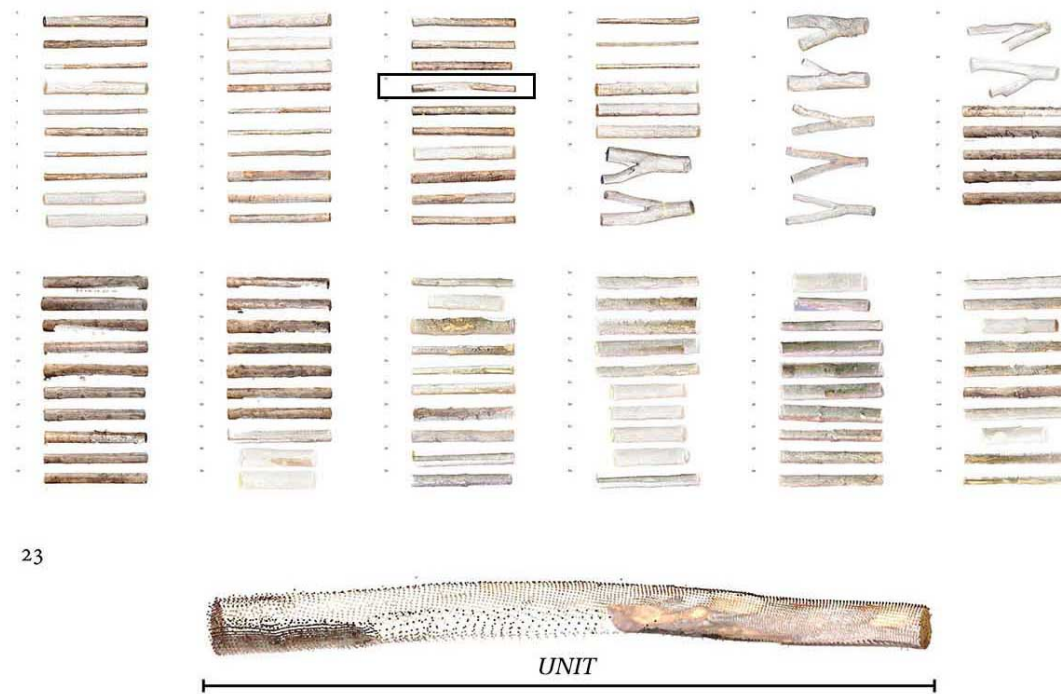


Figure 6.26 – Data-set of tree trunks collected from Lausanne and Rossiniere forests, that are scaled to a unit scale.

Afterwards, points are passed to the Marching-square algorithm. Marching-squares is an algorithm that generates contours for a two-dimensional scalar field. The cell-size of each point is increased by two times because the point-cloud density may vary, and the empty parts would not result in a clean polyline or multiple small segments that are not suitable for computing one outline per one tree-trunk. The data-set of this method could be seen in Figure 6.27.

The largest outline is taken from the Mesh by sorting boundary mesh edges. Only the largest outline is taken as then the rest of the segments are considered artefacts resulting from point-cloud noise or the non-uniform density. The skeletonization of the 2d outline could be performed in several ways, such as Voronoi diagrams or the minimal Mesh triangulation. However, a pixel-by-pixel removal process is applied, also known as the Zhang-Suen Thinning algorithm, that does not require pruning small skeleton branches produced by other methods. The algorithm operates on a black and white Bitmap, meaning the outline must be converted to an image with a solid fill inside the boundary. When the maximum number of iterations is

---

<sup>9</sup>[http://www.open3d.org/docs/0.9.0/tutorial/Advanced/pointcloud\\_outlier\\_removal.html](http://www.open3d.org/docs/0.9.0/tutorial/Advanced/pointcloud_outlier_removal.html)

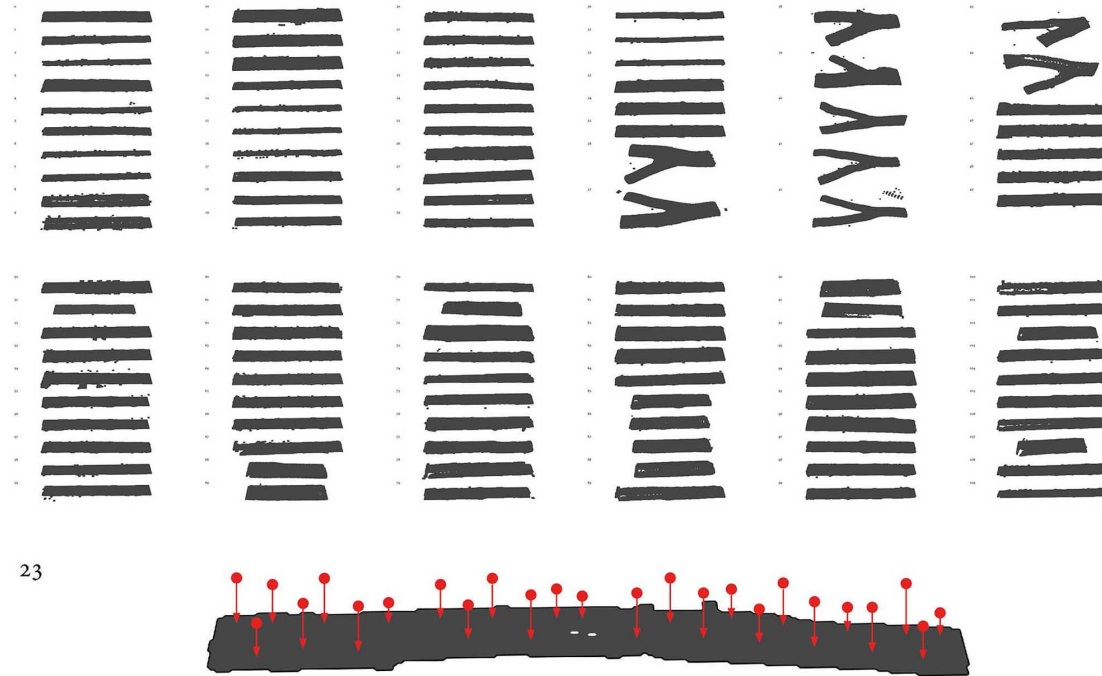


Figure 6.27 – The data-set of Marching-squares method applied for a projected Point-cloud.

reached, or the thinning is finished, the pixel data is converted back to the polyline segments seen in Figure 6.28.

When the axes are found, the polyline segments have to be projected back to the 3D pointcloud. The 2D curves are subdivided into a list of points that searches for the 2D points using an RTree search (RhinoCommon). The 2D indexing of points corresponds to 3D points id. Then pairs of points groups are fit to cylinders. The cylinder fit is formulated by an iterative process when the first points are fit to a line. Then closest-point to a line is moved by an average distance from a line. These points are projected to an iteratively fit line number of times till the distance between points and fit line is equalized. The same procedure is repeated for each pair of points, for each skeleton axis. The centres of tree forks cannot be represented as cylinders. Therefore the previous valid cylinder of the tree fork branch is extended. The overall process is also checked whether the neighbour cylinders follows a gradual taper of a tree and orientation (see Figure 6.29).

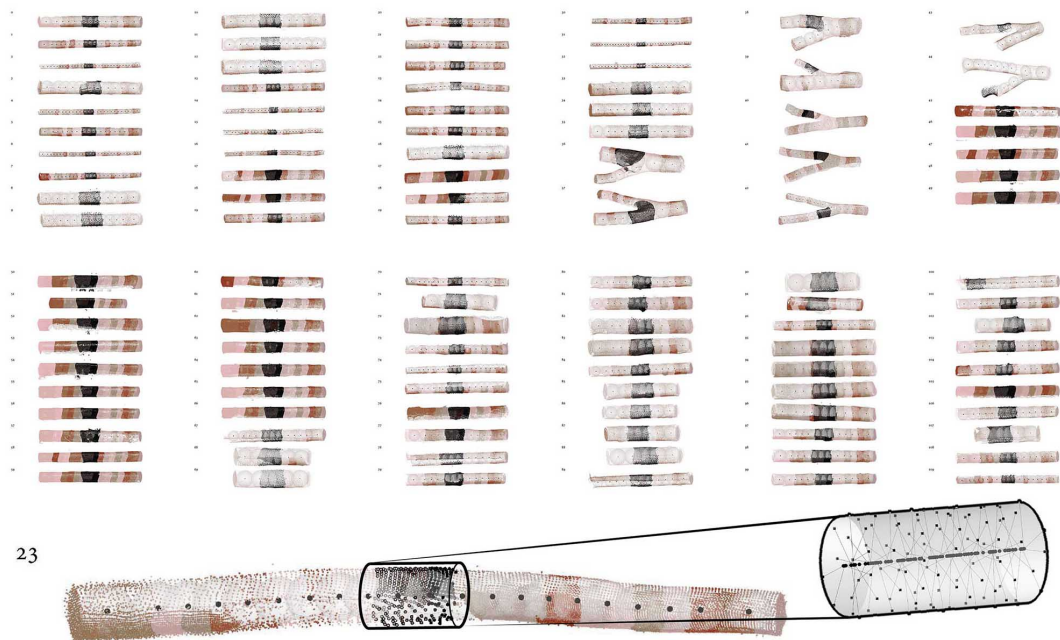
The final result is a 3D polyline and circles at each polyline point. The geometric result is scaled back to its original scale since the point-cloud processing algorithms were performed on a unit scale. These parameters are enough for visualization and fabrication as seen in Figure 6.30. The point-data is not used anymore, and the radial parameters are written for a TXT file to a 3d library or directly used for machining. This method is also implemented within the Unity application and called after the scanner sends point-clouds to the computer.

## 6.4. Point-cloud Processing for Raw Wood Fabrication



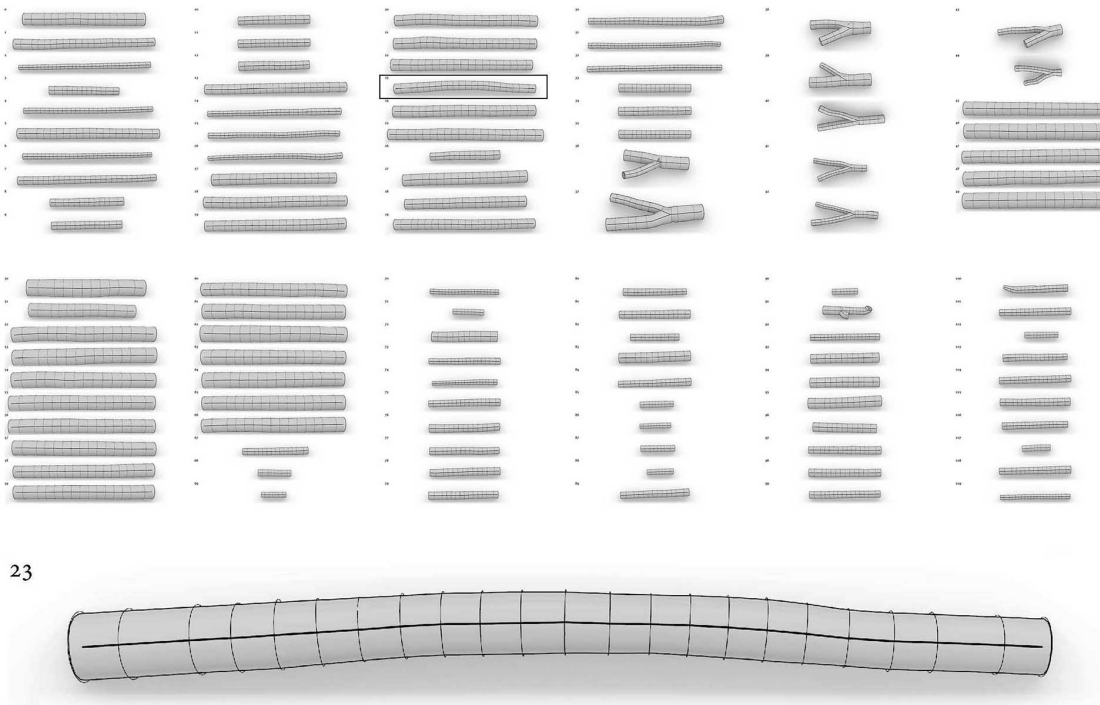
23

Figure 6.28 – Zhang-Suen Thinnning algorithm performed on the 2D outlines converted to a black and white Bitmap picture.



23

Figure 6.29 – Cylinder fit from the 3D Point-cloud to obtain an approximate position of the 2D vertices in a 3D space.



23

Figure 6.30 – Output of the Cylinder-fit method: center Polyline axis, and a series of circles.

#### **Cloud-to-cloud Registration for a Tree Alignment from a Digital Stock to Fabrication Setup**

When the point-cloud is processed, it is serialized for a digital timber stock and machining. While the setup is the same, the manual positioning of straight log can change up to 3-5 cm in translation and rotation. In contrast, the scan taken before the fabrication helps to acquire an accurate position of the object. Furthermore, the positioning corresponds to the wood radius and tangent direction of the axis. There are several ways to reference the digital and analogue models, such as a) the orientation of the digital geometry to the scanned object central axis b) using markers that have are captured using the sharp robot tool, c) cloud-to-cloud registration (see Figure 6.31), d) using the optical triangulation such as OptiTrack.

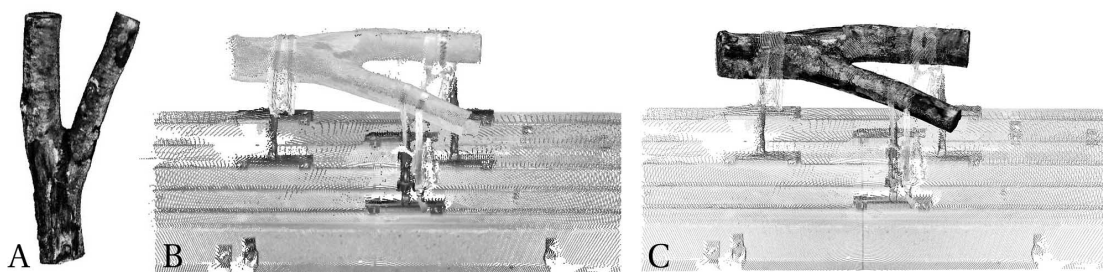


Figure 6.31 – Tree fork (a) scan in a stock (b) scan in fabrication, (c) RANSAC+ICP alignment.

## 6.4. Point-cloud Processing for Raw Wood Fabrication

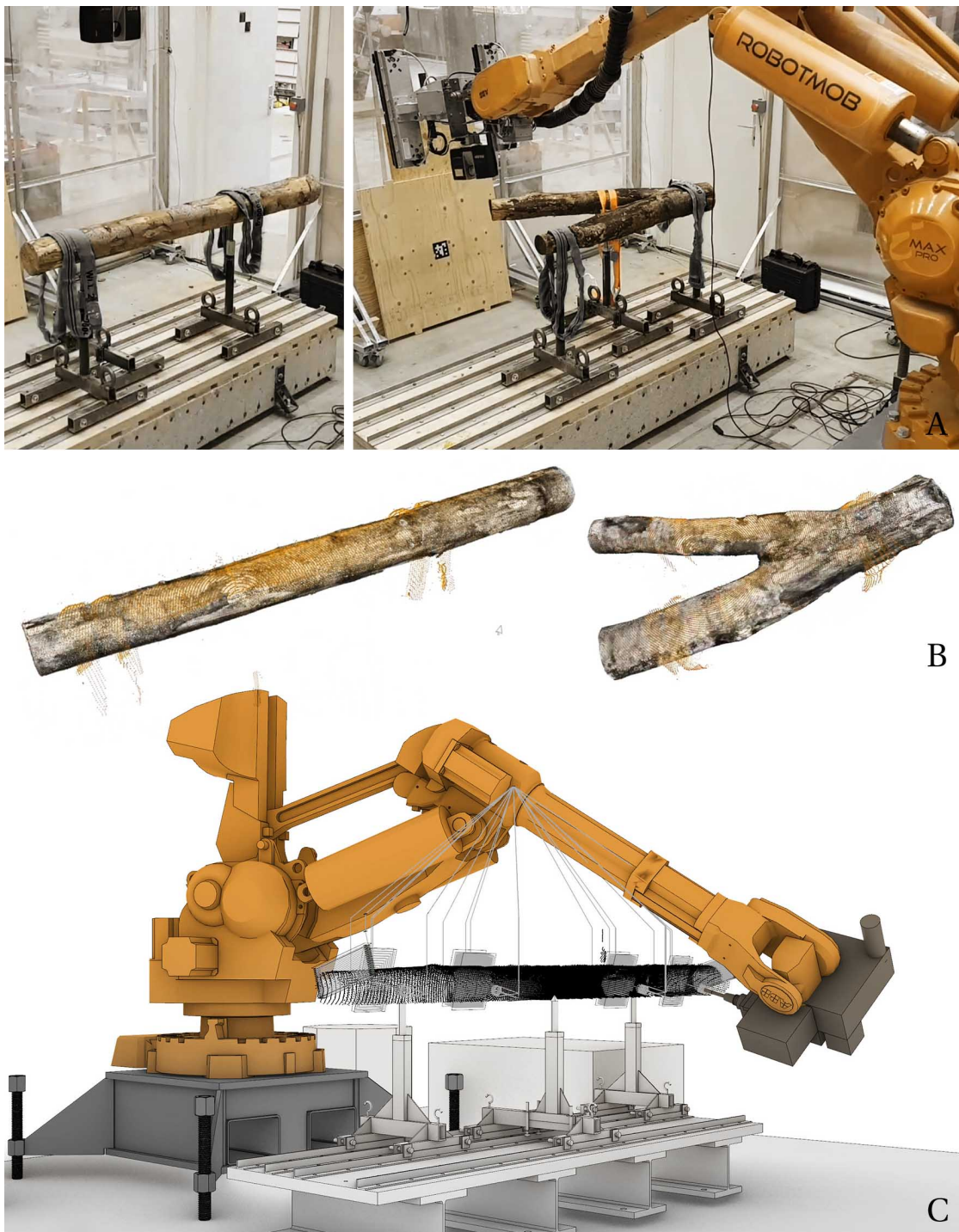


Figure 6.32 – The tool-path is oriented from the design model to the machining space. The overall process: a) scan a tree trunk in the machining setup, b) then perform the alignment from tree stock to the fabrication setup using the cloud-to-cloud registration methods (RANSAC and ICP), c) orient tool-paths based on the transformation matrix from the registration pipeline.

### Point-cloud Processing Framework - Cockroach

The very narrow and specific problem of the scanning requires investigating other means of software tools that are not present in the standard CAD modelling applications. The necessity to link different algorithms into one computational workflow resulted in a search for the open-source libraries without relying on the third-party commercial software due to the automation goal. The problem lies in the CAD interfaces that do not offer software development kits (SDK) to connect with other tools. In other words, licensed CAD interfaces do not provide automation for design methods. This issue belongs to a bigger problem when an architectural design is driven by tools put forward by computer scientists that do not have any architectural or structural training. Here, the open-source research software libraries helped to intertwine the needed tools to solve a) the point-cloud processing problem and, at the same time, b) design timber joints and c) control an industrial robot arm. Since point cloud processing algorithms are absent in current CAD tools, this section opened the new opportunities because known low-level algorithms are implemented in the higher-level CAD interfaces and openly shared under the name of Cockroach.

Cockroach [116] is a plugin developed to introduce various commands for point the cloud post-processing and meshing into Rhinoceros3D<sup>10</sup> environment based on the methods already existing in the open-source library Open3D [188], CGAL [161], Cilantro [186] (see Figures 6.33, 6.34, 6.35). It was necessary to develop this tool because there are no point-cloud processing tools for CAD and .NET languages such as C#, VB, Python. Most libraries are situated in the low-level language C++, making it hard to implement to the higher-level languages that architects and engineers often employ. Using a cross-platform method called C# PInvoke, the interoperability between these two languages is enabled. The tool also serves as a teaching platform already employed for IBOIS, EPFL atelier Weinand students.

The pointcloud processing tools focus on:

- fast and easy-to-use geometric manipulation, characterization and decomposition of point clouds directly in Rhinoceros3D [138].
- improving the link between CAD modelling software and point-cloud processing. focus on the integration of point-cloud processing with other frameworks such as easy-to-use .NET programming languages (C#, IronPython, VB) using the interface of Grasshopper, Rhinoceros3D .
- on structures with unpredictable geometries such as raw wood and mineral scraps. These construction elements are scanned and post-processed into low-poly Meshes or NURBS for design, e.g. 3D timber joinery representation and fabrication tool-paths for the 5-axis CNC, 6-axis robot and XR manufacture.

---

<sup>10</sup><https://www.rhino3d.com/>

## 6.4. Point-cloud Processing for Raw Wood Fabrication

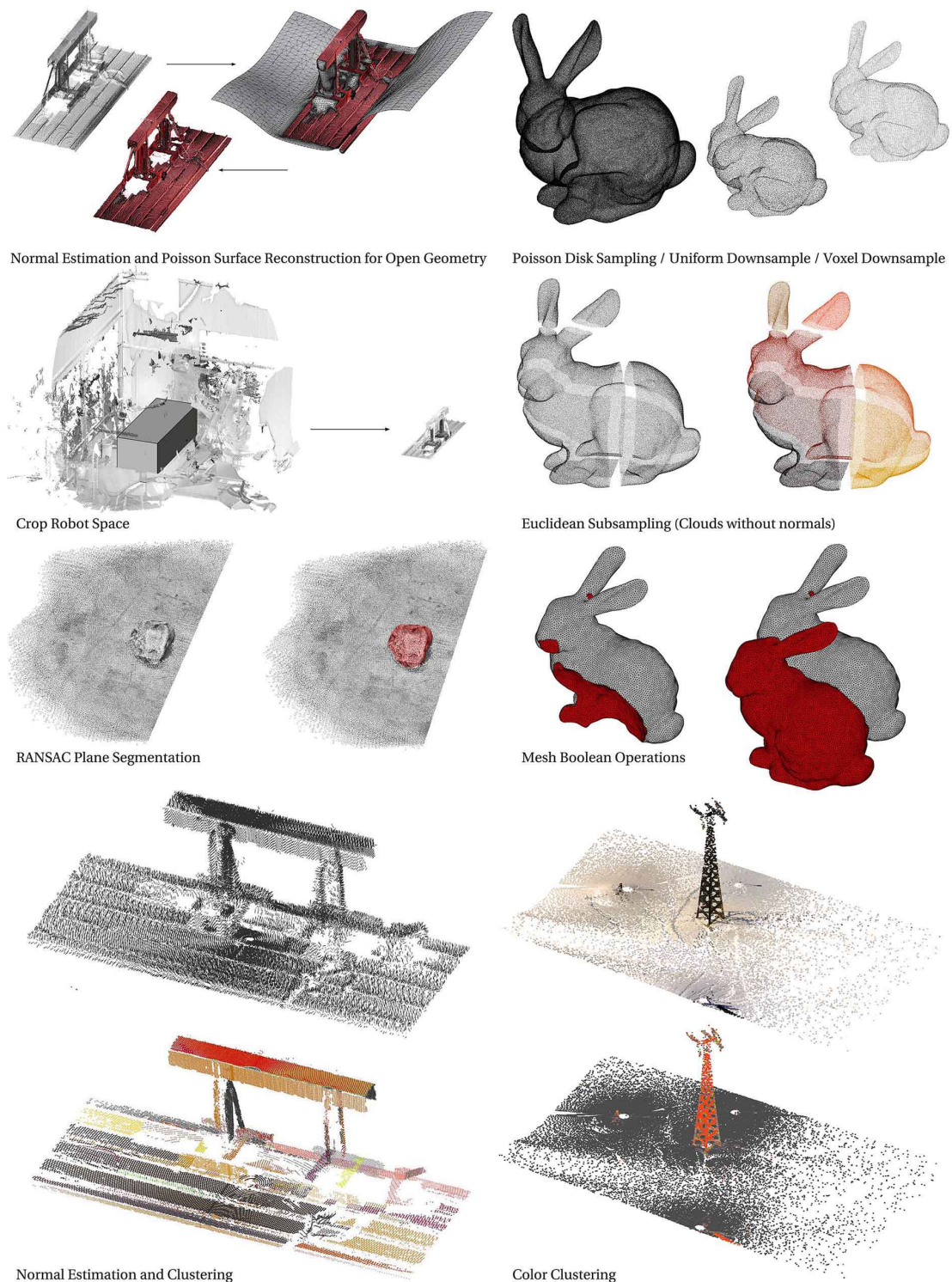


Figure 6.33 – Cockroach plug-in application outside timber context, including small scale objects and large interior and landscape scenes.



Figure 6.34 – Cockroach framework. CGAL methods: Point-cloud normal estimation, Poisson Surface Reconstruction, Mesh Skeleton from a closed Mesh, Euclidean clustering. Cilantro methods: Cluster by Point-cloud normals. Open3D methods: Voxel sub-sampling, remove every  $N$ -th point from a Point-cloud.

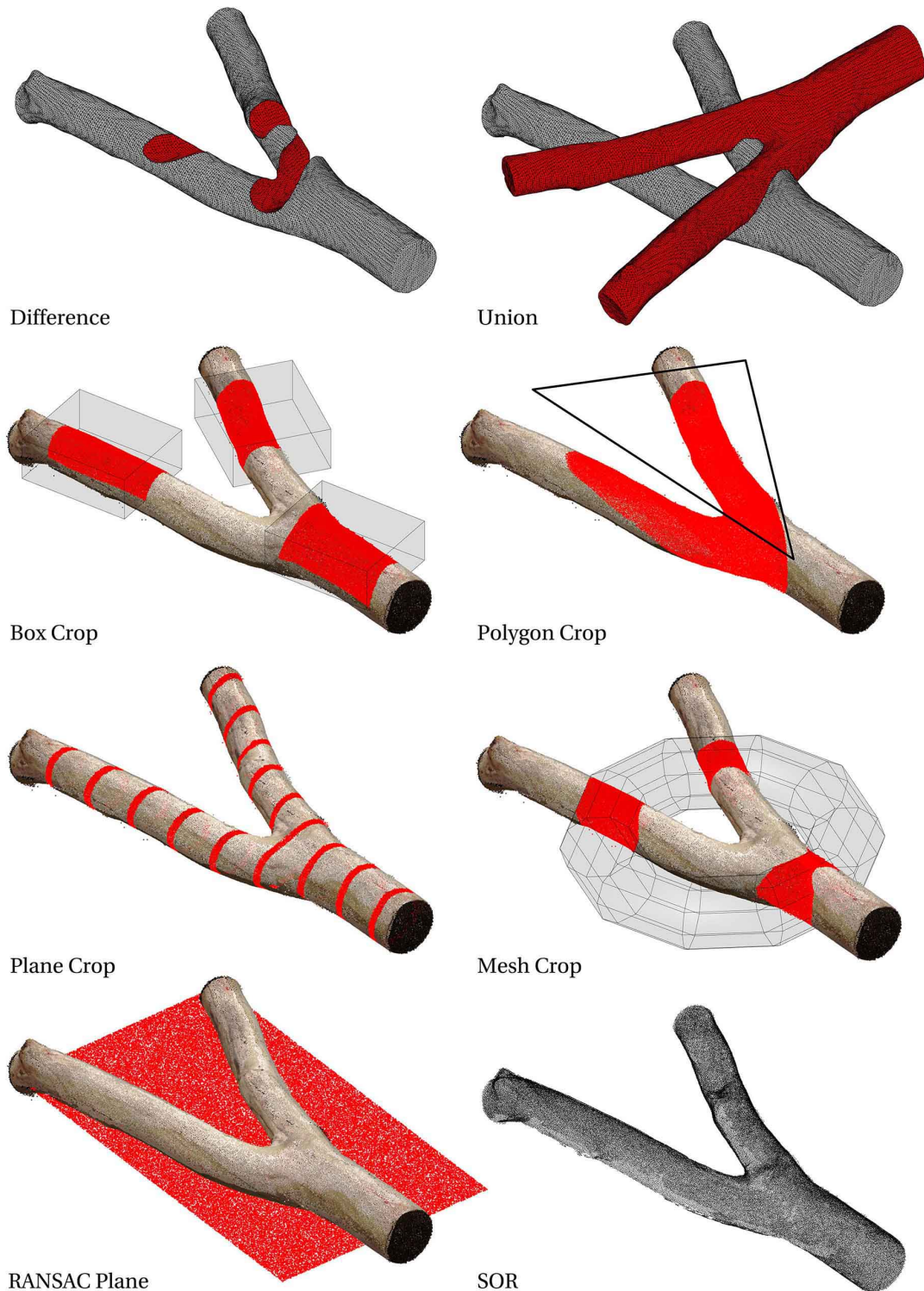


Figure 6.35 – Cockroach framework. CGAL methods: Mesh Boolean, Statistical-Outlier-Removal. Open3D methods: RANSAC plane segmentation. Standalone methods within Rhino3D: Box, Polygon, Plane, and Mesh crop.

## **6.5 Conclusion**

The SDK of the Scanner, robot control software and tool-changer allowed to automate the scanning and fabrication workflow. The scanning precision is achieved within the limit of Faro Focus specification and registration process ( $x<0.25$  mm), the addition of the robot tolerance ( $x<0.1$  mm) and manual target measurement precision ( $x<0.5$  mm). The total laser scanning precision could be in the range of +/- 1 mm. The precision that is needed to machine raw wood is sufficient because wood imperfection such as branches, chain-saw cuts, cracks are discarded.

Furthermore, multiple point-cloud processing algorithms are tested, and the cylinder-fitting method is proved to be the most successful because it works when a point-cloud is incomplete and if there are outliers within the fewer scans are taken per one tree. The proposed scanning application is relatively fast comparing to the fabrication time needed for each timber. Another challenge would be to investigate low-cost scanners to decrease the cost of the application. Several scanners such as Kinect, Orbec, and RealSense were tested, but the amount of noise and imprecision made the robotic calibration difficult. The low-cost application also has a minimal scanning range suitable for small object scanning only. The situation is likely to change due to the increasing interest in the automotive industry. As a result, it is worth to keep studying point-cloud processing methods regardless of the hardware specifications.

The laser-scanner and the industrial robot arm integration speeds the geometry acquisition of raw timber from the 45 min manual process to a 3-4 min automated solution, including robot movement, scanning and point-cloud processing. Twenty-four beams were scanned without additional manual processing that directly guided the machining process, shown in the Demonstrators part 9. The scanning method is essential to get a tree trunk position that helps position cutting tool-paths within. The prototyping demonstrates the feasibility of the proposed workflow for low-value tree trunks harvested from the local forests. The software workflow is open-sourced to ease the point-cloud processing outside the research scope.

It could be relevant to discuss how other scanning setups could be engaged in similar workflows. For example, cameras positioned in the robot space allows scanning the robot space without dependency on the robot precision for real-time applications. Also, the high-cost LIDAR could be replaced by a series of low-cost RGBD cameras. Although RGBD cameras have much lower quality and are harder to calibrate, the raw wood fabrication allows the lower precision surface scanning. Furthermore, volumetric scanning could give more information about the inner structure of a tree that could be used not only for fabrication but also for the tree stock quality analysis.

# 7 Robotic Fabrication

## 7.1 Foreword

The robotic fabrication chapter is divided into three parts (see Figure 7.1) : a) the physical setup for raw wood fabrication, b) the robot control starting from the CNC machine and extending the method to the industrial robot arm, and c) the Joinery Solver and tool path integration. This chapter is focused on the research equipment used in the thesis: a) the 5-axis CNC Maka, and b) the industrial robot ABB IRB 6400R.

The Joinery Solver algorithm is first tested with a CNC machine and then with a 6-axis robotic arm. The methodology is better suited to the robotic fabrication as it has a wider reachability. Additionally, the robot can be connected with a scanner, whereas the CNC machine only runs G-Code files without a feedback loop that is necessary for the raw wood fabrication.

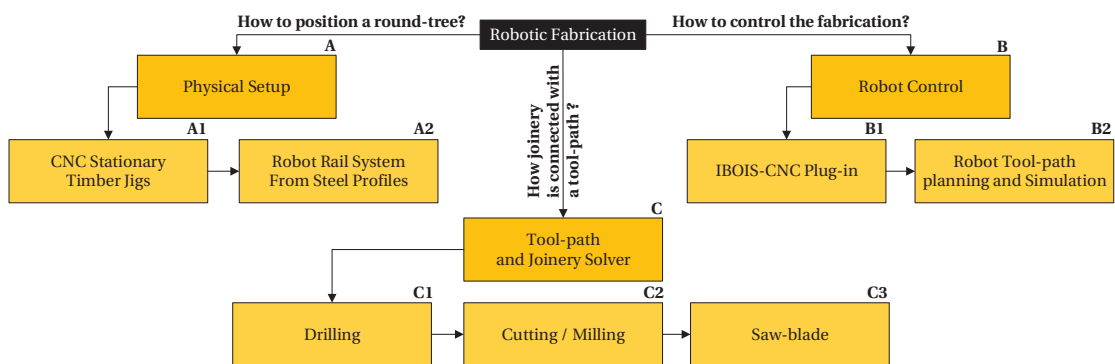


Figure 7.1 – Robotic fabrication chapter is made from three sections: a) the physical setup, b) the robotic control, and c) the tool-path integration in the Joinery Solver.

## Chapter 7. Robotic Fabrication

---

The Robotic Fabrication chapter is the last part of the overall thesis workflow, as seen in Figure 7.2. The robot tool path generation is integrated with Joinery Solver by using the same data structure (Cut) for visualization and fabrication. The robotic movement instructions may vary depending on the employed cutting and scanning tools. Therefore, specificity such as contouring, notches, saw-blade L-shape cutting, drilling is discussed as an integral part of the overall tool-path generation.

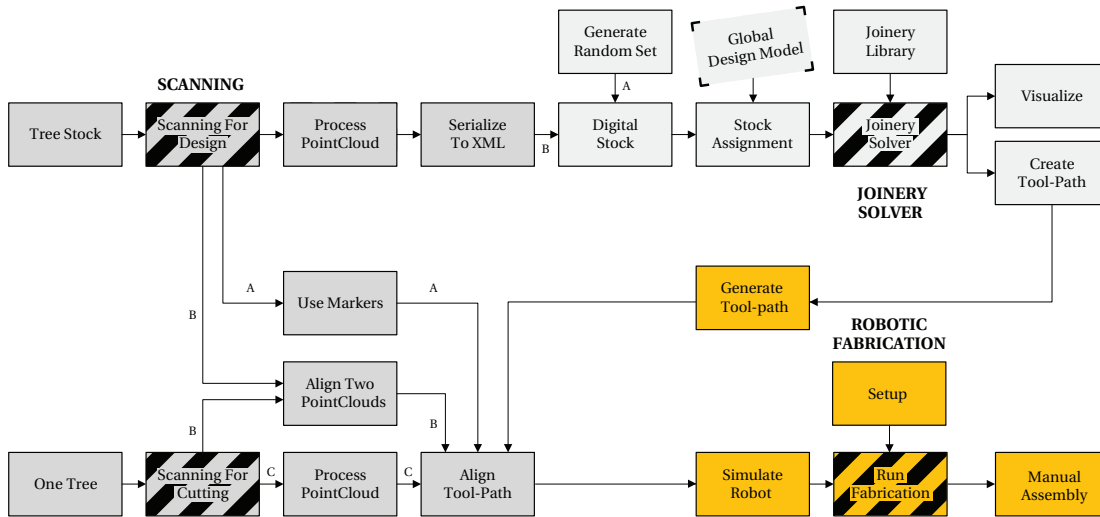


Figure 7.2 – Robotic fabrication integration in the thesis workflow.

---

The Robotic Fabrication chapter is structured as follows:

- Section 7.2 introduces the physical fabrication workflow employed in the thesis.
- Section 7.3 describes the mounting process of timbers for fabrication:
  - CNC setup
  - Robot setup
- Section 7.4 demonstrates the control of the CNC and the industrial robot:
  - CNC control and simulation
  - Industrial robot arm control and simulation
  - Cutting-tool calibration
- Section 7.5 explains how Joinery Solver is connected with the tool-path generation
  - Drilling
  - Milling
  - Saw-blade
- Section 7.6 summarizes the practical part of the research showing the translation between digital joinery geometry and physical experiments.

## 7.2 Introduction

The research starts with the development of the IBOIS CNC plug-in for translating the joinery tool-path to G-Code. CNC machines are most often equipped with a post-processor to translate physical movement into a list of programmable operations (G-Code) such as XYZ positions of TCP (tool-centre point) and A, B rotations. CNC fabrication could be applied for raw wood cutting based on the literature review [94, 175]. Furthermore, there are instructions to take a specific cutting tool, move to TCP to an origin point, start rotation of a spindle and control spindle rotation per minute (RPM). The G-Code plug-in development for the CNC machine is a tradition that is gradually advanced within a chain of IBOIS, EPFL PhD researchers by transferring their knowledge from one student to another [64, 134]. However, this methodology is not specific to current research workflow but also extensible to other application following G-Code ISO6983 standards [75].

The contribution of this study are: a) timber cutting lifted from the machining table and b) collision detection algorithm to ensure safety. Before the raw wood research started, only timber plates were cut, and beam elements were not considered [134]. The main difference between the two methods is the reference object position. The reference object for the plate-cutting is the CNC table and for the beam-cutting is the object itself. The plate-cutting is a 2D problem where a spindle cannot be lowered more than approximately 30 degrees in relation to the table, considering the thickness of a plate [137]. The raw wood cutting is a 3D problem, where a spindle must always point outwards to a beam and must not collide with a table leaving only 30 cm height available for cutting. Additionally, raw wood fabrication depends on saw-blade movements that differs from the flat-end milling process. Consequently, the CNC cutting methods result in a G-Code plug-in extension for the beam fabrication by building upon the previous work of IBOIS research.

Robotic manufacturing was developed in the last years of research after many limited trials of CNC manufacturing. The differences in the two systems could be seen in Figure 7.3. It is necessary to have a feedback-loop from the fabrication setup because the scanning integration is needed. The overall robotic framework is divided into the following parts: a) mounting timber on the fabrication setup, b) scanning a tree trunk, c) orienting machining tool-path to the scan, d) checking the reachability of the robot six-axis and e) running the program. The robot is rented from ImaxPro<sup>1</sup> company that imposes its own robotic ABB control initiated from the Unity software. The Unity application offers a custom text code used to program the movement of the robot that translates simplified commands to RAPID code. In principle, the concept of tool-path programming is similar to G-Code by using txt single-line operations. This workflow addresses the interoperability issue where Unity Game Engine is not compatible with the Rhino CAD interface used for the joinery development. Both applications have different coordinate systems requiring integration of Rhino and Unity geometry methods.

---

<sup>1</sup><https://www.imaxpro.be/>

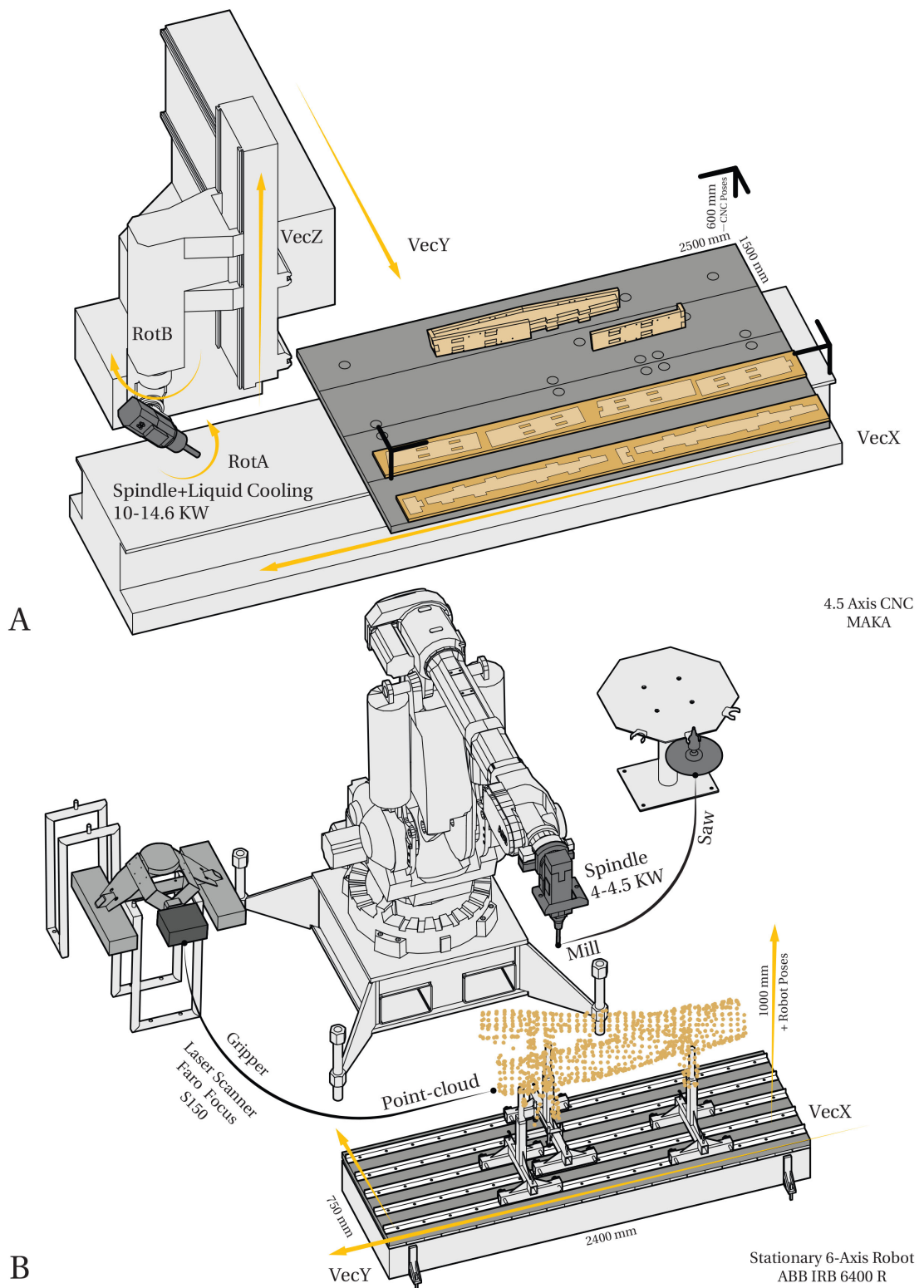


Figure 7.3 – Two digital fabrication methods tested during the thesis: a) the 5-axis CNC Maka, and b) the 6-axis ABB IRB 6400R robot with a tool changer between the spindle and the laser scanner.

The proposed method's added value results in a) the standalone .NET library for controlling the Faro-Focus S 150 and b) the standalone .NET library for simulating the robot movement outside both software. The aim is to integrate the joinery tool-path and scanning workflow independently from the given 3rd party ImaxPro software as it might change in the future. The goal is to run the robot simply as the CNC machine while obtaining the scanning feedback loop. In summary, the industrial robot's work-space is more flexible than the CNC machine for the raw wood joinery fabrication.

Lastly, the robotic fabrication chapter expands on the Joinery Solver tool-path generation. Joinery Solver mentions that wood-wood connections are connected with the machining process, without showing the robot control. The robotic fabrication chapter explains this part of the Joiner Solver Cut data structure that contains the necessary information to translate a joint geometry to robotic movements. Consequently, this chapter focus on the physical robotic workflow and the digital tool-path generation to validate the fabrication process of the wood-wood connections generated from the Joinery Solver.

## 7.3 Physical Setup

### CNC Setup

The physical setup requires a description of the existing workspace that shapes the way timber elements are manufactured. CNC setups follow available workspace dimensions. In the current research context, the maximum bounding box's size is 2500×1500×600 mm. Only 300 mm height out of 600 mm is available because timber must be lifted from the CNC table. The raw timbers have to be machined potentially from all sides except the support areas.

When designing a fabrication rig, two conflicting parameters must be considered: a) work-object must be maximally accessible to cut timber joints, b) while ensuring a strong attachment to the rig. Raw wood round shape cannot be positioned on a flat surface. Its shape increases the rotation moment during the cutting. Furthermore, the fabrication may encounter cantilever or extended span areas of a beam or fork that is supported punctually. Hence, all these parameters have a significant disadvantage in the fabrication. Timbers are vibrating, resulting in fewer precision cuts (1-2 mm tolerance). As a result, the CNC machine can be decalibrated due to monotonous undulating movement.

There were a series of trials and errors to resolve the design of a timber setup as shown in Figure 7.4. In the first option, a pair of stands are fabricated from the LVL engineered timber panel (see Figure 7.5A). The priority is given to safety during machining. If a milling bit would touch a rig, it should cut through instead of having a hard collision with a stand, for example, steel stands. The stand location can be changed at a 20 cm step size because timber length varies in different study cases. Initially, beam elements were fixed to the stand by screws. This method is too weak to avoid the significant movement during cutting. In the second option, a beam is tightened using belts that ensured the stability but reduced the cutting zone without the possibility to machine the top surface of a beam. This option can change depending on the cutting type (see Figure 7.5B-C-D) : a) rectangular regular beam, b) round-wood strapped by belts, c) end fixation to reach all sides of a tree trunk. The second option is not optimal because the setup is made from timber, and timber is relatively light in weight resulting in the CNC machine decalibration. The scanning of timbers is performed using two methods: a) point-by-point measurement using a Teach-Pendant and manually transferring the coordinates to a computer, b) laser scanner using targets positioned on the CNC machine. The manual preparation and scanning of each beam take 30-45 min excluding the fabrication time that highly questions the proposed method's efficiency. Consequently, raw wood fabrication is continued using an industrial robot with an axial flexibility considering the CNC decalibration and a larger machining space for a more robust timber fixation setup. In the third option a beam is connected from two sides (see Figure 7.5E). This option resulted in the most robust setup that also allows cutting the top part of a beam.

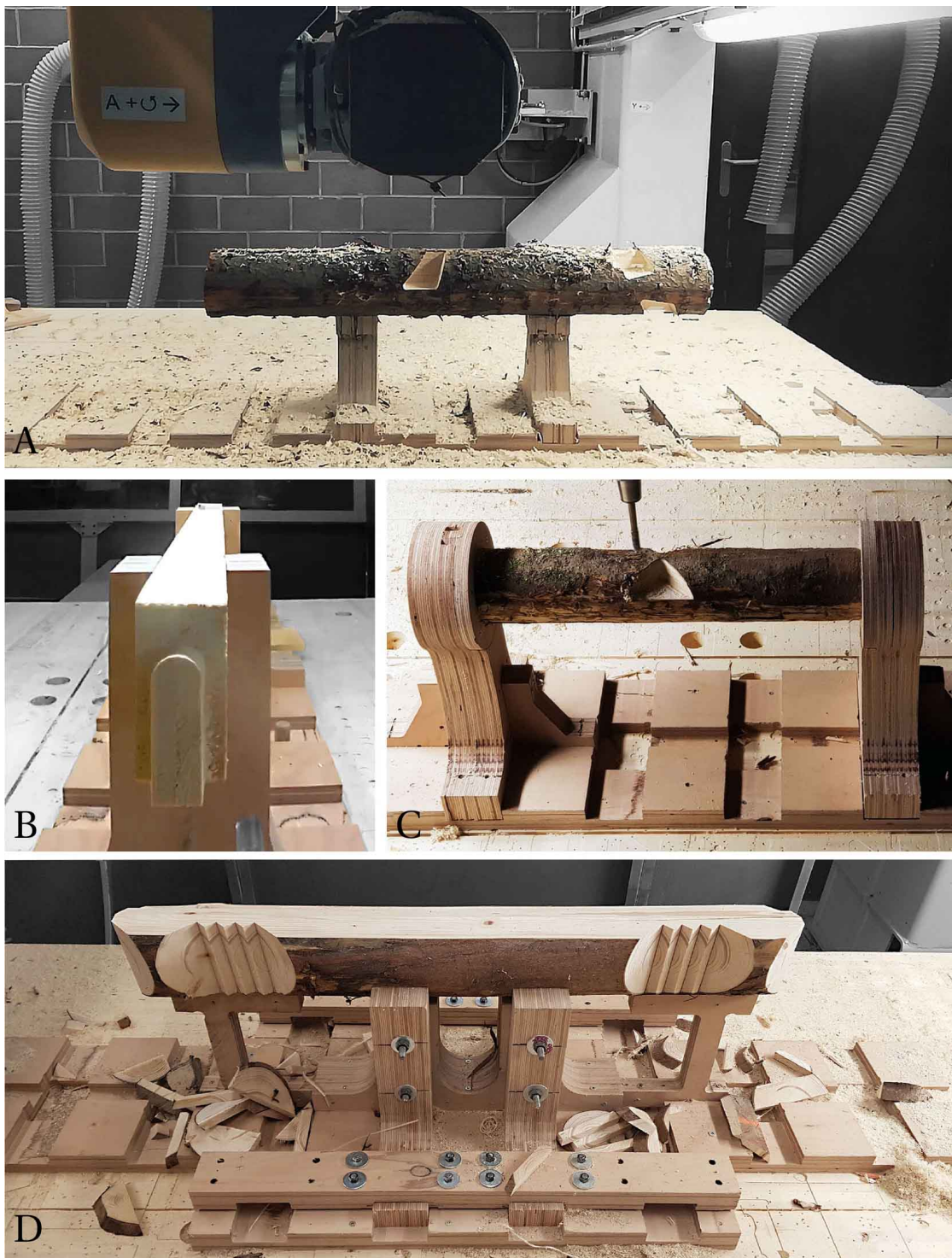


Figure 7.4 – CNC setups for raw wood fabrication: a) screw fixation, b) U-shape setup, c) end clamps for top and side cutting and d) the rig for machining the top part and sides of a beam.

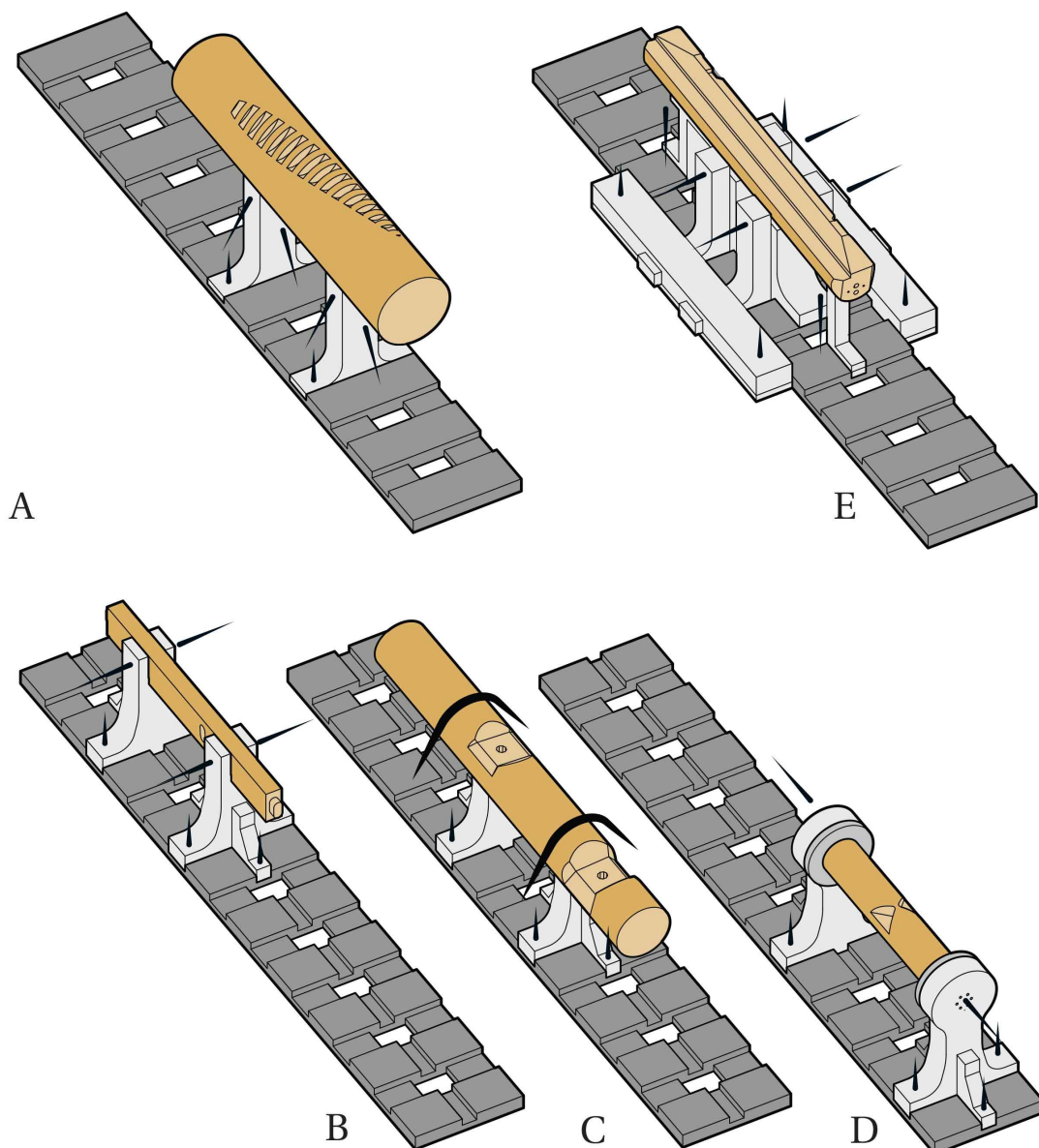


Figure 7.5 – Wooden CNC setups made from four cm LVL panels: a) the screw fixation (black lines), b) the U-shape rectangular beam holder, c) the beam fixation using dowels and belts, d) the end clamps to access the tool-path from all sides of a beam, and e) the setup for machining the upper half of a beam by the side fixation. The base (the dark grey part) has a 20 cm step size to adapt to different sizes of elements.

#### Robot Setup

The introduction of an industrial robot arm ABB IRB 6400R helped resolve technical issues re-occurring within the CNC fabrication. Robotic fabrication is often used for cutting irregular objects due to the larger reachability, shown in Figure 7.6. The robot can also adapt to vibrations of timber without self de-calibration. Moreover, the machining space is much larger (5000x2500x2000 mm) and allows a more robust setup than before. Additionally, the robotic software adds additional features such as scanning integration, reducing the long manual 45 min point-cloud processing to an automated 2-4 min scanning.

There is a need to change the initial concept of the setup after learning from the technical tests performed using the CNC cutting. Steel is chosen as a primary material to hold the timber. The development of the Joinery Solver and Laser Scanning integration allowed detection of a potential collision removing a need to have a setup made from timber. The change of material explained issues hardly visible using wooden setups. The vibration of steel could be heard during the robotic milling that suggested changing steel stands to 8 mm strong and heavy supports as shown in Figure 7.7. The heavier support has neither bending nor vibrations resulting in a fixed connection between the timber and a machining table.

The table is designed as a rail system (see Figure 7.8). The stands can move linearly, extending the stationary robotic movement that is limited to two meters reach. Also, stands are designed with an additional axis that helps adapt to varying fork geometry (see Figure 7.9). Straps are used to ensure rigidity between raw-timber and the overall setup. Depending on the timber's size, different types of belts could be used to withhold a weight of up to 1000-2000 kg. These technical details show the strength needed to prevent any additional movement during the joinery cutting. These trials suggest that fabrication setups must be heavier and more robust than a timber piece. The experiments are validated using empirical studies as no prior methodology is available as a design guideline. This knowledge is transferred by empirical studies by constant testing and improvement using local observations.

Moreover, for flexibility reasons the setup is designed without a connection to the floor. It means that neither robot nor the fabrication setup can be screwed to the ground. In other words, the objects must be heavy enough to withstand mechanical movements. This rule is changed due to two observations: a) robot started to move from its original location b) fabrication table changed its position. The robot base is modified to avoid loose connection to the ground. Moreover, the rig's base was changed from the four steel I-beam to reinforced concrete blocks (see Figure 7.6). The fabrication setup is composed of reused material due to material costs and environmental considerations. The I-beams are reused from past engineering tests. Furthermore, the concrete block is cut to 2400x750 mm size from the past IBETON laboratory studies of reinforced concrete slabs. Finally, the fabrication setup is bolted to the ground.

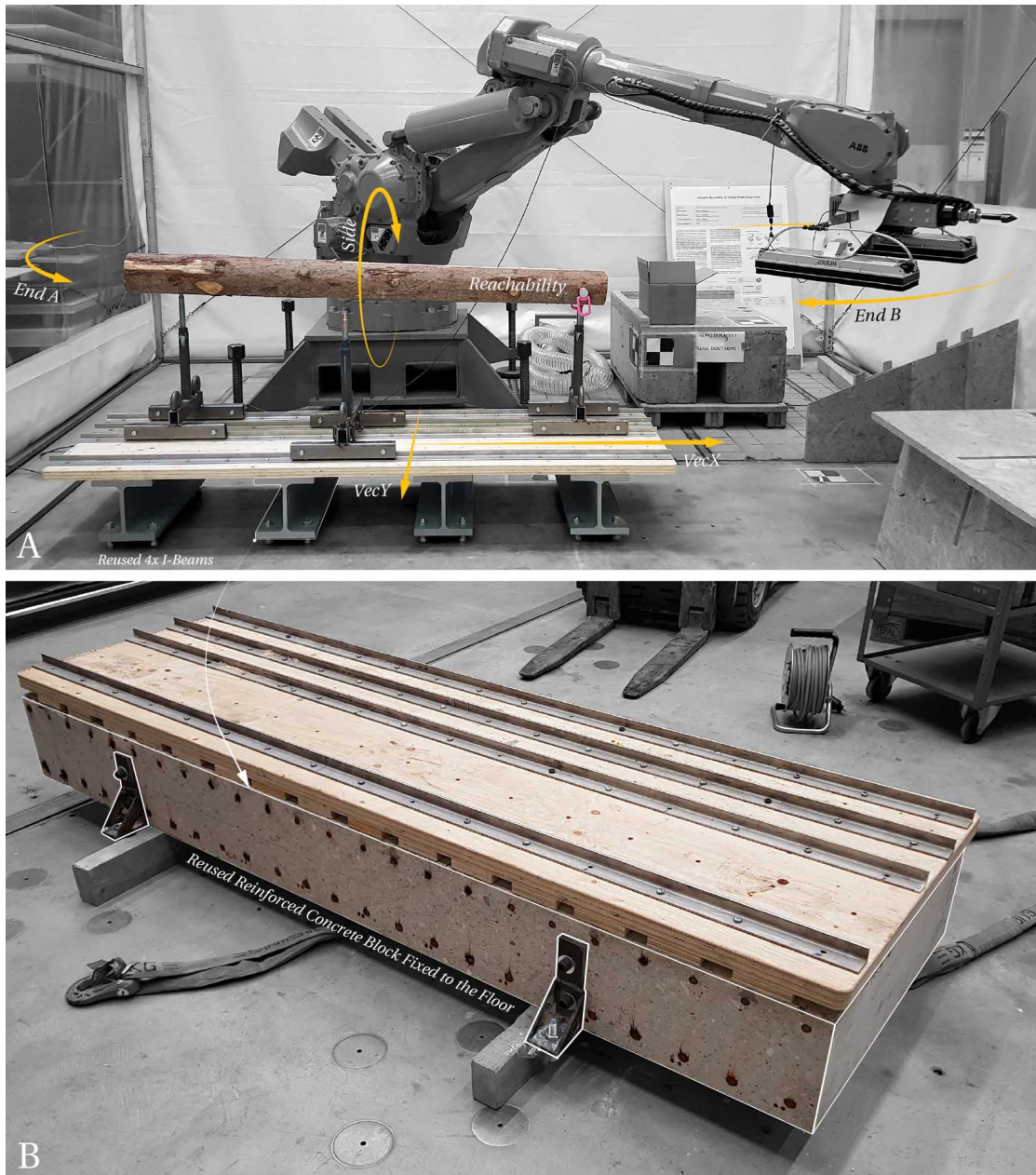


Figure 7.6 – The rail system is employed for the robotic fabrication to have a larger accessibility from all the sides of timber. The base of the setup is made from re-used a) steel I-beams, b) reinforced concrete block from EPFL, IBETON laboratory experiments cut to dimensions of 2400x750 mm and bolted to the ground. The robotic workflow has up to 5000x2500x2000 mm reachability that helps to cut wood-wood connections without the major constraints in a given space.

A series of manual tools accompany the overall scanning to fabrication setup (see Figure 7.7), including a) metallic dowels for either strapping or bolting depending on a joinery type, b) hex-keys to fix the sliding stands to the rail, c) additional keys to mount the laser-scanner Faro

### 7.3. Physical Setup

Focus S 150. The scanner is often used outside the research scope such as building scanning for studio teaching that requires an additional flexibility. The setup already allows the multi-use exploitation, including robotic and manual stationary scanning using the automation adapter. The manual rail fixation could be developed further using an air-pressure mechanism or bolting stands directly to the ground. For the research studies, the current setup is sufficient to perform small and large scale experiments.



Figure 7.7 – Different types of stands are used as part of the rail system: a) 3 mm rectangle profiles are changed to less vibrating b) 8 mm stands, and c) the additional translation axis. Besides the fabrication setup, a series of secondary tools are needed (d): steel dowels for different machining types (sharp, flat-end and bolted, belts, hex-keys and a key to place a Faro Focus laser scanner on the robot vacuum-gripper.

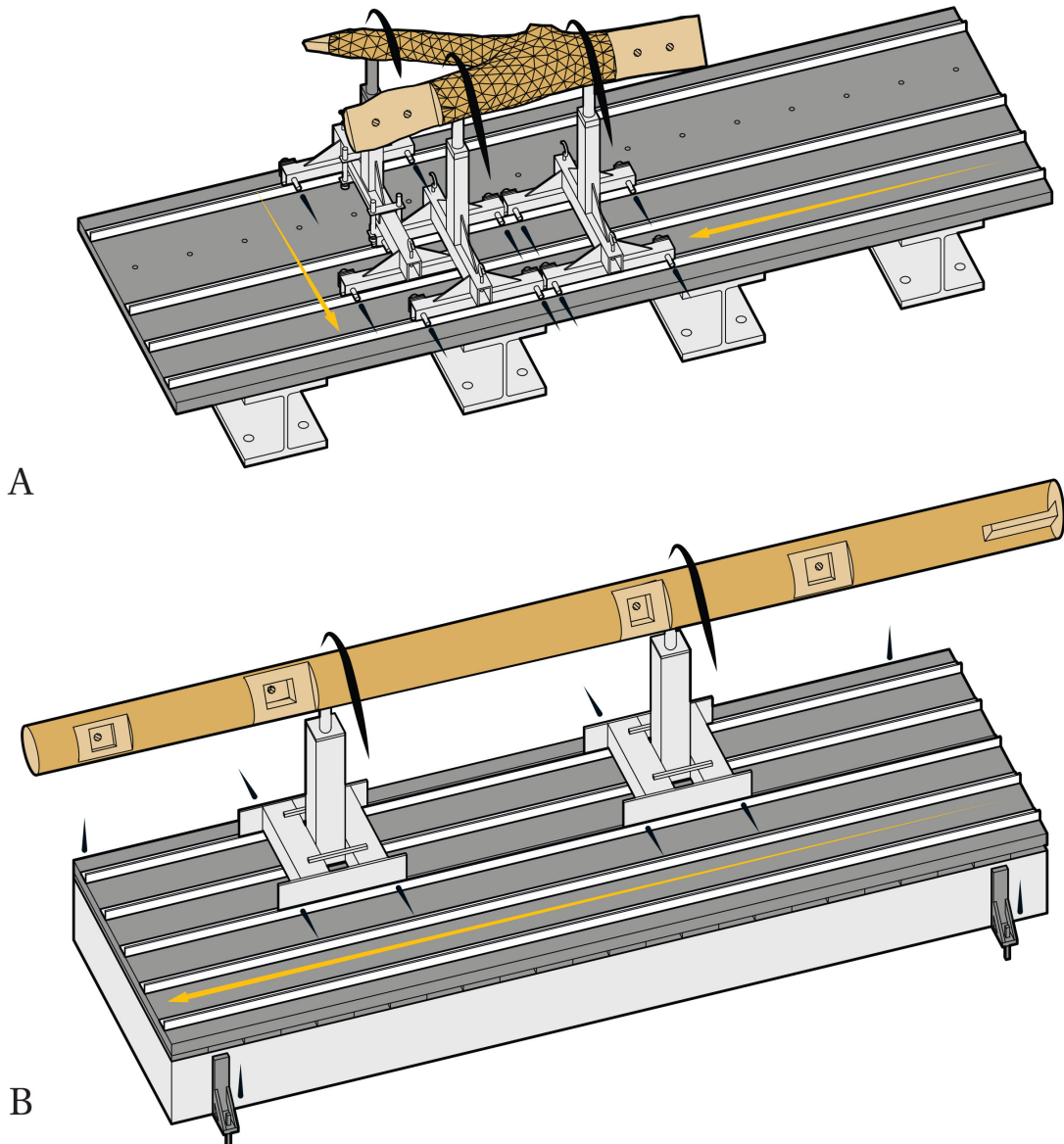


Figure 7.8 – Raw wood setup for a) the fork, and b) the straight beam fabrication. The first rig rests on four steel I-beams that are too light to prevent vibrations or the movement of the table (the robot can push the whole base during the fabrication). The base is later changed to the reinforced concrete block that is fixed to the ground.

To conclude, the development of the fabrication setups are essential to start the joinery manufacturing for irregular raw wood shapes. The setup has to be strong enough to transfer forces from the robot to the timber and the floor without vibration or movement. Practical experience is necessary to develop setups suitable for robotic cutting acquired via close collaboration with the technical support at the research facility. Furthermore, these critical details are often not

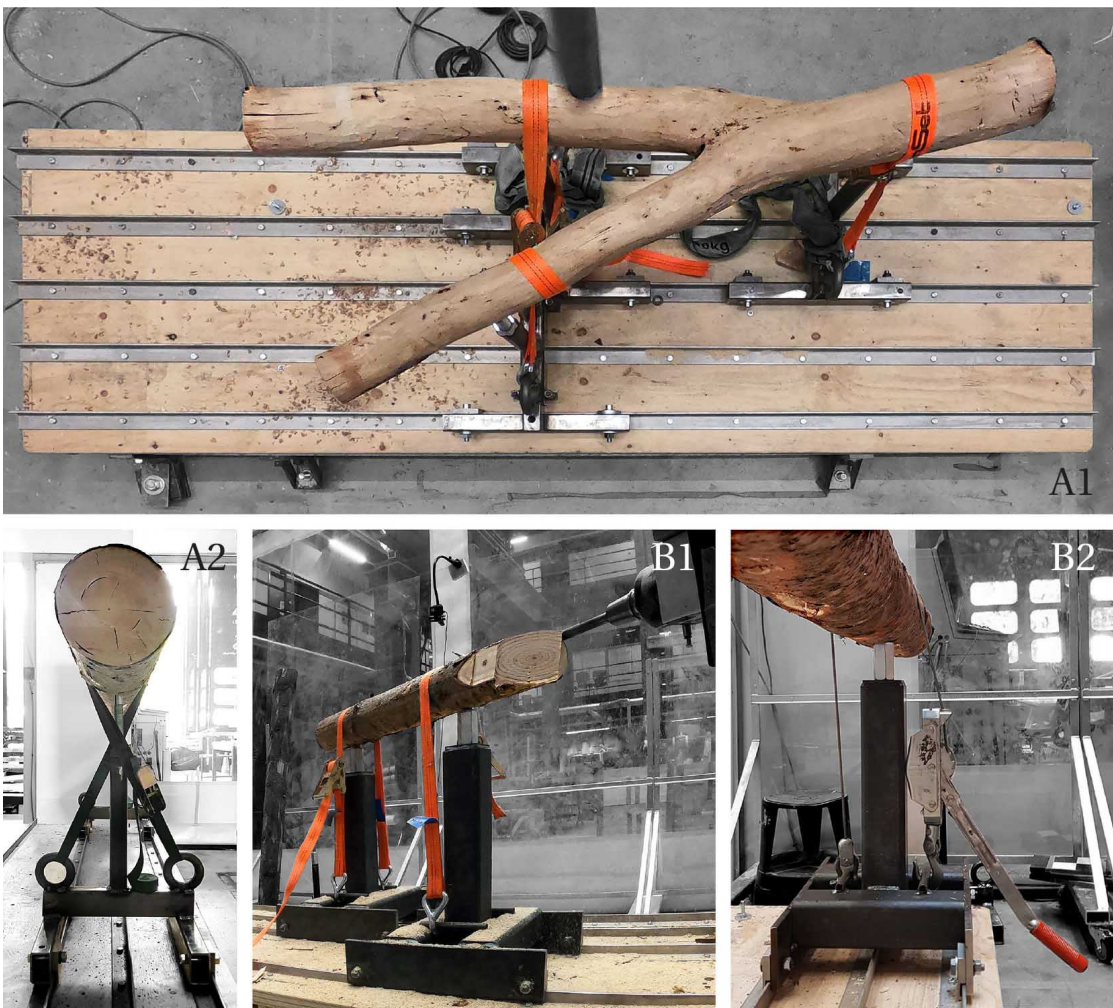


Figure 7.9 – Belt fixation methods: a1) 3 mm steel setup for fork cutting, a2) 3 mm steel fixation for a straight tree trunk, b1) 8 mm steel stands positioned diagonally for a better reachability, b2) lever-arm mechanism to reduce the strength needed to tighten the belts.

discussed in research work and are equally crucial in line with design methods, especially in the raw wood research context. Differently from timber plate structures where CNC machines are optimized to process regular wood, it is obligatory to develop fixation setups to adapt to timbers' variability and topology. Industrial applications have fewer issues like previously described ones because only longer and heavier timber is employed as a construction element. The collaboration between industrial raw wood manufacturing (ImaxPro) did not lead to relevant results, leading to individual investigation needed to design a flexible yet robust fabrication setup. The smaller a beam is, the stronger the fixation mechanism is needed. The setup's final version is still in use, resulting in precise robotic cuts for straight, bent, bifurcated raw woods and regular-sized beams. Lastly, the base is designed to adapt to timber plate assembly because the robot space must be shared between different researchers.

### Cutting-tool Calibration

The cutting tool calibration has an essential role in the precision of the overall assembly when using timber joints. If there is an imprecision in one joint, it will be challenging to assemble an overall structure due to the tolerance accumulation. A typical tool centre point calibration (TCP) is performed by orienting the robot in different angles while keeping the tool-tip at the same point [65]. This calibration method resulted in a 5-10 mm tolerance using the second hand industrial robot ABB IRB 6400R. The inaccuracy is relatively significant because each joint is cut in different angles where each cut has around 2 mm imprecision. This calibration is limited to the human vision. A solution to this problem is proposed using two low-cost USB microscopes by simply increasing the level of vision, demonstrated in Figure 7.10., resulting in tolerance of 1 mm.

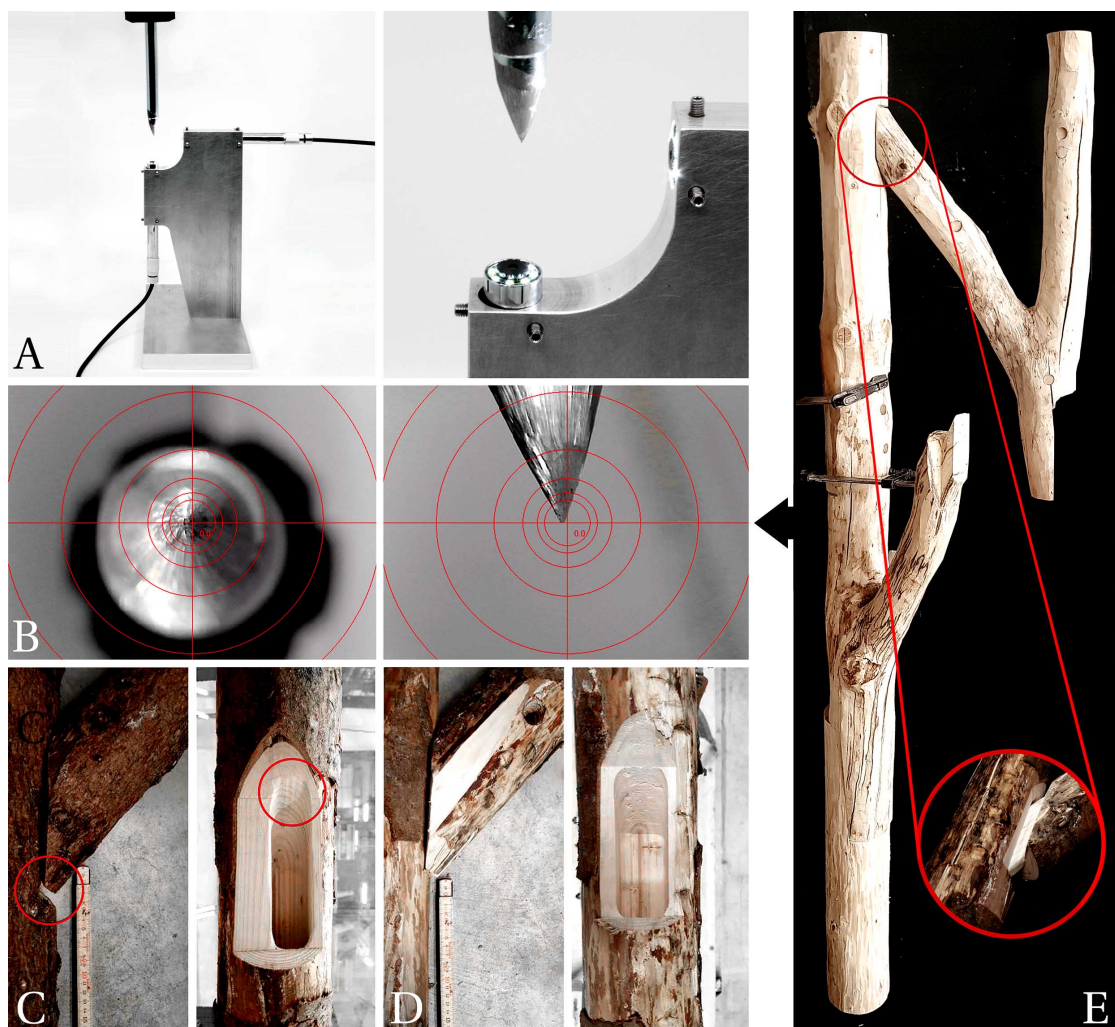


Figure 7.10 – Calibration using a) two low-cost microscopes and b) visual information for TCP calibration. The initial hand-eye calibration results in c) low quality 5-10 mm imprecision, whereas d) the proposed method decreases the tolerance to less than 1 mm. The calibration is necessary because the tolerances accumulate over e) the larger assemblies.

## 7.4 Robot Control

Two simulation methods are developed during research experiments: a) Rhino3D CNC, b) Unity-Rhino3D tool-path simulation. The translation of tool-path geometry to machine code has one critical difference in how the end-effector orientation and position are found. CNC tool-path preparation is more straightforward than robotic fabrication because there is no need to specify a target plane's X and Y axes. Instead, only the normal plane Z-Axis is needed that eases the tool-path planning significantly comparing to the robotic workflow. Such simplification is possible because CNC machines have a 3-axis linear movement and 2-axis rotations. Contrary, industrial robots employ an Inverse Kinematics solver to find 6-axis rotation angles to move the robot end-effector to the desired plane. The fixed plate rotation makes the tool-path generation significantly slower because rotary tools such as milling or saw-blade that have to be incrementally checked by gradually rotating target planes until the reachable target position is found. Both systems are described in detail in the following sub-sections.

### CNC Control and Simulation

Every vector in the CNC machine space is reachable due to the arc tangent approximation as described in the Algorithm 3 for the A and B rotations. The linear XYZ CNC movements allow the relocation of the end-effector without employing Inverse Kinematics. When a tool-tip is moved to a user-specified location, it is rotated first by the vertical axis and second by the horizontal axis, resulting in the additive rotation sequence. The sequential addition of two angles gives the orientation of a tool (see Figure 7.11).

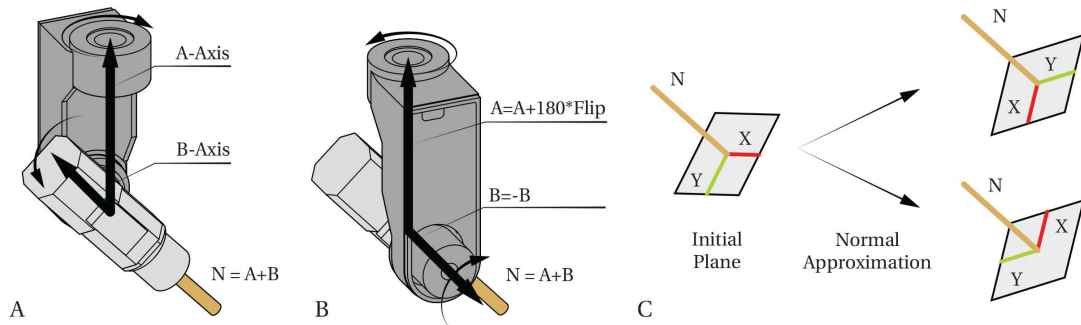


Figure 7.11 – CNC 3D orientation is approximated by a) the two angular rotations A and B, that can be flipped b) by the addition of 180 degrees to the axis A and reversing the rotation of axis B. Therefore, the tool-path is approximated c) to two possible planes at a current position.

The orientation of a plane is the same as the user-specified one, but the in-plane rotation is highly likely to differ. The in-plane rotation difference is irrelevant because only conical and cylindrical tools are employed in CNC cutting. The only optimization available in this algorithm is the 180-degree rotation of a spindle that could be needed to reduce the rotation time during cutting or avoid collision with a work-piece. This simple model allows reaching

every plane during the machining process unless there is a collision with a timber. The CNC workflow is accompanied by a mesh-mesh collision detection where each line of G-Code is first translated into CNC position and intersected with a work-space and the work-piece. If there is no collision, the G-Code program is saved as a text file and processed by the CNC computer to run the program physically as shown in Figure 7.12.

---

**Algorithm 3:** CNC a and b rotation angles from input Plane pl

---

**Result:** a b

```
// Convert Plane to Normal and Origin
Vector3d n = pl.ZAxis;
Point3d p = pl.Origin;
// Get A and B rotation of the CNC machine
double a = Math.Atan2(n.X, n.Y);
double b = Math.Atan2(Math.Sqrt(n.X*n.X + n.Y*n.Y), n.Z);
a = Math.Round(-1*Rhino.RhinoMath.ToDegrees(a),3);
b = Math.Round(-1*Rhino.RhinoMath.ToDegrees(b),3);
// Minimize a and b rotations
Plane f1 = new Plane(p,p+new Vector3d(-1,0,0), p+new Vector3d(0,-1,0));
f1.Rotate((Math.PI/180)*a,f1.ZAxis);
f1.Rotate((Math.PI/180)*-b,f1.ZAxis);
if (Vector3d.VectorAngle(plane.XAxis,f1.XAxis>Math.PI*0.5) then
    double Flip = (Math.Abs(A - 180) < Math.Abs(A + 180)) ? -1 : 1;
    a += 180 * Flip;
    b *= -1;
end
```

---

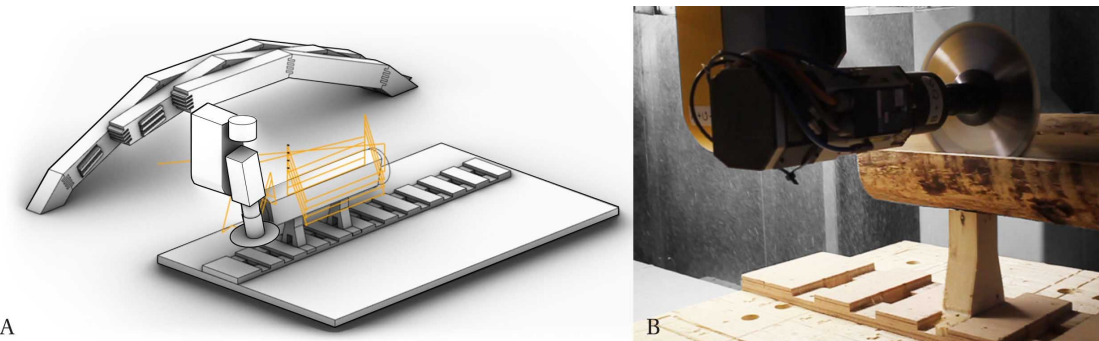


Figure 7.12 – CNC tool-path simulation a) that outputs a G-Code for b) the saw-blade cutting.

The total list of added new features to existing IBOIS-CNC<sup>2</sup> plugin is following: a) video simulation, b) merge several G-Codes, c) security checks from a text file, table and work-object collision detection, d) volumetric milling, e) saw-blade cutting, f) easier file export, h) tool-path generation for objects lifted from a table, i) faster 3-axis cutting without A and B rotations, j) serialization of MAK and documentation of the G-Code.

---

<sup>2</sup><https://github.com/petasvestartas/IBOIS-CNC>

### Industrial Robot Control and Simulation

When the industrial robot ABB IRB 6400R was introduced to IBOIS, EPFL researchers, a new digital fabrication workflow had to be developed. There are existing open-source robotic control methods suited for Rhino3D<sup>3</sup><sup>4</sup><sup>5</sup><sup>6</sup>. However, the current application is specific to ImaxPro-IBOIS collaboration because the robot must follow a contract requiring to employ a custom-built Unity application. The application has a text interpreter to transfer the Rhino tool-path information to the robots poses translated by the Unity application. The workflow has the advantage of being open-source to integrate the 3rd party tools, such as a) Faro Focus control to create a scanning-to-fabrication process, b) interconnect distinct research topics using an automatic tool-changer. It also poses an interoperability issue because Joinery Solver employs CAD Rhino3D software that highly differs from the Unity game-engine. Geometry types and tool-path targets must match in both software. Furthermore, the current robot application does not have any tool-path planning algorithms essential for the timber fabrication. Therefore, an automated simulation method is developed for the robotic cutting in Rhino3D to simulate robots poses and transfer files to Unity once the actual fabrication is needed (see Figure 7.13).

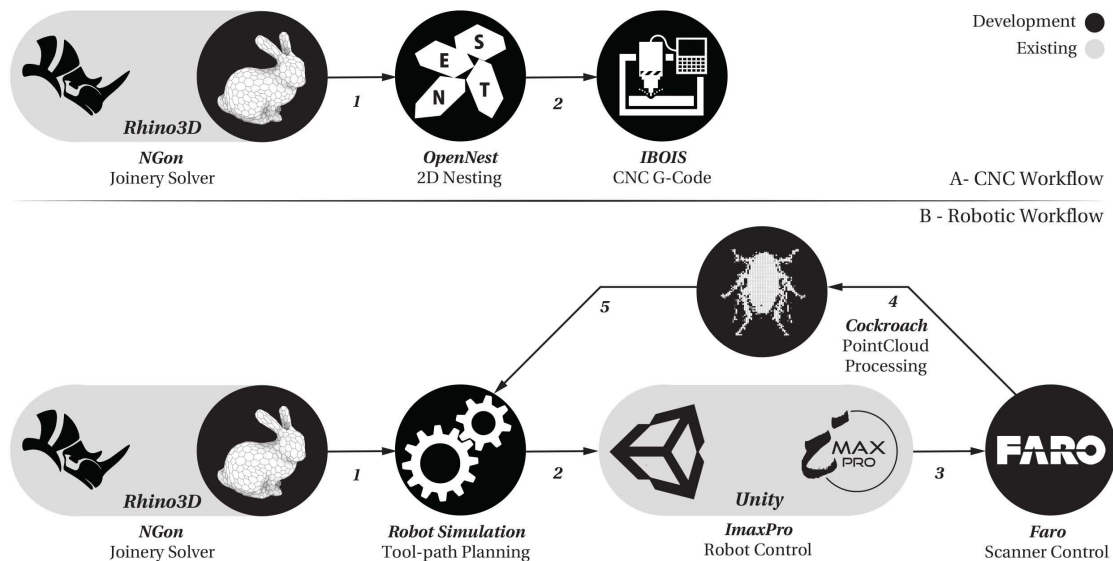


Figure 7.13 – Different set of tools employed for the CNC and robotic fabrication. The previous CNC fabrication was a linear process including: a) the Joinery Solver, b) 2D and 3D Nesting, and c) the IBOIS CNC plug-in. Whereas the robotic fabrication workflow has an inbuilt scanning feedback loop: a) Joinery Solver, b) robot tool-path simulation, c) Unity application to control the Faro laser scanner, d) Point-cloud processing, and e) the feedback loop to reorient a tool-path for the robotic fabrication.

<sup>3</sup><https://github.com/visose/Robots>

<sup>4</sup><https://github.com/HALRobotics/Beta>

<sup>5</sup><https://www.food4rhino.com/app/taco-abb>

<sup>6</sup><https://www.food4rhino.com/app/robot-components>

## Chapter 7. Robotic Fabrication

---

Several attempts were made to create an interoperability workflow between Rhino3D and Unity applications. The company ImaxPro developed Unity robot simulation and a text interpreter to transfer the CAD information from Rhino3D to Unity and control the robot in a real-mode. There is a problem in this workflow because there must be an additional robot simulator in Rhino3D. Else, it is impossible to understand whether the robot can reach a tool path or the tool-path must change. Ideally, such a workflow should be located in one application, but due to the software interoperability this causes the significant slow down of the workflow due to the manual file saving and reopening. To emphasize this problem more, a single person is hired for a reciprocal raw wood prototype, shown in the Demonstrators chapter, for the file checking. A consequent goal is made assuming that the application itself must be able to find a good orientation for tool re-orientation instead of using the manual labour.

The first trial to change this workflow is based on the Robots plug-in in Rhino3D to simulate the robot path virtually and then transfer the text files to Unity. This method's problem lies in how these two algorithms are developed: a) the Unity robot simulator is written by one party, and b) the Robots plug-in has been written by another party. Also, both applications differ from the actual ABB robot control. Furthermore, the robot axial information differs from each method because the Robots plug-in follows the node-plane specification, and the ImaxPro application follows the axial rotation where rotation planes could be located in the same position (see Figure 7.14). The overall problem lies in the application dependent robot simulators that leads to a search of other alternatives than using the Robots plug-in.

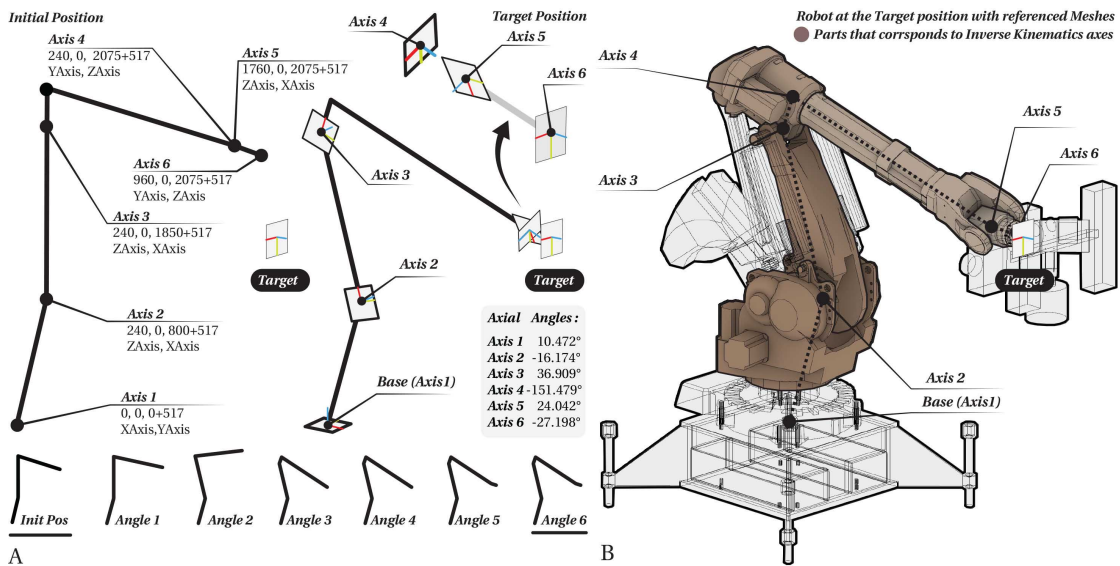


Figure 7.14 – Based on the ABB IRB 6400R documentation, six robotic axes extracted to create a) a skeleton for the Inverse Kinematics solver, and b) the robot part colored in brown is used in the Inverse Kinematics solver.

A better solution is proposed by translating the Unity robot simulator to an application

independent method. The workflow requires understanding how Euler and Quaternion methods are employed in Unity to translate to the Rhino3D notation. The translated version is checked multiple times by running different robot programs, Unity and Windows Console values. The output of the Imax-Pro method results in six angles representing individual axis rotations equally application in all of the software. The absolute robot joint movement called MoveAbs outputs the most optimal six angles between the current and the next target position. The linear movement is formulated as an interpolation between the current and the next target by moving the robot in small increments, e.g. 1cm, using the absolute joint movements. The six angles represent incremental rotations of a robot, as demonstrated in Figure 7.15. For example, the first axis rotates the remaining five parts of the robot, the second axis rotates the four parts of the robot and so forth. It means that the transformation matrices are incrementally added based on the axial sequence. Hence, the Unity application and the Rhino3D could be synchronised using the same algorithm written in distinct platforms.

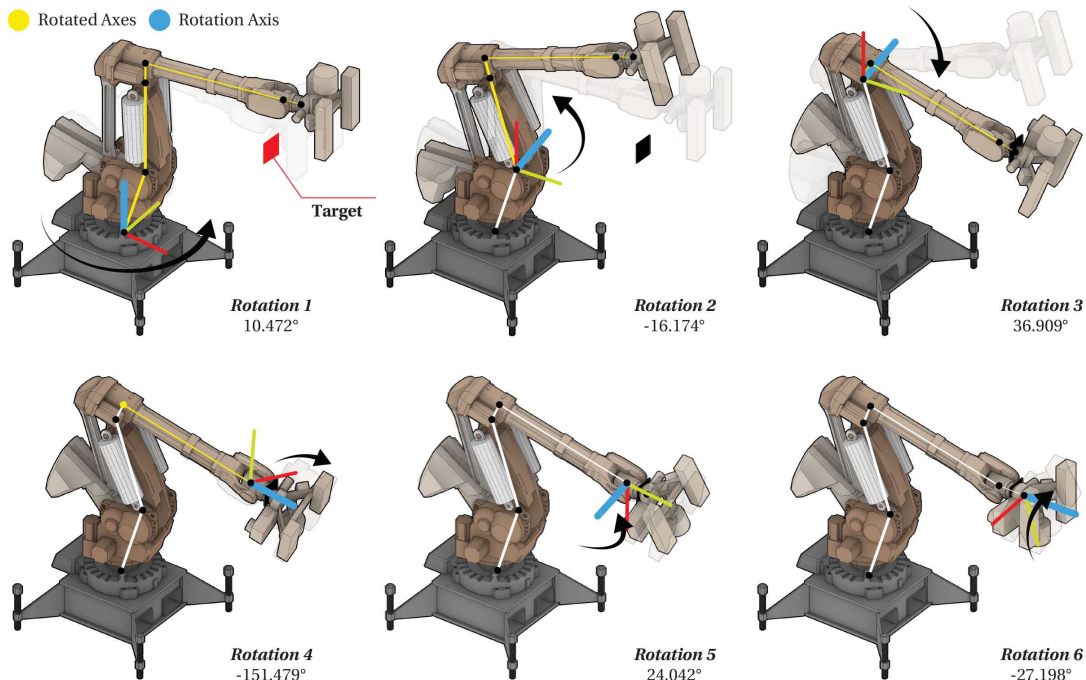


Figure 7.15 – Robotic Simulation is integrated to Rhino Grasshopper interface using the Inverse Kinematics solver. The 3D Meshes that represents the robot are rotated sequentially six times to reach a user-defined target (marked in red). For example, the first angle rotate five axes, the second one rotates four angles and so on.

Several other methods are developed to continue integrating the robot simulation: the optimisation of a tool-path trajectory and that corresponds to the Tool-Center-Point (TCP) between Unity and Rhino (see Figure 7.16). In the current research, three tools are employed: the Faro Focus S 150, saw-blade, and flat-end milling tool. The Tool-Center-Points are obtained using a) calibration methods discussed in the Scanning chapter for the Faro Focus S 150 and b) a standard 4TCP Teach-Pendant method to acquire the position of cutting tools. The calibration

values are stored in Unity and Rhino to have the corresponding simulation based on the different TCPs. The tool-path planning posed another constraint. Depending on the sixth axis' plane rotation, the tool-path could be hardly reachable, requiring multiple attempts to correct tool-path planes' rotation. The employed cutting tools are cylindrical, allowing rotation freedom within the 6th axis plane already discussed in the CNC sub-section. An optimisation strategy is developed by incrementally rotating a sequence of planes in 45 degrees and checking the robot's reachability. If one of the possible rotation is valid, then the cutting process is ready to start. Else, the timber element location must be changed. Consequently, the proposed workflow allows integrating the two different software platforms, including corresponding axis angles, the calibration of the Tool-Center-Points (TCPs), and the cylindrical tool-path optimisation.

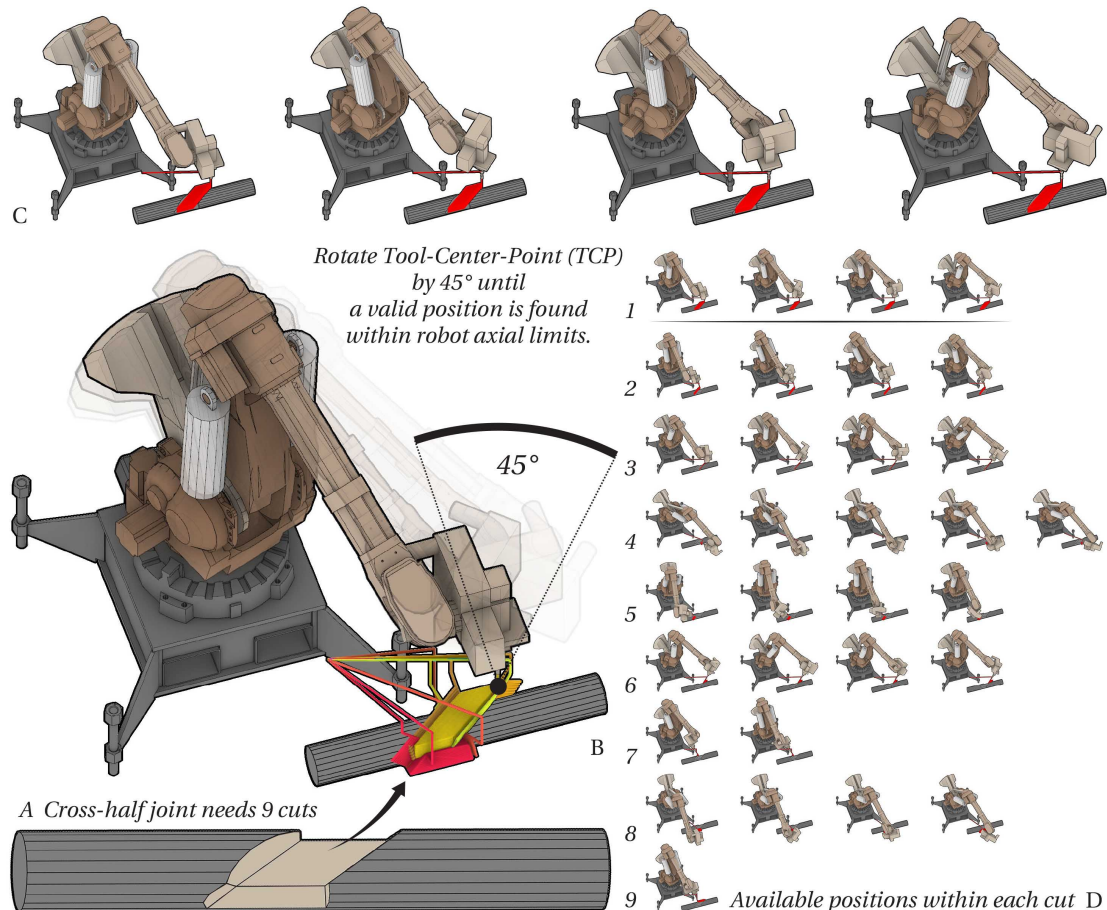


Figure 7.16 – Robotic tool paths are constrained by the robot Tool-Center-Point (TCP) reach. Depending on TCP rotation, the tool path could be reachable or not. The cross joint (a) is taken as an example that has to be cut using nine different TCP orientations. An optimization method is proposed to check the TCP's available orientations by an incremental 45-degree rotation (b) and choose the most optimal one (c). This procedure is needed to automate an else-wise manual checking operation in the possible robot reach at each cut (d).

## 7.5 Robotic Tool-path Generation within Joinery Solver

The Joinery Solver contains a data structure called Cut that transforms the geometric joint data into tool paths. The Cut has three inherited classes corresponding to the available tool-set: a) drilling, b) flat-end milling, c) saw-blade. The author is aware of the band-saw [77, 87, 189], chain-saw [119, 167] cutting and rotary lathe systems that are not available within the current robotic tool-set. Nevertheless, these tools are major ones employed in practice. The digital representation of joints and fabrication follows a similar notation: a) a pair of polylines is used to represent a cut, and b) a line is used to denote a drilling operation. The application considers physical tools geometric properties such as radius, thickness and length and their respective movements. The method must be a collision-free and reachable within the robot work-space (see Figure 7.17). Consequently, the CutDrill, CutMill and CutSawBlade classes are detailed individually in the following sub-sections to explain how a tool path is generated.

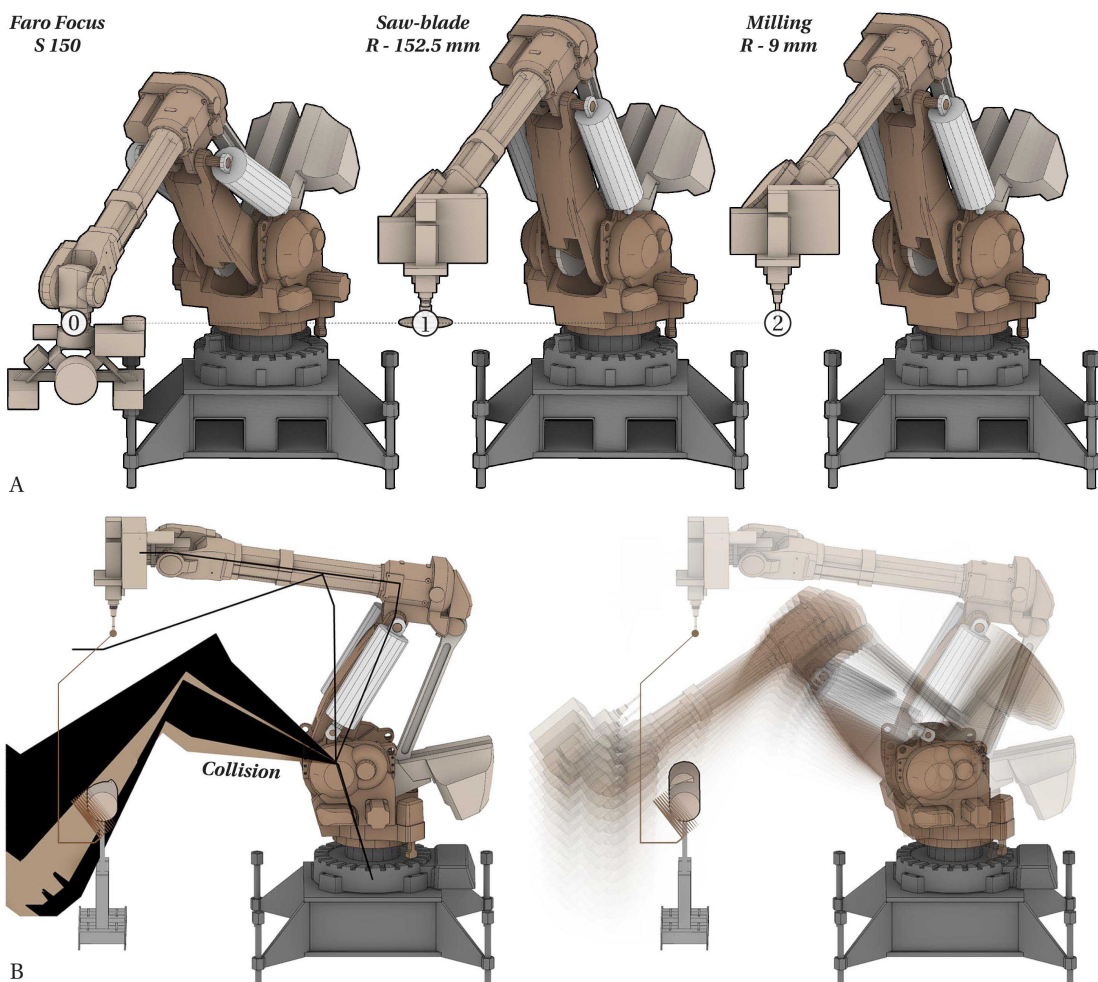


Figure 7.17 – Rhino3D simulation considers three different tools: a0) Faro Focus S150, a1) saw-blade, a2) milling tool. The tool-path generation includes a collision detection (b) to ensure safety during the fabrication.

## Drilling

The drilling tool path has two possible operations: a) the cut is performed following a line direction, b) the tool moves in a spiral path because the cutting hole is greater than a tool radius. The robot follows a circular movement instead of the standard linear or joint movement. Before each tool path is executed, the spindle stops and starts within 20 000 rotations/minute (RPM) for security reasons. The robot movement starts and finishes in a so-called Home-target, ensuring that the following path is reachable. For example, the Home-Target is located at the point (1694.93, 65.95, 1749.00) within Z-Axis (0.00, 0.00, -1.00) for the specific ABB IRB 6400R IBOIS EPFL robotic application. Afterwards, the program iterates a list of lines and converts them to circular arc movements (see Figure 7.18). The tool path includes two additional targets: a) Retreat-target that moves the tool-tip away from the timber piece, b) RetreateZ-target – returns to a safe Z coordinate concerning the last target. The robotic movement is controlled by a list of planes that must be reachable by the robot. Therefore the overall procedure is incrementally rotated by 45 degrees until a valid orientation is found. Consequently, the drilling operation performs a secure circular movement to cut a series of holes within the robot reach that is optimized by the tool-path planning method.

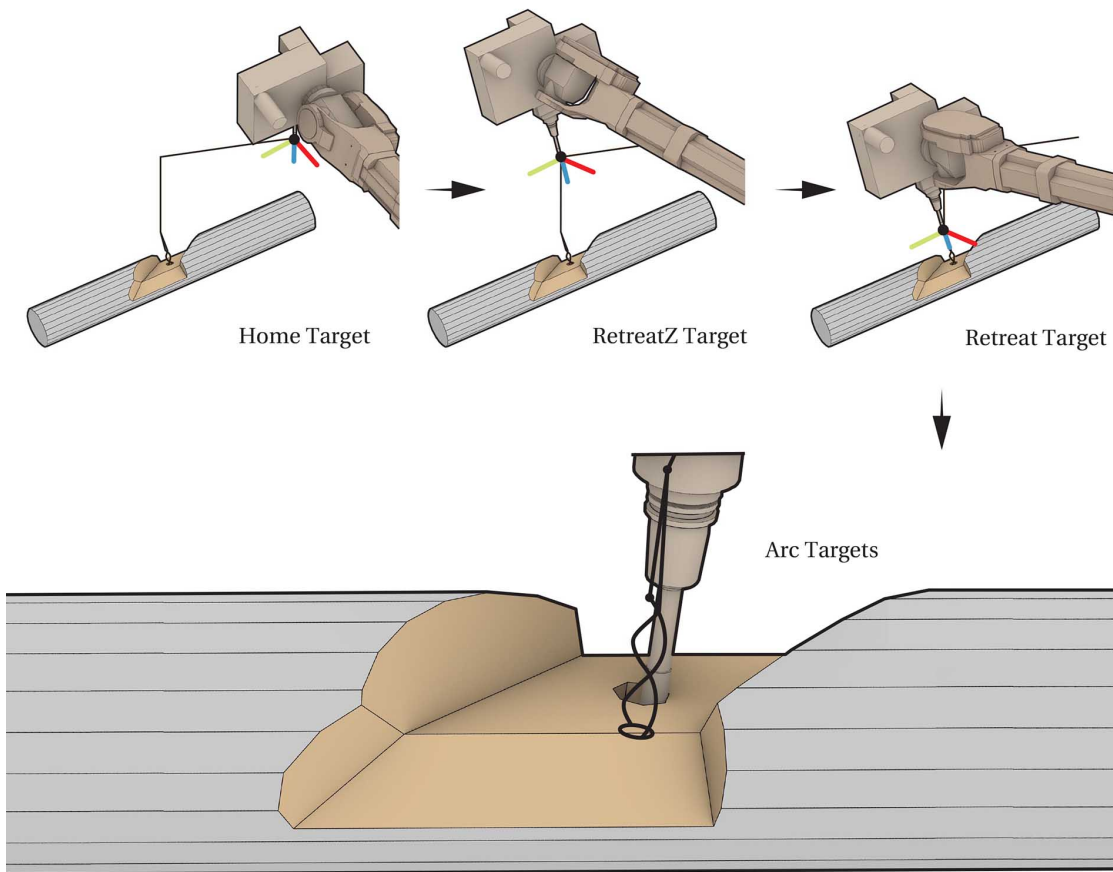


Figure 7.18 – Tool-path for drilling using spiraling arc movements and a series of retreat planes.

### Milling

Pairs of polylines define the milling tool path, where a) the bottom polyline defines a surface that needs to be reached, and b) the top polyline gives information about the tool orientation and the height of a cut. There are four possible tool path options (see Figure 7.19) : a) cutting a closed contour, b) open polyline, c) single line, d) milling a closed contour with or without holes. Due to the radius of the milling tool, the tool path must accommodate notches else timber joints cannot be assembled. The corner pockets have two main categories: a) extension of a cutting line, b) bisector cut. The notches are computed by performing plane-plane intersection constructed from the top and bottom outlines. The planes are offset by the distance of a radius of a tool and the necessary tolerance. Several parallel cuts are often needed to cut through a large volume of timber. A spiral tool path helps to move the milling tool in a slope to ensure the tool's safety. The volumetric milling employs Clipper library to offset polygons in a fast and robust manner. Then the offset pattern is mapped from one contour to the other using a barycentric mapping [71].

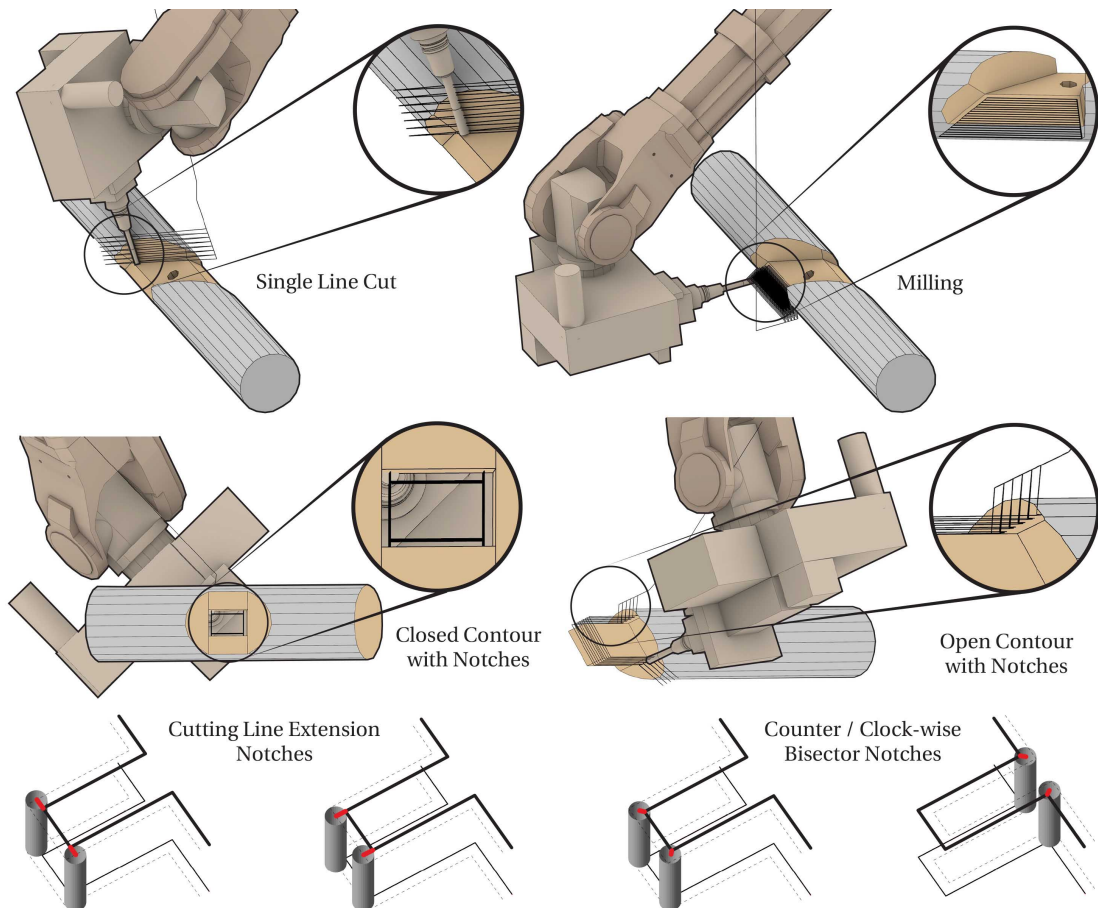


Figure 7.19 – Tool-path for milling and cutting including closed, open and linear polylines. Also, three notch types are included depending on a curve direction. The figures shows a milling tool within the scale of 9.8 mm radius and 110 mm in length.

### Saw-blade

The saw-blade cutting is needed to remove a large amount of timber faster than the milling tool. Several categories of saw cuts are employed (see Figure 7.20): a) cutting along a plane of the circular saw, b) performing the L-shape cut, and c) the 90 degree L-shape cuts. Unlike the milling tool, the saw-blade needs to be rotated more slowly, e.g. 6000 RPM, because the speed at the centre of a blade and its edge differs. The blade must be turned off and turned on for each cut due to the circular saw movement and safety. The L-shape cuts are performed because the saw is limited by the cylindrical holder minimizing the cutting length of the tool radius minus the holder size. Depending on the cut size, the tool path could be interpolated to perform a series of L-shape cuts until the needed volume is removed. These binary cuts limit the reachability of a robot that requires an optimization strategy to shift the cutting tool path polygons until a reachable and secure orientation is found. The two cuts could be performed in an alternating ninety or a user-specified angle. Finally, the tool path is oriented so that the 4th axis of a robot points to the farthest position from timber.

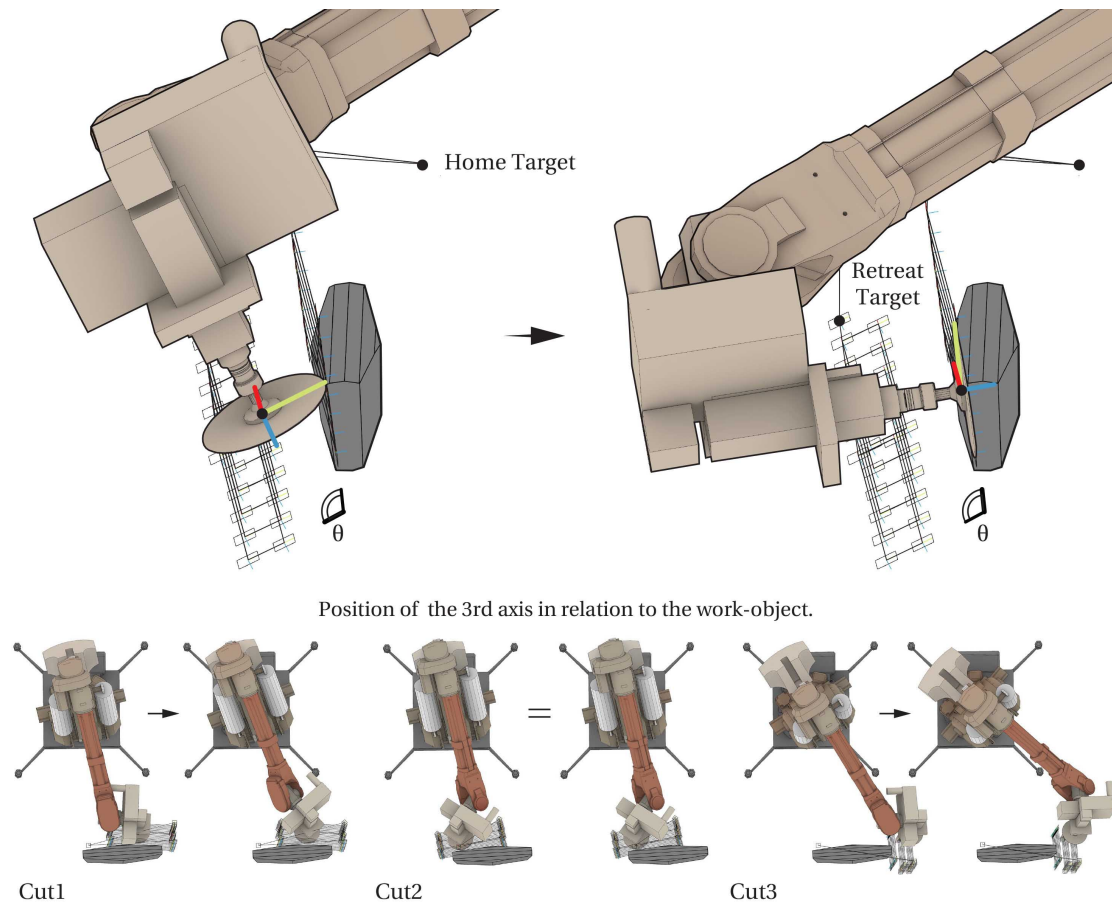


Figure 7.20 – Tool-path generation for the saw-blade that is computed in the singular or the L-Shape cut (top). The robotic cutting must orient X-Axis of Tool-Center-Point pointing outwards from the cutting object to prevent possible collisions (bottom).

## 7.6 Conclusion

This chapter summarizes two parts: a) the physical setup, and b) the tool-path generation within the Joinery Solver. There is a gradual shift from the CNC to the Robotic fabrication due to the flexibility of the robot. The main difference between the engineered timber plates and the crooked lumber is that the timber must be lifted in the middle of a work-space to reach the cuts from all the sides. The lifting operation poses a question of how to fix a tree trunk without limiting the machining space and ensuring as minimal vibration as possible. The trial and error process helped find a stable, solid and flexible enough rig to mount raw timbers using the steel profiles integrally connected to the base of a setup.

Both the CNC and robotic systems need to be understood to interpret the mechanical movement for a tool-path planning algorithm. The CNC machining is simpler because there is a minor interference between the machine and the cutting object. Moreover, all the points of the CNC machine are reachable. On the contrary, the robotic cutting is tightly connected with the tool-path planning. Before the proposed methodology was developed, each tool path had to be manually checked by incrementally rotating the tool-tip, which is a general industrial practice requiring the time-consuming laborious work. This process became highly constrained due to the use of two software: Unity and Rhino. The solution is reached by disconnecting the robotic simulation from the both applications using a stand-alone C# application. The robotic simulation, provided by the industrial partner ImaxPro, is translated from Unity to a stand-alone library to make the physical experiments possible. Understanding the Quaternion and Euler rotation systems and the rotary robot axial system helped synchronize the given industrial simulation with the research needs. Both systems are checked by testing multiple tool-paths within Unity and separately as a Windows Console Application. Any 3rd party software commonly used in Rhino, such as the Robots plug-in<sup>7</sup> could not be employed because the industrial partner developed a slightly different Inverse Kinematics system considering the 3rd and 4th axis rotation of the robot.

The tool path generation follows a notation of two closed polylines for cutting and single line segments for drilling. This method is based on the first experiments with the CNC machine and adapted to the robot control. The drilling, milling, and saw-blade operations have sub-categories such as spiralling cuts, notches for open and closed polygons, and L-Shape cuts that adapt to different types of wood-wood connections. When developing such methods, it is necessary to minimize the initial user inputs to avoid a multitude of variables. The polygons pairs help significantly simplify the tool-path because a pair of polylines already contains information about a cut orientation, concavity and convexity of corners for notch positioning, tool inclination and volume needed to be removed from a single element of timber. Finally, the robot reachability is checked with these individual tool-path operations automatically, and a group of different cuts are performed for a single timber joint as demonstrated in Figure 7.21).

---

<sup>7</sup><https://github.com/visose/Robots>

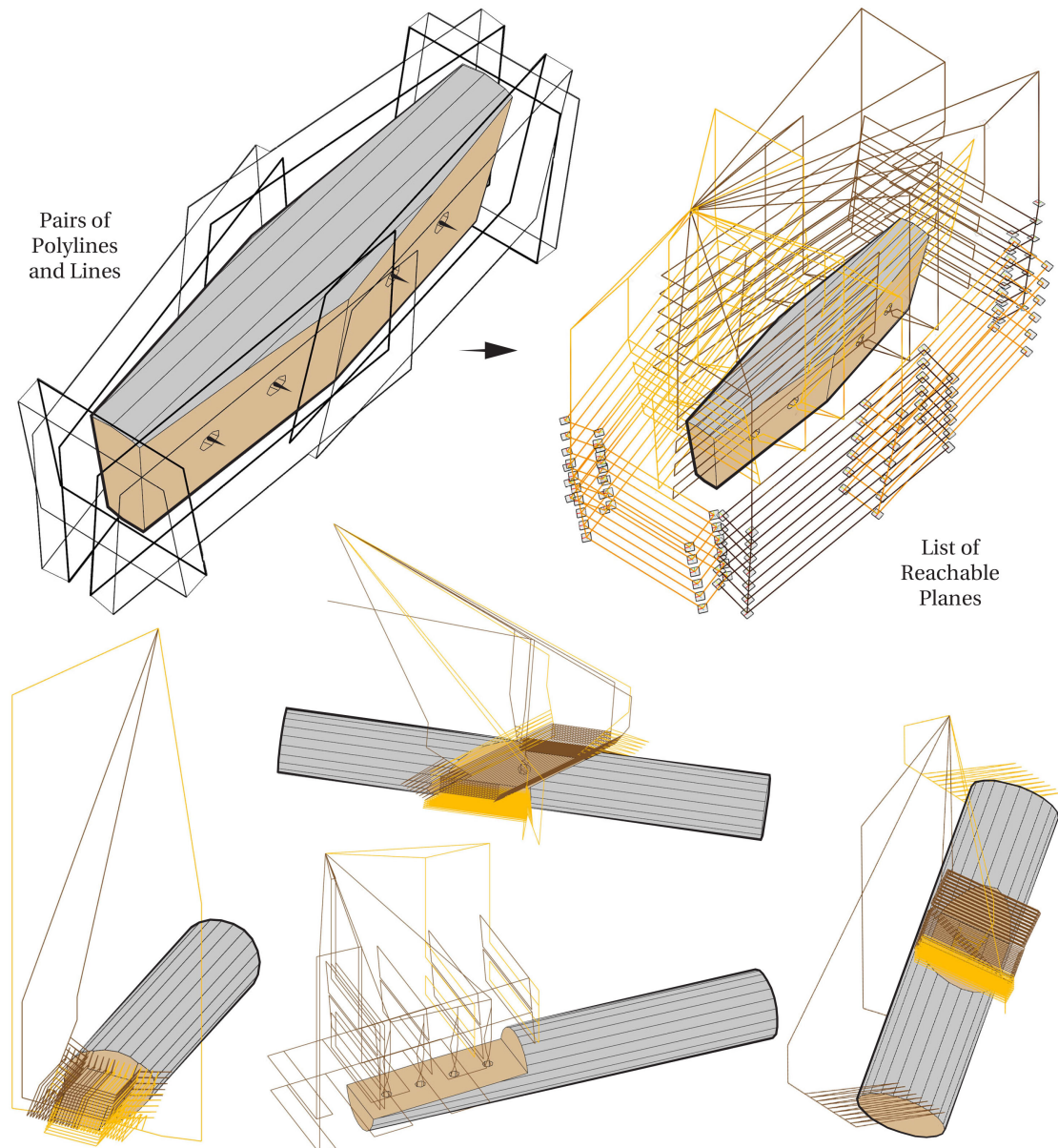


Figure 7.21 – Multiple tool-paths for a timber joint fabrication. The connections in the Joinery Solver are defined as pair of polylines for cutting and lines for drilling.

Cutting operations of raw wood or solid lumber requires large timber removal for each joint. Furthermore, the tree trunks are relatively large elements comparing to cutting tools used in the current research. For example, the most miniature trees that could be machined falls into 15-30 cm diameter range. The smaller woods are unstable, weak, and are non-uniformly twisted and crooked. Therefore, the fabrication tests show that there is a potential to use small radius trees, but they cannot be less than 15 cm in diameter due to the material properties of wood.

The fabrication methods can have additional adjustments needed to adjust to the industrial standards. The fixation of tree trunks poses a complex problem in itself, and it is explained how a customized setup has been developed to enable the production of prototypes. For example, the linear track system could be enhanced using compressed air grippers rather than the manual fixation. Depending on the setup, a U-shape raw wood holder and the metallic dowels could be accompanied by the additional rig for pre-drilling. Future work could elaborate on other means of tool-sets such as rotary lathe system, band-saws, chain-saw operations to speed up the cutting process and ease the robot reachability. Lastly, the generation of tool paths for the fabrication process becomes a challenge when standard software cannot be engaged. The nature of digital fabrication requires constant research and development that can be highly specific to the current equipment and the design. This knowledge is often based on empirical studies due to an individual project design, whereas the primary robotic control could be reused as individual blocks when repeatability from project to project is identified.



# Conclusion of Methodology

The three methodology chapters: a) Joinery Solver, b) Scanning, and c) Robotic fabrication form a design-to-fabrication workflow for raw-sawn-timber. The Joinery Solver provides a design modelling framework as a primary input for prototyping, guided by the laser scanning method and the robotic manufacturing.

The Joinery Solver describes an algorithm that helps to automate wood-wood connection generation using a minimal model representation and a wood-wood connection library. The method allows identifying connection zones and assign timber joints based on an element-to-element orientation. The framework employs a change of basis transformation to a shape of a joint to a connection zone. The framework demonstrates that it is possible to construct timber joints, independently from a timber shape, starting from the local element relations instead of a global form. Lastly, the Joinery Solver links the visualization with the tool-path generation for the digital fabrication.

The Scanning chapter demonstrates two developments: a) the laser-scanner integration with the industrial robot arm, and b) the point-cloud processing framework – Cockroach. The precision of the scanning application is subject to three measures: a) the scanner precision, b) the robot tolerance, and c) the calibration method. The obtained precision of the robotic scanning is around 1 mm using the multi-stationary scanning method. While the scanning method is specific to the research method, the point-cloud processing framework is applicable outside the research scope. Methods such as Skeletonization, cloud-to-cloud registration, clustering and other techniques form a software library named Cockroach.

The robotic fabrication compares the CNC and the industrial robot arm fabrication methods, and explains the advantages of robotic manufacturing over the CNC machining. Physical setups for raw wood fabrication are described in further detail to ensure a stable and secure cutting process. Furthermore, a tool path planning algorithm is proposed to speed up the manual fabrication preparation. The tool path is linked with the Joinery Solver using the pair-wise geometry representation applicable for both systems. Besides the robotic control, all the algorithms are open-sourced and detailed in the Appendix C.



## **Demonstrators Part III**



# Foreword of Demonstrators

The Demonstrators part is divided into two sections: a) Side-to-Side joints for Shell Structures, b) Raw wood Cross and Side-top Joints for Nexorades. The demonstrators are needed to develop and validate the Joinery Solver based on the physical tests (see Figure 7.22). The Joinery Solver is refined through the CNC and the robotic fabrication to enable the design-to-fabrication workflow. Furthermore, global geometry frameworks are developed based on the previous state-of-the-art methods and applied to raw-sawn-timber. Additional studies are developed during teaching that are separately discussed in the Appendix A. The first section is based on stacking timber elements side-by-side to form a shell structure. The surface discretization methods are interlinked with properties of raw wood and possible architectural applications. The second study explores Nexorades connected by Cross and Side-to-Top connections. Nexorades and frame structures employ fewer elements using pair-wise connections. The later system poses a question of how the structure needs to be covered and how to strengthen the joints with a minimal connection area. As a result, two systems are proposed: a) raw wood and plate hybrid and b) a double-layer system.

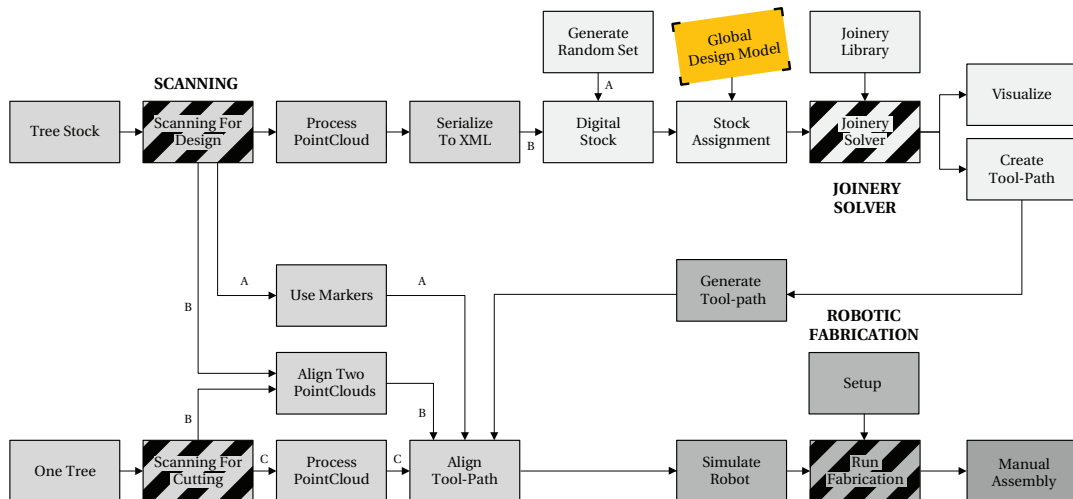


Figure 7.22 – Demonstrators integrated into the global thesis framework.



# 8 Side-to-side Joints for Shell Structures

---

This chapter is based on:

P. Vestartas, N. Rogeau, J. Gamerro and Y. Weinand. Modelling Workflow for Segmented Timber Shells using Wood-wood Connections. *Design Modelling Symposium Berlin 2019. Impact: Design with all Senses, p. 596-607, Berlin, Germany, September 23-25, 2019.*

DOI : 10.1007/978-3-030-29829-6\_46.

---

## 8.1 Foreword

This section presents a modelling method based on a planarization method for double-curved segmented timber shell made from quad polygons and assembled by wood-wood connections. The inspiration is taken from the timber dome structures [37, 103], where solid timber walls were built from planks, connected side by side. The geometry modelling workflow is split into three parts: surface discretization, joint modelling and fabrication. Firstly, the projection-based solver is applied to the planarization of volumetric blocks. Secondly, the joint geometry is computed according to the insertion vectors and the tool-path is generated using G-Code [75] to guide the 4.5 Axis CNC machining. As proof of concept, two prototypes were built, one from planks and another from raw wood. The choice of material influences the segmentation of the timber shell. Finger and Tenon-mortise joinery have been chosen for their simple modelization and fast cutting time. Their placement follows as closely as possible fiber orientation of wood. Even if both study cases share the same discretization method, the first prototype from timber plates takes advantage of lightweight structures, while the second explores a heavy solid round-wood structural system.

Side-side Joints for Shell Structures chapter is structured as follows:

- Section 8.2 Introduction to the surface planarization and joinery framework
- Section 8.3 Description of the surface discretization method
- Section 8.4 Prototypes:
  - Prototype in timber boards
  - Prototype in raw timber
- Section 8.5 Overview of results
- Section 8.6 Conclusion

## 8.2 Introduction

The CAD modelling workflow (see Figure 8.1 B1-B5) is based on a surface subdivision, discretization, planarization, joinery geometrical specification, CNC fabrication and assembly sequence. Two building materials are assessed from the local saw mill: planks and round-wood. The design target is a surface that is discretized according to building material scale and assembled manually using wood-wood connections. It considers geometrical and material constraints: linearity of wood, grain direction, drying and fabrication processes. The proposed method is based on a mesh modelling framework in order to have a low-poly representation of panels and timber blocks.

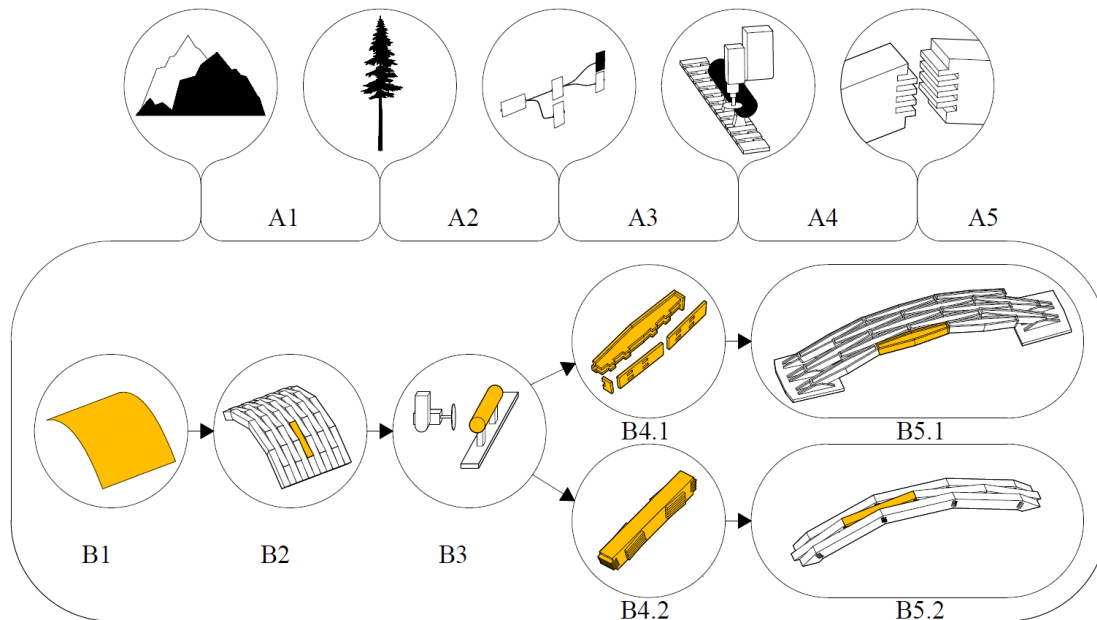


Figure 8.1 – The research context: a1 – Mountain forestry, a2 - Tree species – Épicéa, a3 - CAD interface, a4 - CNC cutting, a5 - joinery. Modelling workflow: b1 - surface, b2 - discretization and planarization, b3 – CNC milling and cutting, b4.1/2 Box component, Solid element component B5.1/2 Prototypes.

### 8.3 Surface Discretization

The planarization method is based on support structures of polygonal cell packing [124]. The aim is to compute polyhedrons, which are solids with only planar face boundaries from arbitrary surface subdivision [133]. Similar research [134] implemented plane projection methods on quad meshes with small gaps at each mesh vertex. Other possibility is to use Voronoi diagrams for planarization [124]. Another technique is to apply a circle packing of triangle meshes whose incircles form a packing [143]. A third method uses circular and conical meshes [90]. Our chosen polygonal pattern does not have such qualities because its shape is linked to the linearity of planks and round-wood. The aim is therefore, to keep the original shape without too much distortion. The proposed planarization method is based on an iterative solver which gradually projects extruded quad faces to an average plane (see Figure 8.2).

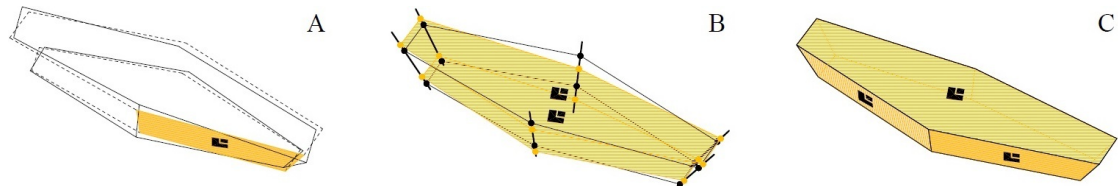


Figure 8.2 – Planarization method consists of two main steps: a) planarization of extruded mesh edges (support structure), b) intersection of lines to the average planes of line ends, and c) the planar polyhedron.

The user has to specify a tolerance of a planar polygon and give a collection of mesh vertex points. While iterating through polygonal mesh faces, the current mesh face vertices are projected to an average plane and the non-planar polygon deviation is recorded. Afterwards the average sum of topologically coincident projected mesh face vertices are assigned to current mesh face vertices. This method is re-iterated multiple times until the deviation is below the user specified tolerance value. The full modelling framework is subdivided into the following steps (see Figure 8.3 C): the target surface is discretized into a polygonal mesh. The mesh edges are extruded and planarized (see Figure 8.3 A). The top and bottom contours of each cell are not planar and are therefore, projected to the average plane of their vertices (see Figure 8.3 B). Projected points form a planar polygon and, together with planarized quads, result in a planar polyhedron.

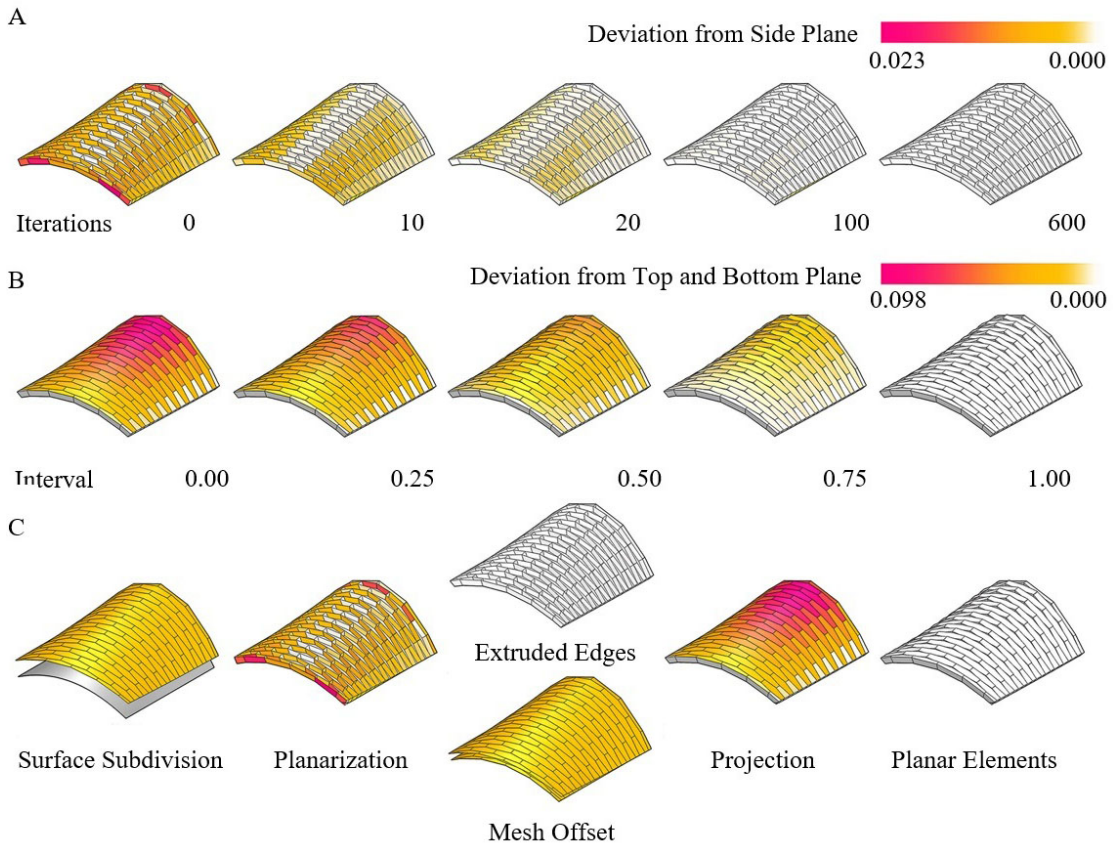


Figure 8.3 – Planarization method shown in iterations: a) planarization of extruded mesh edges 0-600 iteration, b) intersection of lines to average planes, c) the full sequence of planarization.

## 8.4 Prototypes

A series of prototypes was made to validate the planarization algorithm. Planks and roundwoods were specifically chosen as part of a collaboration between a local forestry company and the research institute to use raw timber materials. Consequently, it was important to understand the relationship between material, connection geometry, assembly sequence and fabrication.

### Prototype in Planks

Several existing publications describe the automation of assembly path that influences the joinery geometry (type of joint and an insertion direction) [56, 178, 184]. It is also possible to look at this problem from a user perspective when the assembly path is already known. Proposed methodology is based on the existing state-of-the-art method [136] and extended to polygonal meshes, which are not restricted to triangle or quad discretization. Moreover, graph-search methods such as Breadth-First-Search could be applied to compute an assembly order (see Figure 8.4).

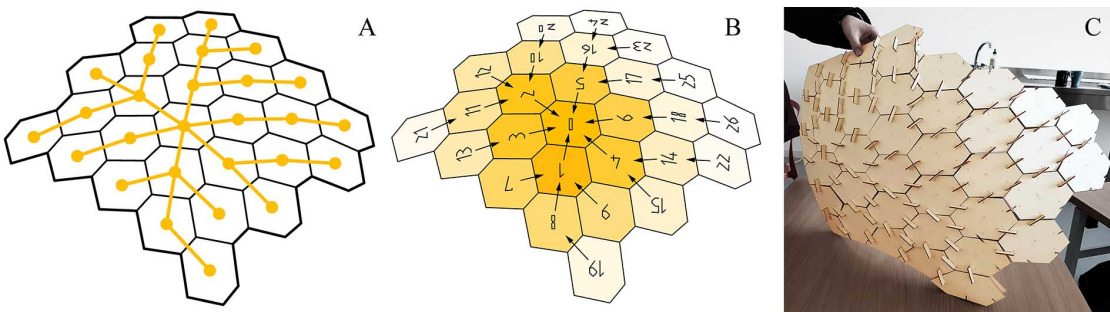


Figure 8.4 – Graph search algorithm – Breadth-First-Search used for an assembly path and joinery orientation (c). BFS connectivity graph from the center points of hexagons (a), graph edge is used as a vector for each polygon edge joint orientation (b), physical test [173].

Edges of this graph whose nodes are polygon centers give insertion direction. This vector has to be compared against connected edge direction to know if the insertion vector is not parallel. BFS is a fast approach when a user does not have a sequential order how to assemble elements one after another. Other methods such as a grid-like assembly could be applied when the initial topology is regular. Lastly, several large patches could be assembled together too. It often requires special details, as multiple edges may not have uniform insertion vector applicable to all elements within a group.

A series of box-to-plates transformations are made after the planarization. First, we get the insertion range based on neighbor faces (see Figure 8.5 A) and second, the insertion angle is computer based on element faces and fabrication constrains a maximum CNC cutting angle 45° (see Figure 8.5 B)). Third, we compute the intersection between the two sets of angles A and B (see Figure 8.5 C). Then, turn each polygonal face into a 3D geometry, with plate-to-plate and box-to-box connections. The insertion direction is used to compute tenon-mortise joints at the top and bottom edges. Edge-wise dovetail joints are chosen for each side. Finally, a set of boxes are assembled from individual boards and connected using dowels (see Figure 8.6).

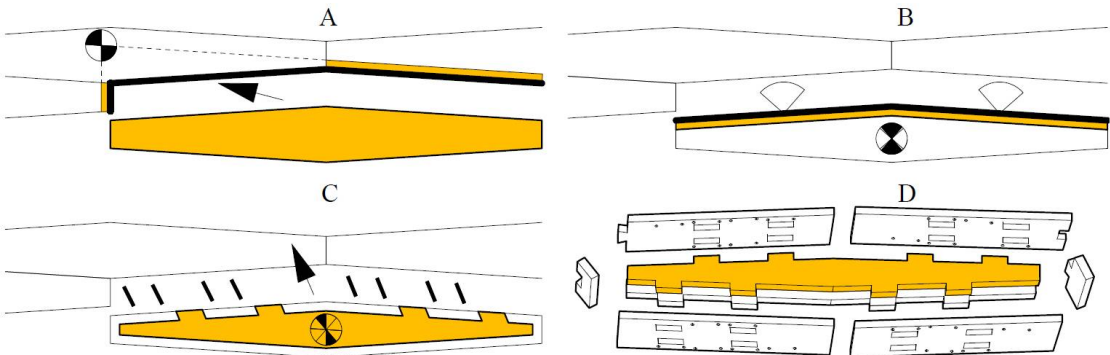


Figure 8.5 – Computing the insertion direction: a) the insertion range based on neighbor faces, b) the insertion range based on element faces and fabrication constrains, c) intersection between set A and B -  $A \cap B$ , and d) – generated geometry.

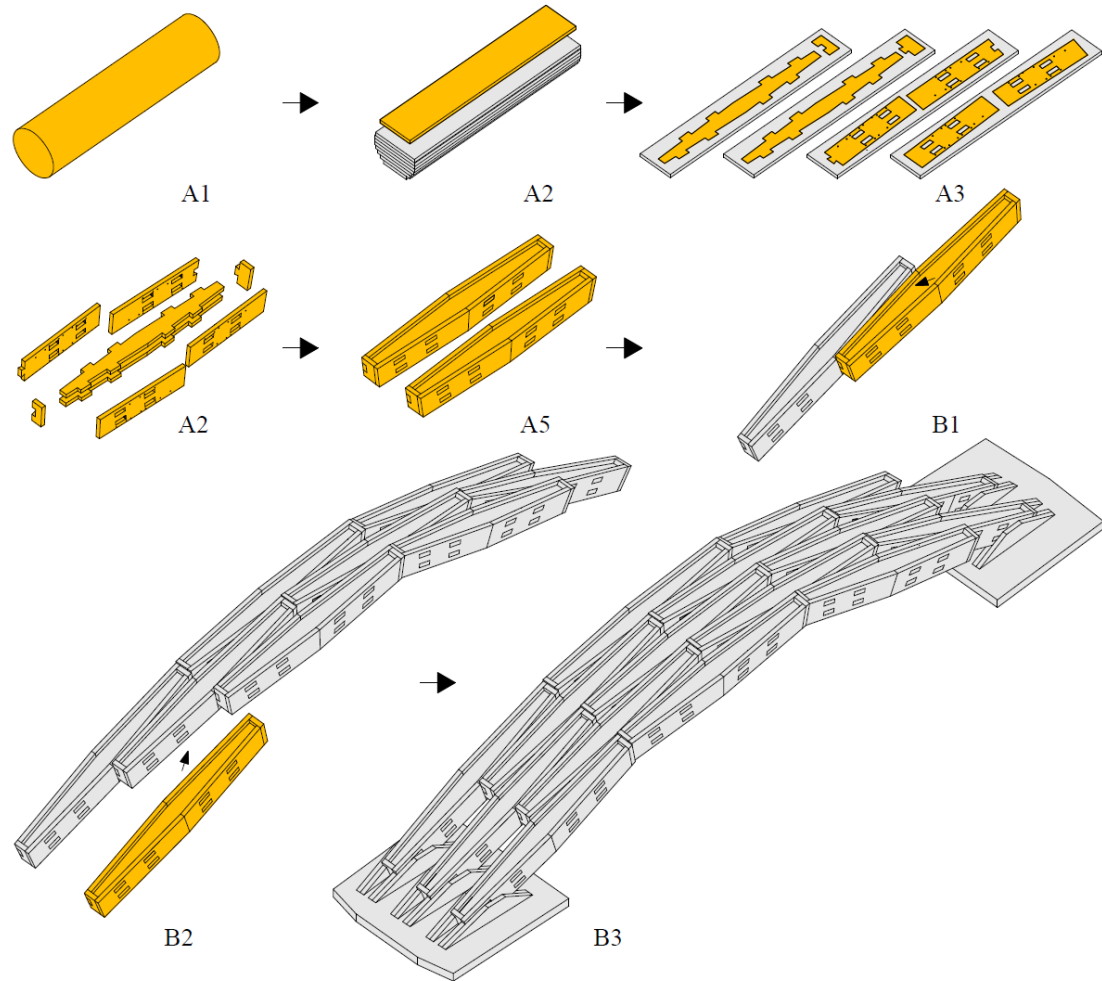


Figure 8.6 – An assembly sequence: (a1) round-wood, (a2) planks, (a3) cutting outlines, (a4–a5) assembly of a box, (b1) connecting boxes by dowels, (b2) boxes assembly (b3) final prototype.

### Prototype in Raw Wood

Stacking modelling methodology is tested for the Round-Wood prototype (see Figure 8.8). It does not rely on mesh topology but rather on basic geometric transformations and tiling operations for single curved arcs. The planar blocks of the arch are generated using five steps (see Figure 8.9). First, curves are divided into points and normal planes are computed from curve derivatives. Two planar outlines are generated using perpendicular planes (see Figure 8.9 A). Second, a finger joint is drawn as a tile to generate the butt connections for each element. This allows the shape of the connector to be changed any other 2D-joint later. The tile is then oriented from the original plane to the perpendicular frames on the curve (see Figure 8.9 B). Afterwards, the tile polyline is inserted into the existing planar outline.

Lateral connections are placed using another set of rules. Rectangles are drawn at the intersec-

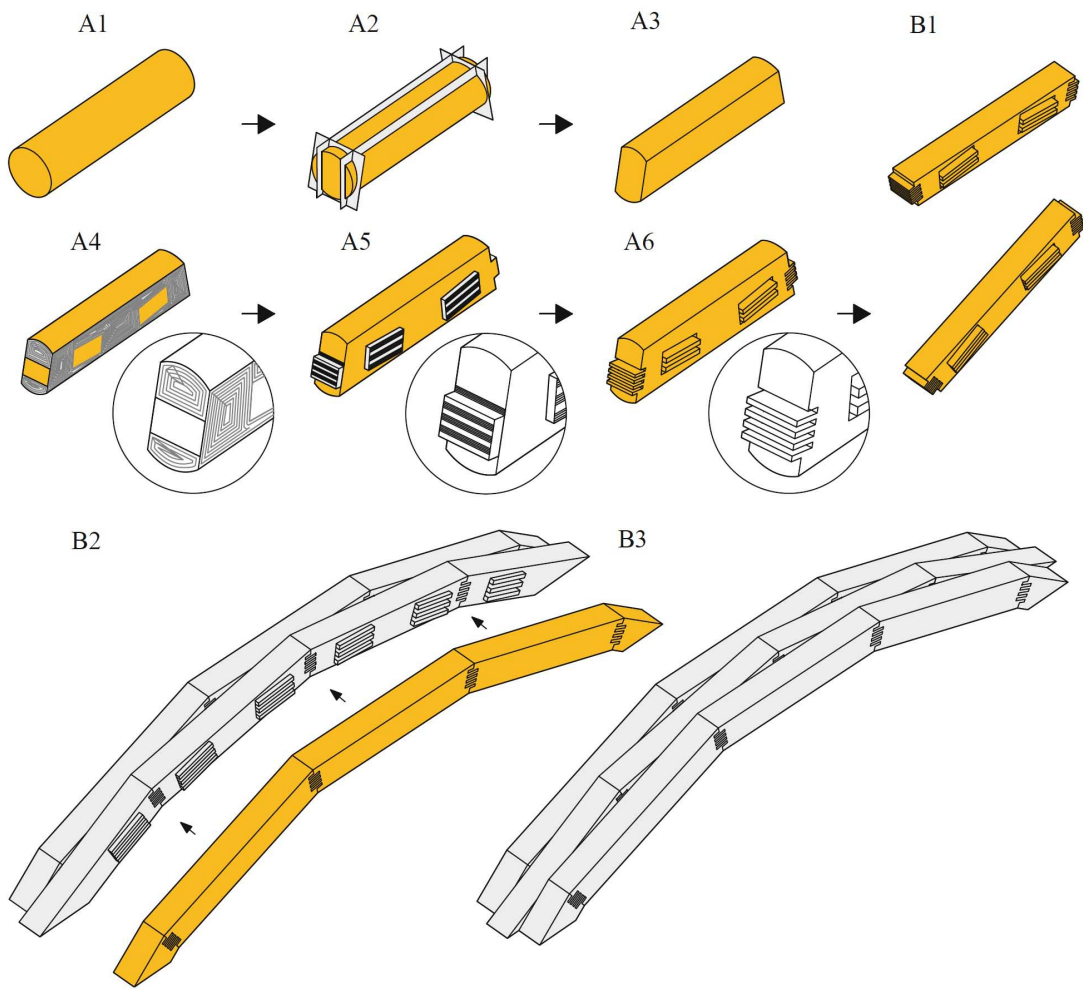


Figure 8.7 – A sequence of fabrication: (a1) round-wood (a2–a3) circular-saw (a4-a5) milling (a6) target geometry. Assembly: (b1) an arch, (b2) arches, (b3) prototype.

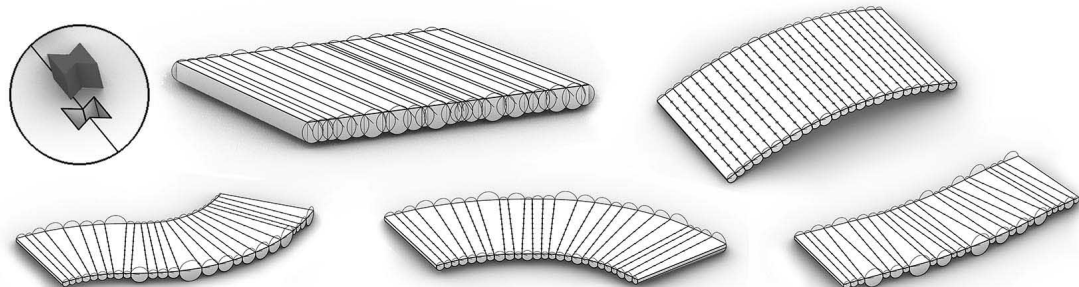


Figure 8.8 – Slab system by stacking solid lumber side-by-side.

tion of the neutral-axis of each row of elements (see Figure 8.9 C), the bisector line allowing to maximize the size of the joint placed in the shared area of adjacent timber blocks. Lateral finger joints are generated by subdividing each rectangle and alternately extruding the stripe in and out of the element (see Figure 8.9 D-E). The divisions within the joints is based on the

CNC machining constraints. Finally, a Boolean operation is used to merge lateral joints with the rest of each element. The fabrication method required two different cutting steps: first saw-blade removed large pieces wood and then surfaces were milled using 14 mm diameter drilling tool (see Figure 8.7).

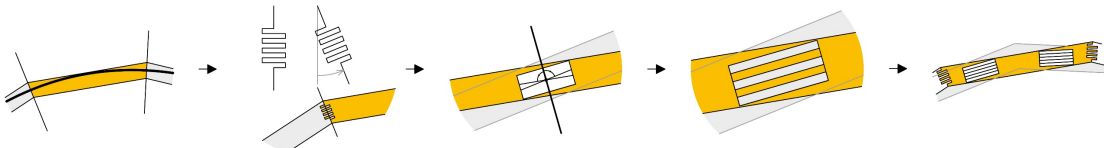


Figure 8.9 – A sequence of modelling steps: a) curve interpolation, b) Butt joint, c) intersection area, d) lateral connection, and e) full model.

## 8.5 Results

### Outlook of the Methodology and Prototypes

The proposed modelling framework was applied for a series of free-from surfaces ranging from low-resolution and high-curvature (see Figure 8.5 A-B) to high-resolution and low-curvature geometries (see Figure 8.5 C-D-E). The shift between polyhedrons is inevitable but acceptable, depending on a Gaussian curvature. In addition, planarized and original polyhedron shapes are similar and do not have large distortions, which makes this workflow useful for our material-based exploration within a specific range of surface curvatures.

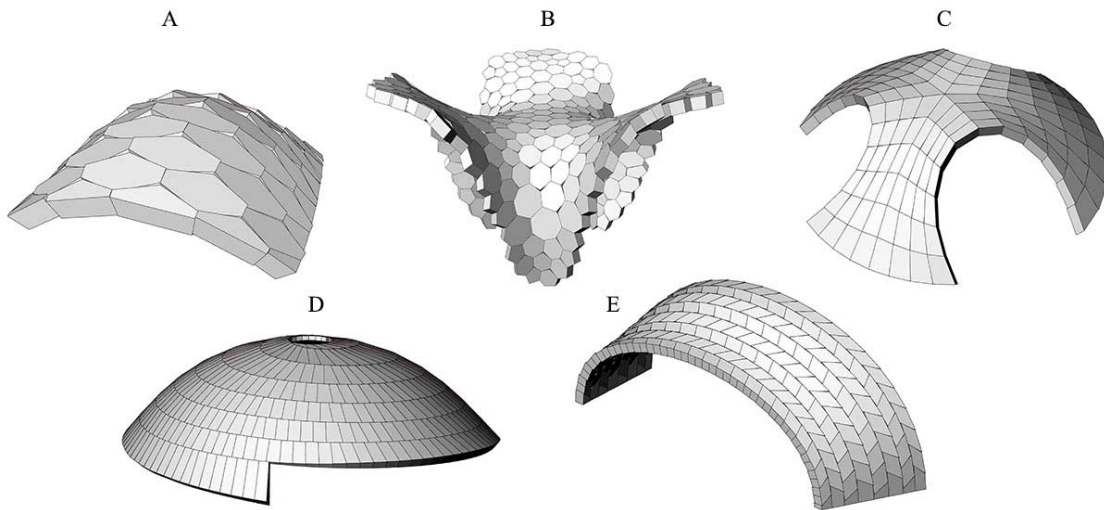


Figure 8.10 – Planarization method performed on a set of free form shapes: a) low resolution hexagonal subdivision, b–c) high-curvature mesh dual, d) dome, and e) low Gaussian curvature.

Two prototypes were made using this modelling framework (see Figures 8.14 - 8.17). While the underlying geometry of both study cases were similar, we used different CNC fabrication approaches. The plate model was fabricated using CNC cutting while the round-wood specimen required a combination of tools (saw-blade, milling and drilling) and an additional rig for lifting the trunks. Both models were assembled manually with the arch resting on one side so that the elements could be easily assembled on top of each other sequentially. Upon the completion of the assembly the whole specimen was lifted and rotated by 90° to its intended position.

A geometry mesh library was made for this polygonal surface discretization workflow. It is based on triangle meshes that are grouped to N-Gon representation. The library contains Mesh adjacency queries, subdivision, transformation and planarization methods applicable not only for this material-based research. Finally, a G-Code library was made to translate the CAD geometry to CNC tool-path such as two open-polyline cutting, surfacing, u-shape saw-blade cutting and collision detection simulation. The tool-path was verified by fabrication tests to avoid damaging tools or de-calibration.

### Challenges in Scaling

Currently, the research is focused on an industrial transfer of a full-scale building application. The project includes a free-form roof made from hexagonal components which was accepted by local municipality (see Figure 8.11). Several geometrical and structural issues have to be addressed for the future development: assembly methods such as element by element, arch by arch or clustering, roof cladding based on the local carpentry methods, facade detailing, supports. Since the study is currently performed in a research environment, the methodology needs to be transferred to the local fabricator. The material characterization for the spruce is performed by non-destructive testing for 1 m<sup>3</sup> of planks, but further destructive analysis is needed.

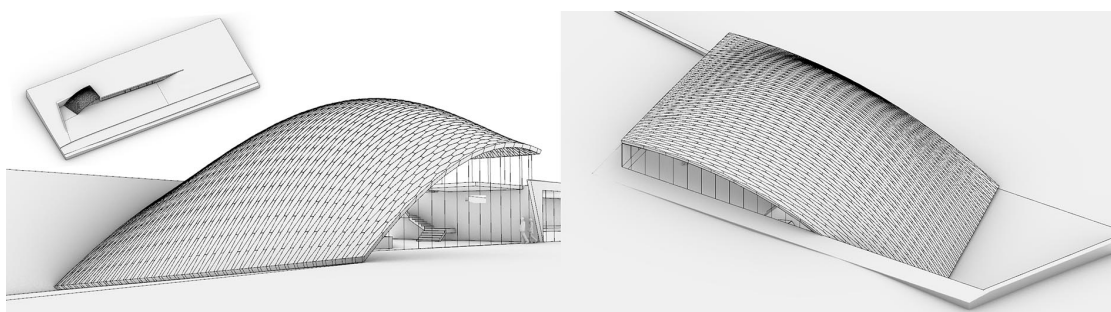


Figure 8.11 – Shell structure composed, from solid hexagonal elements.

## Chapter 8. Side-to-side Joints for Shell Structures

---



Figure 8.12 – Assembly of one box from a series of timber boards. The timber boards form one hexagonal box component.

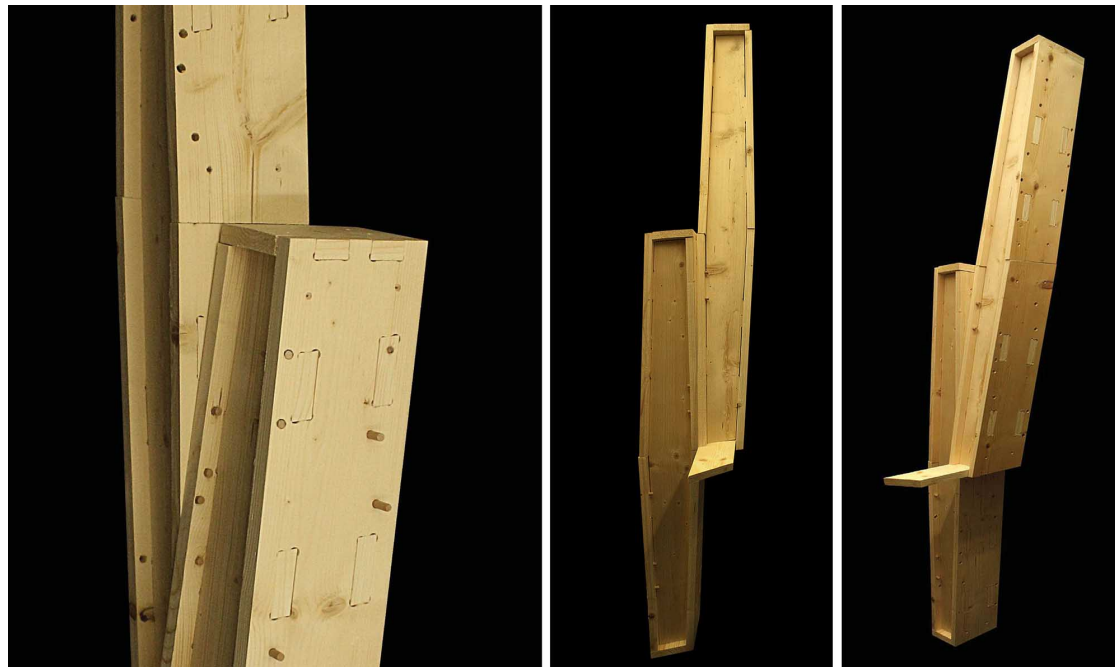


Figure 8.13 – The box components are connected using wooden dowels. External connectors are needed due to perpendicular grain direction.

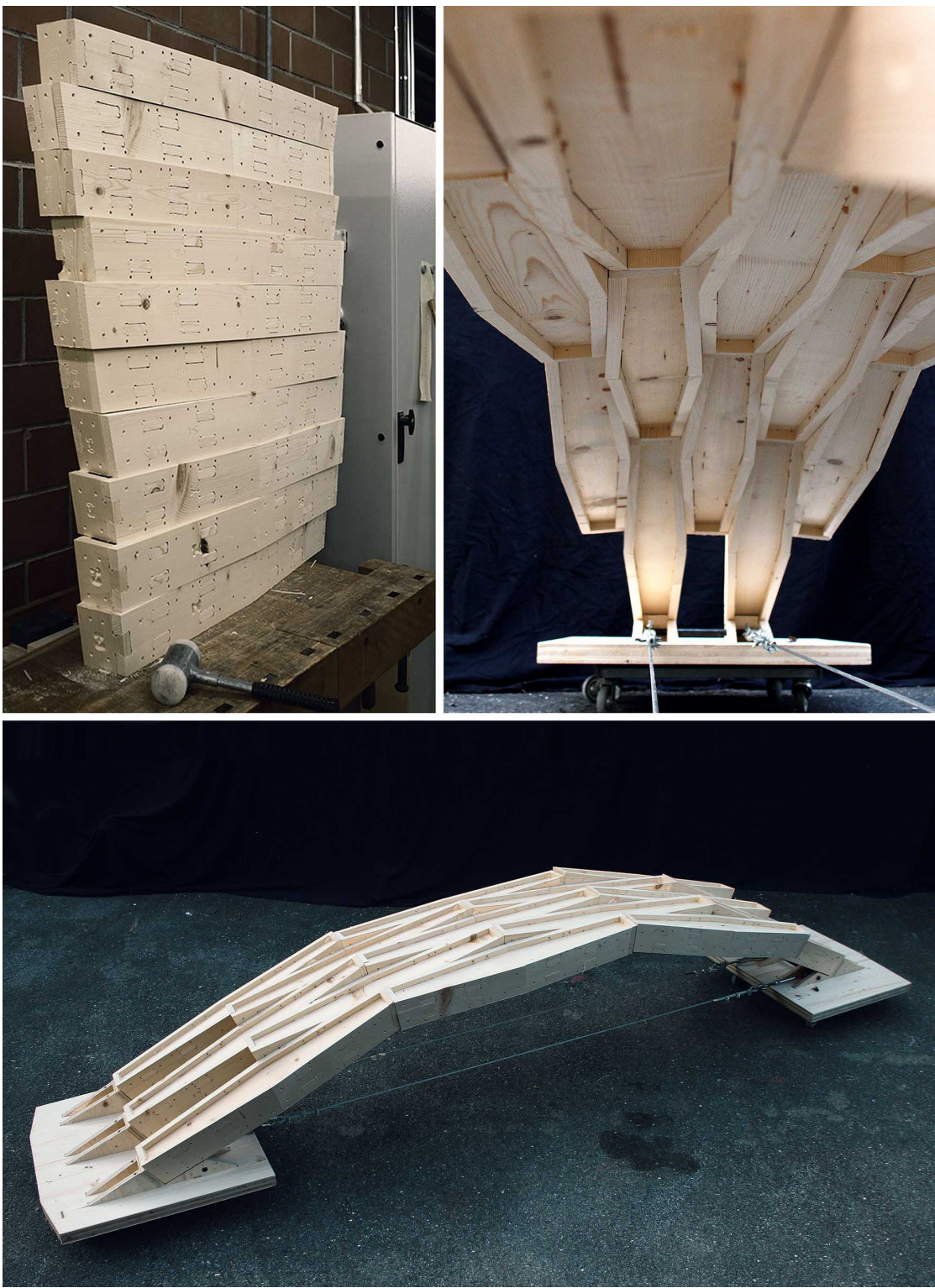


Figure 8.14 – An arch prototype is made from fifteen box elements and custom supports for the connection to the base.

## Chapter 8. Side-to-side Joints for Shell Structures

---

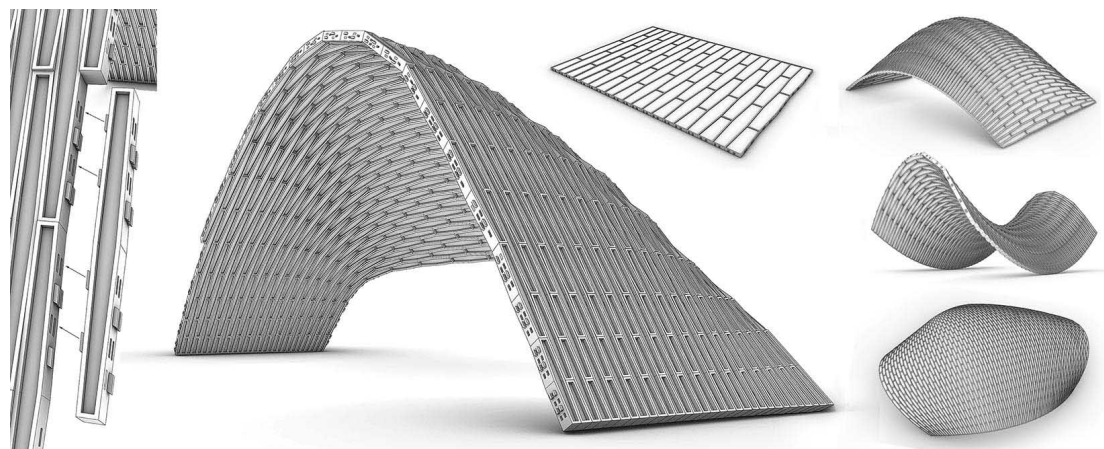


Figure 8.15 – Box component employing through-tenon finger joints. This option was discarded not only due to fibre discontinuity but also the maximum width of a timber board.

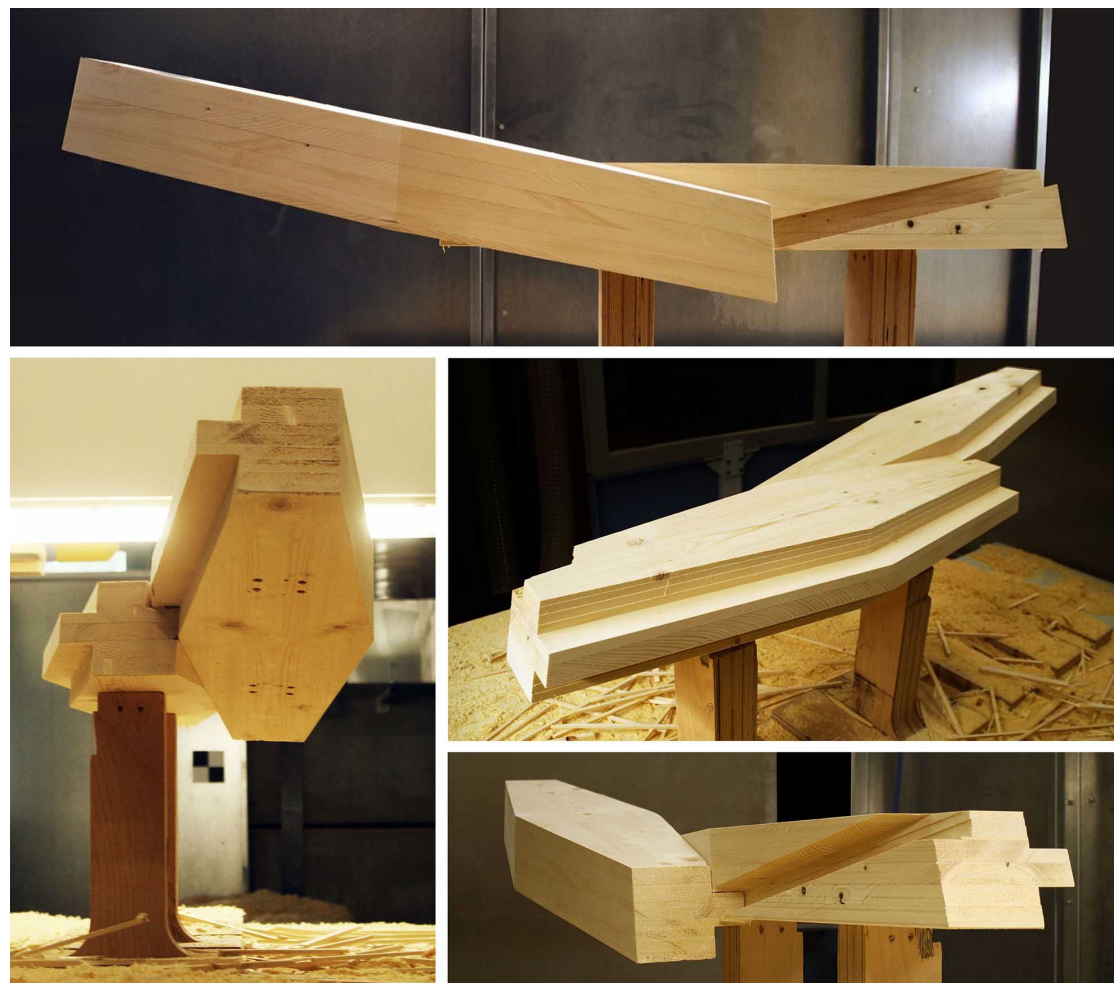


Figure 8.16 – A groove joint interconnecting two solid elements.

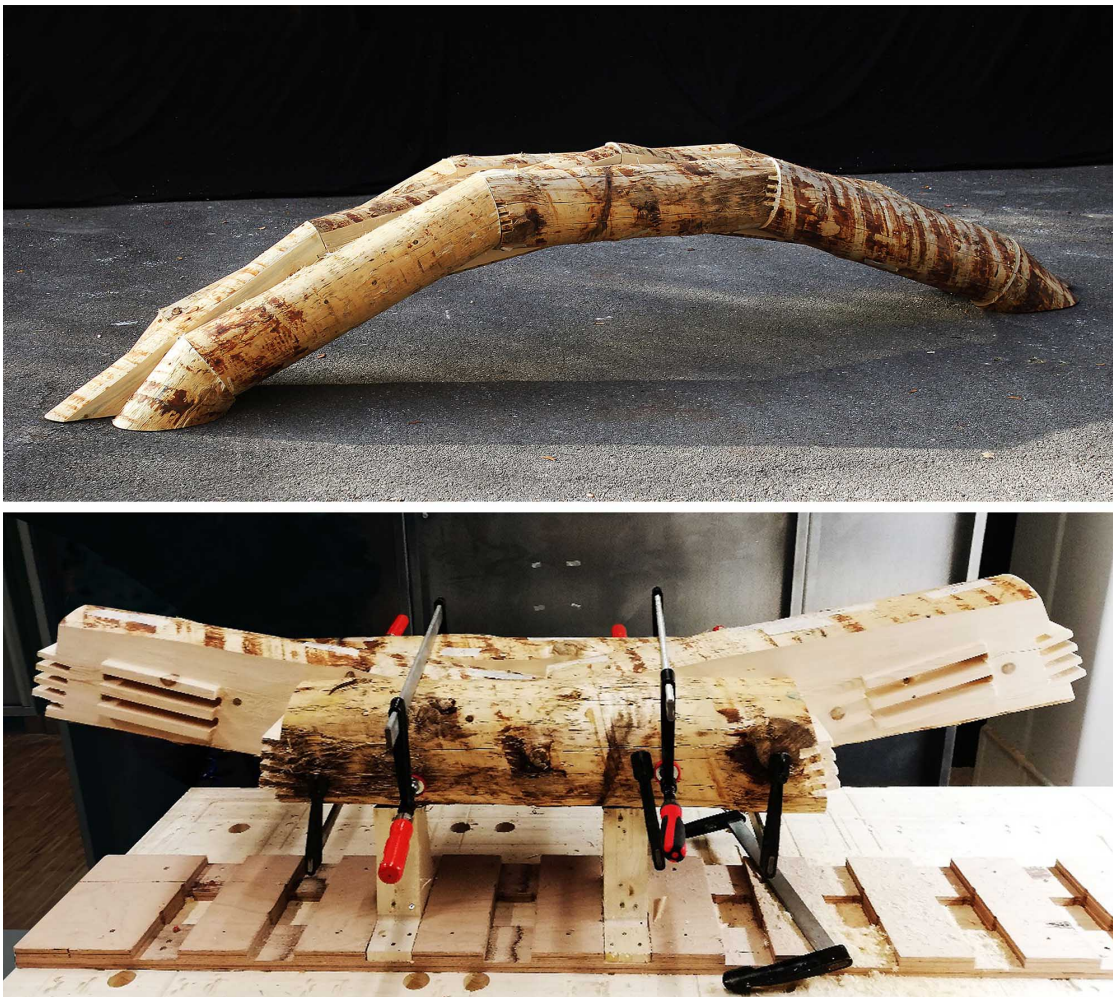


Figure 8.17 – Arch prototype made using raw-timber.

## 8.6 Conclusion

The present study shows a series of experiments based on a vault discretization. The aim of this workflow is to consider the actual shape of local wood stock, the discretization of a design target, the assembly sequence, joinery generation, 3D model representation and tool-path generation. In addition, an interoperability issue is avoided when two models were successfully executed within one software framework from graphical representation to CNC cutting. The physical model, that was made from planks has a fluent setup when the 3d model and the tool-path are modelled equally by a pair of polylines, while the round-wood prototype took more time to prepare the cutting tool-path, thus require more investigation.

There is a series of sub-topics that could be addressed in a more detail such as joinery, assembly logic (BFS), tool-path development and the collaboration frame-work with industrial partner for a full scale application. The assembly logic and configuration of joinery are highly

## **Chapter 8. Side-to-side Joints for Shell Structures**

---

interlinked, since the joint orientation follows the direction of insertion. Also, larger assemblies have to be taken into account to understand how clusters of components could be assembled and what connection methods could be applied at boundary condition.

The most constrained part when working with timber from local forests is that it is strongly direction dependent. It requires specifying the wood joinery according to the fiber direction which limits the geometry exploration within the surface subdivision approach. We are aware that timber in its natural form points to timber frame assemblies when joints are positioned at each end of a beam, else-wise additional connectors are required such as screws, dowels or keys.

The global scope is the development of a methodology based on a performative use of the raw sawn timber available in the local forestry to increase the use of timber biomass. The economical consideration is related to forest investigation that shapes and defines the input library for the modelling workflow. It contributes as a study case based on a material given by the research partner. It is an economical and sustainable reasoning where geometrical exploration is applied for a combined chain value.

# 9 Raw wood Cross and Top-to-side Joints for Nexorades

---

This chapter is based on:

P. Vestertas, A. Rezaei Rad, and Y. Weinand. Robotically-Fabricated Nexorades from Whole Timber. *International fib Symposium on the Conceptual Design of Structures*. Switzerland, 2021.

---

## 9.1 Foreword

This chapter presents a workflow for systematically generating Nexorades using tree-driven round woods. The system is designed based on an integrated framework combining resources from local forestry, knowledge from geometry processing, joinery of round woods, laser scanning and digital fabrication. Particular focus is given to Cross and Top-to-side joint geometry. Also, the global structural performance of the system is assessed. The results indicate that the proposed design methodology can offer an efficient and sustainable construction technique. The methodology is reflected in a demonstrator for testing the proposed methodology.

Inspired by digital fabrication, the aim is to foster bio-based timber construction using tree-driven round woods in reciprocal structures. Employing wood-wood connections with external fasteners, the proposed framework embraces sustainability in building technology and enhances the digitalization of infrastructure. In particular, the goal is to embed timber, in its natural form, in spatially-optimized Nexorades that can offer a new conceptual design perspective. The methodology has four main parts: a) global geometry generation, b) local joinery generation, c) structural analysis, d) laser-scanning and robotic fabrication. Accordingly, the system is designed based on an integrated framework combining resources from local forestry, Computer-Aided Design (CAD) for geometry manipulation, joinery of round woods, virtual scanning, digital fabrication, and Computer-Aided Engineering (CAE) and numerical simulations.

Raw wood Cross and Top-to-side Joints for Nexorades chapter is structured as follows:

- Section 9.2 Introduction to Nexorades using raw wood
- Section 9.3 Description of a tiling method for generating Nexorades
  - Linear Pattern Generation on a Quad-Mesh
  - Dynamic Relaxation of Nexorades
- Section 9.4 Fabrication of prototypes
- Section 9.5 Assignment of trees from a tree stock
- Section 9.6 Overview of results

## 9.2 Introduction

This section aims to re-read past research in Nexorades, publicly available only in a written format, then replicate the work and open-source it for educational purposes. The open-sourcing is performed using the polygonal mesh processing framework NGon [168] developed within the 3d modelling software Rhinoceros3D [138]. Nexorade bars mutually support each other as a load-bearing system. The configuration of reciprocal frames simplifies the construction system because only two members are connected at each node instead of multiple beams such as space-frames or trusses. The n-valence of one node changes to the two-valence node, where the total number of joints is equal to a single joint valence. As a result, fabrication of such nodes is more easily manufactured due to the low valence connectivity (see Figure 9.1).

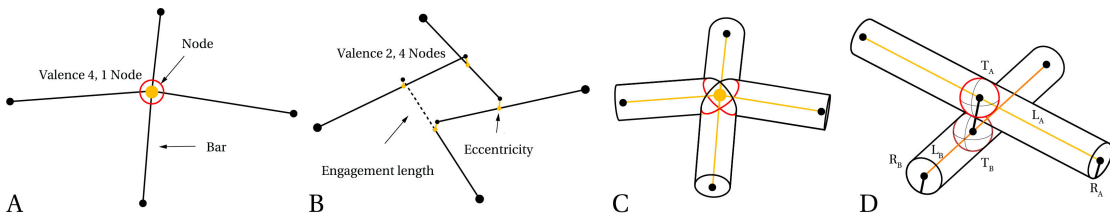


Figure 9.1 – Node valence: a) a 4-valence node, b) a 2-valence node in 4 joints, c-d) joint connectivity using a series of cylinders representing raw timbers.

Key features of Nexorades according to [20] are:

- Nexors of a Nexorade can have identical length and cross-section.
- By varying the engagement length, different sizes of Nexorades can be built using the same basic configurations.
- Nexorades have only one type of joint that connects only two Nexors.
- None of the components requires complex fabrication technology.

Nexorades could be controlled by a series of interconnected geometrical parameters such as rotation or translation of an engagement window, bar length and curvature of a target shape. Several methods are proposed for form-finding of Nexorades:

- Genetic algorithms [19].
- Dynamic relaxation [122] in a double layer system [40] and a non-linear method that can converge to a local minimum but do not converge to a global minimum [102].
- Analytical solution by rotation edges of a regular polyhedra [147]
- Analytic translation of regular polyhedra [20].
- Soft constraints method for eccentricities to perform iterative least-square optimization for form-finding of Nexorades [156].

Besides platonic objects (cubes, tetrahedra, icosahedra) and planar tiling, no theoretical results have been found for curved geometries (see Figure 9.2). The form-finding of Nexorades requires efficient non-linear solvers that do not provide any certainty about their output. Also, the mathematical models do not apply to structures in raw wood due to natural irregularities, thus the form-shaping processes described before are not entirely viable for raw wood.

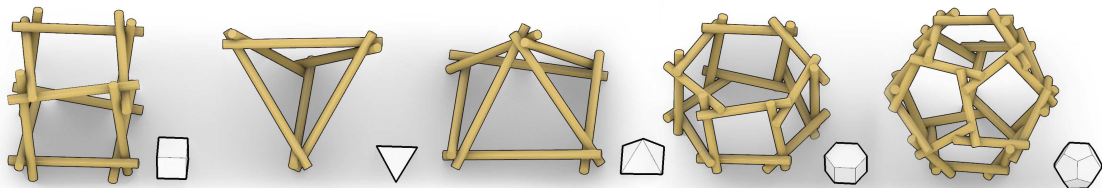


Figure 9.2 – Nexorades applied to platonic objects by rotating Mesh edges.

The cladding of reciprocals has to be addressed too. Before mentioned projects are either covered with membranes, uncovered, or employ timber panels. Covering Nexorades with panels is a challenge that could open new possibilities. The cladding could be used as a bracing system to transform the linear beam model into a shell-structure.

There are two possible connection methods: a) cross-halving connection (see Figure 9.3), and b) a side-top connection (see Figure 9.8). The joints reflect the critical difference between regular and irregular lumber: industrialization of timber tries to regularize wood to simplify and uniform the fabrication of wood-wood connections, whereas irregular lumber needs to adapt a design of a joint and a raw wood shape that is not fully known. For this reason, angle cuts are made on each side of a joint. Even if the scanning gives information about a tree surface's qualities, the joinery methods must follow a low-resolution model notation to guide the robotic fabrication.

The flexibility of Nexorades restricts the scalability of these type of structures. Additional bracing of cables or panels or a double-layer system could improve the structural performance of Nexorades. The further analysis of shell-Nexorade advances on previous research in shell Nexorades [102] by extending the method to hexagonal patterns (see Figure 9.5). The rule for modelling shell-Nexorades is equal to solving a graph colouring problem resulting in two colours, such as a checker-pattern. Elements in these tilings have to be composed of even numbers of edges.

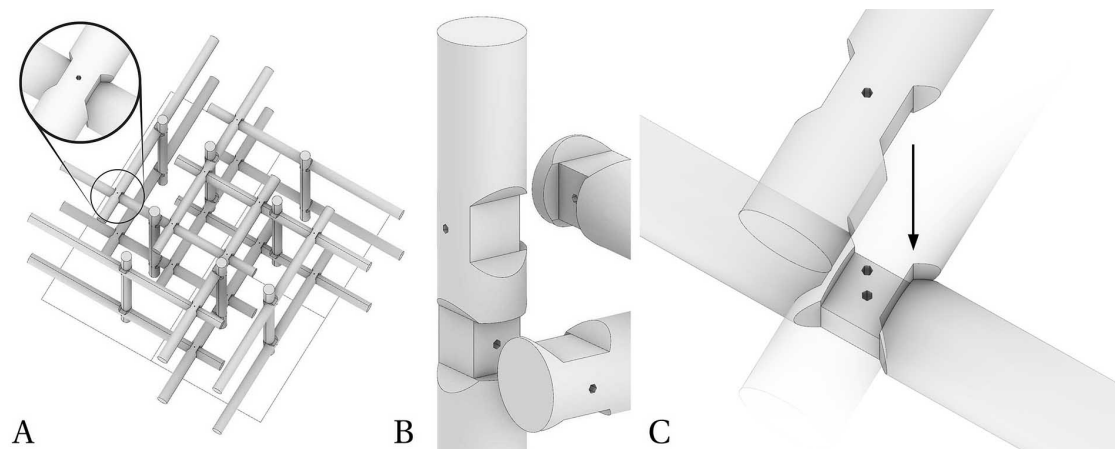


Figure 9.3 – Quad reciprocal model using cross connections.

The Nexorade, in a single plane translation (see Figure 9.4), requires even more complexity in fabrication comparing to the joinery in standardized lumber. Nevertheless, timber structures that can afford such transformation through CNC fabrication (see Figure 9.5). The top part of a beam has to be milled to gain one continuous surface due to the eccentricities of Nexors. This profiling is both decorative for hiding the shift of beams due to curvature. Additionally, a single line groove is made to connect panels with beams that also explains the edge eccentricity between panels.

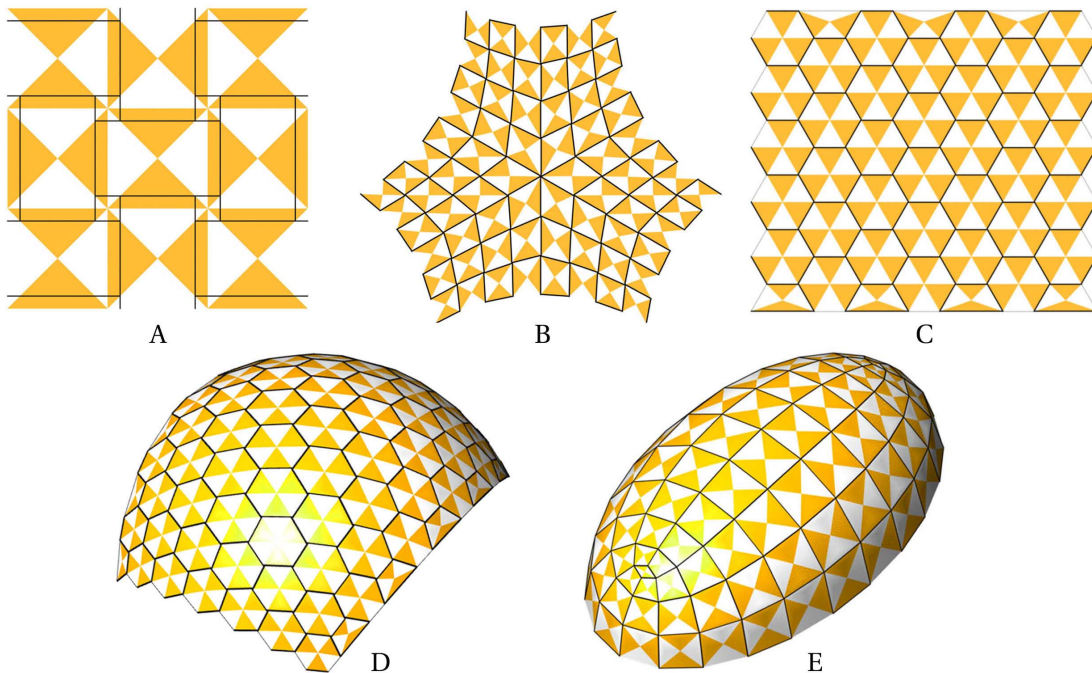


Figure 9.4 – Translation method: a) a square grid, b) a square grid with a singularity, c) a hexagonal grid, d) a mixed grid with hexagons and quads, and e) a quad grid with two singularities.

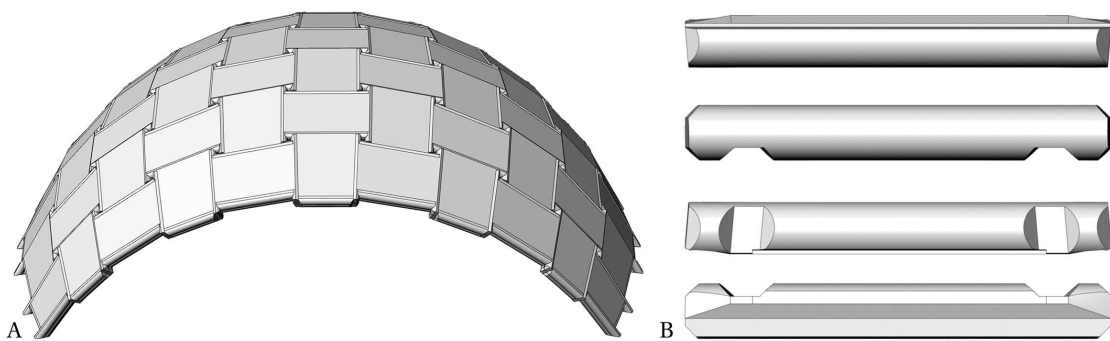


Figure 9.5 – Shell structure developed using a translation method (a), detailing of a beam (b).

The studied quad Nexorade follows a form-finding of conical meshes (see Figure 9.7 A). The translation of beams has to be as minimal as possible to reduce eccentricities. The movement of each beam could be individually controlled to optimize the eccentricities depending on a surface curvature (see Figure 9.7 B). The conical surface is form-found using a constraint based solver [122] that helps to adapt to additional constraints such as a ground-level (see Figure 9.7 C-D). Lastly, a single and double-layer system is detailed as Figure 9.7 E-F.

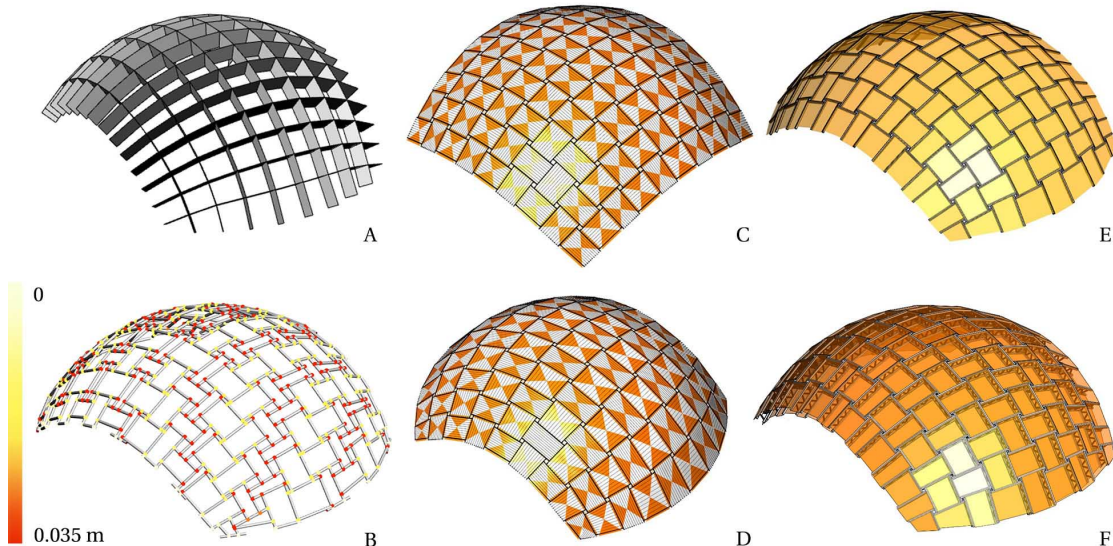


Figure 9.6 – Form-finding of the translational Nexorade: a) conical extruded meshes, b) individual bar translation option, c) checker pattern to cull mesh edges, d) extension to the flat level, e) a single, and f) a double layer system.

The fabrication is made using a 5-axis CNC machine. An individual beam is fixed to a timber rig that allows machining from three sides of an element (see Figure 9.7). The cutting process involves the following steps: a) top surfacing using a saw-blade, b) pre-drilling dowel holes, c) chamfering ends of beams to hide eccentricities, d) milling side-end connections, e) saw-blade bisector cuts, and f) pre-drilling for screws.

## Chapter 9. Raw wood Cross and Top-to-side Joints for Nexorades

---

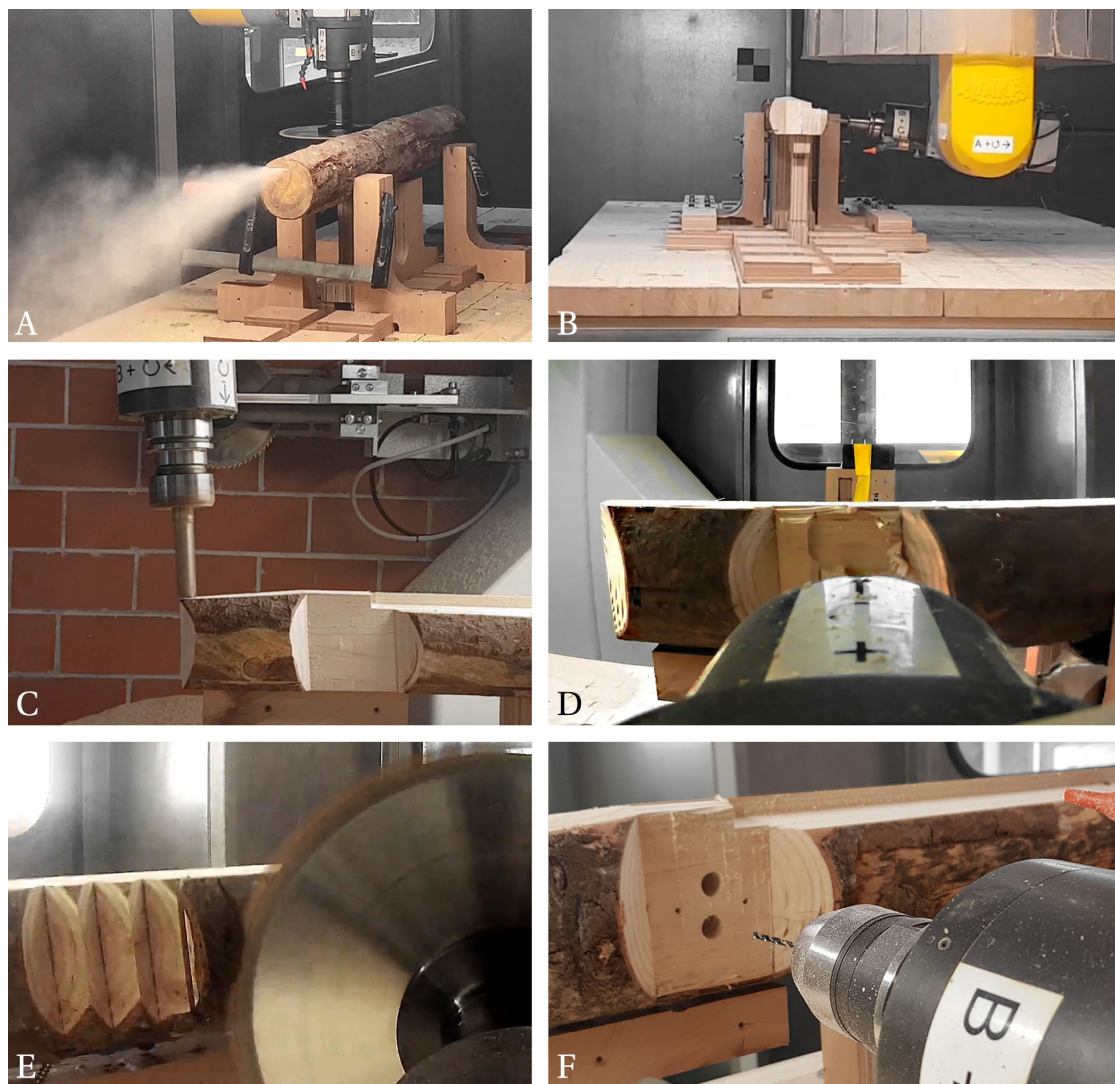


Figure 9.7 – Fabrication process of an individual beam: a) top surfacing, b) dowels holes, c) milling eccentricities, d-e) different fabrication methods for side-to-end joint, and f) pre-drilling for extra fasteners.

The assembly is blocked using external fasteners incrementally forming top-to-side connections. Four top-to-side joints form an engagement window (see Figure 9.8 A-C). There is no particular assembly sequence because beams do not employ any integral mechanical attachments. The connection is blocked by dowels. The joint is not rigid and result in a shear moment. Therefore, an additional bracing is needed such as a) extra beams for triangulation of the rectangular cells, b) cables that would not work in compression, or c) panels. The later option is chosen to fix the shear between beams using screws along each edge of the panels. The shear action between beams occurs due to the minimal connection area and "soft" timbers fasteners such as 10 mm dowels.

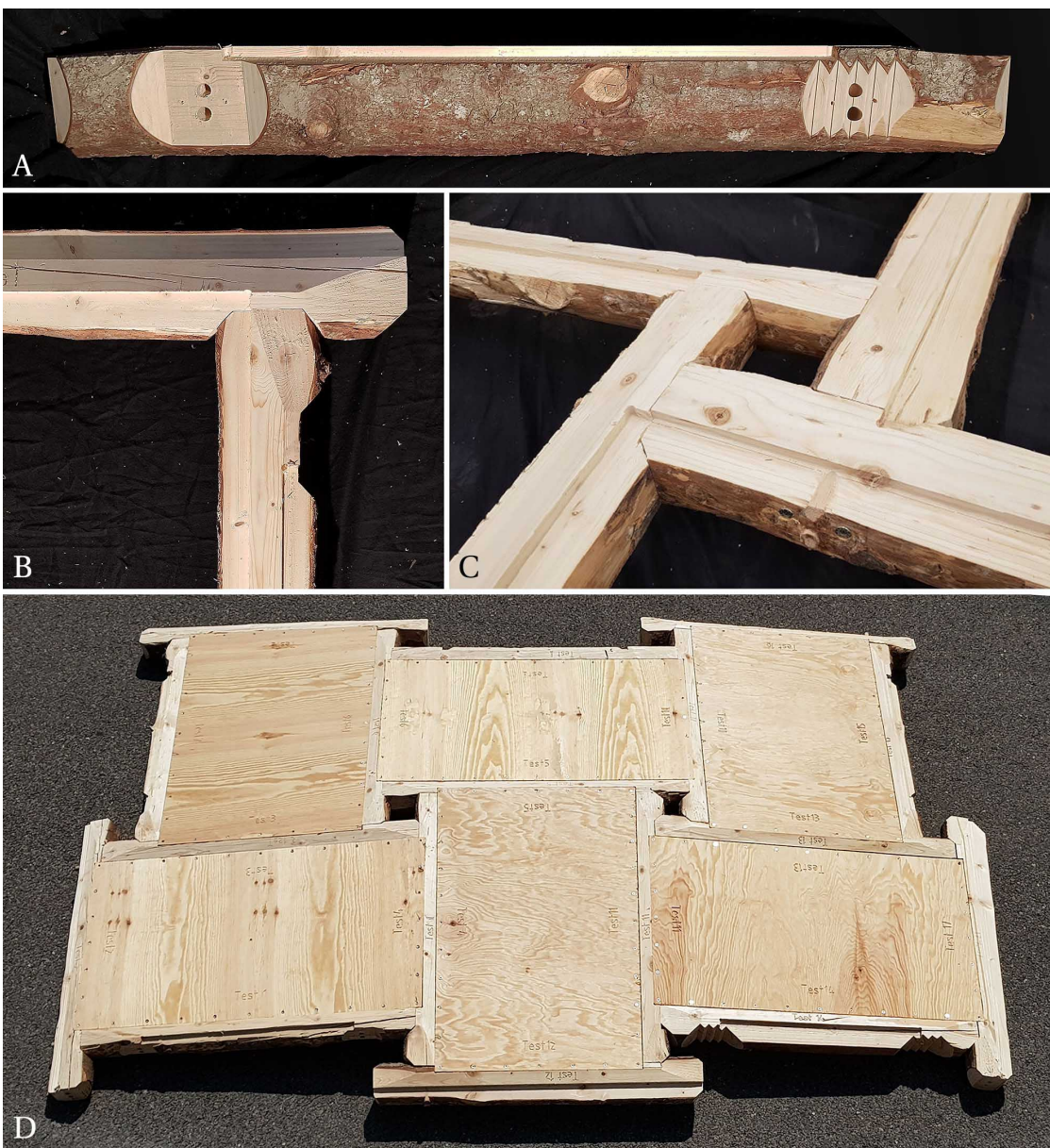


Figure 9.8 – Assembly of a raw wood Nexorade: a) two types of side-to-top joints and a groove to fix a timber panel, b) one assembled connection, c) four side-to-top joints forms an engagement window, and d) a prototype with attached panels.

### 9.3 Workflow for Nexorades in Raw Timber

The second workflow tackles a double-layer Nexorade system. The design methodology starts with a quad-triangle mesh transformation to a Nexorade pattern. An assumption is made that Nexorade patterns can be generated from quad meshes composed of tessellated patches. Given such a geometry, it is possible to map the beam-like geometry from XY plane to Mesh faces. Afterward, the tiled faces can be connected to individual bars representing a tree trunk. The method proposed herein contains indexing, adjacency, eccentricities, and volumetric geometry generation methods. The dynamic relaxation method is also performed based on the elements' eccentricity to obtain a minimal connection area. One of the main features of the methodology is that every beam can have zero length eccentricity. The zero-tolerance constraint is not obtainable because each tree is different and has natural imperfections such as tree knots. Instead, it follows a rule of not exceeding two-thirds of a beam section [29] to have a good contact surface between beams. Then, each connection node employs a traditional wood-wood cross-lap joint. The joint is a geometric feature for visualization purposes and a tool-path for robotic fabrication as one entity. The reason to connect machining with geometry generation is due to possible collision errors during fabrication. The resulting data structure is then transformed into an open-source computer-aided engineering platform for structural analysis. The global structural performance of the system is assessed. Physical tests are performed utilizing ABB IRB 6400R robotic arm and Faro Focus S 150 laser scanner in terms of fabrication. The machining method employs scanning to accurately recognize timber trunks in machining space and select the best fit tree trunks from a timber stock. Visual recognition is needed because timber trunks vary from one beam to another within the shape and position when mounting timber on a fabrication rig [171]. Finally, the methodology is reflected in a recently-designed prototype, which demonstrates that the design framework.

#### Linear Pattern Generation on a Quad-Mesh

The tiling method aims to obtain a principle pattern representing the Nexorade system using a finite set of tiles [168] as Figure 9.9 F. The tiles' finite set consists of nine tiles drawn as a polygon unit measuring 1x1x1 containing line segments. These line segments represent a part of the Nexorade beam where each side of the polygon is numbered. Colors are used to visualize the indexing to track adjacency between the edges as Figure 9.9 A. The sides of the polygon are indexed to identify the rule-set as Figure 9.9 B-C. This process is done to improve the visual reflection of the tiles' edges, where each triangle color represents an index. The rule-set as Figure 9.9 C (i.e. [0,1,2,3] – [3,0,1,2]) is then used to match neighbouring tiles. The structure of the tiling is computed using the mesh face-edge graph data when matching tile edges. The matching procedure is detailed in the following paragraph. Finally, the tiling workflow is applied to a particular quad-dominant mesh topology as Figure 9.9 E composed of mesh patches as Figure 9.9 D.

In the next step, the mesh has to be unified, and the tile order has to be computed before

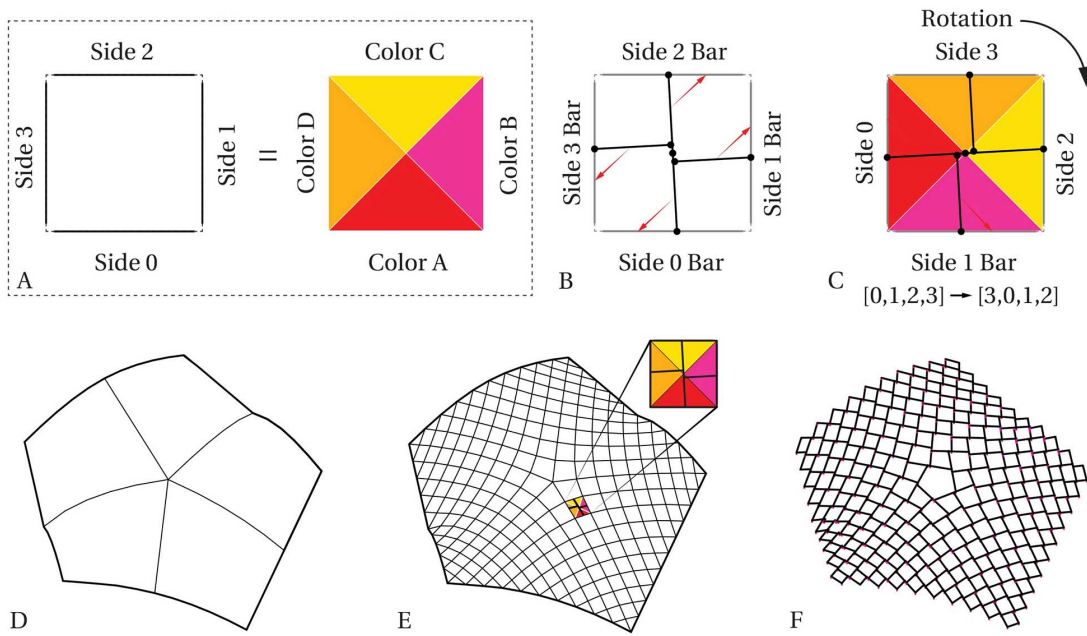


Figure 9.9 – Tiling notation: a) sides of a Tile are indexed, b) sides are colored for visualization purpose, c) each side has an associated bar element, d) Mesh topology composed of multiple patches, e) Barycentric mapping, and f) linear pattern of the mapped tiles.

the tiling method is applied. The first tile represents a mesh quad-face, and the triangular tiles are used to create the boundary faces. For the mesh generation, the neighboring edges are directed to have an opposite orientation as Figure 9.10 B. This condition is obtained by traversing mesh faces and assessing whether edges are opposite to the neighboring peer. Furthermore, the tiles are added to the mesh using the algorithm. Graph traversing algorithms such as Breadth-First-Search (BFS) are used to obtain the tiles' sequence. Such algorithms contain a sequence that indicates the adjacency of the tiles. The BFS algorithm, as Figure 9.10 C is used to traverse mesh faces because it explores all the neighbor nodes at the existing depth before exploring the nodes at the next depth level [107]. When the tiling sequence is determined, the 2D tiles, as Figure 9.10 D, are assigned to the mesh-faces according to the BFS sequence algorithm. This is done by checking whether it is possible to choose one of the nine tiles and the number of times a tile has to be rotated. The mapped tiles are colored by an index (0-9) as Fig 2 E. Furthermore, the associated edges are colored to form triangles (-1:grey, 0:red, 1:pink, 2:yellow, 3:orange) as Figure 9.10 F. This tiling method produces the Nexorade pattern obtained by duplicating, rotating, and mapping the tile-set as Figure 9.10 G.

Rotation of the tiles and their appropriate mapping are determined through the adjacency rule as Figure 9.9 C. The rule has a notation of the current-edge-index and the next-edge-index. The indexing follows 0,1,2,3 for the existing tile' face edges and 3,2,1,0 for the next tile. These numbers say that the quad must be connected, i.e., by edge 0 to the other tiles by edge 3, then 1-3, 2-1, 3-0. The edges that form the boundary are indexed as -1 and empty. The current tile and its rotation in the meshing scheme at each are shown in Figure 9.11 3. Figure

## Chapter 9. Raw wood Cross and Top-to-side Joints for Nexasades

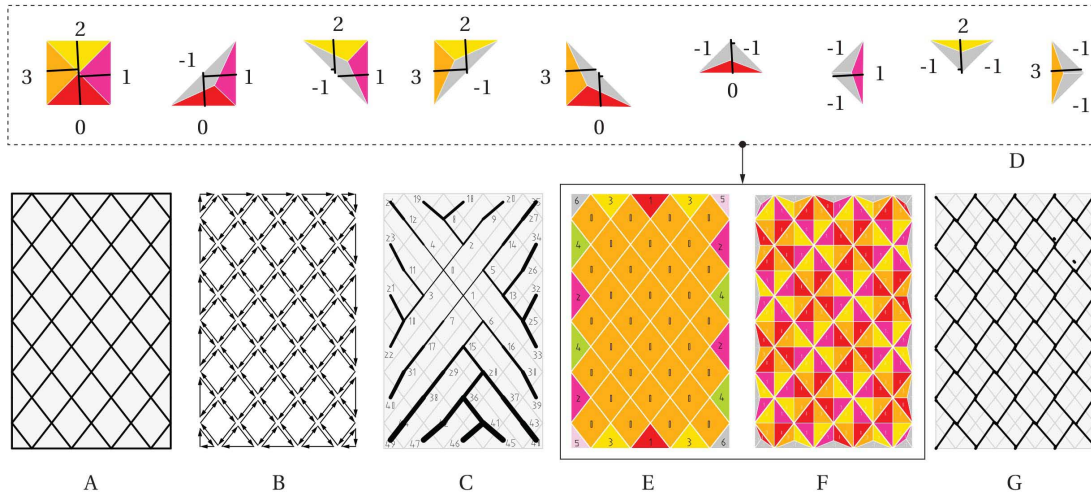


Figure 9.10 – Tiling method for a planar diamond mesh grid: a) a diamond mesh, b) a polygonal mesh with the unified edge winding, c) Breadth-First-Search, d) 2D tiles, e) Tiling, f) Tiles with colored edges that show the edge indexing, and g) pattern generated from tiling.

9.11 B illustrates a tile connected with the existing tile following the 2-1 rule (yellow-pink triangles), where index 2 belongs to the tile shown in Figure 9.11 A. Sequentially, the tile is placed following index pair 3-0 as Figure 9.11 C. Furthermore, it is possible to match several edges at once as Figure 9.11 D-E, while traversing through the BFS sequence order. To match these sequences, the algorithm compares strings and is determined as true for the tile string (3,2,1,0), if the current mesh faces are indexed as (0,1,2,x) or (x,x,x,3), or (x,x,3,0) or (x,x,x,x). If the tile has a match, then it is selected, and the number of rotations is revised to shift the array of tile-edge indices. The iteration stops when all mesh faces are checked or none of the tiles are chosen. The overall aim of applying such a procedure is to use this methodology for multiple patches where the target geometry is more complex than one rectangular surface.

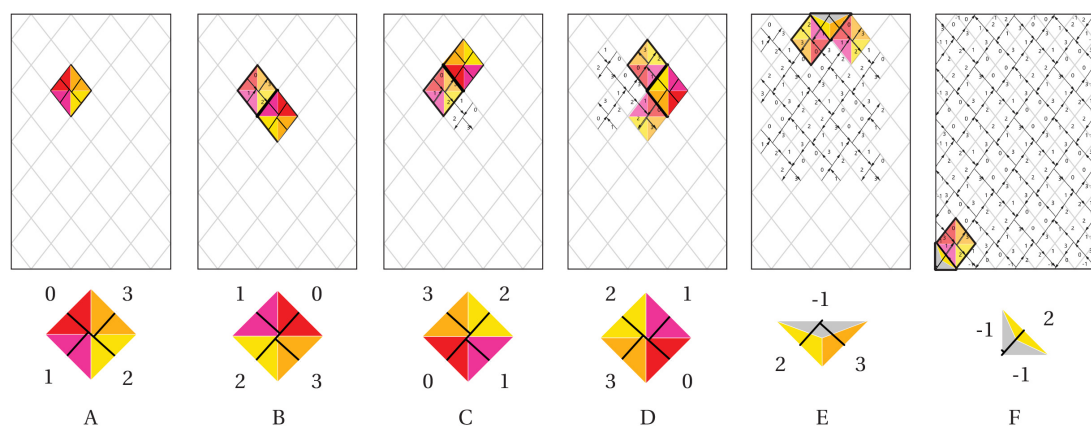


Figure 9.11 – Tiling is based on the Breadth-First-Search method: a) first tile, b) second tile and a common edge, c) third tile and a common edge, d) sixth tile, and e-f) boundary tiles.

So far, the tiles are disconnected from each other. However, they contain adjacency information to reconstruct the beam's geometry (see Figure 9.12). Consequently, the tiles are connected, forming a Beam data-structure containing ordered line segments, connectivity information, and axes' planes (see Figure 9.13). Tiles are transformed into individual beams by converting the tile's sides into an undirected graph. Subsequently, the connected component method is applied to identify the interconnecting beams. Thus, the connected components are simplified as lines, where the corresponding orientation depends on the sum of the mesh face's normal vectors of the tiles. The axis perpendicular to the plane is determined for each beam. The line axis is trimmed between the ends of two neighbouring planes. The tiling sequence and the resultant volumetric geometry are tested to correspond within a set of meshes within multiple singularities, including open and closed geometries, as Figure 9.14.

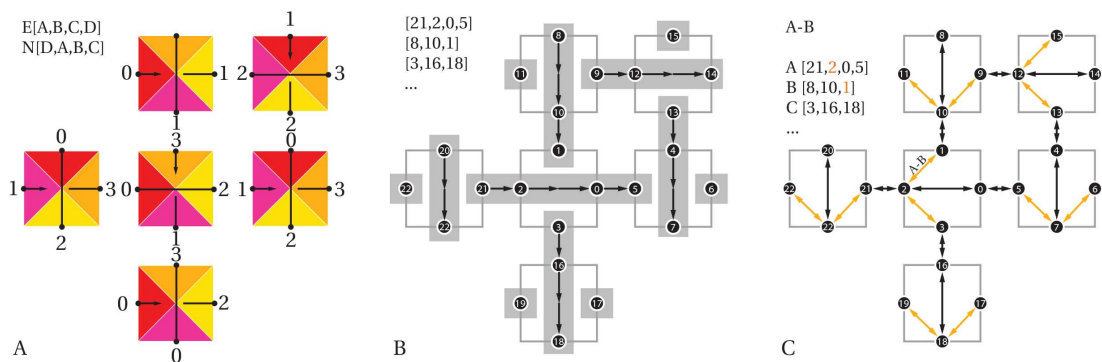


Figure 9.12 – Tiling based on Breadth-First-Search: a) first tile, b) the second tile and a common edge, c) third tile and a common edge, d) sixth tile, and e-f) boundary tiles.

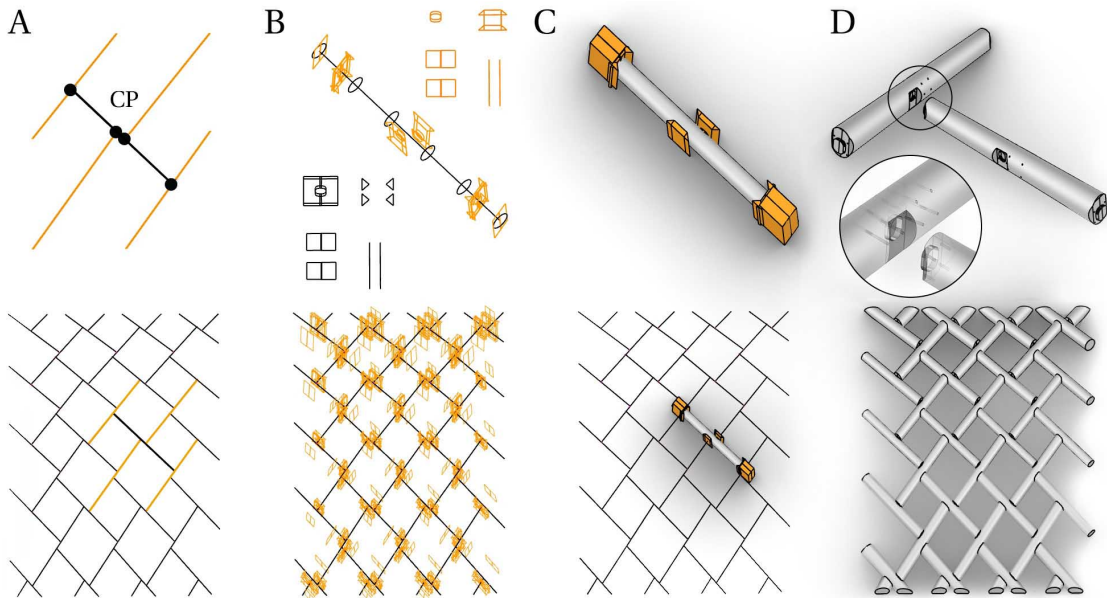


Figure 9.13 – Tiling workflow: a) elements and their adjacency, b) joinery fabrication data, c) boolean operation for solids, and d) the resultant geometry for a display.

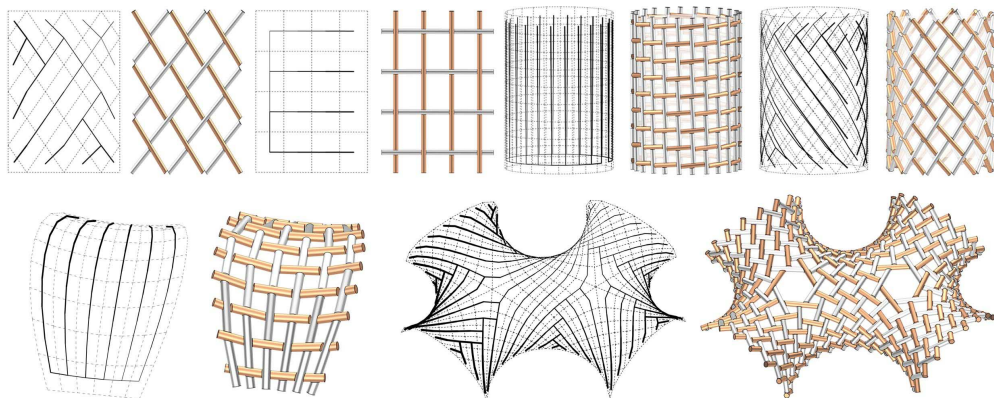


Figure 9.14 – Visualized Breadth-First-Search (left) and geometry output (right).

### **Dynamic Relaxation of Nexorades**

Connection zones between beams in Nexorades depends on a mesh curvature, the thickness of elements, rotation of a tile, and the Eccentricity between beams. If the distance between a pair of elements is too large, then the area to connect the two is not sufficient. Consequently, either the mesh topology has to be changed, or the distance between bar elements must be reduced. The eccentricities' minimization goal is used, employing a constraint-based solver [39, 122]. In the current study, the dynamic relaxation reduces the maximum deviation between beams, as Figure 9.15. Tessellated geometries with a changing curvature mostly have different eccentricities. Therefore, dynamic relaxation aims to reduce or equalize the interval of eccentricities to a given limit, e.g., less than one-third of a given raw-wood diameter. Consequently, the joinery generation adapts to each joint scale depending on a mesh curvature, as Figure 9.15.

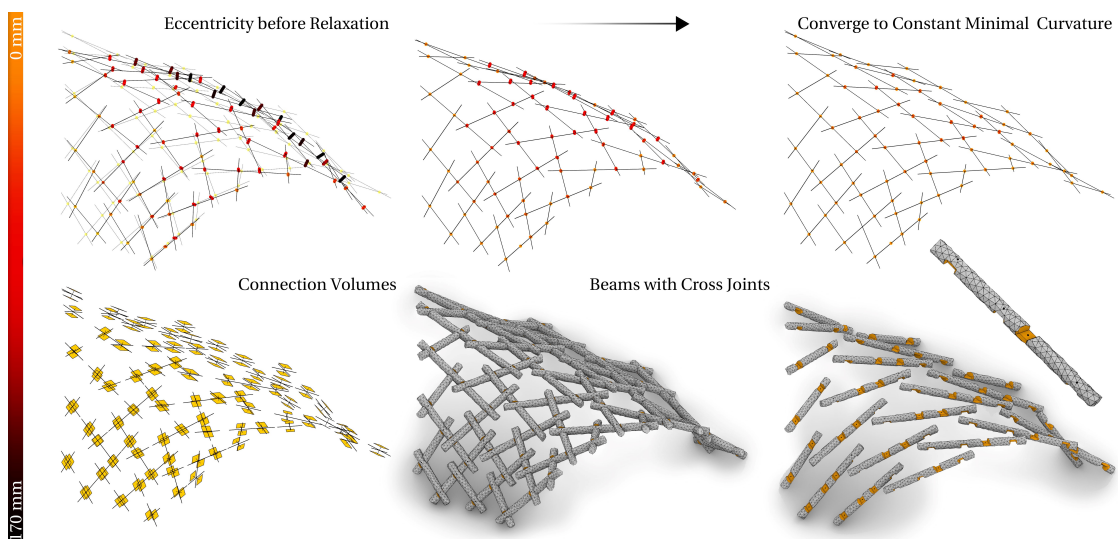


Figure 9.15 – Top – dynamic-relaxation of central axes to minimize and equalize eccentricities. Bottom – joinery generation at the lowest eccentricities and the connections cut-outs.

## 9.4 Prototypes

Two main algorithms are used in the conceptual tiling method to obtain the Nexorades pattern: a) cross cuts when joints are intersecting within less than two-thirds of the timber section and b) side-to-top connection, which refers to Zollinger systems when beams are in-plane to each other. The current research explores the first option of a cross joint. The digital joinery generation follows timber joinery existing in regular rectangular structure, and it applies this methodology to round sections (see Figure 9.16).

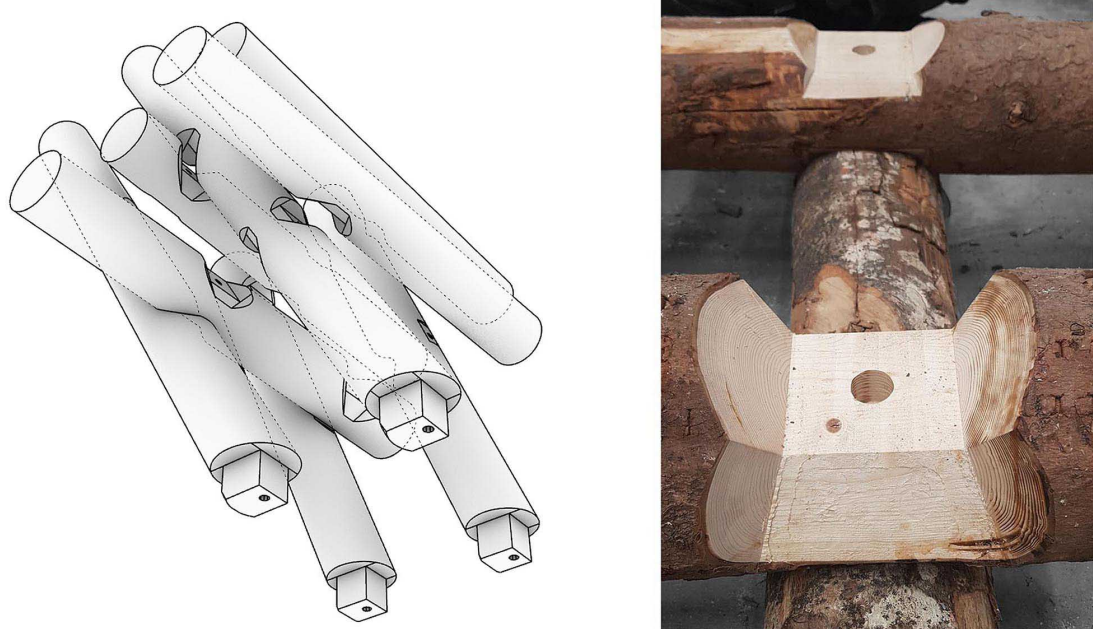


Figure 9.16 – Cross-lap joints for 8 element prototype (left). Fabrication of joints shows varying eccentricity between beams (right).

Raw timbers are not generally straight or regular in shape and section, but they stay relatively constant within the connection zone. Also, the definition of joints relies on fabrication tools and their movement relative to a timber piece (see Figure 9.17). The milling tool is limited to its flat cylindrical movement, whereas the saw blade is constrained within the flat surface area resulting in rectilinear cuts. Due to timber irregularities and requirements to have as much contact area as possible, a conical timber joint is proposed. The joint is generated using a Joinery Solver that can adapt to various design geometry angles and add necessary fasteners to interlock the cross joint. For more information refer to Joinery Solver chapter, the Cross joint section.

The cutting process requires a scanning methodology because timber shape and location vary from element to element, and at least a few cm misalignment can cause issues during the assembly. Consequently, the fabrication workflows require the following steps: a) scanning and point-cloud processing to obtain timber central axis b) tool-path that is generated together with the joint geometry c) automatic tool-changer to switch between sawblade and milling.

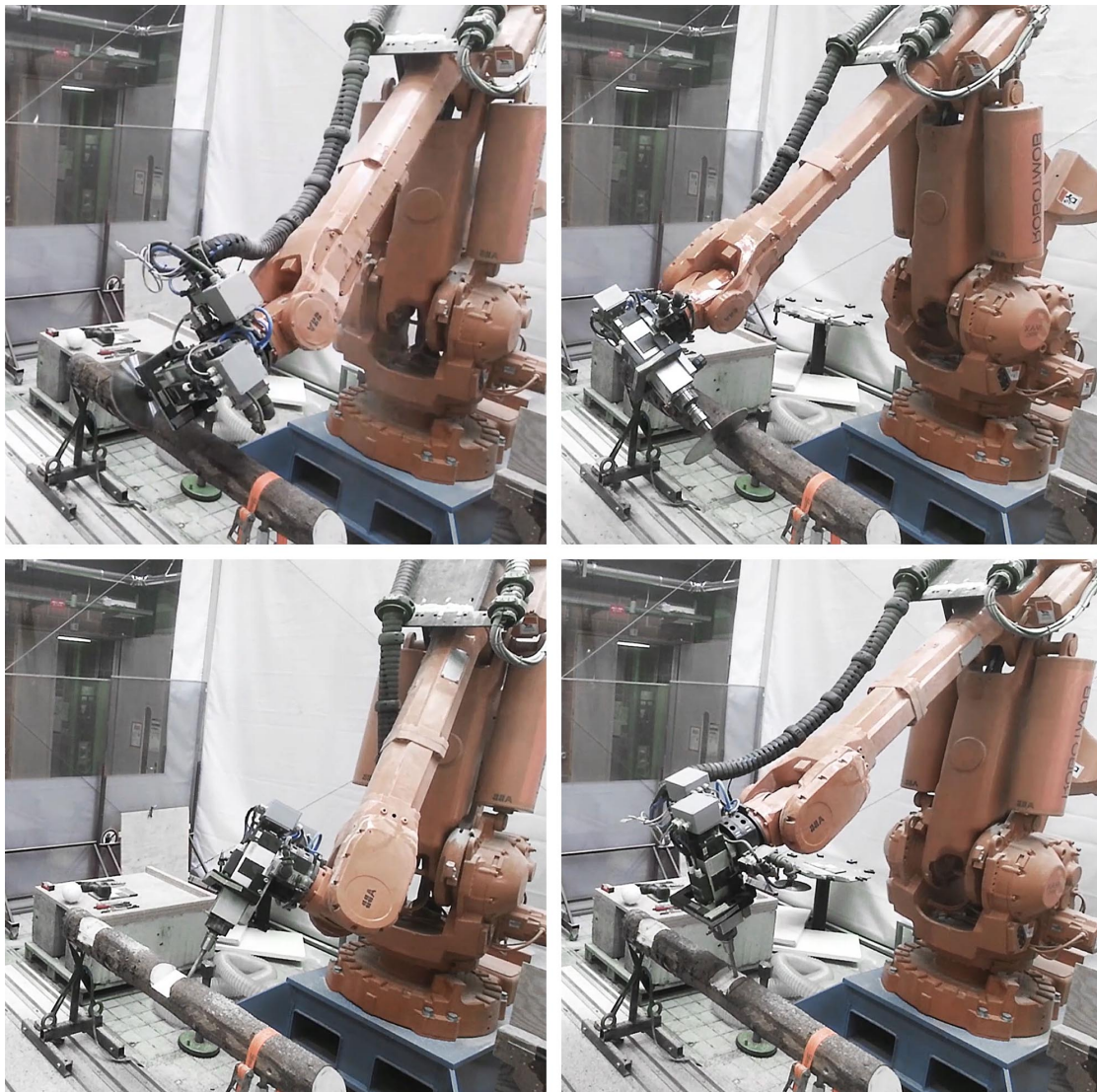


Figure 9.17 – Fabrication of the Cross joint using the saw-blade and flat-end milling tool.

The scanning process is automated to orient timber joinery without manual point-cloud processing. The robotic space stays constant, limited by the maximum reach of the robot. The reachable space can be scanned repeatedly using the same tool-path around the fabrication setup even though the object position and shape changes. This idea simplifies the procedure even though robots can have varying imprecision in different poses if a thorough calibration is made. Furthermore, the scanning operation is decreased from manual 45 minutes 3rd party software processing to 3-4 min scanning and central-axis approximation. No point-cloud registration is used because the fixed robotic poses could help to align multiple scans detailed in the Scanning chapter. The only visible output from the scanning process is the central axis and radial parameters used to orient the tool path. The described method that is not visible to a user is shown in Figure 9.18.



Figure 9.18 – Element identification from a) a larger scan, b) the simplification to radial parameters, and c) the joint alignment.

## 9.5 Assignment Problem

A given set of timbers alters the initial design (see Figure 9.19). When trees were ordered from the forest within 15 cm radii, the delivered wood had taper, curvature and sectional differences up 15-22 cm in radius. The assignment strategy is needed because two large timbers might be colliding, or smaller beams might not form a connection zone. First, all the beams are scanned at one time, and the point cloud is cropped to individual beams. Second, skeletonization is performed on each point cloud using a Cylinder-fit method. Third, the cost is assigned for each beam based on length and radii. Fourth, the assignment is made using a Hungarian method<sup>1</sup>. The search criteria for the Hungarian Algorithm was a length of a beam. The indexing is needed to select the suitable geometry for fabrication within a group of self-similar elements. When the assignment solution is found, the initial design is updated concerning the oriented point clouds. These assignment findings resulted in the global design changes such as reducing layer thickness, reorientation of conical parameters, and better cost estimation per element so that too small or too large beams would not be positioned close to each other (see Figure 9.20). Lastly, a small change like a few centimetre difference in a tree radius influences tool-path generation, requiring less or more milling to ensure fast and secure fabrication.

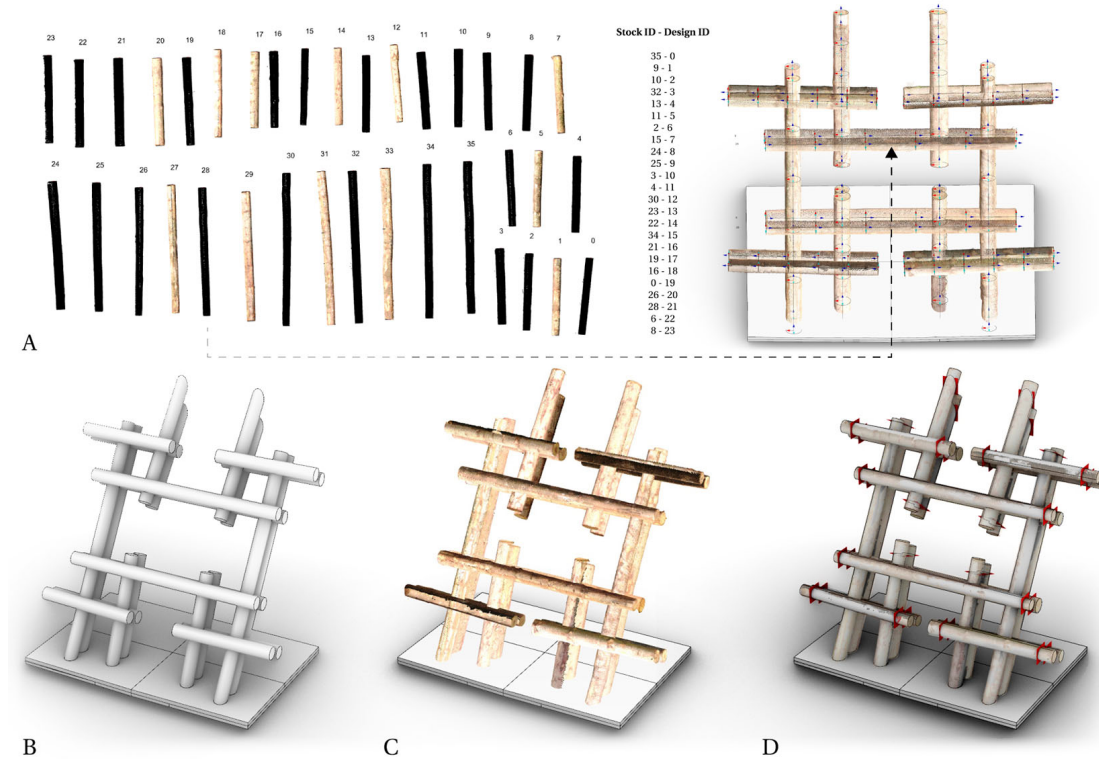


Figure 9.19 – Beam assignment from the real to the digital stock: a) Hungarian algorithm, b) initial model with equal radii beams, c) oriented scans, d) altered design.

<sup>1</sup><http://accord-framework.net/>

## 9.5. Assignment Problem



Figure 9.20 – Prototype comparison between the digital model and the scanned trees. The scan is not made after the assembly but before to check if beams are colliding and alter the design model based on a given stock of timber.

## 9.6 Conclusion

A new methodology to design bio-based spatial timber structures from round woods is proposed. A series of geometrical steps are employed to obtain a Nexorades pattern, including tiling, dynamic-relaxation, joinery solver, and digital fabrication (see Figure 9.21). The framework enables the use of discrete tile mappings in non-manifold meshes to obtain a Nexorades pattern while reconstructing the beam-like geometry following the graph methods. The irregular beams are automatically generated using a stock of wood harvested from the forest. The methodology is verified by evaluating simple 2D quad-grids. The beams' volumetric representation included changing radii along the beam axis, and taper assignment based on curvature and elevation is also considered. Meshes with multiple singularities and variation of curvature with optimized eccentricity are also validated. Lastly, experiments were conducted using laser-scanner and point-cloud processing to create a raw wood library and alignment of beams in the robotic workspace.

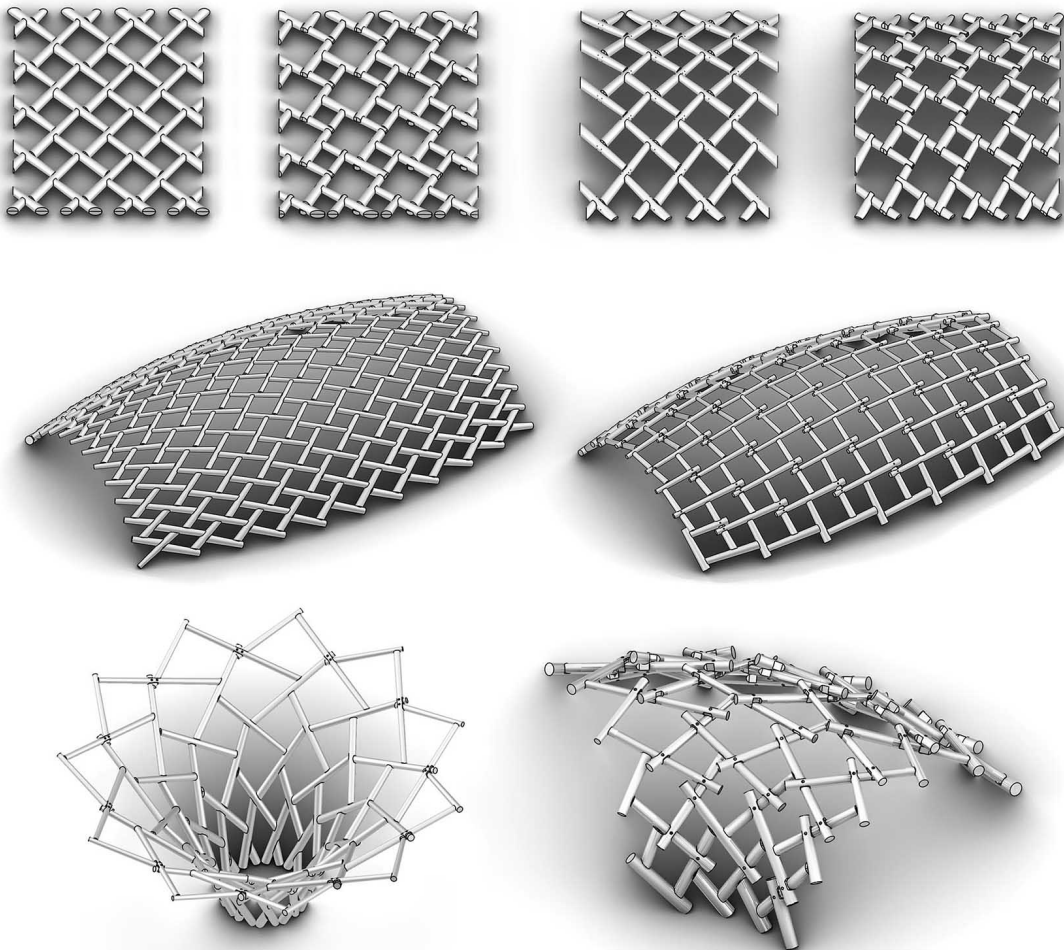


Figure 9.21 – Nexorade system with cross and side-to-top wood-wood connections.

## Conclusion of Demonstrators

The Demonstrators section shows a link between the methodology and applications. Two systems are detailed: a) the shell structure, and b) the Nexorades. Additionally, technical experiments of tree forks are developed in the Appendix A. The selection of these specific structural topologies is related to the local forestry collaboration in Rossiniere and the past IBOIS research in the double-layer plate structures. Shell structures in raw-sawn-timber require many interconnected elements, whereas the simpler and less structurally performative Nexorade could be used to span a similar size structure. Furthermore, multiple small scale experiments, such as the truss from tree forks, are needed for the development of the design-to-fabrication workflow. The fork fabrication is necessary to understand if it is possible to extend the current setup independent of a timber shape, whether it is straight, curved or forked. The market-less point-cloud registration helps to align varying timber shapes within a millimeter precision, and the Joinery Solver automates the modeling of wood-wood connections. The case studies are related to the so-called “the chicken and the egg problem”: which comes first, an architectural design or the technique of cutting and joining? Both are needed. Design imposes its own contextual decisions, whereas the technical developments require a more rigorous systematic formulation of a solution that could be re-used though-out multiple case studies. Lastly, it could be interesting to discuss the research implication more broadly beyond small-scale raw wood and the available robotic fabrication equipment considering the scalability and repeatability of the proposed methodology including structural performance and relation to other systems such as enclosures and facades.



## **Conclusion and Future Work Part IV**



## 10 Conclusion

The research of raw timber started in AA, Hooke Park and was followed by numerous researchers afterwards. In 2015, Frei Otto explained the fabrication process of the actively bent grid-shell from raw wood, quoting his teacher, a famous German wooden engineer, who always asked his students: "What is the biggest enemy of wood?" and the teacher wanted the students to answer "The saw". Following this, explained that it is always good to use raw wood that has not been cut by a saw. However, at the same time, it is challenging to employ whole timber without a saw.

In the following two decades of the architectural research linked with the introduction of digital fabrication such as industrial robot arms and CNC machines, there has been a continuous increasing interest in raw timber. The role of a carpenter has changed overtime because the hard and time-consuming labour is partly replaced by the collaborative work of a human and a robot. While industrial methods focus on mass production of equal-sized straight tree trunks, the research explores the low-value timber. The topological differences in timber in its natural form could be divided into three types: a) straight, b) crooked-bent, and c) forked. The architectural projects search for new design and fabrication methods following the relation between structure and a tree topology.

Contrary to the educational research prototypes, a new branch of robotic timber companies is seizing the economic and structural advantage of raw wood. The downside of such commercial models is that they follow the centralization scheme. Often only one company in a large region can produce structural raw timber resulting in a monopolization. At the same time, the small timber companies, such as Rossiniere, Lausanne, Chavornay, could hardly exist without the government help. The large centralized companies do not share the R&D developments to ease the current forestry situation.

The centralization scheme will probably not change, as a result the local timber companies are willing to cooperate with universities. For example, the dissertation started from the collaboration as an extension of the studio Weinand inquiry in the local Swiss forestry Rossiniere. Following the quote from Rossiniere in the 24 heures newspaper: "Si l'on n'innove pas en

## Chapter 10. Conclusion

---

tenant des risques, on n'aura plus que les yeux pour pleurer", there is an interest and acknowledgement that there is a lack of digitalization in the local timber companies. The researchers have already been demonstrating that it is feasible to exploit local timber and provide an additional value towards the circular economy.

Also, the research methodology is related to an industrial robotic framework that did not exist before at IBOIS, EPFL. The methodology is developed by first re-examining the state-of-the-art workflows. Following this, methods are replicated at the scale of raw wood fabrication and extended further. The past research methods employed for timber panels could not be equally adapted to raw wood fabrication due to the CNC manufacturing method. A feedback loop between laser-scanning and robotic cutting is enabled when the industrial robot arm is introduced at IBOIS, EPFL.

At the same time, IBOIS research has a strong focus for re-visiting wood-wood connections, the so-called "integral mechanical attachment" that allows reducing the use of steel fasteners employed in timber construction. The Joinery Solver algorithm is developed to transfer the knowledge from previous research in timber plates to beam elements, while considering the irregularities of raw-sawn-timber. The timber joinery, which is applied punctually, could ensure fibre continuity while adding the information for the assembly through prefabrication.

There is a gradual shift between timber boards to regular sized timber during the thesis experiments, and then finally applying the methodology to raw wood. Most of the used timber is delivered from the Rossiniere forest, as described in Appendix B. Spruce is the main soft-wood tree species growing in Rossiniere that has a relatively straight tree trunk. The natural bending, known as the reaction wood, could only be observed locally at the base of a tree due to the mountain terrain. Also, tree forks are found as well. However, they usually break after falling due to the complicated harvesting process, as explained by foresters. Nevertheless, bifurcations of tree trunks are considered as part of the design-to-fabrication workflow to show the broader applicability of the developed tools. The main focus is given to small-radius trees that are less than thirty cm in diameter because they have little economic value but have potential in structural applications with a minimal fabrication time.

The Joinery Solver method employs a novel algorithm that starts not from a parametric model such as Mesh or NURBS, but a list of timber elements. The element strategy is employed to ease the timber joint modelling without a need to hard-code the timber details for each case study. There are two joinery specification models: a) developer creates a mathematical model of each joint or, b) user draws a 3D joint which is serialized for the future use. Furthermore, this idea allows reusing the previous joints by gradually collecting the timber joinery library from more than one project. The idea seems to have much more advantages than the previous mesh-based models. The past method relies on the real-time mesh adjacency graph, whereas collision check, face intersection and curve proximity methods could be relatively slow. The described methodology explains how to create an equivalently fast workflow that helps to transform solid models to fabrication aware parts. Another joinery integration into

---

the element problem is addressed considering volumetric 3D beam joints. Past IBOIS case studies demonstrate that a timber plate joint belongs to a set of 2D problems resulting in close to real-time applications. Subtraction of beam joints requires costly Boolean operations that were before neither fast nor robust. Consequently, Mesh Boolean methods are implemented into the Rhino modelling environment to visualize timber joinery. The overall framework is open-sourced and further detailed in Appendix C.

The joinery generation had to be validated through physical experiments. Unique setups are manufactured to enable robotic cutting. The provided industrial robotic application had to be extended employing a tool-path planning algorithm to automate the reachability of the 6-axis ABB IRB 6400R. The knowledge in CNC machining is gradually translated to the provided workflow even though G-Code and the custom Inverse Kinematics solver belongs to two different systems. The translation shows that the Joinery solver is not machine-specific and could be adapted to other methods such as Virtual Reality fabrication tools that are currently developed at IBOIS.

Additionally, the tool path generation method considers a series of machining tools integrated into the Joinery Solver based on the robot movement. The joint visualization and fabrication are interconnected using a notation of pair cuts that could be directly translated for 3D Mesh and 2D Polyline Boolean operations and manufacturing processes such as milling, cutting, saw-blade, and drilling. The method considers specificity of digital fabrication such as types of notches, and slope cuts for the tool safety, including concave and convex polygon pairs. In addition, the collision detection and simulation method is developed, and the overall ImaxPro Inverse Kinematics solver is implemented into Rhinoceros3D visual interface.

The interoperability between different software libraries, applications and laser scanning hardware is an inherent practical part of this research. The scanning methods are needed for two reasons: a) to collect a digital library of irregular tree shapes and transform scans to minimal models, and b) to know a position of a tree before fabrication starts. The Faro Focus S 150 is integrated into the robotic workflow and interconnected with robotic movement via a thorough calibration process. The fabrication starts by a) scanning a tree trunk, b) re-positioning reachable tool paths, c) automatically changing the tool via the Schunk adapter and d) executing the cutting process. Besides the laser scanner hardware automation, the research shows that there is a lack of point-cloud processing tools for architectural applications in the higher-level languages. A point-cloud tool is developed to gather state-of-the-art efficient low-level libraries adapted to the CAD modelling environment Rhinoceros3D. Additional effort is made for the documentation to enable collaboration through the open-source library.

Two types of demonstrators are developed based on the Joinery Solver: a) a segmented timber shell and b) Nexorades. Additionally, the joinery algorithms were involved in teaching to adapt the methodology to tree forks and regular-sized lumber. The physical tests helped to interconnect the 3D representation of timber joints with constraints of fabrication. The manufacturing of joints is seen as an integral part of a connection design. Finally, the assembly

## **Chapter 10. Conclusion**

---

sequence is developed as part of the Joinery Solver in relation to the direction of a joint and the interlocking of a structure. Also, the framework considers individual elements such as beams and the level of nesting to reflect on the modular assembly composed from a series of elements. The Joinery Solver is not limited to these two case studies. It is known that raw timber could be used for other structural topologies: frames, trusses, shells, grid-shells, post and beam systems, solid walls, slab and hybrid models. The goal is to solve the local micro joinery generation through the pair-wise joint identification, whereas the global macro model is subject to an individual design.

## 11 Future Work

The research methodology results in the stand-alone software libraries and plug-ins that allow extending this work further. The applications are open-sourced and described in further details in Appendix C. Developing and maintaining applications requires a constant refinement, updates, reflection on the varying nature of case studies and user needs.

The Joinery Solver method has been already taught at the studio Weinand, and it has been incorporated in the final master thesis, workshops and individual case studies throughout the dissertation. Each project gives an additional input and allows to find possible bugs. The framework is designed to show that the joint library could be extended based on a planar polygon and an axial search methods. For example, if a new joint needs to be implemented, there is flexibility to add a new type of joint to the joinery library. Furthermore, the Joinery Solver is not limited to plates or beams, but can combine both using a hybrid timber system.

The wood-wood connection algorithm also shows the need to address the assembly and constructive aspects in the early stage of design. This problem is discussed numerous times by Fabian Scheurer (Design to Production), yet is still an issue starting from an educational standpoint. Often, taught BIM software is designed to produce 2D drawings for visualization and does not consider the assembly and material practices.

The proposition to develop the Joinery Solver could be seen in many research models made at IBOIS, EPFL, e.g., Christopher Robeller, the current dissertation, and the ongoing work of Nicolas Rogeau. Also, more known tools such as Cadwork are linked with the past timber research of IBOIS, emphasizing the need to develop the methodology further. The challenge of such methodologies is not to make a new modelling framework each time, but to develop a common model that could be gradually enhanced using the open-sourced collaborative methods.

Development of applications is often seen as a highly individual work when each researcher creates his/her own tool without sharing it to enhance its functionality. The point-cloud processing framework Cockroach takes a different route by emphasizing the importance of a

## **Chapter 11. Future Work**

---

collaboration. A new doctoral thesis, initiated by Andrea Settimi in 2021, combines similar research through point-cloud processing. Furthermore, documentation and continuous maintenance are needed to invite external collaborators. The point-cloud processing could help analyze ancient timber joints using, for example, mesh clustering methods, and in a more global picture provide methods for developing catalogs for reuse of discarded timber elements in construction. Besides software integration, synchronization of multiple low-cost, low-range scanners could open new research paths and applicability considering the overall precision of such tools.

The given methodology could be highly advantageous to local timber forest companies that exhibit a lack of digitalization. The open-sourced tools could help to reduce the dependency on centralized timber companies. There is a limited access how raw wood is machined at an industrial scale, resulting in a fewer companies able to cut raw woods. Thus, the collaboration could be enabled by installing digital tools, and providing software training for development of small scale applications. Also, automation in wood-wood joinery could gain an advantage when combined with traditional carpentry to ease and learn from the manual timber processing. Timber companies currently freely supply wood for research purposes, and in return, the developed methodology could be transferred outside the closed lab environment. It is unlikely that timber transportation will decrease due to the economic reasons and rugged mountain forestry, however, the circular economy could be re-started through the local digitalization.

Extra fasteners of wood-wood connections in raw wood need to be investigated further. A rotary system such as a lathe would ease the reachability of the industrial arm, allowing it to tackle the more complex timber joinery and speeding up the machining process. The rotary mechanism could initiate a new research line using a winding process based on fibrous timber joinery methods. An investigation was carried out using rope for tightening cross joints that resulted in a discussion regarding the search of possible automation.

The fabrication methods employed in the current research could be upgraded. For example, robotic band-saw and chain-saw cutting could help find new joinery fabrication methods and speed up even the simple cutting processes.

Larger-scale experiments such as hexagonal braced Nexorades, solid raw wood slabs, raw timber frame systems, and solid lumber shell structures could be investigated further. It is necessary to address the roof cladding, insulation and overall detailing to transform the experimental structural models for the actual use. Additionally, frames and Nexorades could be covered using bio-materials that could open new research lines as well. Many questions arise besides the scope of raw wood structural systems. Besides the emphasis on the sustainability discourse, the cultural shifts and other impediments beyond the technological and integration with the building systems such as facades or structural skins need to be investigated further.

## **Appendices Part V**



# A Timber Joinery and Teaching

## A.1 Introduction

Teaching is a key part of research studies that takes at least one or two days per week. The involvement in teaching revealed the contradiction between the common architectural training for students and the craftsmanship of building techniques. The so-called detail is understood as 2D drawings taken from previously published articles, without the knowledge of how to generate an assembly sequence of a construction process. The initial software (BIM) and tool teaching limits the thinking of students and constrain their design language to the hard-coded digital systems, instead of sketching or generating new ideas. Also, the tools limit the understanding of the material based building processes, such as those of timber. Furthermore, the 2D references, mostly taken from social search engines, are not understood in-depth. Differently from other disciplines, there is no common practice of reading state-of-the-art research of architecture. Therefore, how can one link the design and construction techniques with a knowledge of materials and assembly?

There is a particular gap in academic research that results from the narrow focus on finding novelty, rather than re-developing existing workflows of timber construction. Current contemporary research in timber structures focuses on advancing architectural geometry, whereas there is a more significant necessity is to build better digital models. The models have to be as lightweight and flexible as possible to detail in the further design stage. One large parametric model often tries to solve a complex non-linear problem, yet it fails to do this due to its limitations to one structural system. One of the most straightforward examples of timber manufacturing is that we do not want to model each drilling hole for a toolpath, but rather make correct instructions for digital manufacturing. In this context, BIM and NURBS models do not work because the 3D visualization of a detailed model has no relation to manufacturing instructions. Consequently, the modelling needs to attach and detach attributes to limit the costly remodelling process.

Architectural practices relies on a labour-intensive, repetitive processes such as a) make a 3D model, b) dispose of a 3D model and c) repeat the same process until the building is built.

## **Appendix A. Timber Joinery and Teaching**

---

The reason why digital BIM practices fail is due to the fact that BIM delivers 2D drawings but not the production data. Therefore, these models have too much information that is not usable at a later stage. However, there is no perfect way to design a sketch design to a crisp and precise model for construction. These systems are advertised for small-scale demonstrators and pavilions, but large projects require a greater complexity. One of the possible solutions is to employ Minimal Models, as described by Fabian Scheurer. A model is a simplified reproduction of reality that must contain information necessary for the given purpose and audience. To understand the purpose and the audience, the designer must study the project in depth from the very beginning to find the worst cases and develop a systematic, rule-based approach if resizing or resurfacing is needed.

Thoughtful detailing – such as seen in Ikea furniture – it is possible to make the assembly easier without confusing or rethinking how parts have to come together. In the timber context, joinery helps to remove the complexity of the assembly and constructability, as the connection already has the insertion information. In this section, two student projects shortly describe how design decisions were made to transfer the digital model to fabrication. The first case study describes the modelling of Ari-kake side-to-top joint added to Joinery Solver to display and robotically fabricate a wood-wood connection. The second study explores tree forks, including design, scanning and cutting of side-to-top and side-to-side joints. In both cases, the digital detailed Rhino3D models could not be used for manufacturing, therefore minimal models are used with the help of the Joinery Solver to generate the tool-path and visualize geometry.

### **A.2 Side-to-top Joints Multi-valence Joint**

The simple case of the Arikake joint demonstrates the modelling problem where a 3D model cannot be directly used for fabrication (see Figure A.1). The geometry is created for visual architectural purpose only and contains no information for a tool-path or joinery generation. A single joint can be produced using the digital fabrication method by manually drawing a tool path and incrementally checking the robot's orientation. However, a slight variation of joint angles or multiple node fabrication is worth automating to reduce the manual labour and avoid manual user mistakes that often result in a collision and damage of the overall setup.

From an educational point of view, there is an absence of coding lessons that cannot be taught quickly. Therefore, a Joinery Solver is used to ease the automation process by describing a set of rules on how the Arikake joint is drawn. Each joint in the Joinery Solver is described by a function that allows to change the proportions of a joint, and that specifies the cutting method and its details such as notch types visible in the fabrication process (see Figure A.1 B). The function specification is a more time-intensive than a single joint modelling but could be reused more once, including angular changes.

The Joinery Solver is developed for pair-wise connections only. Nevertheless, when two joints are located in the same node, it is possible to obtain multi-valence joints. Visually it looks

## A.2. Side-to-top Joints Multi-valence Joint

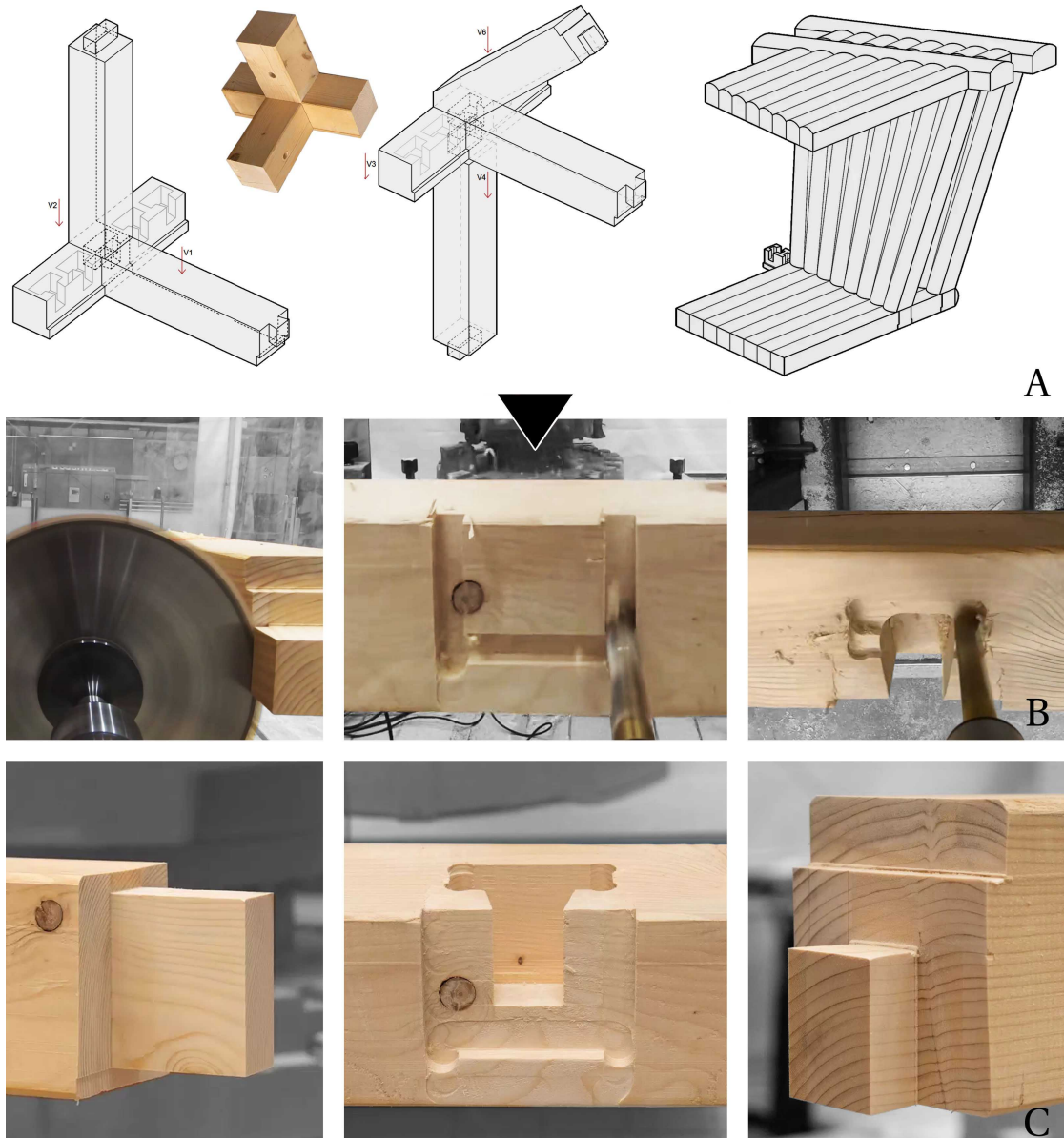


Figure A.1 – Ari-kake joint fabricated using the Joinery Solver: a) the joint shape is described b) by the robot movements, to get c) a physical result. Student project by Maxim Andrist.

like a 3-valence joint, but it is composed of two pair-wise connections. The same principles were applied to the Annen structure when coupling two side-to-end connections. The Arikake joint is composed of a through-tenon joint and a half-dovetail joint. Two tests were made to arrive at the result, including notch testing and balancing fast saw-blade cutting versus a more reachable milling process. The overall joint is fabricated from one single beam and cut into three parts to test the assembly. Consequently, this relatively simple example shows the need to have different models than the initial one used for the 2D representation only.

### A.3 Truss from Tree Forks

The second project is developed for a half-year studio project, exploring tree forks (see Figures A.2 and A.3). The case studies are developed using the Joinery Solver. A small scale prototype is made using three tree forks and four straight timbers brought from Rossiniere. In order to start the design phase of the truss, the available tree stock at IBOIS, EPFL is scanned to document the physical properties of wood such as the radii, the length and the fitting parameters of the truss system.

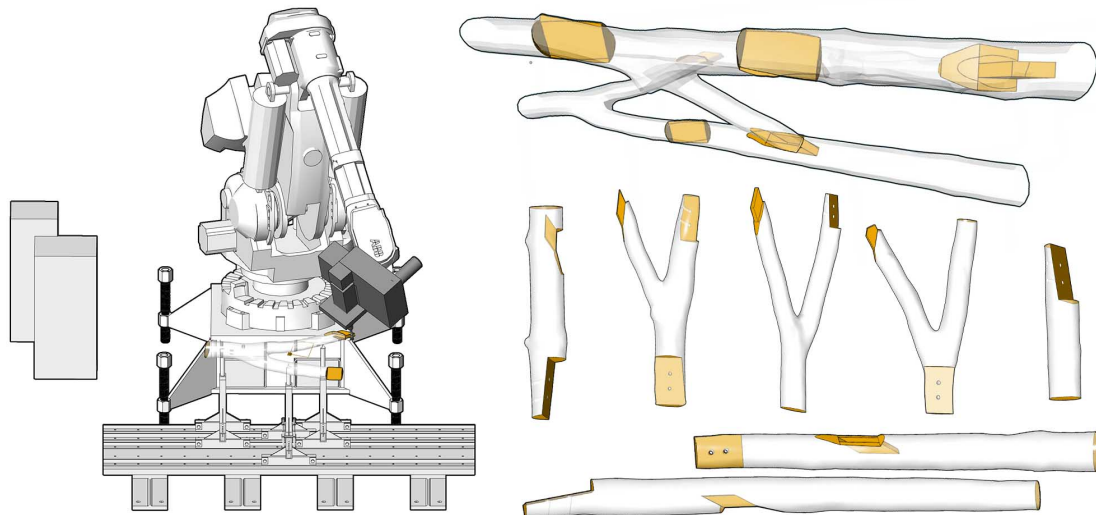


Figure A.2 – The case study of Vierendeel truss using Joinery Solver for both the geometry generation and robot control (Student Maxence Grangeot).

The truss model is created using a set of rules for the iterative optimization solver: a) pairing forks with straight beams, b) equal distribution, c) orientation of connection points between the pairs, and d) deviation between tree forks truss and regular Vierendeel truss. Often tree forks are understood as three lines interconnected at the centre; yet in reality, there is a curvature, twisting and irregularities that need to be considered when adding wood-wood connections. There are two possible solutions: a) select similar size forks, and b) machining a large amount of timber to fit design needs. Both methods have advantages and disadvantages, depending on how well natural shapes fits the design shape versus how it may disrupt the fibre continuity.

Moreover, we did not have an extensive library of tree crotches selected explicitly for this project. Three forks could be used for the project while the rest of the elements differ too much in radii. Consequently, it is worth studying tree topologies in the forest long before fabrication occurs to interconnect the fitting strategy with the available tree trunks. The uniqueness of tree forks questions the fabrication strategy. For example, what will happen if a tree trunk is accidentally destroyed during fabrication, or if a structural element must be replaced in the lifespan of a built structure?

### A.3. Truss from Tree Forks

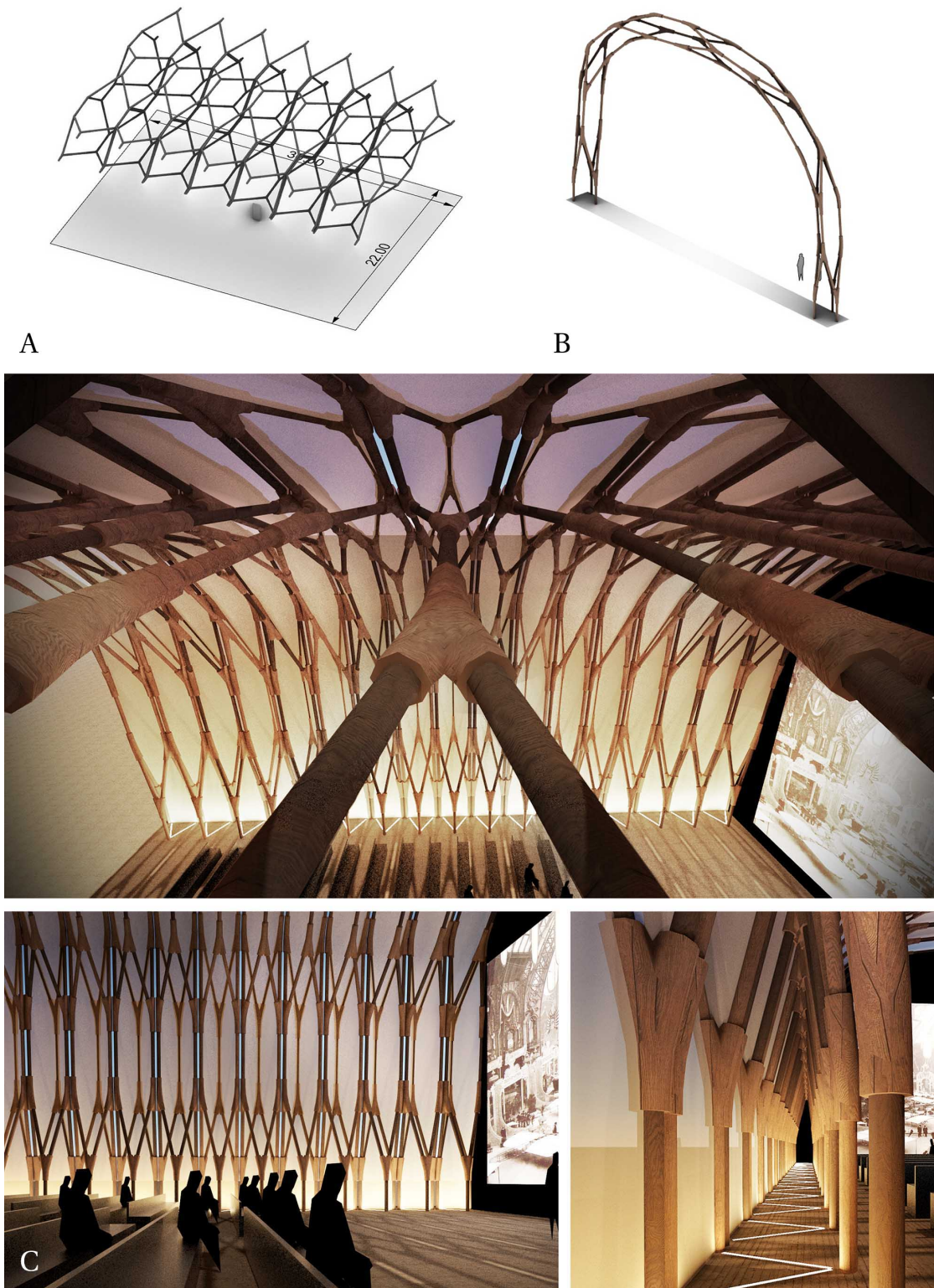


Figure A.3 – Modelling sketches for structural topologies employing tree forks: a) a hexagonal cylinder subdivision, b) a frame system, c) views of the system.

## Appendix A. Timber Joinery and Teaching

---

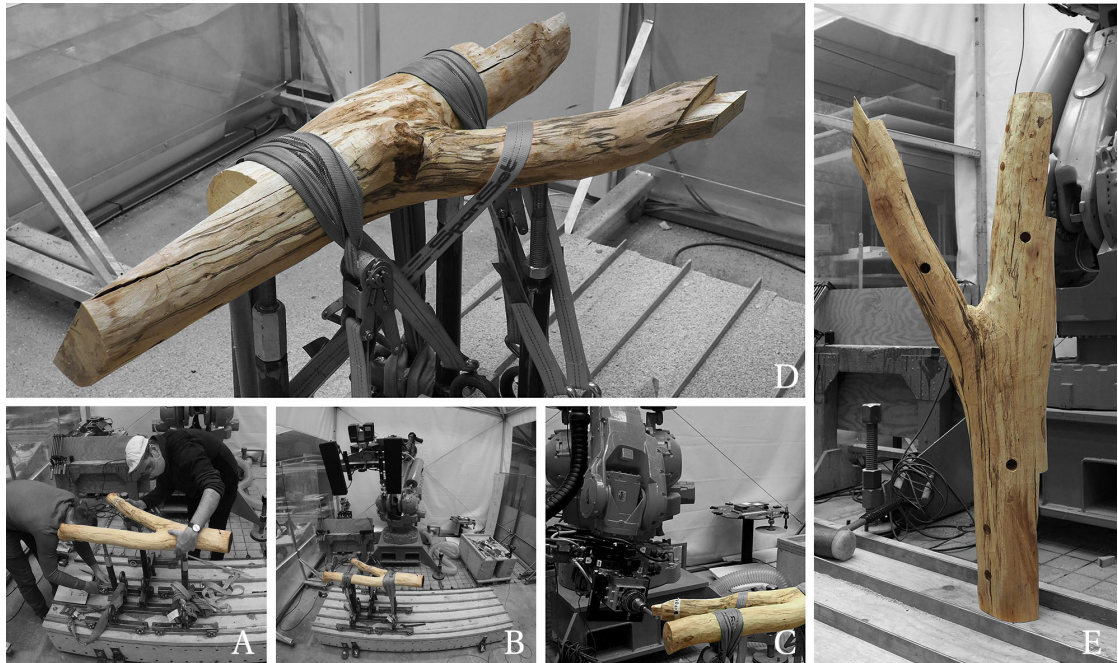


Figure A.4 – Main steps of fabrication: a) mounting, b) scanning and alignment, c) fabrication, d) removal of belts, e) result showing pre-drilling holes for fixation.

To avoid any mistakes, first, multiple tests are carried out using straight timbers (see Figure A.5), and only then a similar tool-path is performed on tree forks. The tests included: a) plain scarf joint cutting, including the search of the proper hole size for dowels, b) tenon-mortise fabrication, and c) end cuts from two sides of a beam (see Figure A.4). After intensive physical modelling and understanding of the poorly calibrated robot tolerances, the fabrication is started.

The support of the fabrication setup helped adjust to varying shapes of trees that must not be positioned at a joint location. The mounting process includes the following steps: a) predrilling dowel holes, b) fixation of belts, and c) automatic scanning to align the digital model with the physical one. Initially, it was thought that we could follow a similar strategy described by Design and Make studio Tree Truss; however the mounting process revealed that tree trunks could change their initial position of dowels due to the rotation moment when adding belts. One of the central questions for this prototype was to find the precision of scan alignment and joint positioning, which ultimately surprised us due to highly accurate scanning and point-cloud processing. The only inaccuracy is related to the robotic cutting of 2-3 mm, knowing that the robot was not calibrated well initially; this problem is solved afterwards by performing a two-microscope TCP calibration method developed by Simon Lullin.

Another challenging part of the project is a collision-free tool-path generation. The tree fork experiment leads to a development of a tool-path planning algorithm to avoid the manual procedure applied in this prototype. The algorithm is described in the last methodology

chapter. Prior to solving this problem, a student had to be hired for one week to align multiple tool-paths by constant manual checks between Unity and Rhino (see Figure A.5). The given Unity application from industrial partner ImaxPro could only be used to simulate a robot that cannot flexibly adapt to rotary tool like CNC machines. Therefore, the tool-path planning for robotic cutting proved to be an effective option for designing timber joints from design to fabrication.

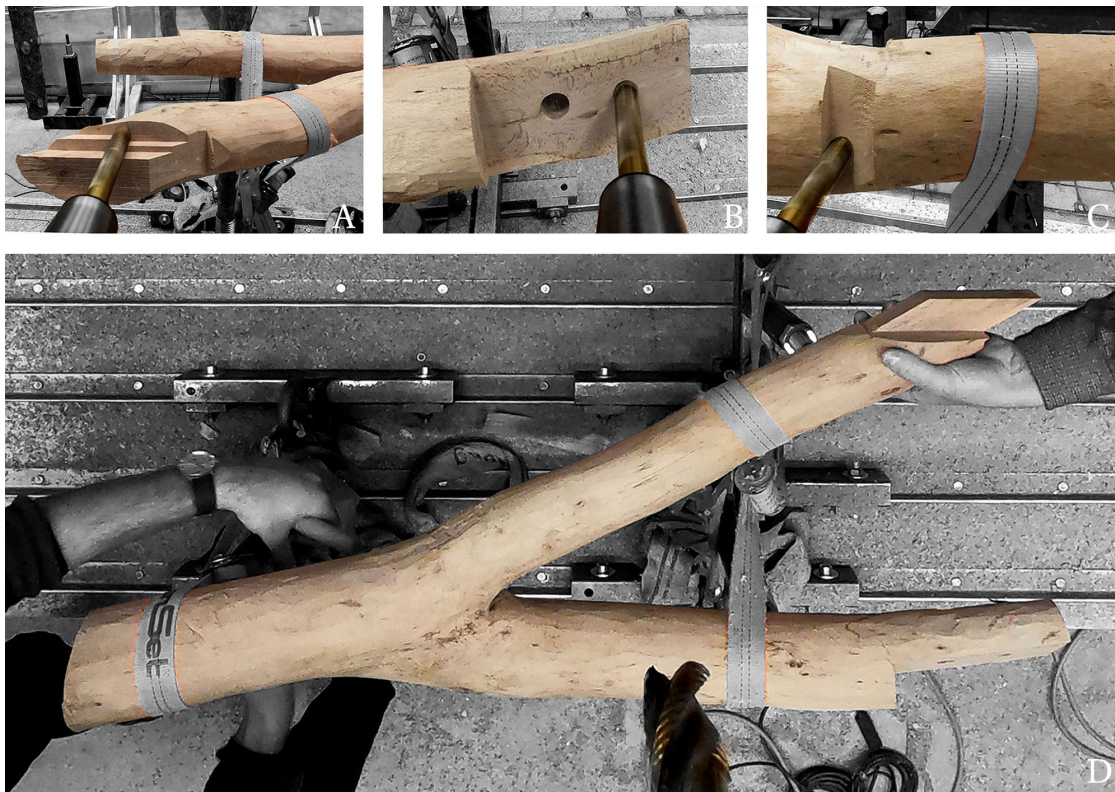


Figure A.5 – Detailed steps of fabrication: a) milling of the side-to-top joint, b) side-to-side scarf joint, c) end cuts, and d) two timber joints and one end cut.

The Fork fabrication experiment also reflects on the modelling process interconnected with the Joinery Solver. Compared to the Arikake joint prototype, the fork modelling cannot follow the standard NUBRS modelling process. The joints had to be adjusted until all fabrications constraints were known, which shows a need to have lightweight and flexible models without changing the initial design intention (see Figure A.7). For example, side-to-side scarf joints had to be rotated depending on the reachability of the robot. Also, the truss system had to be adjusted by measuring the maximum angle of the milling. The milling angle of forks was close to 30 degrees, which falls into the maximum limit of a collision-free path. As a result, the tenon-mortise joint could be changed either perpendicular to the connection area or by limiting the maximum cutting angle. The changes are solved in the overall model using only axis and radii information, while the local joinery information is automatically generated together with the tool-path. Consequently, the Joinery Solver generates the micro joint scale with a flexibility to

## **Appendix A. Timber Joinery and Teaching**

---

change macro design scale, resulting in the multi-scalar modelling methodology.



Figure A.6 – Side-to-top Tenon-Mortise Joint test fabrication prior to the full-scale prototyping. Each joint is manufactured separately to know the calibration precision.



Figure A.7 – Tree forks with a) wood connections, and b) scarf joint with straight elements.

## A.4 Conclusion

The Joinery Solver and Teaching section describes two experiments with solid lumber and crooked bifurcated trees. The timber joinery generation method is also taught each semester as an introductory course for master's students. The tool teaching must be coupled with physical experiments to explain why these models are helpful. The teaching method is divided into two parts: a) giving a general introduction to the algorithm utilizing Grasshopper tutorials, and b) working individually for a specific student project that targets timber joinery. Most students attending the studio do not have any coding experience and primarily employ BIM software for standard CAD modelling. Semester projects are relatively short, leading to pre-planned automation for timber joinery fabrication. The very first projects (see Figures A.8, A.9) demonstrate case studies for Nexorades in raw wood. The global models designed by students did not have fabrication and joinery data leading to a time-intensive and challenging fabrication, whereas the Arikake and Fork Truss prototypes addressed this question in the early design stage, enabling the data transfer from the design to fabrication. Consequently, there is a need to have automation even in teaching in order to acknowledge students with building and assembly techniques.



Figure A.8 – Prototype for reciprocal structures from regular lumber (Matthias Pengg, François Loison).

## **Appendix A. Timber Joinery and Teaching**

---



Figure A.9 – Prototype for reciprocal structures from raw wood (Nordine Mahmoudi, Tobias Richterich).

# B Rossiniere Forestry

## B.1 Introduction

The raw wood research started from a collaboration with a local mountain forestry of Rossiniere, Switzerland. The following chapters illustrate the current situation by describing a series of visits made in Rossiniere (see Figure B.1). The first visit explored the local sawmill and available tools for timber processing. The second visit focused on the laser-scanning of the forest harvesting sites. The third visit was made to understand the technology required to cut wood in the mountains. The three visits resulted in a future research interest – a study of small-diameter raw wood.

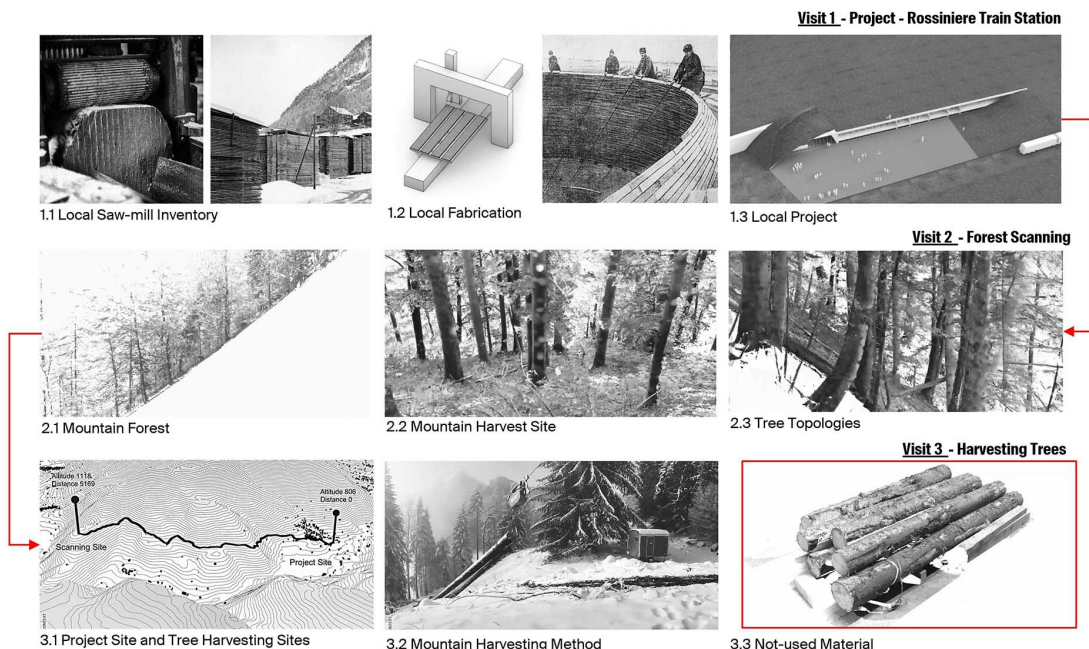


Figure B.1 – The research context is explained by a series of visits to understand the harvesting process of raw wood and the level of digital fabrication employed locally.

## **B.2 Local Circular Economy**

In the larger scope of the research, the interest is given to the circular economy of the local mountain forestry, where timber is harvested, processed and used locally. Currently, the situation is centralized as timber is sold to large timber companies and delivered back to Rossiniere as a construction material. This situation becomes economically difficult as the timber no longer covers harvesting costs. This is due to the fact that mountain forestry requires additional tools, such as a cable-system, to transport trees from the high altitude to the local sawmills. The cutting process mostly relies on skilled manual labour. The local sawmills transform trees into boards, planks and beams for export, as there is a minimal local application in construction, such as mountain Chalets made by the local carpenters. As a result, it is more efficient to import wood from the neighbour countries of Switzerland, rather than cut trees locally. In this context, the only available timber product is the solid lumber, namely boards, beams and raw wood. Industrial timber products are not available, and the structures have to follow the design methodology based on a wood grain orientation – e.g. connections cannot beam positioned perpendicular to fibers, otherwise external connectors are needed. The political and economical situation cannot be changed from a research point of view, however it is a starting point to question whether it is possible to use local wood without relying on large companies and the industrialized timber products.

## **B.3 Visit 1 - Absence of Digital Fabrication**

The first visit to Rossiniere is planned as a site and forestry inventory review to understand the local context and application of the digital tools (see Figure B.2). The village is composed of a small number of Chalets situated in a valley of the Alps and a mountain forest. There are only a few local industries connected in a chain of neighbouring towns by a railway and the main-road. There is a number of cutting sites surrounding Rossiniere, which are used twice per year, in the summer and winter. It is possible to notice vertical cuts of the forest that marks the cable-system used to transport tree trunks after they have been cut manually by ax-men. Local sawmills transforms logs into standardized timber products such as planks, beams, chips, and are then sold to larger factories to produce industrialized timber products such CLT, GLT, and PLY. There are no industrial drying facilities, manual labour is present at the processing scale, and there is an absence of digital fabrication in construction by strongly relying on carpenters. The only existing CNC machine is used for decorative work of windows and doors to construct mountain Chalets.

### B.3. Visit 1 - Absence of Digital Fabrication



Figure B.2 – Timber forestry in Rossiniere: a) marking trees before the harvest, b) forest line for the cable system, c) harvested wood, d) outdoor drying, and e) the use of the same plain-sawn cutting pattern.

## B.4 Visit 2 - Available Tree Topologies

The second visit helped to gather information about tree species in the forest (see Figure B.3). The most frequent tree species is spruce - softwood (*Epicea*). At lower altitudes beech is often naturally dominant, whereas in mountain forests the dominant species is spruce, larch and Swiss stone pine. The Faro laser scanner is brought to the harvesting site when trees are marked for future cutting. The slope of the mountain is close to forty-five degrees, depending on the area. Multiple scans were made in a range of 150 m to understand both the topology of trees and their height. It was considered that mountain slope influences the growth of a tree in a result of bent wood, also known as the reaction wood. The bending is visible but only in a small portion of a tree within less than 50 cm, and from this point it is straight with a minimal amount of bifurcations. The data is processed using Faro Scene and CloudCompare software and visualized using Rhino.

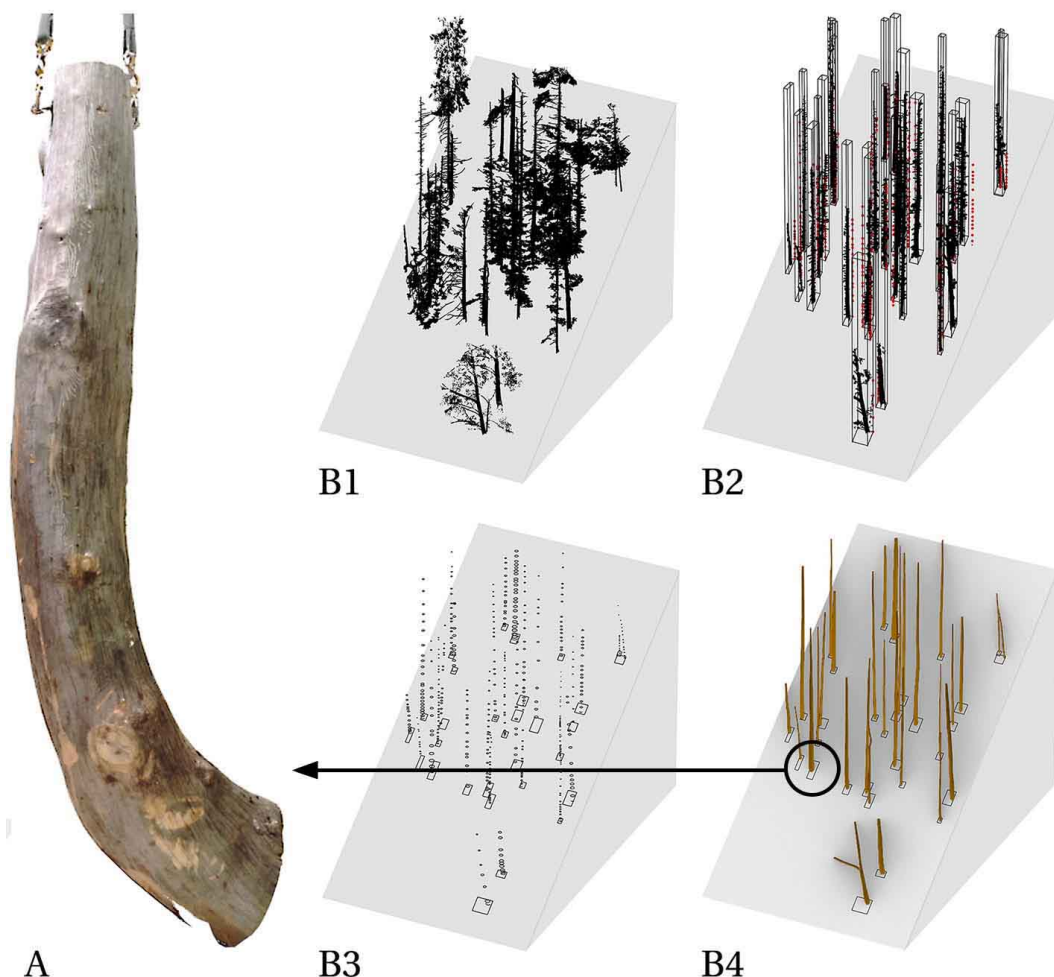


Figure B.3 – Scan taken from the Rossiniere forest during the second visit: a) reaction wood is formed only at the base of a tree (approx. 1-2 meters in length), b1) base scan, b2) cleaning the point-cloud and identification of individual trees, b3) sectioning, and b4) meshing for display.

## B.5 Visit 3 - Harvesting Trees

The third visit took place during the harvesting period in winter (see Figure B.4). The meeting is held in the Alps forest by asking to cut nine trees: three straight, three bent, and three forked trees. The cable system brings large tree trunks cut in half for further processing, in 5m length segments, as the mountain truck can only carry this length due to the narrow mountain road. Afterwards, a selection of trees are made for straight and bifurcated types, as there were no bent tree topologies around. The ax-men explain that forks mostly break after falling down. Following this, the cutting site was cleared for scanning to document the tree types. During the geometry survey, a small truck arrived and took no less than 30 cm in radii straight beams, whereas the small radius trees are left to rot at the cutting site or sold to paper industries and burnt as fuel. Consequently, the low value timber – i.e. that is less than 20 cm – and forked trunks were transported to EPFL for further analysis in structural applications.

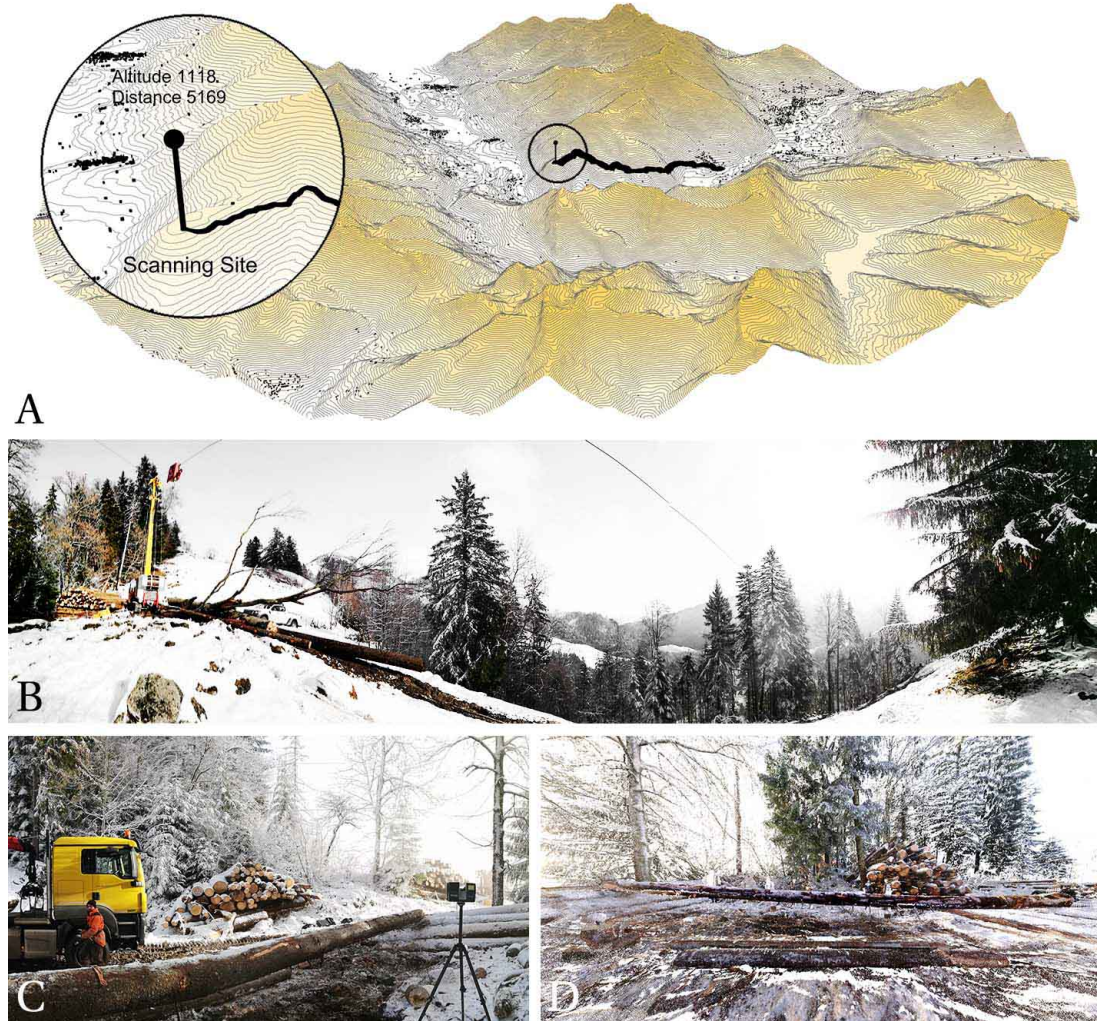


Figure B.4 – The third visit during the harvest: a) site distance from Rossiniere, b) crane, c) scanning site, d) point-cloud.

## B.6 Conclusion

Several attempts were made to order timber from Rossiniere for the fabrication testing. The ordering and transportation process takes months and shows that this material, and especially small-radii beams, are only available at certain time of the year. Also, the local sawmill is scanned, as shown in Figure B.5. Other attempts were made to buy raw wood commercially by collaborating with forestry companies around Lausanne to avoid the delay. The Chavornay sawmill was the first commercial supplier that delivered small logs bigger than 30 cm in diameter, because smaller beams are not considered to be a construction material. It is not possible to buy bent or forked wood, therefore the selection process was highly limited in research. The other collaboration was established with Lausanne forestry by asking specifically to cut trees in the diameter of 10-15 cm and 15-20 cm. These orders were possible due to closed cooperation between university and known forestry guards, since this is not a sellable product. These attempts show that there is a need to have a close collaboration between forest companies to apply digital fabrication methods for selected tree types and species.



Figure B.5 – Blum Sawmill in Chateau-d’Oex. The sawmill (top) is used only during the winter while the rest of the site is used during the full year. The raw timber is temporary stored in front of the sawmill building and then cut into boards.

# C Software Frameworks

## C.1 NGon - Mesh Processing and Joinery Solver

The NGon<sup>1</sup> plugin contains a collection of methods for polygonal mesh processing and wood-wood joinery generation (see Figure C.1). The Joinery Solver algorithm is implemented in this tool-set as it is closely related to mesh operations. Additionally, there is a collection of methods for designing timber structures, including shell structures and Nedorades. The plugin has a library NGonsCore.dll that combines existing geometry processing algorithms without Grasshopper user interface.

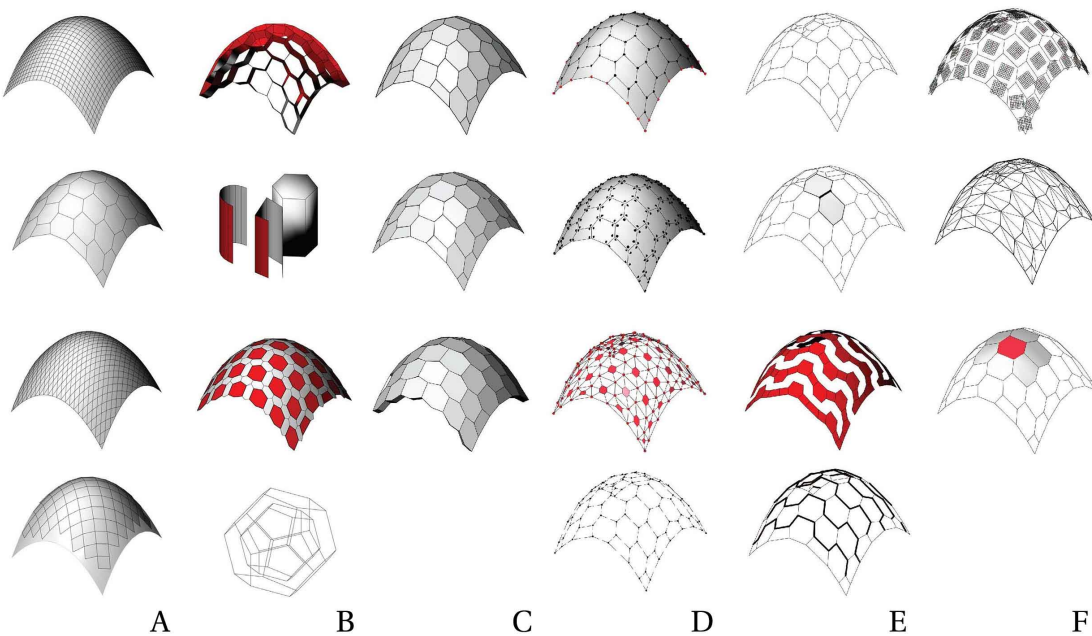


Figure C.1 – Polygonal Mesh processing: a) tesselation, b) transformation, c) planarization, d) vertex adjacency, e) edge adjacency, f) face adjacency.

<sup>1</sup>The framework is open-sourced: <https://github.com/petasvestartas/NGon>

## C.2 OpenNest - Packing 2D Objects for Fabrication

OpenNest<sup>2</sup> is a Grasshopper and Rhino plugin to optimally pack 2D closed planar polylines to closed polygons (see Figure C.2). The algorithm considers concave and convex polygons with and without holes, including an element and sheets. The main algorithm is based on No-Fit-Polygon generation using the Boost library method - Minkowski difference. The method is initially developed for the Nabucco project to nest timber panels for CNC fabrication. The algorithm proved to be helpful outside the project context and thus applied for the broader use. Besides the 2D packing method, there are additional methods for computing minimal bounding-box (principal-component-analyzing), 3D bin-packing, single-line text, object orientation to a grid and other functions used for fabrication. Lastly, OpenNest could be used as a stand-alone library to customize the algorithm and implement into other software applications.

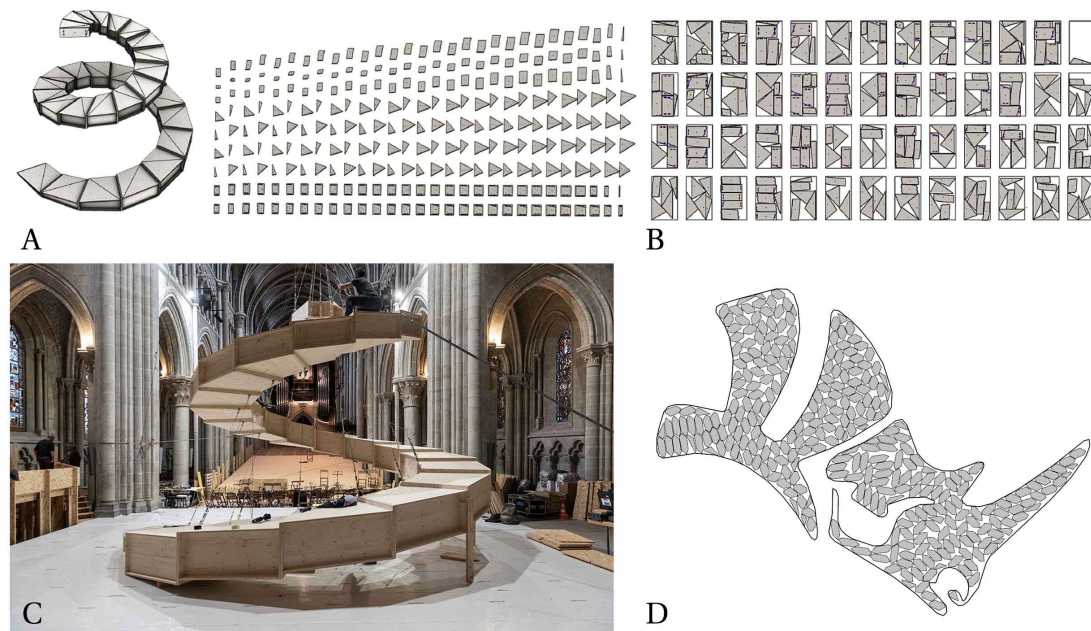


Figure C.2 – OpenNest started from the Nabucco project: a) grid packing, b) 2D nesting, c) study case, d) nesting to concave and convex polygons.

---

<sup>2</sup>The framework is open-sourced: <https://github.com/petasvestartas/OpenNest>

### C.3 Cockroach - PointCloud Processing

Cockroach<sup>3</sup> is a tool for PointCloud processing (see Figure C.3). A series of algorithms are developed to introduce various commands for point cloud post-processing and meshing into Rhinoceros® environment based on the functions existing in the open-source libraries Open3D, CGAL, Cilantro. The pointcloud processing tools focus on: a) the fast and easy-to-use geometric manipulation, characterization and decomposition of point clouds directly in Rhinoceros3D, b) improving the link between CAD modelling software (Rhinoceros®) and point-cloud processing, and c) integration of point-cloud processing with other frameworks such as easy-to-use .NET programming languages (C#, IronPython, VB) via the Grasshopper interface .

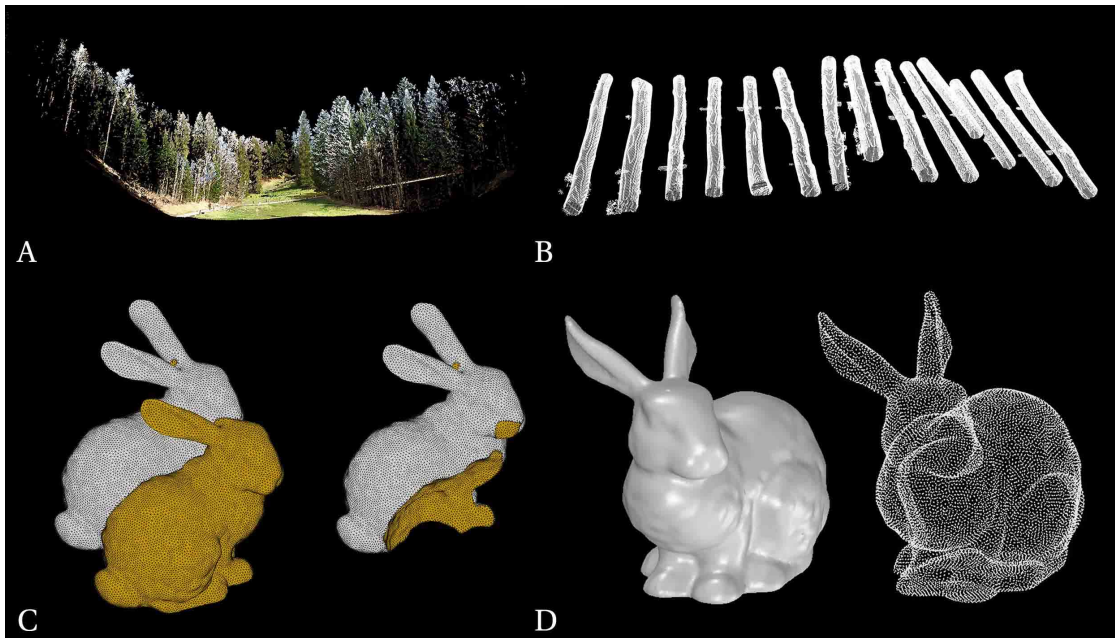


Figure C.3 – Pointcloud processing applications: a) architectural and landscape scans, b) object processing, c) mesh Boolean operations, d) point-set meshing.

---

<sup>3</sup>The framework is open-sourced: <https://github.com/9and3/Cockroach>

## C.4 FaroSharp - Laser Scanner Control for .NET Applications

FaroSharp<sup>4</sup> is a .NET library to control Faro Focus laser scanners (see Figure C.4). The library is based on the Faro C# SDK to automate the process of scanning and point-cloud transfer. There are four different types of the FaroSharp integration: a) stand-alone console application, b) Rhino plugin, c) Grasshopper plugin, and d) Unity plugin. The library is communicating with C++ SDK, and each implementation has differences. For example, the Unity application can only read .fls files line by line instead of the complete file transfer. The Grasshopper application needs to manage the garbage collector. Rhino and Console applications can use all Faro SDK methods. Additional methods are made to orient and crop point clouds without dependency on third-party software. Lastly, the interface for Unity and Rhino are developed.

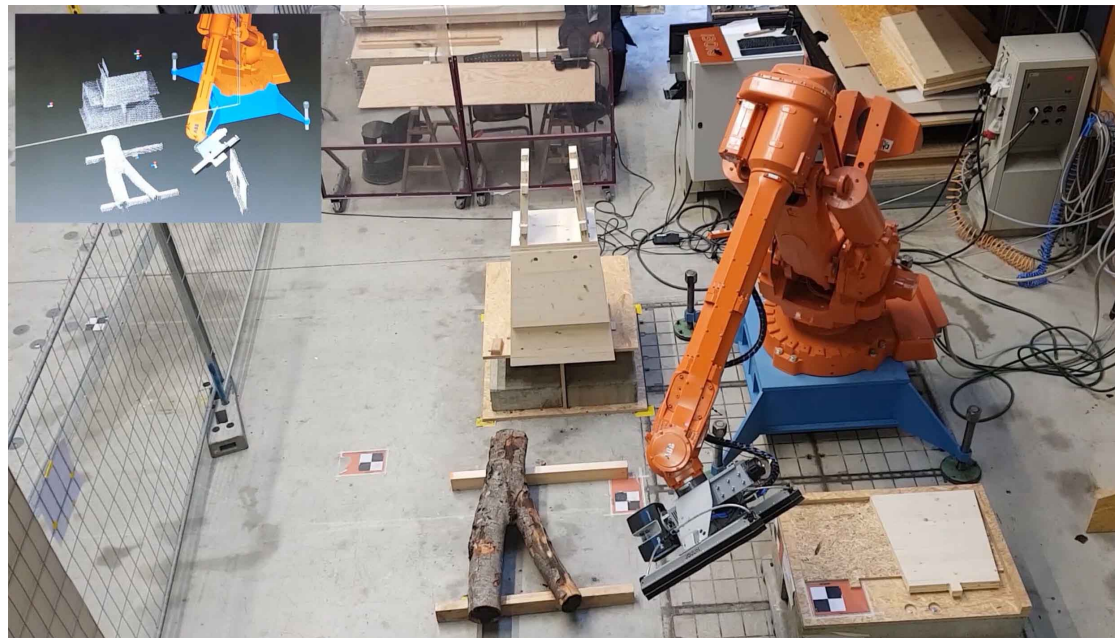


Figure C.4 – Faro integration to ABB IRB6400R (IMaxPro software): Unity point-cloud viewer (top left) and a stationary scan performed by the robot.

---

<sup>4</sup>The framework is open-sourced: <https://github.com/petasvestartas/FaroCSharp>

## C.5 IBOIS-CNC - Tool-path Generation for 5-Axis CNC

IBOIS-CNC<sup>5</sup> Grasshopper plugin translates polygonal geometry to the tool-path of the 5-Axis CNC machine Maka (see Figure C.5). The application employs the G-Code using A and B rotations and XYZ values for translation. The algorithm also considers additional methods such as the tool-changer, zero referencing, speed of movement, etc. The CAD to G-Code translation works for the following operations: milling, cutting, drilling, saw-blade movement, and engraving. The cutting methods consider bisector and translation notches. Multiple tool paths can be combined into a single path to speed the cutting process, and there is an optimization method for 2D cutting. Finally, the tool path can be simulated, and possible collisions between the CNC, the work-object, and the table can be detected.



Figure C.5 – CNC tool-path generation and simulation: a) digital model, b) physical setup.

---

<sup>5</sup>The framework is open-sourced: <https://github.com/petasvestartas/IBOIS-CNC>



# List of figures

1	Reviewed Papers	4
1.1	Research and industry workflow	6
1.2	Timber element cost and tree species in Switzerland	7
1.3	Timber strength after processing	8
1.4	Tree topologies	9
1.5	Timber use in Switzerland	10
1.6	Local timber companies	11
1.7	Timber harvesting	12
2.1	Scanning - OptiTrack and Faro Focus	14
2.2	Scanning - Photogrammetry	15
2.3	Scanning - 2D Photos	15
2.4	Scanning - ArUco markers	16
2.5	Scanning - Photogrammetry, rotating an object	16
2.6	Scanning - Artec	17
2.7	Scanning - Kinect	17
2.8	Scanning - Kinect, Indoors and Outdoors	17
2.9	Scanning - Skanect	18
2.10	Scanning - Faro Focus and Sectioning	19
2.11	Scanning - VR - phone camera	19
2.12	Scanning - CT	20
2.13	Connections - 7xCabin	21
2.14	Connections - Tree Fork Truss	22
2.15	Connections - Conceptual joining	23
2.16	Connections - Zollinger system and crooked bent wood	23
2.17	Connections - Boiler House	23
2.18	Connections - conical cross-lap	24
2.19	Connections - multi-valence joint	24
2.20	Connections - fibrous joints	25
2.21	Manual cutting, flattening	26
2.22	Robotic fabrication - milling	27
2.23	Robotic fabrication - chainsaw cutting and milling	28
2.24	Robotic fabrication - chainsaw cutting	28

## List of figures

---

2.25 Robotic fabrication - chainsaw cutting and jigs . . . . .	28
2.26 Robotic fabrication - chainsaw cutting and manual finishing . . . . .	29
2.27 Robotic fabrication - ImaxPro milling . . . . .	30
2.28 Robotic fabrication - band-saw curved cutting . . . . .	30
2.29 Robotic fabrication - band-saw cutting and re-assembly . . . . .	30
2.30 Robotic fabrication - band-saw cutting for timber boards . . . . .	30
2.31 Robotic fabrication - 5-axis CNC milling . . . . .	31
2.32 Robotic fabrication - 3-axis CNC milling - scarf joint . . . . .	31
2.33 Robotic fabrication - 3-axis CNC milling - cross-lap . . . . .	32
3.1 Historical record - straight trees . . . . .	36
3.2 Historical record - crooked trees . . . . .	36
3.3 Applications - slabs . . . . .	37
3.4 Applications - frames . . . . .	38
3.5 Applications - truss . . . . .	39
3.6 Applications - grid-shells . . . . .	40
3.7 Applications - Nexorades . . . . .	42
3.8 Applications - forked columns . . . . .	43
3.9 Applications - forked hexagonal frame . . . . .	44
3.10 Applications - forked truss . . . . .	45
3.11 Applications - column-beam system . . . . .	45
3.12 Applications - 3D truss . . . . .	46
3.13 Reaction wood . . . . .	47
3.14 Applications - crooked Zollinger system . . . . .	48
3.15 Applications - crooked Nexorade . . . . .	48
3.16 Applications - crooked wall . . . . .	49
3.17 Applications - facade cladding . . . . .	49
4.1 Thesis name explanation . . . . .	52
4.2 Small radius straight trees . . . . .	54
4.3 Multi-scalar modelling . . . . .	55
4.4 Thesis framework . . . . .	61
5.1 Joinery Solver data-types and methods . . . . .	63
5.2 Joinery Solver integration in the thesis . . . . .	64
5.3 Joinery Solver connection types . . . . .	65
5.4 Joinery Solver - Data-structures - fabrication types . . . . .	68
5.5 Joinery Solver - Data-structures - Element . . . . .	68
5.6 Joinery Solver - Data-structures - element grouping . . . . .	70
5.7 Joinery Solver - Data-structures - Tile . . . . .	70
5.8 Joinery Solver - Data-structures - graph . . . . .	71
5.9 Joinery Solver - Data-structures - Change-basis transformation . . . . .	72
5.10 Joinery Solver - Data-structures - Change-basis transformation . . . . .	72

5.11 Joinery Solver - Data-structures - Tile transformation example . . . . .	73
5.12 Joinery Solver - Data-structures - Model . . . . .	73
5.13 Joinery Solver - Search - search methods . . . . .	74
5.14 Joinery Solver - Search - curve-curve intersection . . . . .	75
5.15 Joinery Solver - Search - face-face search . . . . .	76
5.16 Joinery Solver - Search - plane-face search . . . . .	76
5.17 Joinery Solver - Search - mesh-mesh search . . . . .	77
5.18 Joinery Solver - Connection-types - side-side connection area . . . . .	78
5.19 Joinery Solver - Connection-types - side-side connection area in an angle . . . . .	78
5.20 Joinery Solver - Connection-types - side-side joint generation . . . . .	79
5.21 Joinery Solver - Connection-types - round section . . . . .	80
5.22 Joinery Solver - Connection-types - side-side profiling . . . . .	81
5.23 Joinery Solver - Connection-types - side-side connection area profile subdivision	81
5.24 Joinery Solver - Connection-types - side-side connection area in a slab . . . . .	82
5.25 Joinery Solver - Connection-types - side-side connection in a shell . . . . .	82
5.26 Joinery Solver - Connection-types - side-side connection area physical tests . . . . .	83
5.27 Joinery Solver - Connection-types - side-side short-end connections . . . . .	84
5.28 Joinery Solver - Connection-types - side-side short-end physical model . . . . .	84
5.29 Joinery Solver - Connection-types - side-side short-end in a bent beam . . . . .	85
5.30 Joinery Solver - Connection-types - side-side short-end in forks . . . . .	85
5.31 Joinery Solver - Connection-types - side-side plate example . . . . .	86
5.32 Joinery Solver - Connection-types - side-side plate examples and angles . . . . .	87
5.33 Joinery Solver - Connection-types - side-side plate with miter joints . . . . .	87
5.34 Joinery Solver - Connection-types - side-side plate with Tile rebuilding . . . . .	88
5.35 Joinery Solver - Connection-types - side-side plate example scalability . . . . .	88
5.36 Joinery Solver - Connection-types - side-side plate examples in multiple elements	89
5.37 Joinery Solver - Connection-types - side-side physical examples . . . . .	90
5.38 Joinery Solver - Connection-types - side-top connection method . . . . .	91
5.39 Joinery Solver - Connection-types - side-top connection and orientation . . . . .	92
5.40 Joinery Solver - Connection-types - side-top in beams and plates . . . . .	93
5.41 Joinery Solver - Connection-types - side-top differences in plates and beams . . . . .	93
5.42 Joinery Solver - Connection-types - side-top raw wood prototype . . . . .	94
5.43 Joinery Solver - Connection-types - side-top raw wood fork prototype . . . . .	95
5.44 Joinery Solver - Connection-types - side-top rounded . . . . .	95
5.45 Joinery Solver - Connection-types - side-top joint orientation . . . . .	96
5.46 Joinery Solver - Connection-types - side-top joint orientation in prototype . . . . .	97
5.47 Joinery Solver - Connection-types - side-top dowel-nut . . . . .	97
5.48 Joinery Solver - Connection-types - side-top extension to plates . . . . .	99
5.49 Joinery Solver - Connection-types - side-top extension to plates and scalability	100
5.50 Joinery Solver - Connection-types - side-top extension to plates - Annen . . . . .	101
5.51 Joinery Solver - Connection-types - cross-lap Tiles . . . . .	102
5.52 Joinery Solver - Connection-types - cross-lap, elements and graphs . . . . .	103

## List of figures

---

5.53 Joinery Solver - Connection-types - cross-lap, rotational assembly . . . . .	104
5.54 Joinery Solver - Connection-types - cross-lap, assemblies and graphs . . . . .	104
5.55 Joinery Solver - Connection-types - rectangular and round . . . . .	105
5.56 Joinery Solver - Connection-types - cross-lap, conical cuts . . . . .	105
5.57 Joinery Solver - Connection-types - cross-lap, connectors . . . . .	106
5.58 Joinery Solver - Connection-types - cross-lap, bending . . . . .	106
5.59 Joinery Solver - Connection-types - cross-lap, grid-shell . . . . .	106
5.60 Joinery Solver - Connection-types - cross-lap, Bunraku Theater . . . . .	107
5.61 Joinery Solver - Connection-types - cross-lap, two-layer Nexorade . . . . .	108
5.62 Joinery Solver - Connection-types - cross-lap, geometry studies . . . . .	109
5.63 Joinery Solver - Connection-types - cross-lap, connection physical tests. . . . .	110
5.64 Joinery Solver - Boolean types . . . . .	111
5.65 Joinery Solver - Mesh Boolean . . . . .	112
5.66 Joinery Solver - 2D Polyline Boolean . . . . .	112
 6.1 Scanning - Methods . . . . .	115
6.2 Scanning - Methods integration in thesis . . . . .	116
6.3 Scanning - Fabrication problem . . . . .	118
6.4 Scanning - Collection of scans . . . . .	119
6.5 Scanning - Stock of timbers from Rossiniere . . . . .	120
6.6 Scanning - Tree harvesting . . . . .	121
6.7 Scanning - Tree topologies in Rossiniere . . . . .	122
6.8 Scanning - Robot setup and aim . . . . .	124
6.9 Scanning - Calibration process . . . . .	125
6.10 Scanning - Setup . . . . .	126
6.11 Scanning - Application . . . . .	127
6.12 Scanning - Calibration goal . . . . .	128
6.13 Scanning - Calibration and Faro arm . . . . .	129
6.14 Scanning - Calibration and markers . . . . .	129
6.15 Scanning - Scanning types . . . . .	130
6.16 Scanning - Calibration tests . . . . .	131
6.17 Scanning - Calibration and multiple TCPs . . . . .	132
6.18 Scanning - Skeletonization problem . . . . .	133
6.19 Scanning - Flat-cut Skeletonization . . . . .	135
6.20 Scanning - Flat-cut Skeletonization - section fitting . . . . .	136
6.21 Scanning - Flat-cut Skeletonization . . . . .	136
6.22 Scanning - Normal estimation . . . . .	138
6.23 Scanning - Mesh Skeletonization . . . . .	138
6.24 Scanning - Mesh Skeletonization extension . . . . .	139
6.25 Scanning - Cylinder-fit Skeletonization . . . . .	140
6.26 Scanning - Cylinder-fit Unit Scale . . . . .	141
6.27 Scanning - Cylinder-fit Skeletonization Project . . . . .	142

6.28 Scanning - Cylinder-fit Skeletonization 2D Thinning . . . . .	143
6.29 Scanning - Cylinder-fit Skeletonization least-square problem . . . . .	143
6.30 Scanning - Cylinder-fit Skeletonization result . . . . .	144
6.31 Scanning - Cloud-to-cloud registration . . . . .	144
6.32 Scanning - Cloud-to-cloud registration and robotic workflow . . . . .	145
6.33 Scanning - Cockroach examples . . . . .	147
6.34 Scanning - Cockroach examples for a fork - A . . . . .	148
6.35 Scanning - Cockroach examples for a fork - B . . . . .	149
7.1 Robotic Fabrication - Workflow . . . . .	151
7.2 Robotic Fabrication - Workflow in the thesis framework . . . . .	152
7.3 Robotic Fabrication - Setup . . . . .	154
7.4 Robotic Fabrication - Jigs and test . . . . .	157
7.5 Robotic Fabrication - Jigs . . . . .	158
7.6 Robotic Fabrication - Robot jig . . . . .	160
7.7 Robotic Fabrication - Stands . . . . .	161
7.8 Robotic Fabrication - Robot jig for straight and forked beams . . . . .	162
7.9 Robotic Fabrication - Belt fixation . . . . .	163
7.10 Robotic Fabrication - Cutting tool calibration . . . . .	164
7.11 Robotic Fabrication - CNC control . . . . .	165
7.12 Robotic Fabrication - CNC simulation . . . . .	166
7.13 Robotic Fabrication - Difference between CNC and Robotic control . . . . .	167
7.14 Robotic Fabrication - Robot motion . . . . .	168
7.15 Robotic Fabrication - Robots angle rotations . . . . .	169
7.16 Robotic Fabrication - Tool-path planning . . . . .	170
7.17 Robotic Fabrication - Tools and collision detection . . . . .	171
7.18 Robotic Fabrication - Drilling . . . . .	172
7.19 Robotic Fabrication - Milling . . . . .	173
7.20 Robotic Fabrication - Saw-blade . . . . .	174
7.21 Robotic Fabrication - Tool-paths . . . . .	176
7.22 Scanning - Tree harvesting . . . . .	183
8.1 Demonstrators - Shell - Global Scheme . . . . .	186
8.2 Demonstrators - Shell - Planarization B . . . . .	187
8.3 Demonstrators - Shell - Planarization A . . . . .	188
8.4 Demonstrators - Shell - Insertion sequence . . . . .	189
8.5 Demonstrators - Shell - Box insertion angles . . . . .	189
8.6 Demonstrators - Shell - Hex-boxes . . . . .	190
8.7 Demonstrators - Shell - Arch modelling . . . . .	191
8.8 Demonstrators - Shell - Slab modelling . . . . .	191
8.9 Demonstrators - Shell - raw wood joint modelling . . . . .	192
8.10 Demonstrators - Shell - Planarization examples . . . . .	192
8.11 Appendix B - Rossiniere train station study case . . . . .	193

## List of figures

---

8.12 Demonstrators - Shell - Assembly of one box . . . . .	194
8.13 Demonstrators - Shell - Assembly of two box components . . . . .	194
8.14 Demonstrators - Shell - Assembly of a prototype . . . . .	195
8.15 Demonstrators - Shell - Method applications . . . . .	196
8.16 Demonstrators - Shell - Solid lumber application . . . . .	196
8.17 Demonstrators - Shell - raw wood application . . . . .	197
9.1 Demonstrators - Nedorades - Node valence . . . . .	200
9.2 Demonstrators - Nedorades - Platonic solids . . . . .	201
9.3 Demonstrators - Nedorades - Quad shell . . . . .	202
9.4 Demonstrators - Nedorades - Translation method . . . . .	202
9.5 Demonstrators - Nedorades - Joinery detailing . . . . .	203
9.6 Demonstrators - Nedorades - Planar edge extrusion . . . . .	203
9.7 Demonstrators - Nedorades - Fabrication of Nedorade-shell hybrid . . . . .	204
9.8 Demonstrators - Nedorades - Prototype of the Nedorade-shell hybrid . . . . .	205
9.9 Demonstrators - Nedorades - Tiling method . . . . .	207
9.10 Demonstrators - Nedorades - Tiling method and Tiles . . . . .	208
9.11 Demonstrators - Nedorades - Tiling method sequence . . . . .	208
9.12 Demonstrators - Nedorades - Tiling method and connected components . . . . .	209
9.13 Demonstrators - Nedorades - Tiling method and joinery . . . . .	209
9.14 Demonstrators - Nedorades - Tiling method examples . . . . .	210
9.15 Demonstrators - Nedorades - Tiling method and form-finding . . . . .	210
9.16 Demonstrators - Nedorades - Conical joints . . . . .	211
9.17 Demonstrators - Nedorades - Conical joint fabrication . . . . .	212
9.18 Demonstrators - Nedorades - Conical joints fabrication and scanning . . . . .	213
9.19 Demonstrators - Nedorades - Stock assignment and Hungarian algorithm . . . . .	214
9.20 Demonstrators - Nedorades - Stock and design intention . . . . .	215
9.21 Demonstrators - Nedorades - Tiling method results . . . . .	216
A.1 Appendix A - Multi-valence joint . . . . .	231
A.2 Appendix A - Forks truss and the stock . . . . .	232
A.3 Appendix A - Tree fork fabrication . . . . .	233
A.4 Appendix A - Tree fork fabrication . . . . .	234
A.5 Appendix A - Tree fork fabrication tool-paths . . . . .	235
A.6 Appendix A - Tree fork side-end joint fabrication . . . . .	236
A.7 Appendix A - Tree forks element and the prototype . . . . .	236
A.8 Appendix A - Joinery Solver and teaching . . . . .	237
A.9 Appendix A - Joinery Solver and teaching . . . . .	238
B.1 Appendix B - Rossiniere Context . . . . .	239
B.2 Appendix B - Rossiniere forest and timber products . . . . .	241
B.3 Appendix B - Rossiniere forest tree types . . . . .	242
B.4 Appendix B - Rossiniere harvesting site . . . . .	243

---

**List of figures**

B.5 Appendix B - Rossiniere sawmill . . . . .	244
C.1 Appendix C - NGon . . . . .	245
C.2 Appendix C - OpenNest . . . . .	246
C.3 Appendix C - Cockroach . . . . .	247
C.4 Appendix C - FaroSharp . . . . .	248
C.5 Appendix C - IBOIS-CNC . . . . .	249



# Bibliography

- [1] M. Olson A. Tagliasacchi, I. Alhashim and H. Zhang. Mean curvature skeletons. *Computer Graphics Forum*, 2012. doi:10.1111/j.1467-8659.2012.03178.x.
- [2] M. Agrawala, D. Phan, J. Heiser, J. Haymaker, J. Klingner, P. Hanrahan, and B. Tversky. Designing effective step-by-step assembly instructions. *ACM Transactions on Graphics*, 22(3):828–837, 2003. doi:10.1145/882262.882352.
- [3] E. Akleman, V. R. Krishnamurthy, C. A. Fu, S. G. Subramanian, M. Ebert, M. Eng, C. Starrett, and H. Panchal. Generalized abeille tiles: Topologically interlocked space-filling shapes generated based on fabric symmetries. *Computers and Graphics (Pergamon)*, 89:156–166, 2020. doi:10.1016/j.cag.2020.05.016.
- [4] I. Al-Khattat. Light Prestressed Segmented Arch (LPSA) bridges: A demonstration of sustainable engineering. *Structural Engineering International: Journal of the International Association for Bridge and Structural Engineering (IABSE)*, 18(1):62–66, 2008. doi:10.2749/101686608783726759.
- [5] G. Alemano, P. Cignoni, N. Pietroni, F. Ponchio, and R. Scopigno. Interlocking pieces for printing tangible Cultural Heritage replicas. *2014 Eurographics Workshop on Graphics and Cultural Heritage, GCH 2014*, pages 145–154, 2014. doi:10.2312/gch.20141312.
- [6] L. Allner, D. Kroehnert, and A. Rossi. Mediating Irregularity: Towards a Design Method for Spatial Structures Utilizing Naturally Grown Forked Branches. *Impact: Design With All Senses*, 2020. doi:10.1007/978-3-030-29829-6\_34.
- [7] Y. An and G. S. Schajer. Geometry-based CT scanner for measuring logs in sawmills. *Computers and Electronics in Agriculture*, 105:66–73, 2014. URL: <http://dx.doi.org/10.1016/j.compag.2014.03.007>. doi:10.1016/j.compag.2014.03.007.
- [8] Y. Anastas, L. Rhode-Barbarigos, and S. Adriaenssens. Design-to-construction workflow for cell-based pattern reciprocal free-form structures. *Journal of the International Association for Shell and Spatial Structures*, 57(2):159–176, 2016. doi:10.20898/j.iass.2016.188.737.
- [9] Angus, J. Clipper, 2020. URL: <http://www.angusj.com/delphi/clipper.php>.
- [10] A. A. Apolinarska, D. Tanadini, F. Gramazio, and M. Kohler. Using Distributed Robotic Clamps. 124:1–10, 2021.

## Bibliography

---

- [11] C. Araujo, D. Cabiddu, M. Attene, M. Livesu, N. Vining, and A. Sheffer. Surface2Volume: Surface segmentation conforming assemblable volumetric partition. *ACM Transactions on Graphics*, 38(4), 2019. doi:10.1145/3306346.3323004.
- [12] VUILD architects. Emarf. URL: <https://www.food4rhino.com/app/emarf>.
- [13] M. Attene. Shapes in a Box: Disassembling 3D Objects for Efficient Packing and Fabrication. *Computer Graphics Forum*, 34(8):64–76, 2015. doi:10.1111/cgf.12608.
- [14] J. Ballu. *Bois de marine : les bateaux naissent en foret*. Compagnie des éditions de la Lesse, Editions du Gerfaut, Aix-en-Provence, 2008.
- [15] S. S. Barnes and R. C. Green. From Tongan meeting house to Samoan chapel: A recent Tongan origin for the Samoan fale afolau. *Journal of Pacific History*, 43(1):23–49, 2008.
- [16] M. Batchelar and M. Newcombe. Hollow timber poles: Te Wharehouse O Tuhoe Living Building Challenge. *WCTE 2014 - World Conference on Timber Engineering, Proceedings*, pages 1–2, 2014.
- [17] M. Batchelar and M. Newcombe. Structures Using Hollow Timber Poles. *Australasia Structural Engineering Conference*, pages 1–2, 2014.
- [18] P. Baudisch, A. Silber, Y. Kommana, M. Gruner, L. Wall, K. Reuss, L. Heilman, R. Kovacs, D. Rechlitz, and T. Roumen. Kyub. (Chi):1–12, 2019. doi:10.1145/3290605.3300796.
- [19] O. Baverel, H. Nooshin, and Y. Kuroiwa. Configuration processing of Nexorade using genetic algorithm, 2004.
- [20] O. L. S. Baverel. *Nexorades: A Family of Interwoven Space Structures*. Thesis (doctoral), University of Surrey, 2000. URL: <http://epubs.surrey.ac.uk/id/eprint/795820>.
- [21] A. Berglund, O. Broman, A. Gronlund, and M. Fredriksson. Improved log rotation using information from a computed tomography scanner. *Computers and Electronics in Agriculture*, 2013. doi:10.1016/j.compag.2012.09.012.
- [22] F. Bianconi and M. Filippucci. Innovative Techniques of Representation in Architectural Design. *Digital Wood Design*, 24(February 2020):1524, 2019. URL: <http://link.springer.com/10.1007/978-3-030-03676-8>, doi:10.1007/978-3-030-03676-8.
- [23] D. Bozsaky. Historical Development and Special Building Structures of In-earth Embedded Houses. *Acta Technica Jaurinensis*, 8(2):113, 2015.
- [24] L. D. Brit and Carlito C. J. Types of Connections for Structural Elements Roundwood used in Brazil. *WCTE*, 2012.
- [25] A. Bukauskas. New structural systems in small-diameter round timber. *MIT Master Thesis*, page 53, 2015.

- [26] A. Bukauskas, P. Mayencourt, and P. Shepherd. Whole timber construction: A state of the art review. *Construction and Building Materials*, 213:748–769, 2019. doi:10.1016/j.conbuildmat.2019.03.043.
- [27] M. J. M. Burgos, H. S. A. de Toledo, R. A. G. Lezcano, and A. G. de Mera. The sedentary process and the evolution of energy consumption in eight native American dwellings: Analyzing sustainability in traditional architecture. *Sustainability (Switzerland)*, 12(5):1–28, 2020. doi:10.3390/su12051810.
- [28] R. Burton, M. Dickson, and R. Harris. The use of roundwood thinnings in buildings – a case study. *Building Research and Information*, 26(2):76–93, 1998. doi:10.1080/096132198370001.
- [29] CEN European Committee for Standardization. EN 338: Structural timber - Strength classes. Technical report, 2016.
- [30] M. Chablot and P. Dupraz. Forestry School in Lyss. *Structural Engineering International*, 10(1):14–15, 2000. doi:10.2749/101686600780620928.
- [31] L. Chen and L. Sass. Fresh Press Modeler: A generative system for physically based low fidelity prototyping. *Computers and Graphics (Pergamon)*, 54:157–165, 2016. doi:10.1016/j.cag.2015.07.003.
- [32] X. Chen, H. Li, C. W. Fu, H. Zhang, D. Cohen-Or, and B. Chen. 3D fabrication with universal building blocks and pyramidal shells. *SIGGRAPH Asia 2018 Technical Papers*, *SIGGRAPH Asia 2018*, 37(6), 2018. doi:10.1145/3272127.3275033.
- [33] Y. S. Chen and W. H. Hsu. A modified fast parallel algorithm for thinning digital patterns. *Pattern Recognition Letters*, 7(2):99–106, 1988. doi:10.1016/0167-8655(88)90124-9.
- [34] P. Cignoni, N. Pietroni, L. Malomo, and R. Scopigno. Field-aligned mesh joinery. *ACM Transactions on Graphics*, 33(1):1–12, 2014. doi:10.1145/2537852.
- [35] R. W. Conners, C. W. Mcmillin, K. Lin, and R. E. Vasquez-Espinosa. Identifying and Locating Surface Defects in Wood: Part of an Automated Lumber Processing System. *IEEE Transactions on Pattern Analysis and Machine Intelligence*, PAMI-5(6):573–583, 1983. doi:10.1109/TPAMI.1983.4767446.
- [36] G. Decio, D. V. Luciano, L. C. Andre, and F. A. R. Lahr. Tree-Shaped Timber Structural System: An Ecological Way of Designing Spatial Structure. *Journal of Civil Engineering Research*, 4(1):1–7, 2014. doi:10.5923/j.jce.20140401.01.
- [37] P. Delorme. *Illustrations de Nouvelles inventions pour bien bastir et a petits fraiz* (1561). Republished in 2003 by Okmhistoire, 1561.
- [38] E. Denison and G. Ren. Transgression and progress in China: Wang Shu and the literati mindset. *Architectural Design*, 83(6):38–43, 2013. doi:10.1002/ad.1672.

## Bibliography

---

- [39] M. Deuss, A. Deleuran, S. Bouaziz, B. Deng, D. Piker, and M. Pauly. ShapeOp—A Robust and Extensible Geometric Modelling Paradigm. In *Modelling Behaviour*. 2015. doi: 10.1007/978-3-319-24208-8\_42.
- [40] C. Douthe and O. Baverel. Morphological and Mechanical Investigation of Double-Layer Reciprocal Structures. *Nexus Network Journal*, 16:191–206, 2014. doi:10.1007/s00004-014-0185-9.
- [41] N. Duncan, L. F. Yu, and S. K. Yeung. Interchangeable components for hands-on assembly based modelling. *ACM Transactions on Graphics*, 35(6):1–14, 2016. doi: 10.1145/2980179.2982402.
- [42] A. V. Dyskin, Y. Estrin, A. J. Kanel-Belov, and E. Pasternak. Topological interlocking of platonic solids: A way to new materials and structures. *Philosophical Magazine Letters*, 83(3):197–203, 2003. doi:10.1080/0950083031000065226.
- [43] J. J. Edward. *A user's guide to principal components*. Wiley series in probability and mathematical statistics. Wiley, 1991.
- [44] J. Enns. Intelligent wood assemblies: Incorporating found geometry and natural material complexity. *Architectural Design*, 2010. doi:10.1002/ad.1171.
- [45] G. Erber, F. Holzleitner, M. Kastner, and K. Stampfer. Effect of multi-tree handling and tree-size on harvester performance in small-diameter hardwood thinnings. *Silva Fennica*, 50(1):1–17, 2016. doi:10.14214/sf.1428.
- [46] P. Eversmann, F. Gramazio, and M. Kohler. Robotic prefabrication of timber structures: towards automated large-scale spatial assembly. *Construction Robotics*, 1(1-4):49–60, 2017. doi:10.1007/s41693-017-0006-2.
- [47] K. Evgeny and Skjold L. *Historic Wooden Architecture in Europe and Russia*. 2015. doi:10.1515/9783035605426.
- [48] Paul A. F. Neue projektbezogene Anwendungen von Holzbauelementen an der Westküste von Kanada. *Holzbau-Forum*, 2020.
- [49] W. Fairham. *Woodwork Joints*. Anboco, 2016.
- [50] G. Fallacara, M. Barberio, and M. Colella. *Topological interlocking blocks for architecture: From flat to curved morphologies*, volume 282. Springer International Publishing, 2019. URL: [http://dx.doi.org/10.1007/978-3-030-11942-3\\_14](http://dx.doi.org/10.1007/978-3-030-11942-3_14), doi:10.1007/978-3-030-11942-3\_14.
- [51] J. I. Fernandez-Golfin, M. R. Diez-Barra, E. Hermoso, and R. Mier. Mechanical characterization of visually classified, small-diameter laricio pine round timber. *Spanish Journal of Agricultural Research*, 5(3):304–311, 2007. doi:10.5424/sjar/2007053-251.
- [52] M. Fischler and R. Bolles. RANSAC. *Graphics and Image Processing*, 24(6):381–395, 1981.

- [53] European Science Foundation. The Reconstruction of the Danubian Neolithic House and the Scientific Importance of Architectural Studies. pages 5–9, 2013.
- [54] M. Fredriksson. Log sawing position optimization using computed tomography scanning. *Wood Material Science and Engineering*, 9:110–119, 2014. doi:10.1080/17480272.2014.904430.
- [55] U. Frick, T. V. Mele, and P. Block. Decomposing Three-Dimensional Shapes into Self-supporting, Discrete-Element Assemblies. *Modelling Behaviour*, pages 187–201, 2015. doi:10.1007/978-3-319-24208-8.
- [56] C. W. Fu, P. Song, X. Yan, L. W. Yang, P. K. Jayaraman, and D. Cohen-Or. Computational interlocking furniture assembly. *ACM Transactions on Graphics*, 34(4):1–11, 2015. doi:10.1145/2766892.
- [57] M. Fujimoto, S. Katayama, and T. Kaname. Numerical study on effect of member length error on structural properties of single layer pin-joined grid dome composed of wooden truss system. (October):444–455, 2009. URL: <https://riunet.upv.es/handle/10251/6536>.
- [58] F. Giudiceandrea, E. Ursella, and V. Enrico. PRÄSENTATION - A high speed CT scanner for the sawmill industry. *Forestry Journal*, (July 2015):22, 2011.
- [59] T. Gobin, R. Mesnil, C. Douthe, P.e Margerit, N. Ducoulombier, L. Demont, H. Delmi, and J. Caron. Form Finding of Nedorades Using the Translations Method. In *Robotic Fabrication in Architecture, Art and Design 2018*, pages 232–241. sep 2019. doi:10.1007/978-3-319-92294-2\_18.
- [60] J. GonzalezdeTanago, A. Lau, H. Bartholomeus, M. Herold, V. Avitabile, P. Raumonen, C. Martius, R. C. Goodman, M. Disney, and S. Manuri. Estimation of above-ground biomass of large tropical trees with terrestrial lidar. *Methods in Ecology and Evolution*, 2018. doi:10.1111/2041-210X.12904.
- [61] R Gower, A Heydtmann, and H Petersen. Lego: Automated Model Construction. *European Study Group with Industry*, pages 81–94, 1998.
- [62] R. Gundersen. US14136253. (12), 2014.
- [63] A. Guttman. R-trees: A dynamic index structure for spatial searching. In *Proceedings of the ACM SIGMOD International Conference on Management of Data*, 1984. doi:10.1145/602259.602266.
- [64] B. Hahn. Upscaling of friction welding of wood for structural applications. 2014. URL: <http://infoscience.epfl.ch/record/202191>, doi:10.5075/epfl-thesis-6442.
- [65] J. Hallenberg. Robot Tool Center Point Calibration using Computer Vision. *Master Thesis in Computer Vision*, 2007.

## Bibliography

---

- [66] P. Haller and M. Cavarese. A new approach to free form wooden shell structures using helical cuts. *Proceedings of the IASS Annual Symposium 2019 – Structural Membranes 2019 Form and Force*, pages 1684–1695, 2019.
- [67] F. Heller, J. Thar, D. Lewandowski, M. Hartmann, P. Schoonbrood, S. Stonner, S. Voelker, and J. Borchers. CutCAD - An open-source tool to design 3D objects in 2D. *DIS 2018 - Proceedings of the 2018 Designing Interactive Systems Conference*, pages 1135–1140, 2018. doi:10.1145/3196709.3196800.
- [68] T. Herzog, J. Natterer, R. Schweitzer, M. Volz, and W. Winter. *Timber Construction Manual*. 2013. doi:10.11129/detail.9783034614634.
- [69] K. Hildebrand, B. Bickel, and M. Alexa. Crdbrd: Shape Fabrication by Sliding Planar Slices. *Computer Graphics Forum*, 31:583–592, 2012. doi:10.1111/j.1467-8659.2012.03037.x.
- [70] M. Holroyd, I. Baran, J. Lawrence, and W. Matusik. Computing and Fabricating Multi-layer Models. *ACM Transactions on Graphics*, 30(6):1–8, 2011. doi:10.1145/2070781.2024221.
- [71] K. Hormann and M. S. Floater. Mean value coordinates for arbitrary planar polygons. *ACM Transactions on Graphics*, 25:1424–1441, 2006. URL: <http://dl.acm.org/doi/10.1145/1183287.1183295>, doi:10.1145/1183287.1183295.
- [72] P. Huybers. Timber Pole Space Structures. *SAGE*, 1:653–660, 1986.
- [73] P. Huybers. Wooden poles for larger structural applications. *Space Structures 5*, pages 1: 173–183, 2002. doi:10.1680/ss5v1.31739.0019.
- [74] K. Imai, Y. Fujita, T. Furukawa, K. Wakiyama, S. Tsujioka, M. Fujimoto, M. Inada, A. Takino, and M. Yoshinaga. Development of the KT-wood space truss system with round timber as a new structural material. *Space Structures 5*, pages 1: 155–160, 2002. doi:10.1680/ss5v1.31739.0017.
- [75] ISO6983. Automation systems and integration—numerical control of machines. program format and definitions of address words—part 1: Data format for positioning, line motion and contouring control systems, 2009.
- [76] A. Jacobson. RodSteward: A Design-to-Assembly System for Fabrication using 3D-Printed Joints and Precision-Cut Rods. *Computer Graphics Forum*, 38(7):765–774, 2019. doi:10.1111/cgf.13878.
- [77] R. L. Johns and N. Foley. Bandsawn Bands. *Robotic Fabrication in Architecture, Art and Design 2014*, pages 17–33, 2014. doi:10.1007/978-3-319-04663-1.
- [78] Darius K. Cedar River Trestle Bridge. *Maple Valley Historical Society Archive*, 1925.
- [79] Dunkelberg K. *IL 31 Bambus - Bamboo*. Karl Karmee Verlag, Stuttgart, Germany, 1985.

- [80] A. J. Kanel-Belov, A. V. Dyskin, Y. Estrin, E. Pasternak, and I. A. Ivanov-Pogodaev. Interlocking of convex polyhedra: Towards a geometric theory of fragmented solids. *Moscow Mathematical Journal*, 10(2):337–342, 2010. doi:10.17323/1609-4514-2010-10-2-337-342.
- [81] G. G. Karlsen, W.W. Bolszakow, M. E. Kagan, and Swiencicki G. *Kurs dieriewiannych konstrukcij cz. I i II*, G. I. C. L. Moskwa, Leningrad. 1943.
- [82] S. Kieran and J. Timberlake. *Refabricating Architecture: How Manufacturing Methodologies are Poised to Transform Building Construction*. Architectural Record S. McGraw-Hill Education, 2004. URL: <https://books.google.fr/books?id=PkxQKygXe2cC>.
- [83] J. W. Kim, K. K. Kang, and J. H. Lee. Survey on automated LEGO assembly construction. *22nd International Conference in Central Europe on Computer Graphics, Visualization and Computer Vision, WSCG 2014, Poster Papers Proceedings - in co-operation with EUROGRAPHICS Association*, pages 89–96, 2014.
- [84] O. D. Krieg and O. Lang. Adaptive automation strategies for robotic prefabrication of parametrized mass timber building components. *Proceedings of the 36th International Symposium on Automation and Robotics in Construction, ISARC 2019*, pages 521–528, 2019. doi:10.22260/isarc2019/0070.
- [85] V. R. Krishnamurthy, E. Akleman, S. G. Subramanian, K. Boyd, C. A. Fu, M. Ebert, C. Starrett, and N. Yadav. Bi-axial woven tiles: Interlocking space-filling shapes based on symmetries of bi-axial weaving patterns. *Proceedings - Graphics Interface*, 2020-May, 2020.
- [86] P. Kvetina and V. Hrncir. Between Archaeology and Anthropology: Imagining Neolithic Settlements. *Anthropologie (Brno)*, 51(2):323–347, 2013.
- [87] N. M. Larsen and A. K. Aagaard. Exploring Natural Wood. *ACADIA19*, pages 500–509, 2019.
- [88] B. Law. Roundwood timber framing. 2009. URL: <http://mirlyn.lib.umich.edu/Record/007298400>.
- [89] J Lim, J. Oh, H. Yeo, and J. Lee. Behavior of center-bored round timber beams in center-point bending test. *Journal of Wood Science*, 59(5):389–395, 2013. doi:10.1007/s10086-013-1346-2.
- [90] Y. Liu, Pottmann H., J. Wallner, Y. Yang, and W. Wang. Geometric modeling with conical meshes and developable surfaces. *ACM Transactions on Graphics*, 25(3):681–689, 2006. doi:10.1145/1141911.1141941.
- [91] A. Lokaj and K.a Klajmonova. Round timber bolted joints reinforced with modified washers and self-drilling screws. *Perspectives in Science*, 7:261–265, 2016. doi:10.1016/j.pisc.2015.12.001.

## Bibliography

---

- [92] R. C. Bolles M. A. Fischler. Random sample consensus: A paradigm for model fitting with applications to image analysis and automated cartography. *SRI International*, 1980.
- [93] M. Bolitho M. Kazhdan and H. Hoppe. Poisson surface reconstruction. *Eurographics Symposium on Geometry Processing*, 2006.
- [94] T. Igarashi M. Larsson, H. Yoshida. Human-in-the-loop fabrication of 3d surfaces with natural tree branches. 2019.
- [95] T. Igarashi M. Larsson, H. Yoshida. Human-in-the-loop fabrication of 3d surfaces with natural tree branches. *Proceedings of the ACM Symposium on Computational Fabrication - SCF '19*, 2019. doi:10.1145/3328939.3329000.
- [96] S. Magrisso and A. Zoran. Digital joinery for hybrid carpentry. *Lecture Notes in Civil Engineering*, 24:441–461, 2019. doi:10.1007/978-3-03676-8\_16.
- [97] C. Malcolm, J. Cairns, and C. Gulland. The development of roundwood timber pole structures for use on rural community technology projects. *Construction and Building Materials*, 17(4):269–279, 2003. doi:10.1016/S0950-0618(02)00114-9.
- [98] A. Markku, P. Raumonen, M. Kaasalainen, and Casella E. Analysis of geometric primitives in quantitative structure models of tree stems. *Remote Sensing*, 2015. doi:10.3390/rs70404581.
- [99] D. J. M. Marshall. Unmaking Architecture : Holding Patterns for Misfit Matter. *University of Cambridge*, 2019.
- [100] C. Mattheck. Learning from trees. *Design in Nature*, 1998.
- [101] P. Matthew. On Naval Timber and Arboriculture. *Harvard University*, 1831.
- [102] R. Mesnil, C. Douthe, O. Baverel, and T. Gobin. Form finding of nexorades using the translations method. *Automation in Construction*, 95:142–154, 2018. doi:10.1016/j.autcon.2018.08.010.
- [103] B. Misztal. *Wooden Domes. History and Modern Times.* Springer, Wroclaw Poland, 2017.
- [104] Z. Mollica and M. Self. Tree Fork Truss: An Architecture of Inherent Forms. *Design and Make*, 2016. URL: <http://zacharymolli.ca/assets/download/Mollica-DMThesis-Tree-Fork-Truss-an-Architecture-of-Inherent-Forms.pdf>.
- [105] Z. Mollica and M. Self. Tree fork truss: geometric strategies for exploiting inherent material form. *Advances in Architectural Geometry 2015*, 2016. doi:10.3218/3778-4\_11.
- [106] V. Monier, J. C. Bignon, and G. Duchanois. Use of irregular wood components to design non-standard structures. *Advanced Materials Research*, 671-674:2337–2343, 2013. doi:10.4028/www.scientific.net/AMR.671-674.2337.

- [107] E. Moore. The shortest path through a maze. 1959.
- [108] J. H. Mork. Reindeer. 2019. URL: <https://www.food4rhino.com/app/reindeer>.
- [109] H. Morris, M. Batchelar, and K. Teh. Full strength round timber pole connection using annular grooves. In *10th World Conference on Timber Engineering 2008*, 2008.
- [110] A. K. Aagaard N. M. Larsen. Robotic processing of crooked saw logs for use in architectural construction. *Design Modelling Symposium Berlin 2020*, 2020.
- [111] J Natterer. A way to sustainable architecture by new technologies for engineered timber structures. *NattererBCN*, 2006.
- [112] A. Nguyen, Vestartas P., and Weinand Y. Design framework for the structural analysis of free-form timber plate structures using wood-wood connections. *Automation in Construction*, 107:102948, 2019. doi:<https://doi.org/10.1016/j.autcon.2019.102948>.
- [113] A. C. Nguyen, B. Himmer, P. Vestartas, and Y. Weinand. Performance assessment of double-layered timber plate shells using alternative structural systems. *Proceedings of the IASS Symposium 2019 – Structural Membranes 2019*, pages 8. 2919–2926, 2019.
- [114] J. Oja, Lars Wallbacks, S. Grundberg, E. Hagerdal, and A. Gronlund. Automatic grading of Scots pine (*Pinus sylvestris L.*) sawlogs using an industrial X-ray log scanner. *Computers and Electronics in Agriculture*, 41(1-3):63–75, 2003. doi:[10.1016/S0168-1699\(03\)00042-5](https://doi.org/10.1016/S0168-1699(03)00042-5).
- [115] Seray Ozden, Duncan Slater, and Roland Ennos. Fracture properties of green wood formed within the forks of hazel (*Corylus avellana L.*). *Trees - Structure and Function*, 31(3):903–917, 2017. doi:[10.1007/s00468-016-1516-0](https://doi.org/10.1007/s00468-016-1516-0).
- [116] Vestartas P. and Settimi A. Cockroach: A plug-in for point cloud post-processing and meshing in Rhino environment, 2020. URL: <https://github.com/9and3/Cockroach>.
- [117] C J Panckoucke. *Encyclopedie methodique: Marine.* chez Panckoucke, 1786. URL: <https://books.google.ch/books?id=Z4RQqs2bseoC>.
- [118] T. Patrick and P. Blair. (12) US9605431B2. 2(12), 2017.
- [119] T. Pawlofsky. Individual Robotic Production Processes. *Robots in Architecture*, pages 167–172, 2013.
- [120] R. Peters. Geographical point cloud modelling with the 3d medial axis transform. *PhD Thesis*, 2018.
- [121] Julio César Pigozzo. The first composed log-concrete deck bridge in Brazil Methodology The Computation Model. 1982.

## Bibliography

---

- [122] D. Piker. Kangaroo: Form Finding with Computational Physics. volume 83. John Wiley & Sons, Ltd, 2013. URL: <http://doi.wiley.com/10.1002/ad.1569>, doi:10.1002/ad.1569.
- [123] L. O. Popovic. Reciprocal Frame (RF) Structures: Real and Exploratory. *Nexus Network Journal*, 16:119–134, 2014. doi:10.1007/s00004-014-0181-0.
- [124] H. Pottmann, C. Jiang, M. Hobinger, J. Wang, P. Bompas, and J. Wallner. Cell packing structures. *CAD Computer Aided Design*, 60:70–83, 2015. URL: <http://dx.doi.org/10.1016/j.cad.2014.02.009>, doi:10.1016/j.cad.2014.02.009.
- [125] A. Rais, E. Ursella, E. Vicario, and F. Giudiceandrea. The use of the first industrial X-ray CT scanner increases the lumber recovery value: case study on visually strength-graded Douglas-fir timber. *Annals of Forest Science*, 2017. doi:10.1007/s13595-017-0630-5.
- [126] M. H. Ramage, H. Burridge, M. Busse-Wicher, G. Fereday, T. Reynolds, D. U. Shah, G. Wu, L. Yu, P. Fleming, D. Densley-Tingley, J. Allwood, P. Dupree, P. F. Linden, and O. Scherman. The wood from the trees: The use of timber in construction. *Renewable and Sustainable Energy Reviews*, 68(October 2016):333–359, 2017. doi:10.1016/j.rser.2016.09.107.
- [127] A. Ranta-Maunus. Round small-diameter timber for construction: Final report of project FAIR CT 95-0091. *VTT Publications*, (383), 1999.
- [128] P. Raumonen, E. Casella, K. Calders, S. Murphy, M. Åkerbloma, and Kaasalainen M. Massive-scale tree modelling from tls data. *ISPRS Annals of Photogrammetry, Remote Sensing and Spatial Information Sciences*, 2015. doi:10.5194/isprsannals-II-3-W4-189-2015.
- [129] P. Raumonen, M. Kaasalainen, M. Åkerblom, S. Kaasalainen, H. Kaartinen, M. Vastaranta, M. Holopainen, M. Disney, and P. Lewis. Fast automatic precision tree models from terrestrial laser scanner data. *Remote Sensing*, 2013. doi:10.3390/rs5020491.
- [130] A. Rezaei Rad. *Mechanical Characterization of Integrally-Attached Timber Plate Structures: Experimental studies and macro modeling technique*. Doctoral dissertation, École Polytechnique Fédérale de Lausanne (EPFL), 2020. doi:10.5075/EPFL-THESIS-8111.
- [131] A. Rezaei Rad, H. Burton, N. Rogeau, P. Vestertas, and Y. Weinand. A framework to automate the design of digitally-fabricated timber plate structures. *Computers & Structures*, 244:106456, 2021. doi:<https://doi.org/10.1016/j.compstruc.2020.106456>.
- [132] A. Rinnhofer, A. Petutschnigg, and J. P. Andreu. Internal log scanning for optimizing breakdown. *Computers and Electronics in Agriculture*, 41(1-3):7–21, 2003. doi:10.1016/S0168-1699(03)00039-5.
- [133] M. Rippmann, T. V. Mele, M. Popescu, E. Augustynowicz, T. M. Echenagucia, C. C. Barentin, U. Frick, and P. Block. The Armadillo Vault: Computational Design and

- Digital Fabrication of a. *Advances in Architectural Geometry 2016*, pages 344–363, 2016. doi:10.3218/3778-4.
- [134] C. Robeller. Integral mechanical attachment for timber folded plate structures. *EPFL PhD Thesis*, 2015. doi:10.5075/epfl-thesis-6564.
- [135] C. Robeller. TPS. 2017. URL: <https://www.food4rhino.com/app/timber-plate-structures-tps>.
- [136] C. Robeller, M. Konakovic, M. Dedijer, M. Pauly, and Y. Weinand. Double-layered timber plate shell. *International Journal of Space Structures*, 2017. doi:10.1177/0266351117742853.
- [137] C. Robeller and Y. Weinand. A 3D cutting method for integral 1DOF multiple-tab-and-slot joints for timber plates, using 5-axis CNC cutting technology. *WCTE 2016 - World Conference on Timber Engineering*, 2016.
- [138] Robert McNeel & Associates. Rhinoceros3D, 2020. URL: <https://developer.rhino3d.com/api/RhinoCommon/>.
- [139] J. Rodrigues, A. Dias, and P. Providencia. Timber-concrete composite bridges: State-of-the-art review. *BioResources*, 8(4):6630–6649, 2013. doi:10.15376/biores.8.4.6630–6649.
- [140] A. Rossi and O. Tessmann. *From Voxels to Parts: Hierarchical Discrete Modeling for Design and Assembly*, volume 809. Springer International Publishing, 2019. URL: <http://link.springer.com/10.1007/978-3-319-95588-9>, doi:10.1007/978-3-319-95588-9.
- [141] D. Rutten. Galapagos: On the logic and limitations of generic solvers. *Architectural Design*, 83(2):132–135, 2013. doi:10.1002/ad.1568.
- [142] J. Rykwert. *On Adam's house in Paradise : the idea of the primitive hut in architectural history*. MIT Press, Cambridge Massachusetts, 1981.
- [143] A. Schiftne, M. Hobinger, J. Wallner, and H. Pottmann. Packing circles and spheres on surfaces. *ACM Transactions on Graphics*, 28(5):1–8, 2009. doi:10.1145/1618452.1618485.
- [144] C. Schindler, M. Tamke, A. Tabatabai, M. Bereuter, and H. Yoshida. Processing branches: Reactivating the performativity of natural wooden form with contemporary information technology. *International Journal of Architectural Computing*, 12:101–115, 2014. doi:10.1260/1475-472X.12.2.101.
- [145] V. Segal, T. Black, E. Geske, D. Kretschmann, A. Gjinolli, D. Russell, N. Speer, and P. Gramaud. Small Diameter Log Evaluation for Value Added Structural Applications. *Wood Engineering*, 50(8996):48–58, 2000.

## Bibliography

---

- [146] M. Self and Z. Mollica. Tree Fork Truss. *Advances in Architectural Geometry 2016*, 2016. doi:10.3218/3778-4.
- [147] B. Senechal, C. Douthe, and O. Baverel. Analytical Investigations on Elementary Nexus orades. *Int. J. Space Struct.* 26 (4) (2011) 313–320, 2011. doi:<https://doi.org/10.1260/0266-3511.26.4.313>.
- [148] B. Sheil. *High definition : zero tolerance in design and production / guest-edited by Bob Sheil*. Number 227. 2014.
- [149] R. Shmulsky and P. D. Jones. *Forest Products and Wood Science An Introduction: Sixth Edition*. 2011. doi:10.1002/9780470960035.
- [150] P. Siekański, K. Magda, K. Malowany, J. Rutkiewicz, A. Styk, J. Krzesłowski, T. Kowaluk, and A. Zagórski. On-line laser triangulation scanner for wood logs surface geometry measurement. *Sensors (Switzerland)*, 2019. doi:10.3390/s19051074.
- [151] J. Skinner, C. Martins, J. Bregulla, R. Harris, K. Paine, P. Walker, and A. M.P.G. Dias. Concrete upgrade to improve the vibration response of timber floors. *Proceedings of the Institution of Civil Engineers: Structures and Buildings*, 167(9):1–10, 2014. doi:10.1680/stbu.13.00057.
- [152] J. Skog. Combining X-ray and 3D scanning of logs. *Wood Science and Technology*, page 81, 2009.
- [153] D. Slater, R. S. Bradley, P. J. Withers, and R. A. Ennos. The anatomy and grain pattern in forks of hazel (*Corylus avellana L.*) and other tree species. *Trees - Structure and Function*, 28(5):1437–1448, 2014. doi:10.1007/s00468-014-1047-5.
- [154] D. Slater and A. R. Ennos. Determining the mechanical properties of hazel forks by testing their component parts. *Trees - Structure and Function*, 27(6):1515–1524, 2013. doi:10.1007/s00468-013-0898-5.
- [155] P. Song, C. W. Fu, Y. Jin, H. Xu, L. Liu, P. A. Heng, and D. Cohen-Or. Reconfigurable interlocking furniture. *ACM Transactions on Graphics*, 36(6), 2017. doi:10.1145/3130800.3130803.
- [156] P. Song, F. C. Wing, P. Goswami, J. Zheng, N. J. Mitra, and D. Cohen-Or. Reciprocal frame structures made easy. *ACM Transactions on Graphics*, 2013. URL: <http://dl.acm.org/citation.cfm?doid=2461912.2461915>, doi:10.1145/2461912.2461915.
- [157] C. Stanton. Digitally Mediated Use of Localized Material in Architecture. *Sigradi*, pages 228–231, 2010.
- [158] T. Svilans. Glulamb, 2020. URL: <https://www.food4rhino.com/app/glulamb>.

- [159] T. Svilans, J. Runberger, and K. Strehlke. Agency of Material Production Feedback in Architectural Practice. *Design Transactions*, pages 98–105, 2020. doi:10.2307/j.ctv13xprf6.19.
- [160] T. Svilans, M. Tamke, M. R. Thomsen, J. Runberger, K. Strehlke, and M. Antemann. New workflows for digital timber. In *Lecture Notes in Civil Engineering*. 2019. doi:10.1007/978-3-030-03676-8\_3.
- [161] The CGAL Project. *CGAL User and Reference Manual*. CGAL Editorial Board, 5.2.1 edition, 2021. URL: <https://doc.cgal.org/5.2.1/Manual/packages.html>.
- [162] L. Thomas, L. Mili, E. Thomas, and C. A. Shaffer. Defect detection on hardwood logs using laser scanning. *Wood and Fiber Science*, 38(4):682–695, 2006.
- [163] U. Thonnissen. *Hebelstabwerke : Tradition und Innovation = Reciprocal frameworks : tradition and innovation*. GTA-Verlag, 2015.
- [164] U Thonnissen. Reciprocal Frameworks - Tradition and Innovation. 2015.
- [165] P. Thornton and P. Blair. (12) Patent Application Publication ( 10 ) Pub. No.: US 2016 / 0271610 A1 Patent Application Publication. 1(19):1–5, 2016.
- [166] O. O. Torghabehi, P. von Buelow, K. Vliet, and S. Mankouche. Limb : Inventory-constrained design method for application of natural tree crotches as heavy timber joinery. *TxA*, (November), 2018.
- [167] E. Vercruyse, Z. Mollica, and D. Pradeep. Altered Behaviour: The Performative Nature of Manufacture Chainsaw Choreographies + Bandsaw Manoeuvres. In *Robotic Fabrication in Architecture, Art and Design 2018*. 2019. doi:10.1007/978-3-319-92294-2\_24.
- [168] P. Vestartas. NGon: Tool for mesh processing and engineering design, 2021. URL: <https://github.com/petasvestartas/NGon>, doi:10.5281/zenodo.4550592.
- [169] P. Vestartas, L. Palletier, M. T. Nakad, A. R. Rad, and Y. Weinand. Segmented Spiral Using Inter-Connected Timber Elements. *IASS 2019 Barcelona Symposium: Timber and Bio-based Structures*, 2019.
- [170] P. Vestartas, A. Rezaei Rad, and Y. Weinand. Robotically-Fabricated Nedorades from Whole Timber. *International fib Symposium on the Conceptual Design of Structures*, 2021.
- [171] P. Vestartas, N. Rogeau, and J. Gamerro. *Modelling Workflow for Segmented Timber Shells Using Wood-Wood Connections*. Springer International Publishing, 2020. URL: [http://dx.doi.org/10.1007/978-3-030-29829-6\\_46](http://dx.doi.org/10.1007/978-3-030-29829-6_46), doi:10.1007/978-3-030-29829-6.
- [172] P. Vestartas and Y. Weinand. Joinery Solver for Whole Timber Structures. *WCTE2020*, 2020.

## Bibliography

---

- [173] L. Vestarte, P. Vestartas, and R. Kucinskas. Corrugated Cardboard Shell: A pavilion Project of An Architectural Workshop. *Advances in Architectural Geometry (AAG)*, 2020.
- [174] P. von Buelow. Paragen: Performative exploration of generative systems. *Journal of the International Association for Shell and Spatial Structures*, 53(174):271–284, 2012.
- [175] P. von Buelow. The combination of SQL database queries and stochastic search methods used to explore generative design solutions. *IASS*, (October 2019):1163–1170, 2019.
- [176] P. von Buelow, O. O. Torghabehi, S. Mankouche, and K. Vliet. Combining parametric form generation and design exploration to produce a wooden reticulated shell using natural tree crotches. *Proceedings of the International Association for Shell and Spatial Structures (IASS) Symposium IASS 2018*, (July), 2018.
- [177] Y. Wang. Hooke park biomass boiler house. *Advancing Wood Architecture: A Computational Approach*, pages 169–181, 2016. doi:10.4324/9781315678825.
- [178] Z. Wang, P. Song, and M. Pauly. Desia: A general framework for designing interlocking assemblies. *SIGGRAPH Asia 2018 Technical Papers*, SIGGRAPH Asia 2018, 37(6):1–14, 2018. doi:10.1145/3272127.3275034.
- [179] R. Wilson. Defining the English mosque. *AJ, The Architect Journal*, 2019.
- [180] R. Wolfe. Research challenges for structural use of small-diameter round timbers. *Forest Products Journal*, 50(2):21–29, 2000.
- [181] R. Woodward and T. Zoli. Two bridges built using black locust wood. 30, 2013.
- [182] G. F. Wu, E. C. Zhu, H. J. Zhou, and J. L. Pan. Testing and modelling of shearwalls studded with small-diameter round timber under cyclic lateral load. *Construction and Building Materials*, 77:288–296, 2015. doi:10.1016/j.conbuildmat.2014.12.005.
- [183] K. Wu and A. Kilian. *Designing Natural Wood Log Structures with Stochastic Assembly and Deep Learning*. Springer International Publishing, 2019. URL: [http://dx.doi.org/10.1007/978-3-319-92294-2\\_2](http://dx.doi.org/10.1007/978-3-319-92294-2_2).
- [184] J. Yao, D. M. Kaufman, Y. Gingold, and M. Agrawala. Interactive design and stability analysis of decorative joinery for furniture. *ACM Transactions on Graphics*, 36(2), 2017. doi:10.1145/3054740.
- [185] H. Yoshida, M. Larsson, and T. Igarashi. Upcycling tree branches as architectural elements through collaborative design and fabrication. *TEI 2019 - Proceedings of the 13th International Conference on Tangible, Embedded, and Embodied Interaction*, pages 589–593, 2019. doi:10.1145/3294109.3295639.
- [186] K. Zampogiannis, C. Fermuller, and Y. Aloimonos. cilantro: A lean, versatile, and efficient library for point cloud data processing. In *Proceedings of the 26th ACM International Conference on Multimedia*, MM ’18, pages 1364–1367, New York, NY, USA, 2018. ACM. doi:10.1145/3240508.3243655.

---

## Bibliography

- [187] Z. Zhang, M. Fujimoto, A. Takino, and K. Imai. An experimental study on the buckling behavior of a single layer roof type cylindrical two directional lattice shell using a thin diameter wood rod with threaded tension in three dimension. *Proceedings of the Architecture Department of the Architectural Society of Japan*, 2013. doi:<https://doi.org/10.3130/aijs.78.781>.
- [188] H. Zhou, J. Leng, M. Zhou, Q. Chun, M. F. Hassanein, and W. Zhong. China's unique woven timber arch bridges. *Proceedings of the Institution of Civil Engineers: Civil Engineering*, 171(3):115–120, 2018. doi:[10.1680/jcien.17.00046](https://doi.org/10.1680/jcien.17.00046).
- [189] S. Zivkovic and L. Lok. Making Form Work. Experiments Along the Grain of Concrete and Timber. *Fabricate 2020. Making Resilient Architecture*, pages 116–123, 2020. doi:[10.1007/978-3-030-03676-8](https://doi.org/10.1007/978-3-030-03676-8).



# Curriculum Vitae

## PERSONAL INFORMATION



## PETRAS VESTARTAS

- Avenue D`Ouchy 58, Vaud, 1006, Lausanne, Switzerland.
- +41787261487, +37067371989
- petrasvestartas@gmail.com
- www.petrasvestartas.com

Male, Date of birth: 13/12/1989, Nationality: Lithuanian, ES

## WORK EXPERIENCE

2017 – 2021

### IBOIS, EPFL

PhD  
IBOIS, EPFL  
[www.epfl.ch/labs/ibois/](http://www.epfl.ch/labs/ibois/), Lausanne, CH.

2016 FEBRUARY

### CITA

2017 APRIL

Research Assistant  
(ComplexModelling5–InflatedRestraint, FloraRobotica)  
[cita.karch.dk](http://cita.karch.dk), Copenhagen, DK.

2014 AUGUST

### DELUGAN MEISSL ASSOCIATED ARCHITECTS

2016 JANUARY

Design Architect  
(Austrian Pavilion – Architecture Venice Biennale, Italy (Commission 2016), Wohnen Am Schweizer Garten, Vienna, Austria (1<sup>st</sup> Place), Fiducia GAD, Karlsruhe, Germany (Competition 2015), Zollhafen, Mainz, Germany (Competition 2015), Elbrucken, Hafencity-Hamburg, Germany (Recognition), U5 – Wiener Linien, Austria (Competition 2015), Porsche Design Tower, Frankfurt, Germany (Competition 2015), Future Art Lab, Vienna, Austria (3<sup>rd</sup> Place), Central Park Taopu, China (Competition 2014) Campus Tower, Hafencity-Hamburg, Germany (1<sup>st</sup> Place), Changchun Forest Park (Competition 2014)  
[www.dmaa.at](http://www.dmaa.at), Vienna, AT).

2012 JUNE

### ANDRE BALDI

2013 FEBRUARY

Architect.

(Vilnius Bajorai masterplan)  
[www.andrebaldi.lt](http://www.andrebaldi.lt), Vilnius, LT.

2011 JUNE – AUGUST

### CEBRA

Practical training  
(Våler Church, Hoje Taastrup masterplan).  
[www.cebra.info](http://www.cebra.info), Aarhus, DK.

### TRANSFORM

2011 AUGUST – OCT.

Practical training

(Hoje Taastrup masterplan).  
[www.cebra.info](http://www.cebra.info), Aarhus, DK.

2010 JULY – AUGUST

### VAKARINIS FASADAS

Architect

(Palanga Sanatorium, Druskininkai cafeteria)  
[www.vakarinisfasadas.lt](http://www.vakarinisfasadas.lt), Siauliai, LT.

# Curriculum Vitae

## EDUCATION/TRAINING

2012 – 2014

### VILNIUS ACADEMY OF ARTS

Master degree.

Thesis “Architecture potential in extreme environments - Beirut”

Vilnius, LT.

2013 – 2014

### ROYAL DANISH ACADEMY OF FINE ARTS

Department 8. Exchange program.

Thesis “London – Generics in Newham”

Copenhagen, DK.

2008 – 2012

### VILNIUS ACADEMY OF ARTS

Architecture bachelor with distinction

(Urbanism, building design, landscape, heritage, construction, arts and programming). Vilnius, LT.

1996 - 2008

### KURSENAI LAURYNAS IVINSKIS GYMNASIUM

Kursenai, LT.

## PERSONAL SKILLS

### MOTHER TONGUE

Lithuanian

### OTHER LANGUAGES

	Understanding		Speaking		Writing
	Listening	Reading	Spoken Interaction	Spoken Production	
English	C1	C1	C1	C1	C1
French	A2	A2	A1	A1	A1

### COMMUNICATION SKILLS

Good communication skills gained while studying and working in a team.

### COMPUTER SKILLS

**CAD** (Rhinoceros 3D, Autocad, Revit, Archicad, Microstation, Maya, ArcGis)

**Coding** (Visual Studio (C#, C++), Visual Studio Code (Python), Eclipse (Java), Processing (Java), CMake)

**Visual Scripting** (Grasshopper)

**Rendering** (V-Ray, KeyShot)

**Adobe Package** (Illustrator, Photoshop, InDesign, AfterEffects, Adobe PremierePro)

**Digital Fabrication** (5-axis CNC, ABB Robot control, 3d Printing, Laser cutting)

**Developed Applications** (Point-cloud Processing - *Cockroach*, Polygonal Mesh

Processing for Wood-wood Connections - *NGon*, 5-axis CNC tool-path simulation -

*IBOIS-CNC*, 2D Packing – *OpenNest*, Faro Laser Scanner Automation – *FaroSharp*,

Populating a large number of objects for rendering – *Scatter*, Aggregation and Graph methods – *Fox*.)

## Curriculum Vitae

### PUBLICATIONS

- 2021  
P. Vestartas, A. Rezaei Rad, and Y. Weinand. Robotically-Fabricated Nexorades from Whole Timber. International fib Symposium on the Conceptual Design of Structures. Switzerland, 2021.
- A. Rezaei Rad, H. Burton, N. Rogeau, P. Vestartas, and Y. Weinand. A framework to automate the design of digitally-fabricated timber plate structures. Computers & Structures, 2021.
- P. Vestartas and Y. Weinand. Joinery Solver for Whole Timber Structures. WCTE2020, Santiago, Chile, August 24-27, 2021.
- 2020  
P. Vestartas and Y. Weinand. Laser Scanning with Industrial Robot Arm for raw wood Fabrication. ISARC2020, Kitakyushu, Japan, October 27-28, 2020. p. 773-780, 2020.
- L. Vestarte, P. Vestartas, and R. Kucinskas. Corrugated Cardboard Shell: A Pavilion Project of An Architectural Workshop. Advances in Architectural Geometry (AAG), 2020.
- 2019  
P. Vestartas, N. Rogeau, J. Gamerro and Y. Weinand. Modelling Workflow for Segmented TimberShells using Wood-wood Connections. Design Modelling Symposium Berlin 2019. Impact: Design with all Senses, p. 596-607, Berlin, Germany, September 23-25, 2019.
- P. Vestartas, L. Palletier, M. T. Nakad, A. R. Rad, and Y. Weinand. Segmented Spiral Using Inter-Connected Timber Elements.IASS 2019 Barcelona Symposium: Timber and Bio-based Structures, 2019.
- A. C. Nguyen, B. Himmer, P. Vestartas, Y. Weinand. Performance Assessment of Double-Layered Timber Plate Shells using Alternative Structural Systems. Proceedings of IASS Annual Symposia, 2019.
- A. C. Nguyen, P. Vestartas, Y. Weinand. Design framework for the structural analysis of free-form timber plate structures using wood-wood connections. Automation in Construction, 2019.
- 2017  
P. Ayres, P. Vestartas, M. R. Thomsen. Enlisting Clustering and Graph-Traversal Methods for Cutting Pattern and Net Topology Design in Pneumatic Hybrids. Design Modelling Symposium (DMS) Paris 2017.
- P. Vestartas, M. K. Heinrich, M. Zwierzycski, D. A. Leon, A. Cheheltan, R. La Magna, P. Ayres Design Tools and Workflows for Braided Structures. Design Modelling Symposium (DMS) Paris 2017.
- M. Zwierzycski, P. Vestartas, M. K. Heinrich, P. Ayres. High Resolution Representation and Simulation of Braiding Patterns. Conference: Disciplines & Disruption, ACADIA 2017

